Australian Government

Geoscience Australia

THE 2001 NORTHEASTERN YILGARN DEEP SEISMIC REFLECTION SURVEY

GEOSCIENCE AUSTRALIA
RECORD 2003/28

by

B.R. Goleby[1], R.S. Blewett[1], P.B. Groenewald[2], K.F. Cassidy[3], D.C. Champion[1], L.E.A. Jones[1], R.J. Korsch[1], S. Shevchenko[4] and S.N. Apak[4].

1. Predictive Mineral Discovery Cooperative Research Centre, c/- Geoscience Australia, P.O. Box 378, Canberra ACT, 2601, Australia
2. Kalgoorlie Regional Office, Geological Survey of Western Australia, P.O. Box 1664, Kalgoorlie, W.A., 6430.
3. Predictive Mineral Discovery Cooperative Research Centre, c/- Geoscience Australia, currently at the Geological Survey of Western Australia, Minerals House, 100 Plain Street, East Perth, W.A., 6004.
4. Geological Survey of Western Australia, Minerals House, 100 Plain Street, East Perth, W.A., 6004

GEOSCIENCE AUSTRALIA

Geoscience Australia
Chief Executive Officer: Dr Neil Williams

ISSN 1039-0073
ISBN 0 642 46789 7

Bibliographic reference: Goleby, B.R., Blewett, R.S., Groenewald, P.B., Cassidy, K.F., Champion, D.C., Jones, L.E.A., Korsch, R.J., Shevchenko, S. and Apak, S.N., 2003. The 2001 Northeastern Yilgarn Deep Seismic Reflection Survey. Geoscience Australia, Record 2003/28. 143pp.

This record was originally prepared as a set of workshop notes for the Northeastern Yilgarn Seismic Workshop that was hosted by the *pmd**CRC, GSWA and GA. This workshop presented results from the 2001 deep seismic reflection survey that was conducted in the Northeastern Yilgarn Craton. The workshop was held in Perth on the 28 August 2002 at the ARRC Auditorium (CSIRO), 26 Dick Perry Avenue, Kensington, Perth, W.A.

Authors have subsequently updated their work based on the results of the workshop and later feedback.

TABLE OF CONTENTS

EXECUTIVE SUMMARY

The 2001 Northeastern Yilgarn Deep Seismic Reflection Survey

Deep-seismic reflection data across the Eastern Goldfields Province, northeastern Yilgarn Craton, Western Australia have provided information on the region's crustal architecture and on several of its highly mineralised regions. The 2001 Northeastern Yilgarn Deep Seismic Reflection Survey data has imaged several prominent crustal scaled features, including an eastward thickening of the crust across the northeastern Yilgarn Craton, the subdivision of the crust into three broad layers, the presence of a prominent east dip to the majority of the reflections and the interpretation of three east-dipping crustal-penetrating shear zones. These three east-dipping shear zones are major structures that subdivide the region into four terranes.

Major orogenic gold deposits in the Eastern Goldfields Province are spatially associated with these major structures. The Laverton Tectonic Zone, for example, is a highly mineralised corridor that contains several world-class gold deposits plus many other smaller deposits. Other non crustal-penetrating structures within the area do not appear to be as well endowed as the Laverton structure. In all the major structures a wedge-geometry is formed at the intersection of the east-dipping shear and a low-angle shear zone within its hanging wall. This wedge-geometry forms a suitable trap where the upward and/or sub-horizontal moving fluids were focused into the wedge's apex and then distributed and deposited into the surrounding complexly deformed greenstones.

The information from this seismic survey, together with as much additional geological and geophysical information is being used to construct a three-dimensional model of the granite-greenstone succession within the Eastern Goldfields Province. This model will provide a geological framework for the mining industry to use for future exploration. The model being developed and refined is providing details on the relationships between the various geological units, the major shear zones and the structures and the known mineral deposits. The model is being used as the framework to answer that important question "Why is Kalgoorlie where it is?"

This document presents the results from the 2002 Northeastern Yilgarn Deep Seismic Reflection Survey.

INTRODUCTION

B.R. Goleby and R.J. Korsch
Predictive Mineral Discovery Cooperative Research Centre, Geoscience Australia,
P.O. Box 378, Canberra ACT, 2601, Australia

Introduction to the deep seismic survey

The granite-greenstone terrains of the Eastern Goldfields Province, Yilgarn Craton, contain numerous world-class gold deposits that are spatially associated with major structures. The three-dimensional geometry of these major structures reveals information on the size and architecture of the gold mineralising systems and the geodynamic processes responsible for their generation. Our current knowledge of the three-dimensional nature of the Eastern Goldfields Province is largely restricted to the Kalgoorlie region, where the collection of deep seismic profiles has allowed the development of detailed 3D geological maps (Goleby et al., 2002). Along with previous seismic interpretations (e.g. Drummond et al., 2000), these 3D maps define the geometry of the major structures and show that the greenstone succession is 5-7 km thick and controlled by interlinked crustal shears that compartmentalise the granite-greenstone succession into distinct domains.

To follow up, a further deep seismic reflection survey was proposed to acquire additional seismic data within other areas of the Eastern Yilgarn Craton to examine the geometry of additional major structures and to enhance our understanding of the 3D structure over a wider area. As a result of feedback from the mineral exploration industry at previous seismic workshops, the next strategic target that was proposed is the northeastern Yilgarn between the Leonora and Laverton mineralised fields. These two areas contain gold deposits that are spatially associated with major structures, although they are in different geological domains. The questions that researchers working in the Yilgarn Craton are concerned with are:

- Did these mineralised areas have a similar crustal structure to the Kalgoorlie region?
- What are the structures that control mineralisation in the area?
- What is the internal structure within these mineralised areas?

Thus, the Northeastern Yilgarn Seismic Survey will concentrate on questions on:

- the geometry of the region,
- the mineral system of the region, and
- the geodynamic history of the region.

Geoscience Australia (GA) and the Geological Survey of Western Australia (GSWA), in conjunction with the Predictive Mineral Discovery CRC (pmd*CRC), acquired a regional deep seismic reflection transect across the northeastern Yilgarn Craton in 2001. This deep seismic reflection transect commenced near Leonora, headed east to the Laverton region, then farther eastwards to the Yamarna greenstone belt and finally into the Officer Basin. It provides new information on the crustal architecture of the northern portion of the Eastern Goldfields Province. The results from the seismic reflection data indicate there are significant variations in structure style between this region and the Kalgoorlie region to the south.

The initial interpretation of this 432 km long, deep seismic reflection transect were presented at the 2002 Northeastern Yilgarn Seismic Workshop, that was hosted by the pmd*CRC,

GSWA and GA. The workshop provided a venue where the northeastern Yilgarn researchers presented the results of their work on the interpretation of seismic reflection data. The workshop also provided an opportunity to discuss implications of this research with the earth sciences community and to get feedback from interested parties.

The workshop focused on:

- Acquisition and processing of the seismic data,
- Regional geology and seismic interpretation of the sedimentary basins,
- Potential field modelling of the Officer Basin area,
- Tectonic evolution of the Eastern Goldfields: an overview of postulated models,
- Seismic interpretation of the Northeastern Yilgarn seismic data,
- Potential field modelling of Northeastern Yilgarn seismic data,
- Implications of the seismic data in the development of a 3D geological maps of the region, and
- Implications of the seismic data for mineral systems, in particular gold.

The Northeastern Yilgarn seismic survey forms another piece in Geoscience Australia's long-term plan to undertake a regional seismic traverse across the entire Yilgarn Craton. This survey, in conjunction with the 1991 Kalgoorlie regional deep seismic reflection traverse, provides crustal architecture information from the easternmost terrains on the Yilgarn Craton to well into the Southern Cross Province.

This record summarises the preliminary results presented at the 2002 Northeastern Yilgarn seismic workshop. Copies of this document will be available through the GA Sales Centre, GPO Box 378, Canberra, ACT, 2601, Australia.

References

Drummond, B.J., Goleby, B.R. and Swager, C.P., 2000. Crustal signature of Late Archaean tectonic episodes in the Yilgarn Craton, Western Australia. *Tectonophysics,* **329**, 193-221.

Goleby, B.R., Korsch, R.J., Fomin, T., Bell, B., Nicoll, M.G., Drummond, B.J. and Owen, A.J., 2003. Preliminary 3D geological model of the Kalgoorlie region, Yilgarn Craton, Western Australia, based on deep seismic reflection and potential field data. *Australian Journal of Earth Sciences*, **49**, 917-934.

AIMS OF THE NORTHEASTERN YILGARN DEEP SEISMIC SURVEY

B.R. Goleby and R.J. Korsch
Predictive Mineral Discovery Cooperative Research Centre, Geoscience Australia,
P.O. Box 378, Canberra ACT, 2601, Australia

Introduction

In developing a set of scientific objectives for the 2001 Northeastern Yilgarn Seismic Survey, we were aware that, for the Eastern Goldfields Province of the Yilgarn Craton, there is already considerable information on the two dimensional structure of the granite-greenstone regions from existing seismic reflection work in the Kalgoorlie region (as shown in Figure 1 and documented by Goleby *et al*., 2000).

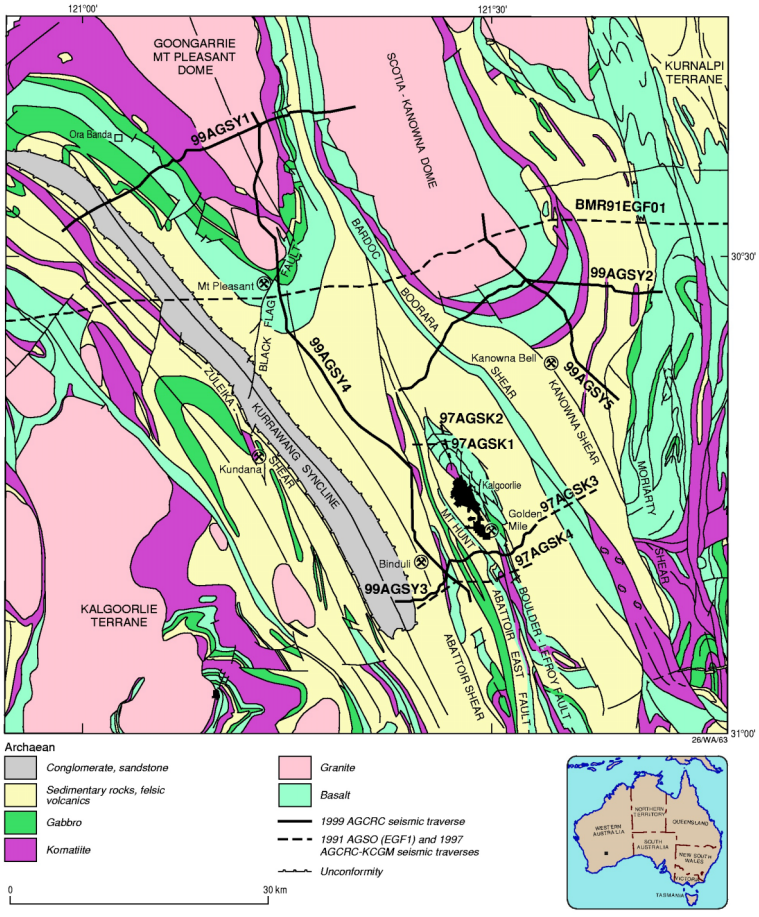

Figure 1: Location of the 1991, 1997 and 1999 deep seismic lines in the Kalgoorlie region, Eastern Goldfields Province, Yilgarn Craton.

Using the seismic reflection technique in the Kalgoorlie region of the Eastern Goldfields Province, detailed seismic sections have been produced that show:

- the thickness of the granite-greenstone succession and topography on a basal detachment surface that lies beneath the Kalgoorlie and Kurnalpi terrains,

- the geometry of the major faults,
- limits to the shapes of granites (although this is dependent on what rock type the granite was intruded into),
- the internal structure within the greenstone succession, and
- possible deformation surfaces and inferred deformational histories.

Given the success of deep seismic reflection techniques within the Kalgoorlie region, it is likely that similar quality seismic sections can be obtained in the northeastern Yilgarn Craton.

Any new work should concentrate on furthering our knowledge of the two (and three) dimensional structure of new areas within the Eastern Goldfields Province to:

- understand the crustal structure of these regions of the Yilgarn Craton,
- investigate similarities and differences between, and within, the various terranes crossed by new seismic traverses and by the earlier seismic traverses in the Kalgoorlie region,
- test the existing models for the Kalgoorlie region in other parts of the Yilgarn Craton,
- develop a geodynamic model of the Eastern Goldfields Province, and
- understand why mineralisation in the Eastern Goldfields Province occurs where it does.

The 2001 Northeastern Yilgarn Seismic Survey will form part of a proposed longer regional transect across the Yilgarn Craton that will investigate new regions and focus on the basic architecture of the craton.

Location of deep seismic traverse

To achieve the broad scientific objectives and specific seismic targets identified below, the 2001 Northeastern Yilgarn deep seismic reflection traverse was oriented approximately east-west to east-northeast-west-southwest. This orientation took advantage of the existing geological information as well as lying within the previously acquired 1 km and 2 km spaced regional gravity data. The route for the traverse is shown in Figure 2.

Objectives of the 2001 Northeastern Yilgarn Seismic Survey

The broad scientific objectives for the 2001 Northeastern Yilgarn Seismic Survey were to:

- Investigate the thickness of the crust within the Laverton-Leonora region and compare it with the thickness of the crust in the Kalgoorlie region and with regions to the east and to the west.
- Investigate variations in the seismic characteristics of the crust between different regions within the Eastern Goldfields Province.
- Determine the presence and geometry of any major boundaries within the Laverton-Leonora region.
- Determine if a detachment surface exists within the Laverton-Leonora region, and if present, determine the lateral extent and depth variation of this surface.
- Determine the thickness and internal geometry of the granite-greenstone succession within the Laverton-Leonora region and the geometry of any major internal structural features within the region. This will be achieved by -
  - ♦ Imaging the internal geometry of the granite-greenstone succession,

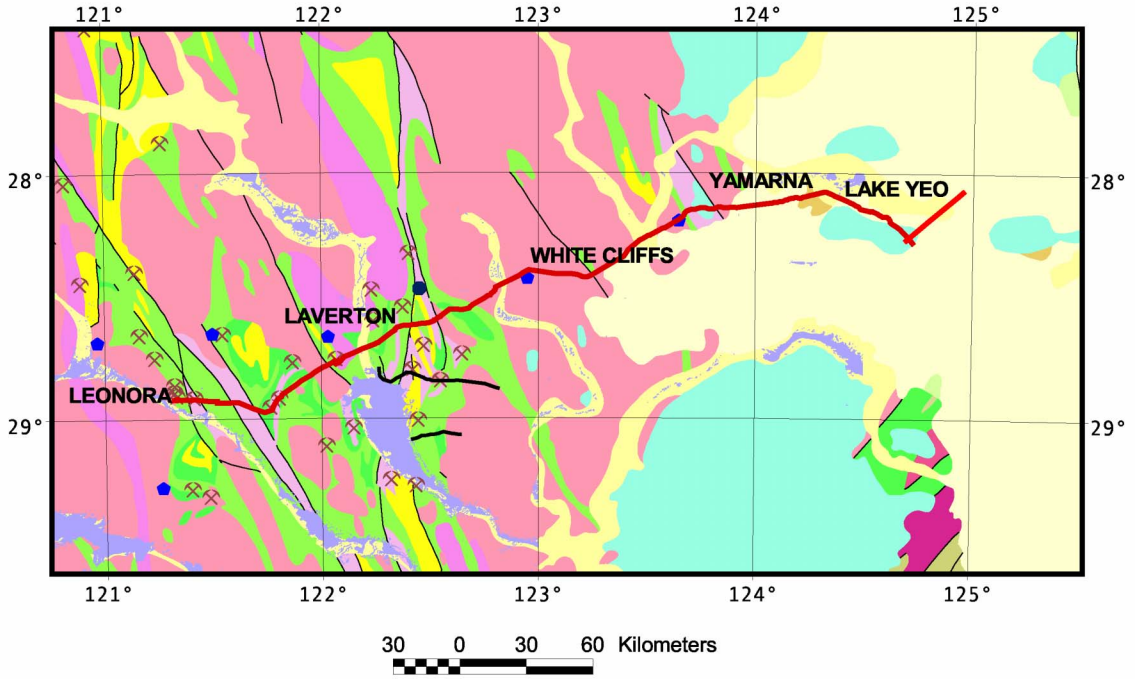

Figure 2: Location map of the deep seismic reflection traverse in the Eastern Goldfields region of the Northeastern Yilgarn Craton. The background is taken from the 1:5m Geology Map of Australia. The deep seismic reflection traverse is shown in red. The blue dots are seismic broadband instrument locations, positioned to determined crustal velocity values for this area and derived using receiver function analysis.

- ♦ Identifying deformation surfaces within and/or bounding the greenstone package,
- ♦ Determining the relationship of the bounding surfaces of a greenstone package to mapped/identified faults systems,
- ♦ Imaging the granite-greenstone contacts, and
- ♦ Determining regional variations of the structure of the granite-greenstone succession,
- ♦ Identifying the sequence of deformational history within the greenstone terrane using kinematic indicators identified within the seismic data and investigate the cumulative effects of the successive deformations (D1 - D4) on the greenstone belt.

- Determine the predominant structural style within the Laverton-Leonora region, both within the deeper crust and in the upper succession, and attempt to provide constraints on the relative timing and importance of contractional, extensional, and strike-slip tectonics during the evolution of the Eastern Goldfields. In particular, determine whether the D2 thrust-stacking model of Hammond and Nisbet (1992) or the D2 vertical folding model of Swager and Griffin (1990) is applicable in the Laverton-Leonora region.
  - ♦ If the thrust-stacking model is valid then it implies duplication and irregularity of greenstone successions within a greenstone belt, with the potential for repetition of mineralised successions, or
  - ♦ If the vertical folding model is valid then it implies a generally laterally extensive stratigraphy with predictable mineralised successions
- Map the form of granite intrusions within the Laverton-Leonora region and compare these with the Kalgoorlie region.
- Image possible fluid flow pathways through the granite-greenstone succession.

Specific Seismic Targets for the 2001 Northeastern Yilgarn Seismic Survey

In conjunction with the broad scientific objectives of the proposed 2001 Northeastern Yilgarn Seismic Survey listed above, specific seismic targets include the following:

- Raeside Batholith - body and margin.
- Sons of Gwalia mineral field and system.
- Mount George Shear Zone.
- Kalgoorlie-Gindalbie terrane boundary.
- Butchers Flat Shear Zone (D_3?).
- Keith-Kilkenny Fault Zone.
- Pig Well (syntectonic) metasedimentary basin.
- Kurnalpi Terrane (Welcome Well region).
- Gindalbie-Kurnalpi terrane boundary.
- Benalla Anticline (D_2?).
- Imbricate stack in greenstones (D_1 or D_3?).
- Folded fault (D1 thrust) separating Welcome Well region and Yundamindera region.
- Imbricate granitoid stack (D_1?).
- Claypan Fault (D_3?) and Celia Lineament.
- Margaret Anticline region (check possible D_2 structures).
- Small granitoid bodies - Laverton Batholith southern margin.
- Chatterbox Shear Zone.
- Structural contact between Margaret Domain and Laverton Tectonic Zone.
- Laverton Tectonic Zone.
- Eastern margin of greenstones, late uplift of granitoid batholith.
- Yamarna greenstone belt.
- Style of Yilgarn Craton under the Gunbarrel Basin and Officer Basin.

Key Acquisition Strategies

Deep seismic reflection profiling is the only scientific technique that can address the above scientific objectives as it can provide detailed information on crustal architecture at depth. In addition to the seismic reflection data, two additional seismic related experiments were acquired to improve our knowledge of the regions velocity structure. These experiments were a receiver function experiment and a passive-listening experiment.

Seismic Reflection Program

The seismic reflection data were collected by ANSIR (Australian National Seismic Imaging Resource), a Commonwealth Government Major National Research Facility. The seismic reflection program consisted of the collection of 432 km of deep seismic reflection data (Figure 2) using a Vibroseis energy source. These data were acquired at a group interval of 40 m, vibroseis interval of 80m, giving 60 fold data redundancy. Record lengths were 16 s (~ 48 km depth) in the west and 18 s (~ 54 km depth) in the east. As part of the seismic acquisition program, accurate location data (X,Y,Z information) were obtained for each station along the seismic traverse. More detailed information on the acquisition of seismic reflection data is provided by Jones et al. (2002, this volume).

The deep seismic reflection profile provided structural information from 0 km (surface) to the base of crust (approximately 40-45 km) along the entire length of the seismic traverse. The seismic reflection technique provided limited velocity information for only the top few kilometres (down to 5 km's depth).

Receiver Function Analysis

Broadband seismic instruments were deployed coincident with the deep seismic reflection traverse to record teleseismic events (S-wave, body-waves and surface-wave seismic arrivals from distant earthquakes). The locations of these recording sites are given in Figure 2. Figure 3 shows the locations of broadband instrument sites in WA.

The new data will be added to the Skippy data set (Kennett, 1998) and will also be used to calculate receiver function values for the region. Receiver Functions are an estimate of the velocity structure of the crust at the recording point.

The Broadband seismic recording provides velocity information from ~80 km to ~300 km depth at the point of recording. Receiver Functions estimate velocity information from 0 km (surface) to 40 km (approximate base of crust) and then to about 70 km at the recording point.

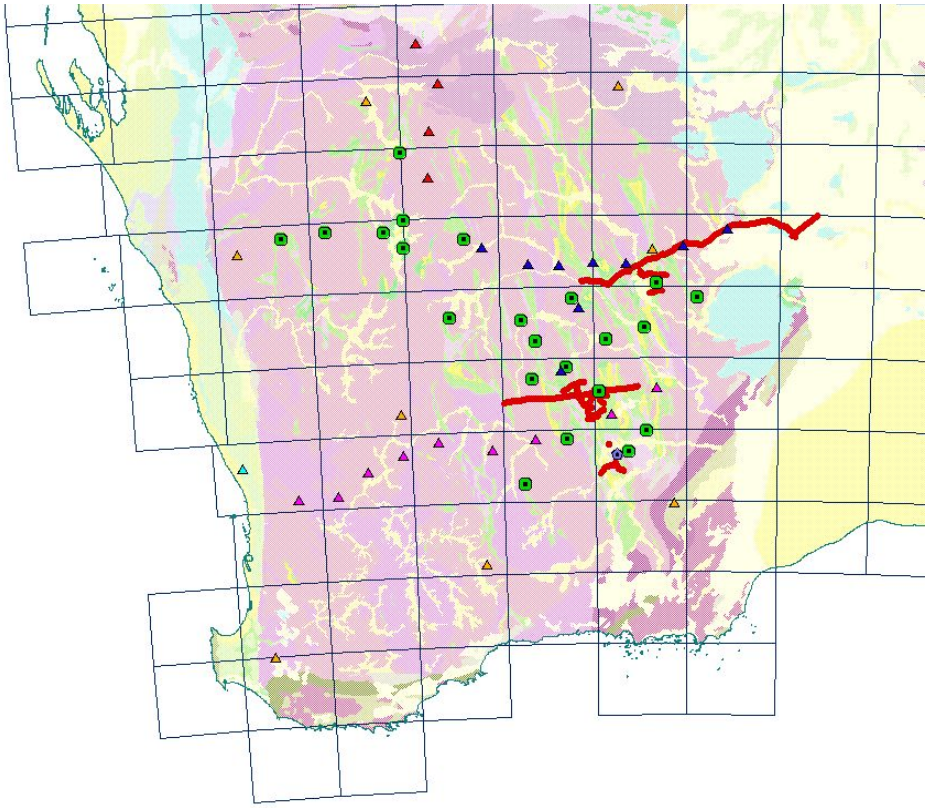

Figure 3: Location of broadband instrument sites in Western Australia. Blue triangles are the location of broadband instrument sites recorded as part of the Northeastern Yilgarn seismic survey. Orange triangles are SKIPPY sites, Red triangles are site from the recent Hamersley Survey and Magenta triangles are from the recent Perth to Kalgoorlie Survey. Green dots are proposed recording sites as part of the ANU - *pmd**CRC's Y2 project.

The objectives for this experiment were to:

- Determine the deeper velocity structure beneath the Northeastern Yilgarn Craton.
- Determine receiver function estimates for the crustal velocity beneath the Northeastern Yilgarn Craton.

- Investigate anomalous material at the base of the crust and within the upper mantle that might provide clues to tectonic evolution.
- Build up the velocity information on the Yilgarn Craton.

These data are currently being processed by staff at RSES, ANU and GA and were not discussed at this workshop.

Passive-Listening Experiment

To obtain additional velocity information and, hence, better lithological information within the Leonora-Laverton greenstone belts, a passive-listening experiment was designed. This experiment recorded wide-angle signal from the Vibroseis trucks as they were working along the seismic reflection traverse. The experiment used the vibroseis energy as the controlled source and recorded into short-period instruments. Hence it was coincident with part of the deep seismic reflection traverse. Station spacing was between 1 km and 1.5 km spacing. The location of the passive listening experiment is shown in Figure 4.

With a large vibroseis source, it was hoped to obtain velocity data from the surface to the base of crust (~40 km). This velocity data can be used to provide structural information beneath the recording sites.

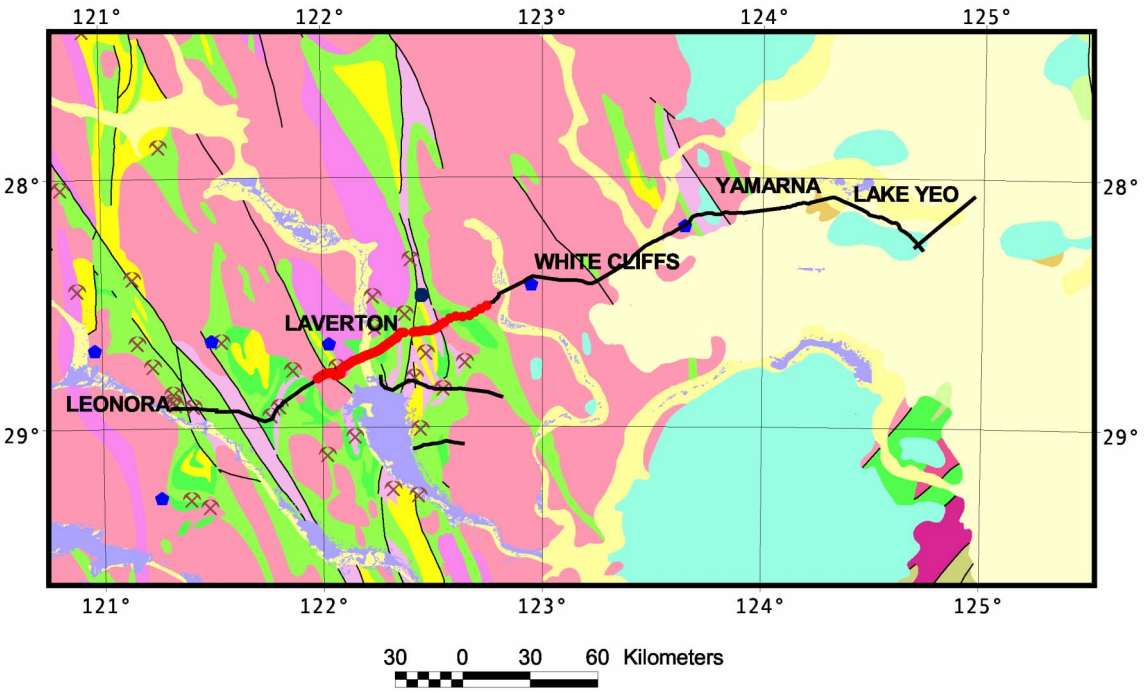

Figure 4: Location map of deep seismic reflection traverse in the Eastern Goldfields region of the Northern Yilgarn. The background is taken from the 1:5m Geology Map of Australia. The red line shows the regions where the short-period instruments were deployed as part of the passive-listening experiment. The deep seismic reflection traverse is shown in black. The blue dots are broadband instrument locations, positioned to determined receiver function values for this area.

The scientific objectives for the Passive Listening Program were to:

- Investigate near-vertical and wide-angle recordings of vibroseis energy at various offsets within the Laverton-Leonora region,
- Investigate variations in the seismic characteristics at larger offsets beneath the different regions within the Laverton-Leonora area,

- Include the high-density first arrival refraction data into the regional refraction analysis to develop higher-resolution images of the velocity structure of the granite-greenstone crust,
- Obtain high-density refraction information with offsets from 0 km up to 50-100 km, and
- Obtain full waveform information at larger offsets.

These data are currently being processed by staff at GA and are not reported in this record.

Potential Field data

Both the gravity and magnetic data coverage are excellent for the majority of the seismic reflection traverse. The project used existing GA and industry data sets.

Geological Data

Detailed geological information was collected in key areas along the deep seismic reflection traverse by staff from GSWA. The collection of the additional data is currently focused to the east of Leonora near the Welcome Well region.

References

Goleby, B.R., Bell, B., Korsch, R.J., Sorjonen-Ward, P., Groenewald, P.B., Wyche, S., Bateman, R., Fomin, T., Witt, W., Walshe, J., Drummond, B.J. and Owen, A.J., 2000. Crustal structure and fluid flow in the Eastern Goldfields, Western Australia. *Australian Geological Survey Organisation, Record,* **2000/34**, 109pp.

Hammond, R.L. and Nisbet, B.W. 1992. Towards a structural and tectonic framework for the Norseman-Wiluna Greenstone Belt, Western Australia. *In* Glover, J.E. and. Ho, S.E., eds., The Archaean: Terrains, Processes and Metallogeny. *University of Western Australia, Geology Department and University Extension, Publication,* **22**, 39-50.

Jones, L.E.A., Goleby, B.R. and Barton, T.J., 2003. Seismic processing - 2001 Northeastern Yilgarn Seismic Reflection Survey (L154), The 2001 Northeastern Yilgarn Deep Seismic Reflection Survey. Geoscience Australia Record, *this volume*.

Kennett, B.L.N., 1998. The SKIPPY Project: Mapping the lithosphere under Australia, Final Report. *Seismology Group, Research School of Earth Sciences, Australian National University Publication*, Unpublished Report.

Swager, C.P. and Griffin, T.J. 1990. Geology of the Archaean Kalgoorlie Terrane, Northern and Southern Sheets, 1:250,000. *Geological Survey of Western Australia, Perth*.

CAPABILITIES AND LIMITATIONS OF THE SEISMIC REFLECTION METHOD IN HARD ROCK TERRANES

L.E.A. Jones[1,2], B.R. Goleby[1,2] and B.J. Drummond[3]
[1] Australian National Seismic Imaging Resource, Geoscience Australia, GPO Box 378, Canberra ACT 2601, Australia
[2] Predictive Mineral Discovery Cooperative Research Centre, Geoscience Australia, GPO Box 378, Canberra ACT 2601, Australia
[3] Geoscience Australia, GPO Box 378, Canberra ACT 2601, Australia

Introduction

The seismic reflection method was developed for petroleum exploration in sedimentary basins, where its accuracy, resolution, and depth penetration result in detailed pictures of structure and stratigraphy. The reflection method uses a controlled source which generates seismic waves that are reflected from interfaces between different rock units, as shown in Figure 1. An explosive or vibratory source is used. Continuous 2D coverage is achieved by moving sources and receivers along a seismic traverse.

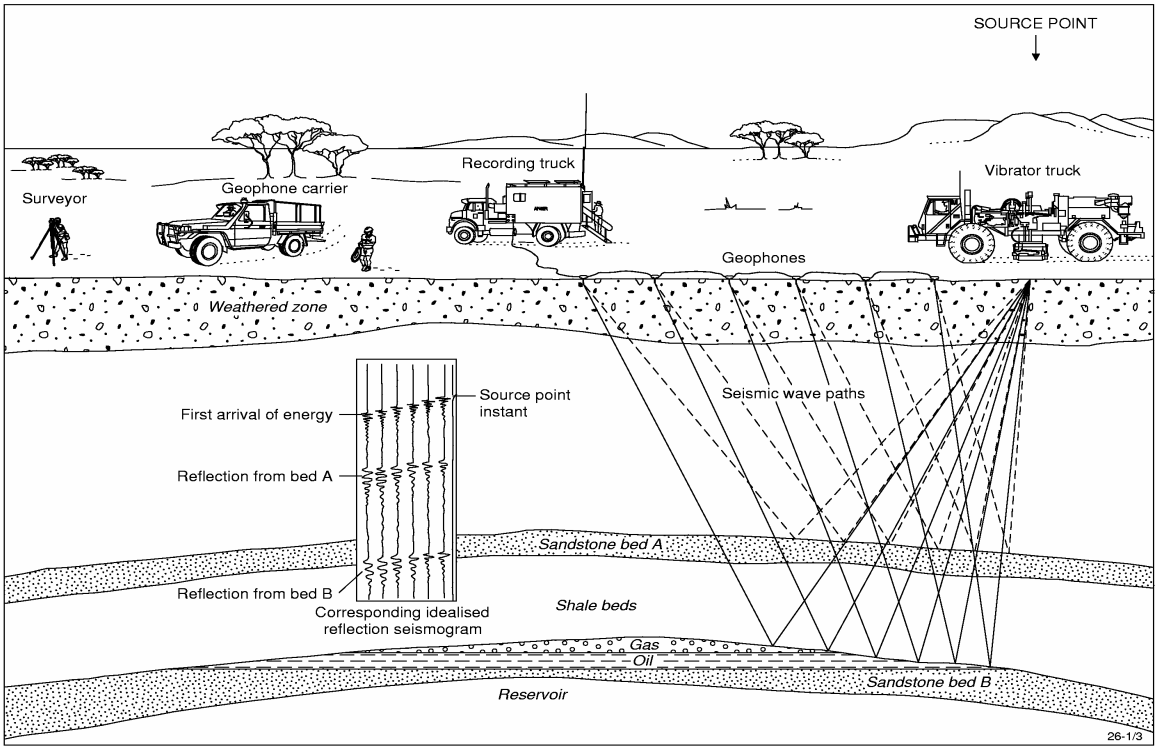

Figure 1. Schematic representation of a seismic reflection survey.

The Earth is not homogeneous or isotropic, but a good approximation in seismology is a system of layers, individually homogeneous and isotropic, which is why the seismic method works so well in sedimentary basins. In hard rock areas too, reflections are indisputably

produced. The salient questions are: What causes reflections? What can't we see? What are the pitfalls?

Some of the key features of hard rocks are steep dips associated with folds and faults, and high seismic velocities. Steeply dipping events can be difficult to image. High velocities affect resolution, but also make it easier to stack reflections since there is less move-out. In hard rock terranes, there may also be more problems correcting for delays in the weathered zone and in getting sufficient energy through it. However, a counteracting factor is that hard rock should have lower intrinsic attenuation of seismic energy, resulting in greater depth penetration of the higher frequencies.

Basic Concepts

Seismic Waves

A seismic (elastic) wave is a propagating oscillatory disturbance that travels as a series of wavefronts (equal amplitude of disturbance). Usually ray paths (path travelled by a point on a wavefront) are drawn, as in Figure 1. The distance between successive peaks (or troughs) is the wavelength, λ. The frequency of the wave, f, is the number of cycles per second, so that the velocity of the wave is $V = \lambda.f$.

Two types of seismic body waves can travel within the Earth, namely P (compressional) and S (shear). In reflection surveys, P waves predominate, being preferentially generated by the commonly used sources. Surface waves (ground roll) can be a source of noise in reflection surveys, travelling along the surface at low velocity and arriving at the same time as reflections from depth.

Factors influencing P wave velocity in rocks include mineralogy, porosity (and cracks), pore fluid content, cementation and texture. For igneous and metamorphic rocks, the dominant factor is mineralogy, although micro-cracks in low concentrations can significantly reduce velocity. Empirical laws for such rocks show that the velocity is approximately proportional to density. In sedimentary rocks, the most important factors are porosity, pore fluid content and cementation. As a general statement, velocities are high in igneous and metamorphic rocks and lower in sedimentary rocks, particularly young sedimentary rocks.

Generation of Reflections

When a seismic wave encounters a boundary where there is an abrupt change in elastic properties, some of the energy is reflected depending on the size of the reflection coefficient, but most is transmitted into the second medium, as shown in Figure 2. Some energy will also be critically refracted along the boundary, and forms the basis of the seismic refraction method. The reflection coefficient RC is the ratio of the reflected wave amplitude Ar to the incident wave amplitude Ai and for near normal incidence (up to 20°) can be expressed as:

$$RC = \frac{A_r}{A_i} = \frac{\rho_2 V_2 - \rho_1 V_1}{\rho_2 V_2 + \rho_1 V_1} = \frac{Z_2 - Z_1}{Z_2 + Z_1}$$

The product ρV (=Z) is known as the acoustic impedance, where ρ is the density and V is the P-wave velocity. The larger the contrast in acoustic impedance, the larger will be the reflection coefficient. An impedance decrease causes a negative reflection coefficient, i.e., the reflected wave is reversed in polarity compared with the incident wave. Typically reflection coefficients are small, generally less than 0.05, but in hard rock terranes could reach 0.075 for a felsic-mafic contact (ρ = 2.7 t/m^3 and V = 6000 m/s overlying ρ = 2.9 t/m^3 and V = 6500 m/s).

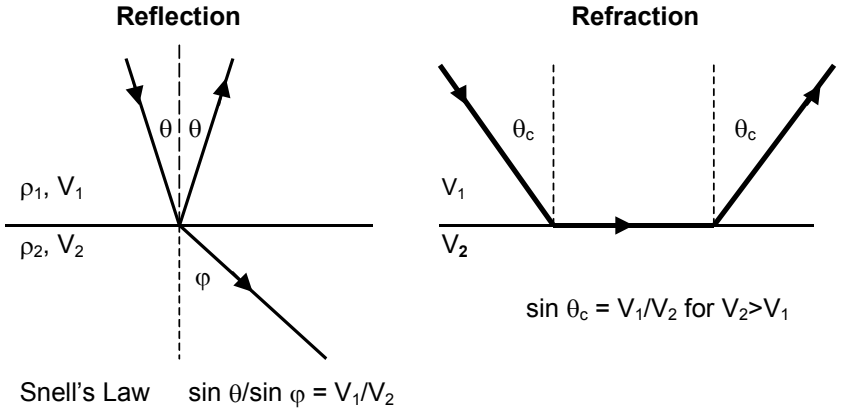

Figure 2. Reflection and refraction of a seismic wave at a boundary between two media with velocity V_1 and V_2 and density ρ_1 and ρ_2, respectively. The angle of incidence equals the angle of reflection. The wave is transmitted into the second medium with angle of refraction φ. For φ = 90°, the refracted ray follows the boundary (critical refraction).

Thus the density contrast governs whether reflections occur at boundaries between different rock types (since velocity is proportional to density for igneous, metamorphic and well-lithified rocks). It is not likely that reflections will result from a foliated fabric within a rock, unless this is strongly developed into alternating bands of material on a macroscopic scale, such as in shear zones.

As a seismic pulse (wavelet) travels down into the Earth, energy will be reflected back at each interface, with an amplitude governed by the reflection coefficient, and an extra time delay corresponding to the extra time down to and back from the interface. Thus a seismic reflection trace consists of a succession of "echoes" of seismic energy, as shown in the reflection seismogram in Figure 1.

Figure 1 also illustrates that the travel time for a reflection increases with increasing offset between source and receiver. It can be shown that the time, T, along a reflection ray path emerging at offset, X, from the source follows a hyberbolic relationship:

$$T^2 = T_0^2 + X^2/V^2$$

where V is the velocity of the layer, and T_0 is the two way travel time for vertical incidence. The difference between T and T_0, known as normal moveout, decreases with both increasing T_0 and increasing V. The high velocities typical of hard rock areas mean that moveout is generally small, so that uncertainties in moveout velocity are not so problematical for stacking the data. However, a corollary is that velocities for depth conversion are very poorly constrained.

For dipping reflectors, the above relationship is modified with V replaced by (V/cos α) where α is the angle of dip, thus increasing the stacking (moveout) velocity.

Seismic Resolution

Seismic resolution deals with the question: How thick and how wide do features have to be to produce recognisable reflections on a seismic section?

Vertical Resolution

The concept of vertical resolution can be illustrated by considering waves reflected from a layer of thickness H and velocity V_1 embedded in a medium of velocity V_0, as shown in Figure 3. The reflection from the bottom will be reversed in polarity (reflection coefficient has opposite sign) and will lag behind the reflection from the top by a time ΔT, as shown in Figure 3. If the layer is thick, ΔT will be large and the two wavelets will appear as separate events. If the layer is thin, ΔT will be small and the two wavelets will almost cancel. A commonly used criterion for resolution is that interference effects are maximised when the wavelets are separated by half a cycle, which corresponds to a layer thickness of $\lambda/4$ (λ being the dominant wavelength for the wavelet).

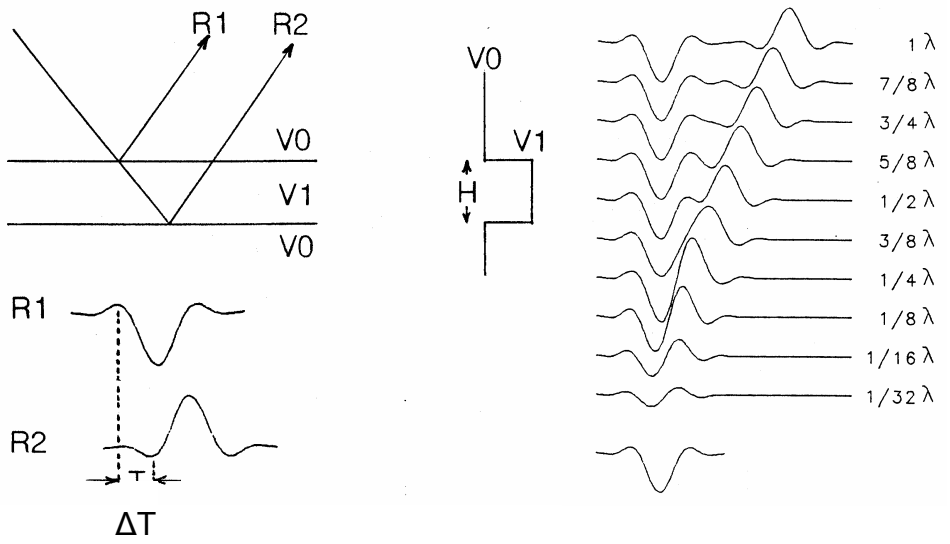

Figure 3. Vertical resolution (identification of an embedded layer) is determined by the superposition of reflections from the top and bottom of the layer. Because the two reflections are of opposite polarity they cancel for thin layers and reinforce for thicker layers.

The seismic response of layers of different thickness is illustrated on the right hand side of Figure 3. Thickness is parameterised in terms of λ. A maximum response occurs for $\lambda/4$, but the top and bottom of the layer are not resolvable and it thus appears as a single interface. In practice, the layer can still be detected as it becomes thinner, but becomes progressively harder to see. Layers thinner than $\lambda/32$ would not be detectable. It is not until the layer thickness exceeds $\lambda/2$ that reflections from the top and bottom of the layer can just be seen as two events.

What are typical values of λ in hard rock areas? The range of frequencies (band width) contained in a seismic pulse is narrow, normally from 5 Hz to 100 Hz. Because the amplitude loss with depth depends on frequency, the highest frequencies are rare at depth. Typically, the

dominant frequency would be 40 Hz or less, corresponding to a wavelength of 150 m for a typical velocity of 6000 m/s. Layers would need to be greater than 75 m thickness to be identified as such. However, a layer of about 37.5 m will produce a strong response, even if it cannot be differentiated from an interface. It would not be possible to detect layers less than 5 m thick (and probably not even less than 10 m). Thus the vertical resolution in hard rock is not as good as in sedimentary basins.

Horizontal Resolution

Horizontal resolution is concerned with the minimum lateral extent of features that can be detected. Consider the case of vertical incidence for a reflecting point P as shown in Figure 4. Geometrical ray theory would predict that only point P contributes to the reflection recorded vertically above on the surface at S. Wave theory shows that not only P, but surrounding points within a certain radius also contribute to the reflection amplitude.

For down-going wavefronts from source S, zones on the reflector can be constructed such that the difference in path lengths from S is λ/4 as shown in Figure 4 (a). For two-way travel, the difference in path length will be λ/2. It can be shown that the innermost zone (known as the first Fresnel zone) makes the dominant contribution to the wave amplitude observed at S.

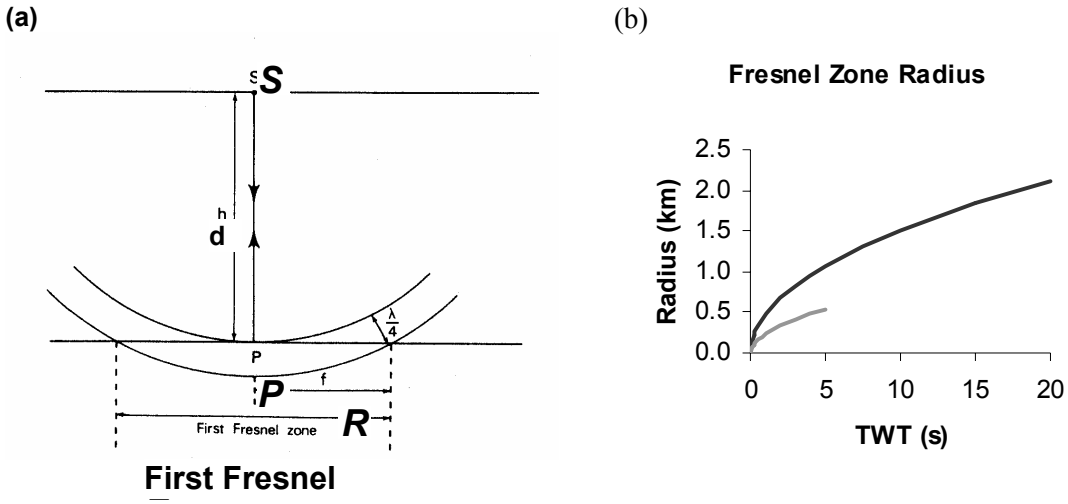

Figure 4. (a) Representation of the reflector zone (first Fresnel zone) contributing to the amplitude of a wave reflected back to S. (b) Radius of the first Fresnel zone for typical hard rock areas (black) and sedimentary basins (grey) versus two-way time (TWT).

The first Fresnel zone has a radius equal to (λd/2)1/2 where d is the depth to the reflector. Thus, the width of the zone increases (resolution decreases) as both depth (two-way time) and dominant wavelength increase. In practice, features smaller than the Fresnel zone will not be resolved, since the reflected wave amplitude depends on the average properties over the width of the Fresnel zone.

In Figure 4 (b), two-way time (s) for the hard rock areas can be converted to depth (km) by multiplying by 3, using a typical velocity of 6000 m/s. For mid-crustal depths of ~24 km (TWT = 8 s), reflecting bodies must extend over a kilometre or two to be visible. As shown in Figure 4 (b), horizontal resolution is poorer than it would be for a typical sedimentary basin, i.e. the Fresnel zone is larger for hard rock areas, because of the greater wavelength (~150 m).

However, because of the mathematical formulation above, the Fresnel zone radius increases by a factor of only 1.4 for a doubling of the wavelength, for features at the same depth.

Diffractions

When a seismic wave encounters a feature whose dimensions are comparable to, or smaller than the wavelength, the wave is diffracted, rather than reflected or refracted. Since the seismic wavelength in hard rock is typically 150 m, there will be many instances where geological features are smaller than this. Diffractions are commonly produced from very small geological structures or where continuous reflectors suddenly stop. Examples such as tight bends on folds, ends of fault-truncated layers, and tips of dykes are illustrated in Figure 5 (a).

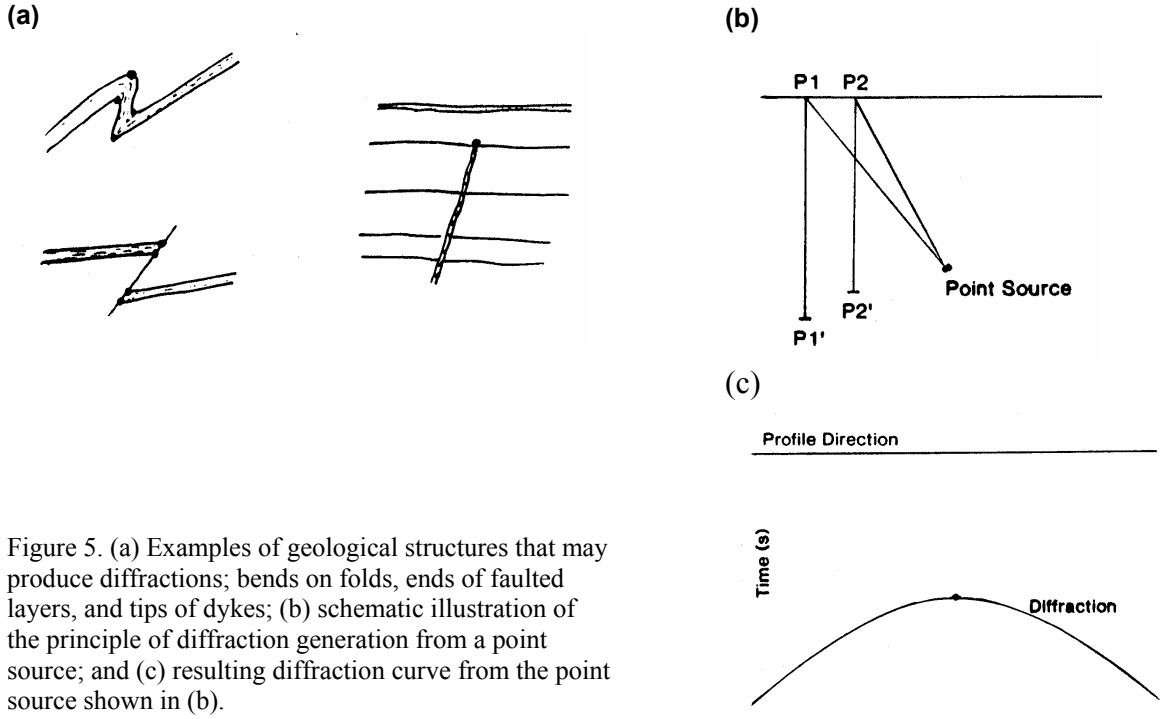

Figure 5. (a) Examples of geological structures that may produce diffractions; bends on folds, ends of faulted layers, and tips of dykes; (b) schematic illustration of the principle of diffraction generation from a point source; and (c) resulting diffraction curve from the point source shown in (b).

The generation of diffractions can be explained by treating the feature as a point from which secondary waves radiate after excitation by the incident wave. An incident wave spreading out from a source at P1 in Figure 5 (b) will generate a returning wave that will travel back along the same path; similarly for point P2. On a seismic section, the returning wave is assumed to come from vertically below P1 and P2, and will lie along a hyperbolic curve as shown in Figure 5 (c).

The crest of the diffraction locates the diffracting point (in time and space). In practice, amplitude is stronger towards the crest of the diffraction curve. The curvature of the diffraction depends on the depth to and the velocity above the diffracting point, but standard overlay curves can be produced to differentiate diffractions from structure. Migration will collapse diffractions as described later. Diffracted waves will also fill in gaps in reflectors, thus making the seismic event appear continuous when the physical interface is not (another way of visualising the concept of horizontal resolution).

Dipping Reflectors

In hard rock areas, rocks are commonly highly deformed, resulting in steeply dipping rock units within folds, as well as faults of varying dips. Since the seismic method was originally developed for sub-horizontal layering within sedimentary basins, a critical issue is the greatest dip that can be imaged by the method in hard rock terranes.

The maximum dip is constrained by two parameters, the length of the seismic line and the duration of the seismic record. The general picture is illustrated in Figure 6. For near coincident source and receiver at P, a reflection will return along a path that is perpendicular to the reflector. To be imaged from P, sub-horizontal reflectors must lie below P, but steeply dipping reflectors will lie off to the side by a considerable distance. Thus a seismic line must be long enough to encompass both the reflecting surface and the seismic reflection system. In addition, recording time must be long enough to record reflections from the offset reflectors.

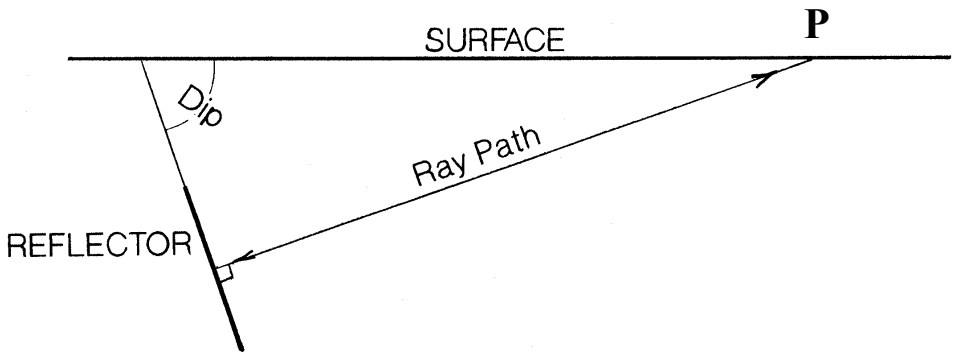

Figure 6. The length of the seismic line and the recording time determine the maximum dip that is imaged. For steep dips, the observation point must be off to the side, and the recording time must be long for energy to travel out to and back from the reflector.

Figure 7 shows this relationship for a typical deep crustal seismic survey in hard rock. Note that a recording time of 20 seconds would be necessary to record reflections from a distance of 60 km, assuming a velocity of 6000 m/s. A semi-circular region in the Earth, centred on the observation point, is divided into equiangular segments. Each segment shows the zone within the Earth where a particular range of dips will be imaged, out to a distance of 60 km. For example, in the segments labelled 70° to 80°, only reflectors with dips in this range towards the observation point will be imaged. In the 0° to 10° segments, only shallow dips will be imaged.

Consequently, shallowly dipping structures are imaged when the observation point is directly above, and continuous coverage will be obtained as the point moves along the line. Very steep dips near the surface can be imaged from the side. For lines of approximately 100 km length, it could reasonably expected that dips as high as 50° in the middle crust may be seen.

A further consideration concerns the survey acquisition parameters - whether these discriminate against steep dips at any frequencies of interest. In the field, geophone arrays are used to attenuate coherent noise and random noise, by summing the individual geophone responses. A source array is also used with typically three vibrators in line with moveup between sweeps. Arrays will pass vertically travelling energy, but will discriminate against horizontally travelling energy with wavelengths shorter than the effective length of the combined source and receiver array.

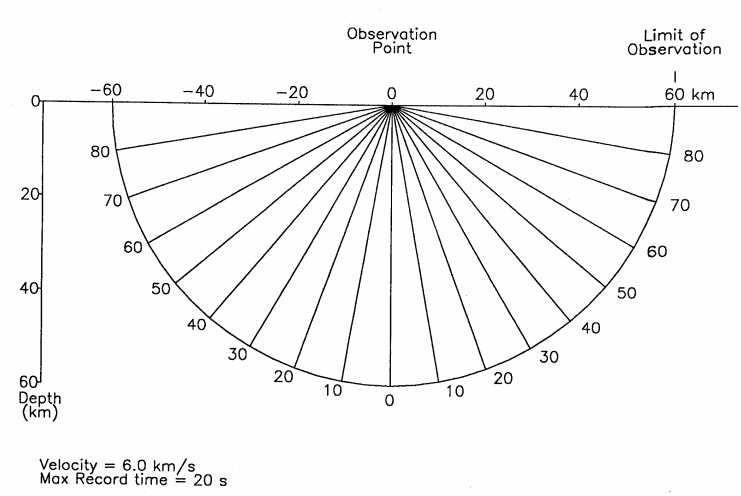

Figure 7. Each segment shows where dipping reflectors must be located, in order to be imaged from the observation point, for the dip range annotated on the segment edges.

For a ray incident at the surface at angle α (to the normal) the apparent velocity across the array is $V_a = V / \sin \alpha$ with corresponding apparent wavelength $\lambda_a = \lambda / \sin \alpha$. For the ray path in Figure 6, α equals the dip angle. Thus, apparent wavelengths will range from infinite for reflections from horizontal reflectors to the true wavelength for reflectors with a dip of 90°. For frequencies from 40-100 Hz, the true wavelength λ will range from 150 m to 60 m. Thus dip filtering by the array is not likely to occur for the typical combined array effective length of approximately 60 m.

A further consideration in imaging steeply dipping reflectors is that dipping reflectors require higher stacking velocities than horizontal reflectors. For example, where a horizontal reflector has a stacking velocity of 6000 m/s, a reflector in the same material dipping at 60° would stack at 12000 m/s ($V/\cos \alpha$). The difficulty of simultaneously stacking reflectors of different dips is more pronounced at shallow depth (and TWT), since normal moveout is greater. Dip moveout (DMO) processing is required, but is difficult to apply correctly for crooked lines where the fold may be low and the offset distribution irregular.

Migration

Migration is the process of moving reflectors to their correct positions and is essential in areas of steep dip and complicated structure. Because of the way seismic data are displayed, dipping reflectors are not correctly imaged, as shown in Figure 8. The ray paths for coincident source and receiver at points P1, P2, and P3 must be perpendicular to the reflector at the corresponding reflecting points. However, on the seismic section, these reflecting points appear to be vertically below points P1, P2, and P3. Thus the reflector segment is shifted downwards and its apparent dip, β, is less than the true dip, α, such that $\tan \beta = \sin \alpha$. Dipping reflectors, such as faults, and the flanks of synclines and anticlines, will not appear in

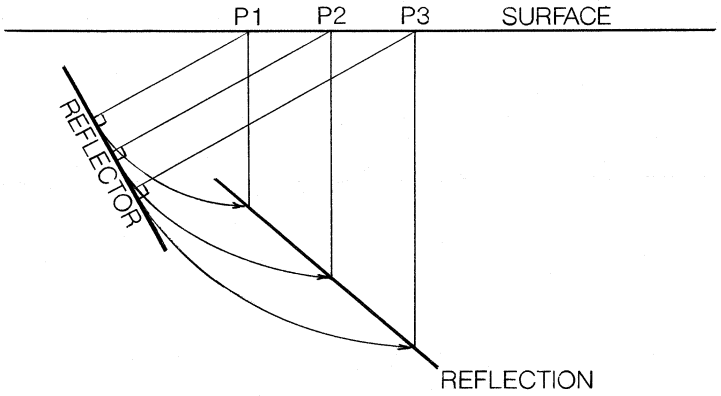

Figure 8. On a stacked seismic section, reflecting points will appear vertically below the coincident source-receiver points on the surface. Thus dipping reflectors will appear deeper than their true position, with a lower apparent dip. The process of moving reflectors to their correct positions is known as migration.

their correct positions. Moreover, such features will appear to have lower dip as illustrated in Figure 9. A consequence of the relationship between true dip and apparent dip is that dips will never appear to be greater than 45° on an unmigrated section.

The effect of lack of migration is shown in Figure 10 (a). In the CDP range 2400-3900, large arcuate features can be seen throughout, crossing one another to give a 'basket-weave' pattern. Some of these are diffractions emanating from lithological discontinuities. Dipping features appear shifted downwards from their true position, for example the westward dipping features below 4 s. Anticlines appear as broad features.

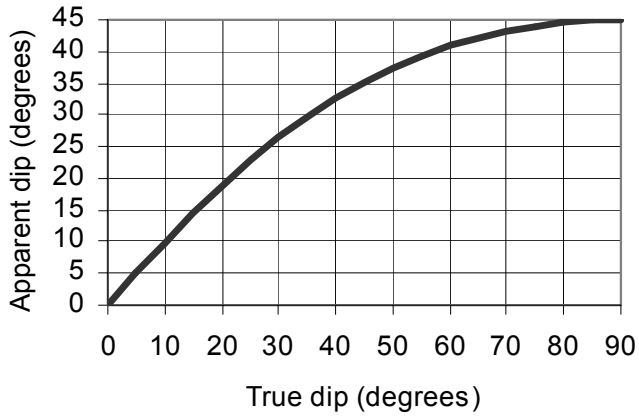

Figure 9. Apparent dip of a dipping reflector on an unmigrated section versus true dip.

Conceptually, migration is a simple procedure. In principle, the position of the reflector shown in Figure 8 just needs to be swung back through an arc equal to the true dip angle. In actual implementation, migration is a complicated process, not only because of velocity variations, but also because of out of plane energy. Because most of the migration algorithms use the wave equation, diffractions will also collapse to a point, thus improving horizontal resolution. It is important to note that 2D migration can only be carried out in the presence of dip. Thus strike lines with apparently horizontal reflectors cannot be migrated. Migration works best for seismic data with strong lateral continuity. However, in hard rock terranes, lateral continuity of reflections is often poor, making it difficult to implement migration successfully.

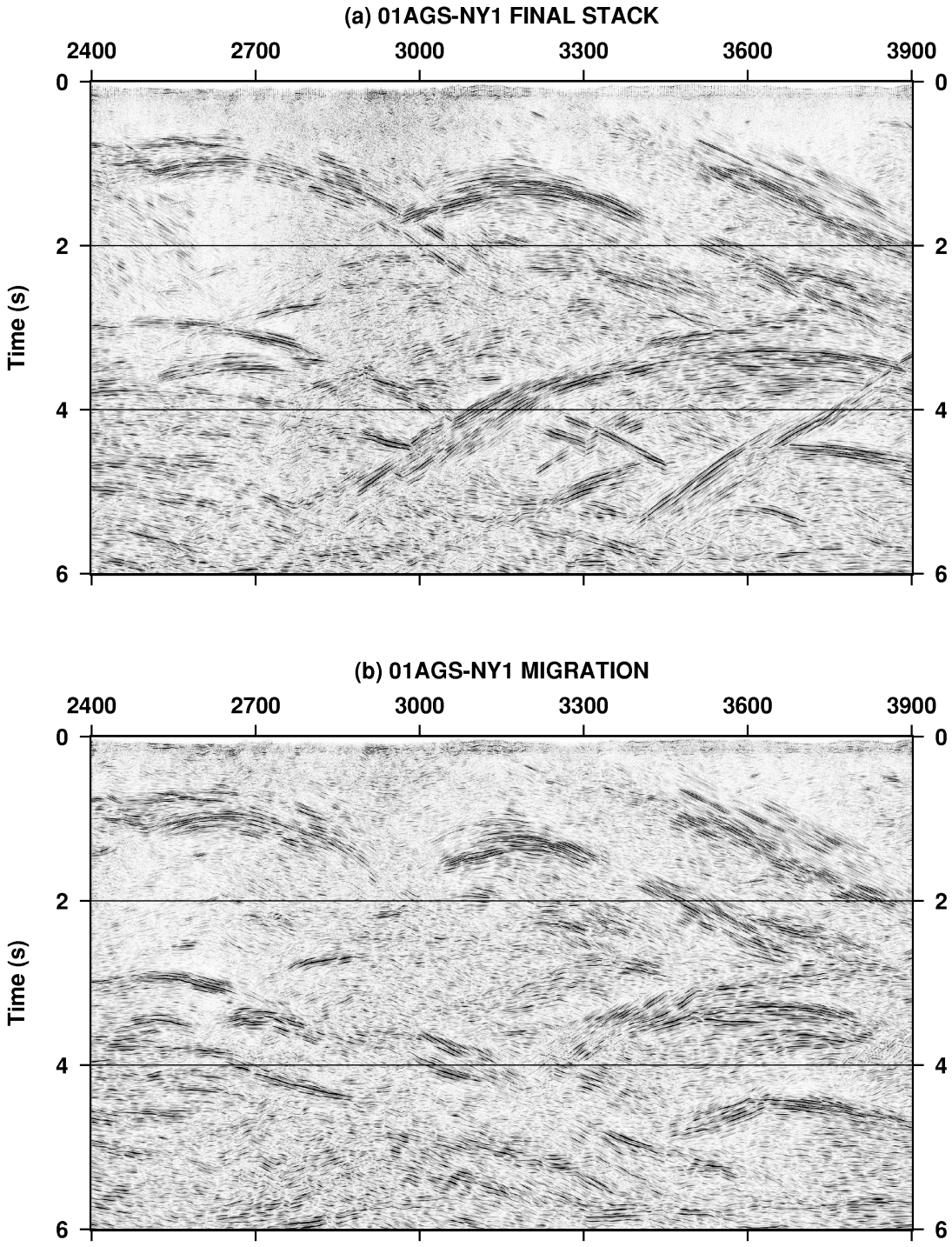

Figure 10. Seismic sections for line 01AGS-NY1 from CDP 2400 to 3900 and 0-6 s TWT. V/H = 1. 100 CDP = 2 km. 1 s = 3 km. (a) Final stack. (b) Migrated section.

The result of migration is shown in Figure 10 (b). Migration has collapsed the diffractions, cleaning up the image and leaving only reflections from continuous surfaces, which are shifted back to their correct position. Dipping parts of reflectors have moved up and become steeper and anticlines have thus become narrower in the process. More steeply dipping events have been migrated greater distances. For example, the reflector around 5 s below CDP 3600 has been moved up to the right beyond the display window.

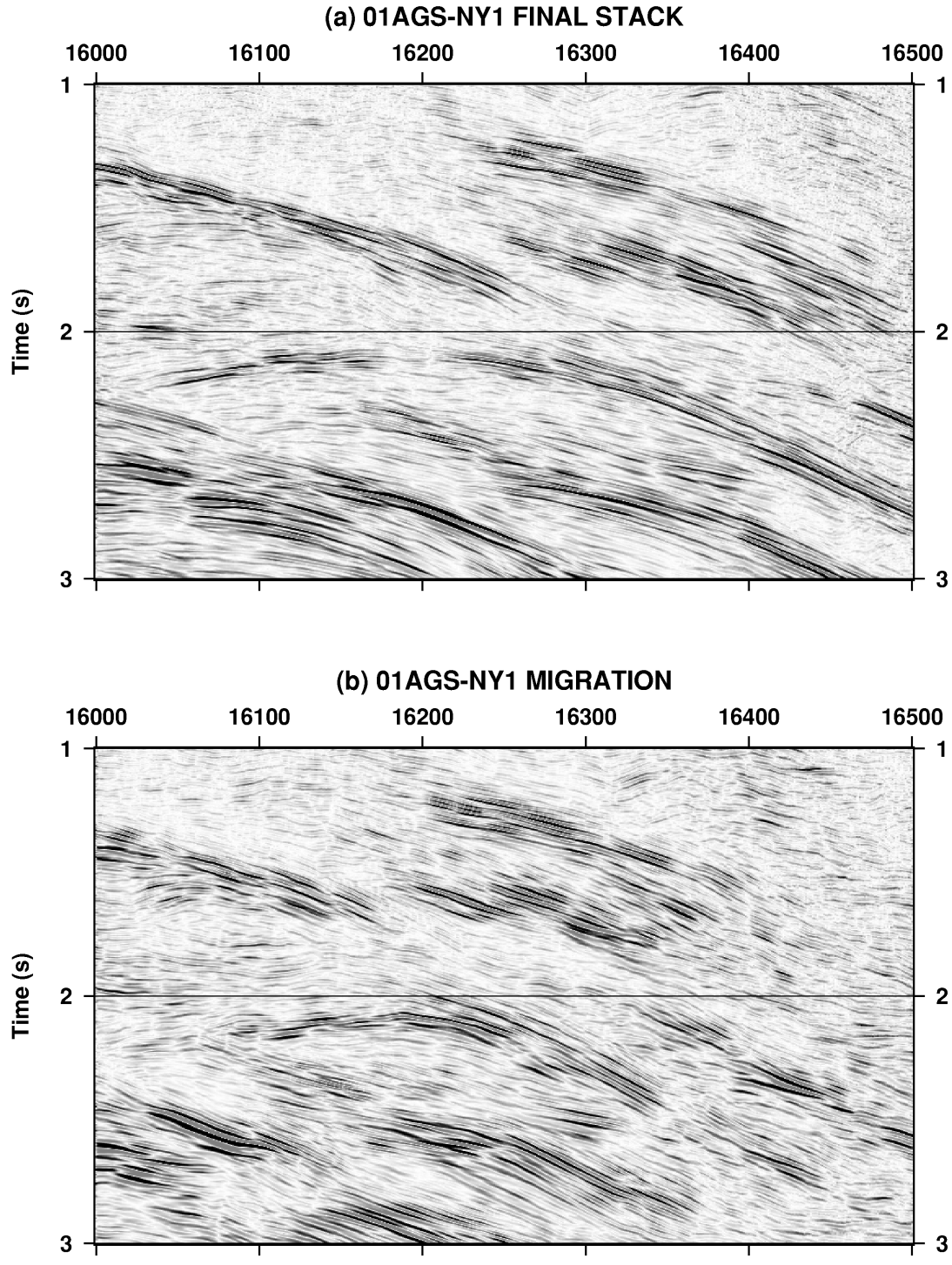

Figure 11 Seismic sections for line 01AGS-NY1 from CDP 16000 to 16500 and 1-3 s TWT. V/H = 1. 100 CDP = 2 km. 1 s = 3 km. (a) Final stack. (b) Migrated section.

Note that care must be exercised in interpreting events on the ends of migrated lines. If events are dipping towards the end of the line, they will be moved updip, but no more data exists to be migrated to fill in the gap.

Several criteria can be used to decide whether the sections are under-migrated or over-migrated. On under-migrated sections, the diffractions still look like diffractions, whereas on

over-migrated sections, the diffractions turn into 'smiles'. Since migration moves reflectors upwards and steepens them, the termination of reflectors against another surface can be used as a guide to the correctness of migration as shown in Figure 11. Figure 11 shows the detailed imaging of thrust duplexes before and after migration. Several separate thrust wedges are apparent on the migrated section.

Examples of features imaged in the Northeastern Yilgarn

In the Northeastern Yilgarn, the seismic reflection survey was able to image features with a range of dips, including shallow to moderately dipping lithology and moderately dipping thrusts and faults. In places, the presence of steeply dipping surfaces could be inferred from the progressive upturn of more shallowly dipping surfaces. It is worth pointing out that for the eastern part of the survey, very little outcrop was present. Other features observed include thrust duplexes, shear zones, and lithological indicators, such as reflective greenstones and poorly reflective homogeneous granites.

Dipping features

The migrated seismic section for line 01AGS-NY1 is characterised by prominent, mostly easterly dipping features along the length of the line, which are variously interpreted as lithology, shear zones and faults. For example, a package of east-dipping parallel reflectors is a prominent feature of Figure 12. Dips of up to 30° appear on the migrated section. These reflectors are characteristic of lithological bedding, but are not identified by surface correlation, as they lie below the Pig Well Graben. Faults and shear zones are discussed in a later section.

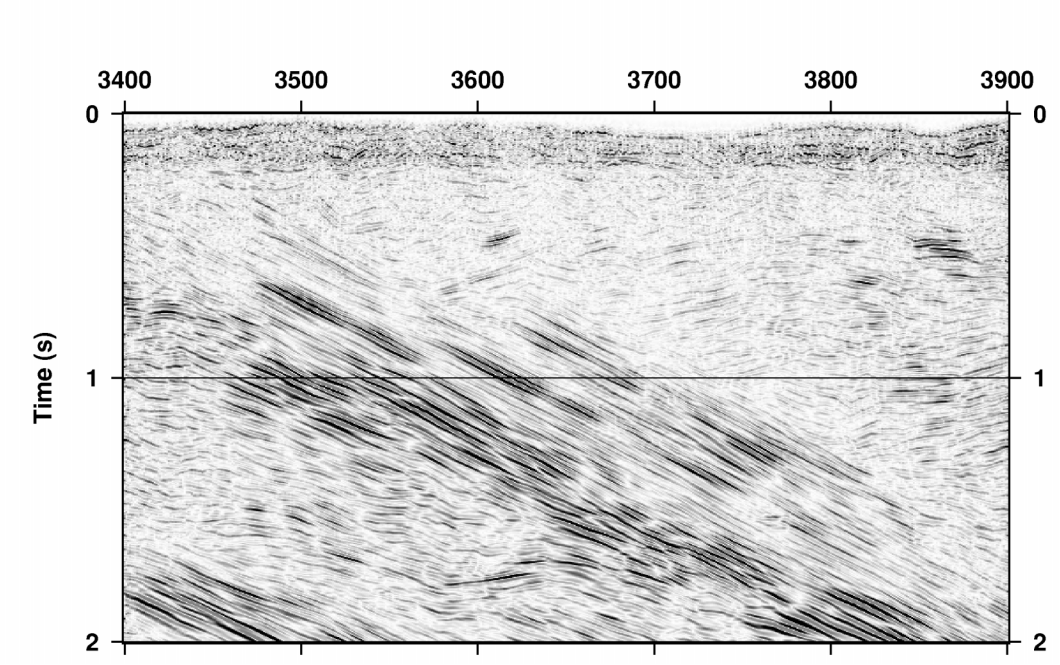

Figure 12. Migrated seismic section for line 01AGS-NY1 from CDP 3400 to 3900 and 0 to 2 s TWT at V/H = 1. 100 CDP = 2 km. 1 s = 3 km. The package of eastward dipping reflectors is interpreted as primary lithological layers. Dip is approximately 30°.

An issue still to be resolved is whether steep near-surface reflectors of limited extent can be satisfactorily imaged, in view of the vertical and horizontal resolution obtainable. Horizontal resolution would be no better than 250 m on an un-migrated section, even at the highest frequencies, for steeply-dipping shallow features. Thus small scale folding will not be seen, but enveloping surfaces may be imaged. In some cases, steep dips may be inferred from a progressive up-turning of layers before entering a reflection-free zone. Resolving these issues needs further research, using seismic modelling and pre-stack migration.

Faults

Faults can be recognised by the way they disrupt layering, with similar criteria to those used for identifying faults in sedimentary basins. These include offset of layers, abrupt change in reflection character or layer thickness, change in dip and the presence of diffractions from truncated layers. Note that vertical faults can be identified in this way, because the fault is imaged by its effects and not by reflections from it.

Figure 13 illustrates listric faults identified by offsets in the top of Yilgarn reflector and in bedding in the overlying Proterozoic basins. These faults are extensional features, which may also be reactivations of pre-existing shears within the Yilgarn, as indicated by reflections off the fault surfaces themselves. Thrust surfaces can also be identified, as in Figure 11, by the truncation of layers and by the occurrence of anticlinal structures in the hanging wall.

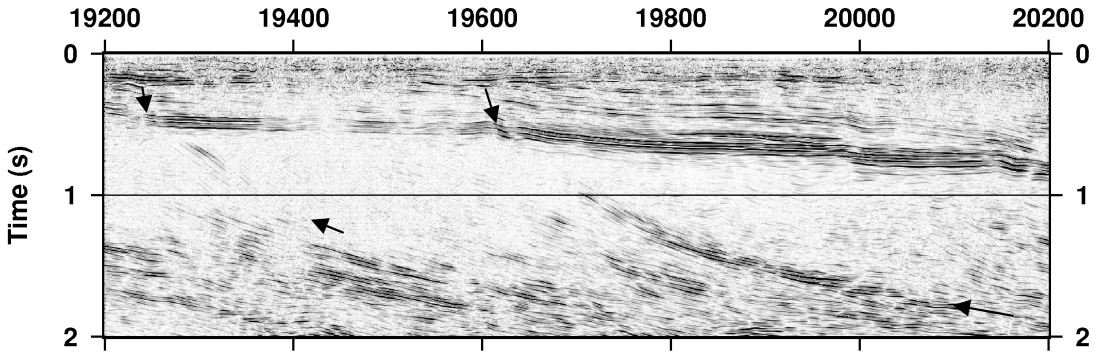

Figure 13. Migrated seismic section for line 01AGS-NY1 from CDP 19200 to 20200 and 0 to 2 s TWT at V/H ~ 1. 100 CDP = 2 km. Arrows indicate listric faults, with normal displacement in the upper section.

Shear Zones

Shear zones are often very strong reflectors of seismic energy, due to their layered nature on a macroscopic scale. Bands of alternating low and high velocity (density) material can explain the seismic response as shown in Figure 14. Tuning of the interference between reflections from tops and bottoms of the layers can result in a much larger seismic response than for a homogeneous layer of the same total thickness (compare Figure 14(a) and (b)). Zones in which layer thickness is variable and less than $\lambda/4$ can still produce strong reflections as illustrated in Figure 14(c) and (d).

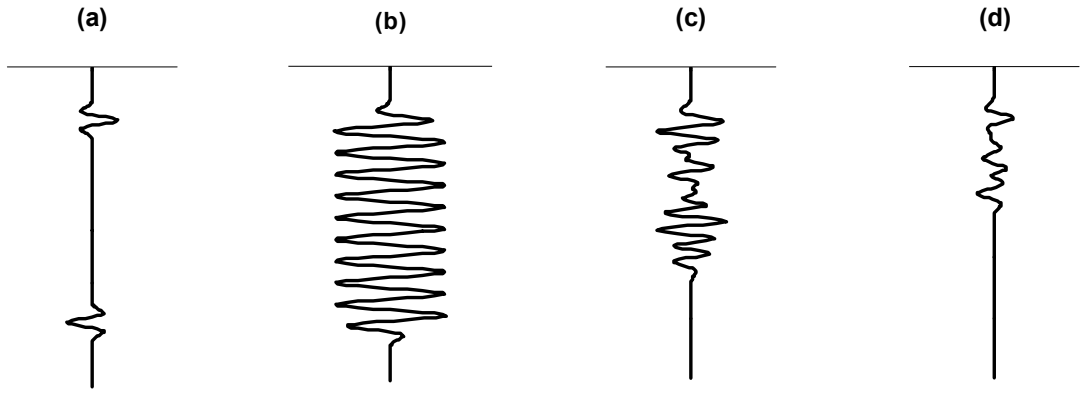

Figure 14. Modelled seismic response for (a) Single layer 4.75 λ thick. (b) 19 layers each of thickness λ/4 with the same absolute reflection coefficient as in (a) alternating in sign. (c) 19 layers as in (b) but with random thickness between λ/16 and λ/4. (d) 19 layers as in (b) but with random thickness between λ/40 and λ/10. Wavelength λ modelled as 120 m.

The interpreted shear zones in the Yamarna Tectonic Zone in Figure 15 show a typical strong amplitude response, which is spatially variable. If the amplitude response is due to constructive interference of reflections from many layers, then lateral change in layer thickness could explain the variability from trace to trace (see Figure 14(b) and (c)).

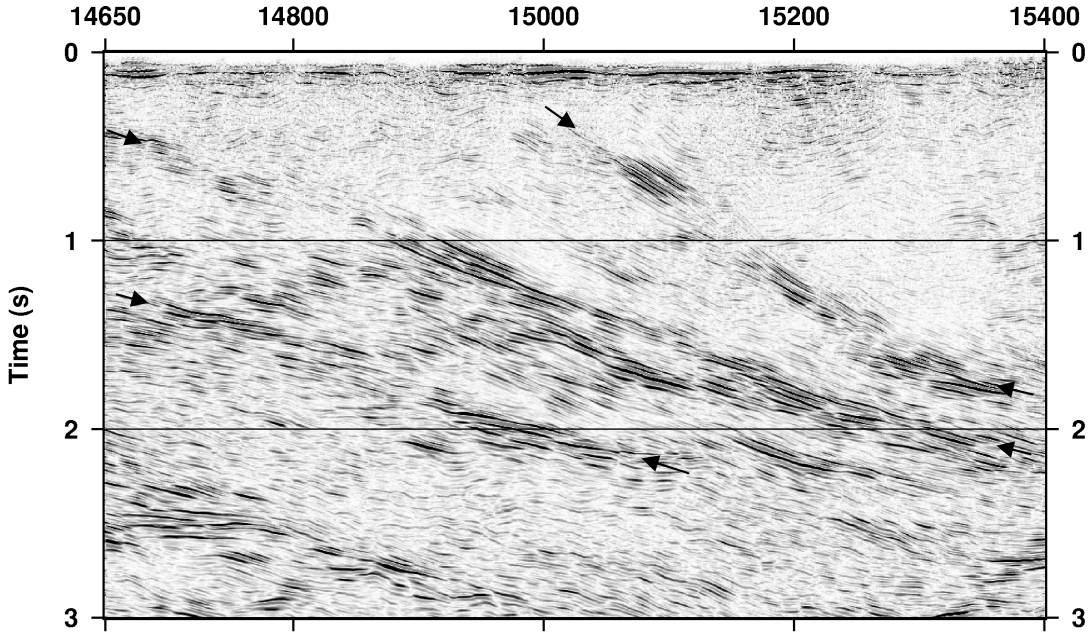

Figure 15. Migrated seismic section for line 01AGS-NY1 from CDP 14650 to 15400 and 0 to 3 s TWT at V/H = 1, showing shear zones within the Yamarna Tectonic Zone (arrows). 100 CDP = 2 km. 1 s = 3 km.

Thrust duplexes

Imbricate thrust stacks occur within the greenstone successions and within the middle crust along most of line 01AGS-NY1. The seismic images indicate the overall geometry of the

stacks as shown in Figure 10 (b). Details of internal geometry are also shown in Figure 11, where the importance of correct migration was demonstrated.

Granites

Since granites are generally homogeneous, they should therefore appear as unreflective zones in the seismic section. Metamorphosed granites should have a similar seismic response, as metamorphism will not alter the density distribution, although it might emplace a structural grain. Shearing within granite could change the density distribution along a shear zone, and thus lead to a reflection from the boundary between sheared and un-sheared granite. In Figure 16, it is difficult to pick the exact bottom of the granite, but its presence above 1 s is indicated by the bland character of the seismic response.

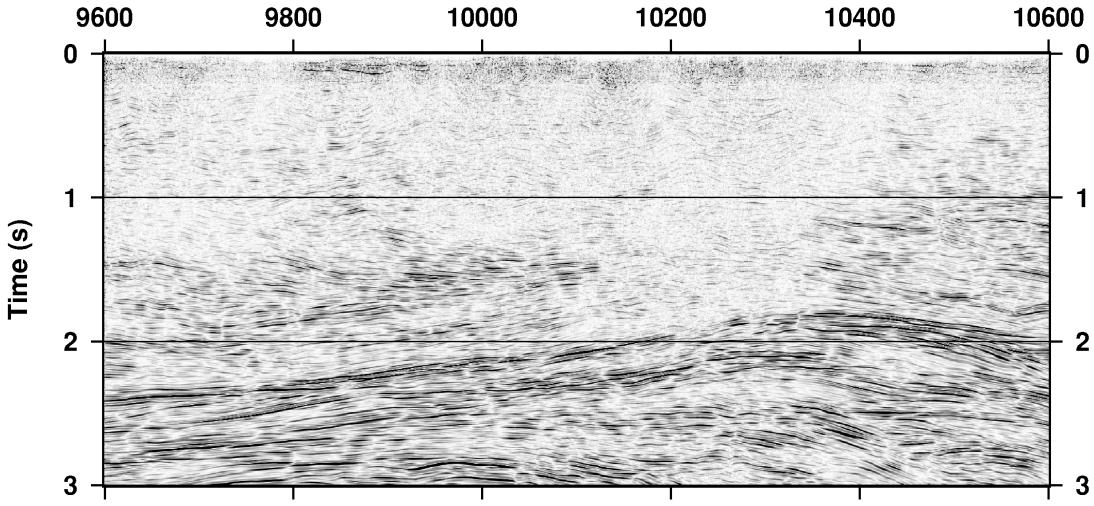

Figure 16. Migrated seismic section for line 01AGS-NY1 from CDP 9600 to 10600 and 0 to 3 s TWT. V/H = 1. 100 CDP = 2 km. 1 s = 3 km. Homogeneous granite is in the upper 1 s.

Summary

The seismic reflection method was originally designed for use in sedimentary basins where the sub-horizontal and continuous layers correspond to primary bedding. Reflections are generated by acoustic impedance contrasts at the boundaries between layers. In hard rock areas, too, reflections are indisputably produced at boundaries between rocks with different densities (and hence velocities). These boundaries may follow bedding, or be thrust surfaces and shear zones.

Some of the key differences between hard rock terranes and soft rock are steep dips associated with folds and faults, and high velocities. High velocities affect resolution, since both vertical and horizontal resolution depend on the seismic wavelength. Compared with sedimentary basins, vertical resolution is probably only half as good, with the situation being slightly more favourable for horizontal resolution. The high velocities make it easier to stack reflections since there is less move-out, but more difficult to use the stacking velocity analysis to determine accurate velocities for depth conversion.

Steep dips can affect the ability to image successfully. The seismic line must be long enough to encompass steeply-dipping reflectors and the seismic acquisition system. Recording times must also be long enough for energy to travel to and from steeply dipping reflectors. Migration is essential in areas of complicated structure in order to move dipping reflectors to their correct positions and to collapse diffractions emanating from discontinuities in the layers. Unless migration is carried out, dips on the seismic section will never appear greater than 45°.

Examples from the 2001 Northeastern Yilgarn seismic survey show that a variety of geological features can be imaged, including primary bedding, unconformities, faults, thrusts, shear zones and granites. Shallow to moderate dips are routinely imaged, with more steeply dipping faults inferred from discontinuities. The migrated sections provide a spectacular set of images that underpin interpretations of the geological structure of the northeastern Yilgarn.

Acknowledgements

This paper is published with the permission of the Chief Executive Officer, Geoscience Australia and the Chief Executive Officer, Predictive Mineral Discovery Cooperative Research Centre.

SEISMIC PROCESSING – 2001 NORTHEASTERN YILGARN SEISMIC REFLECTION SURVEY (L154)

L.E.A. Jones[1,2], B.R. Goleby[1,2] and T.J. Barton[2]

[1] Predictive Mineral Discovery Cooperative Research Centre, Geoscience Australia, GPO Box 378, Canberra ACT 2601, Australia
[2] Australian National Seismic Imaging Resource, Geoscience Australia, GPO Box 378, Canberra ACT 2601, Australia

Introduction

The 2001 Northeastern Yilgarn Seismic Survey (L154) was conducted in August/September 2001 and included the regional traverse consisting of lines 01AGS-NY1 and 01AGS-NY3, jointly sponsored by Geoscience Australia and the Geological Survey of Western Australia, in conjunction with the Predictive Mineral Discovery Cooperative Research Centre (*pmd**CRC). The Australian National Seismic Imaging Resource (ANSIR) was responsible for seismic data acquisition, as well as for field QC and preliminary in-field processing.

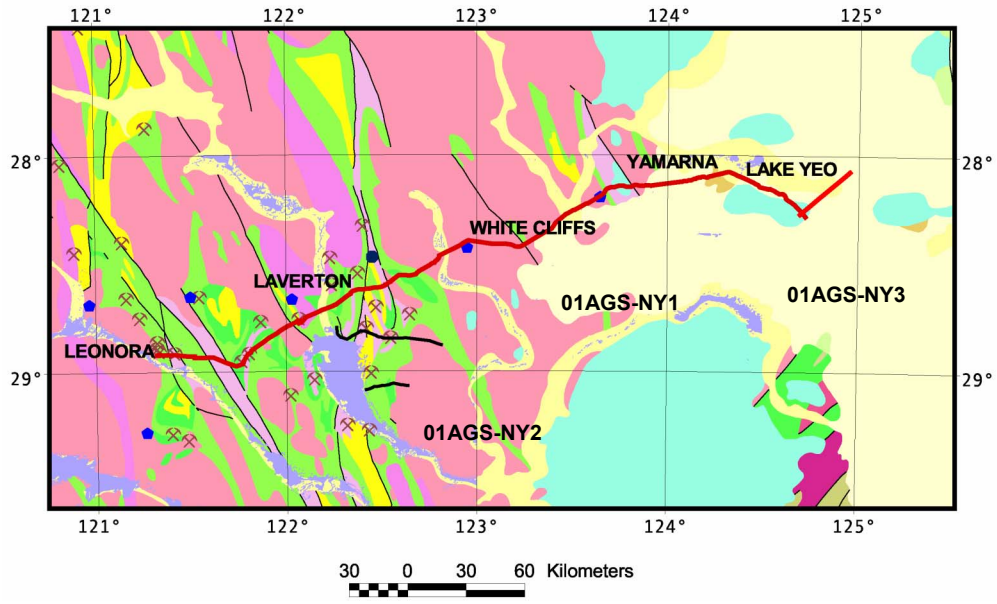

Figure 1. Map of the northeastern Yilgarn Craton showing the locations of the deep seismic reflection lines acquired in 2001. Background is 1:5m geology of the region. Key faults are shown as thin black lines. Major mines are shown as crossed picks.

Two other lines, 01AGS-NY2 and 01AGS-NY4, were acquired in the Laverton Tectonic Zone under the auspices of Geoscience Australia and the Minerals and Energy Research Institute of Western Australia (MERIWA), involving Anglogold, Placer Dome and the University of Western Australia. This paper is concerned only with lines 01AGS-NY1 and 01AGS-NY3. The 384 km line 01AGS-NY1 extended from the vicinity of Leonora eastwards

into the Officer Basin, whereas the much shorter line 01AGS-NY3 lay entirely within the Officer Basin, as shown in Figure 1.

Acquisition

Most of the deep seismic reflection data was acquired along the edge of shire roads, but line clearing was needed for line 01AGS-NY3. Station coordinates were surveyed using differential GPS by Dynamic Satellite Surveys (2001). A split-spread geometry was used with the source nominally at the centre of the spread. Receiver groups were centred between station pegs, while the source array was centred on the peg. Three IVI Hemi-60 (60,000 lb) vibrators were used in-line, with moveup between each of three varisweeps.

A summary of acquisition parameters is given in Table 1. Further details are provided by Barbour (2001). The main differences between the long regional line (01AGS-NY1) and the Officer Basin line (01AGS-NY3) are the group interval, VP interval and source move-up, and the sweep frequency ranges, which were designed to give higher resolution in the Officer Basin sediments.

Table 1: Summary of acquisition parameters for lines 01AGS-NY1 and 01AGS-NY3

LINE	01AGS-NY1	01AGS-NY3
AREA	Leonora to Lake Yeo (WA)	East of Lake Yeo (WA)
DIRECTION	W to E	SW to NE
LENGTH	384 km	52.62 km
STATIONS	992 - 10592	1040 - 2794
CDP RANGE	1984 - 20862	2080 - 5509
GROUP INTERVAL	40 m	30 m
GROUP PATTERN	12 in-line @ 3.33 m	12 in-line @ 2.5 m
# VIBRATION POINTS	4780	1226
VP INTERVAL	80 m	30 m and 60 m
SOURCE TYPE	3 x IVI Hemi-60	3 x IVI Hemi-60
SWEEP TYPE	3 x 12 s: 7-56, 12-80, and 8-72 Hz	3 x 8 s: 8-72, 12-100, and 6-80 Hz
SOURCE PAD-PAD	15 m	15 m
SOURCE MOVE-UP	15 m	10 m
# CHANNELS	240	240
FOLD (NOMINAL)	60	120 and 60
RECORD LENGTH	16/18 s @ 2 ms	16 s @ 2 ms

Processing

Production processing utilised the Disco software package, while the interactive version Focus was used for parameter tests, first break picking and QC. Brute stacks were produced in the field as part of the QC process, using dummy (straight line) geometry and generic stacking velocity functions with very little additional processing.

Table 2 shows the final processing flow, including migration, for the 18 s data for line 01AGS-NY1. Data resampled to 4 ms provided adequate resolution. Essentially the same flow was used for final processing of the 16 s data for line 01AGS-NY3. The first pass for 01AGS-NY3 employed different processing streams for shallow and deep data but was subsequently revised after processing the eastern end of line 01AGS-NY1.

The processing flow was designed with the aim of enhancing reflections and preserving amplitudes, while avoiding processes that could potentially degrade data, particularly in the

shallow section. Comprehensive parameter testing was done on shot records, CDP gathers or stack panels for the processing steps that were used. The key processing steps are discussed in the following sections, with particular emphasis on those that resulted in the most improvement in data quality.

Table 2: Final processing flow for 18 s data for line 01AGS-NY1

[1]	line geometry and crooked line definition (fixed CDP interval)
[2]	field segy to 'disco' data format; resample to 4 ms
[3]	quality control displays and trace edits
[4]	spectral equalization (with removable 1000 ms gate AGC)
[5]	common mid point sort
[6]	gain recovery (spherical divergence option)
[7]	trace amplitude balance across user defined gates
[8]	surgical air wave mute
[9]	bulk shift +100 ms
[10]	application of refraction statics, datum 350 m (AHD)
[11]	application of automatic residual statics
[12]	bandpass filter
[13]	velocity analysis using velex, 1st pass after refraction statics, 2nd pass after automatic residual statics
[14]	normal moveout correction (15% stretch mute)
[15]	common mid-point stack (alpha trimmed mean)
[16]	trace amplitude balance
[17]	finite difference migration with dip corrected velocities
[18]	bandpass filter
[19]	signal enhancement (digistack 0.85)
[20]	linear gain and trace amplitude scaling

Crooked line definition and CMP/CDP sort

Prior to actual seismic data processing, the geometry for each line was defined (i.e., station coordinates and station locations for shots and receivers). Since the receiver groups were centred between the surveyed stations, the receiver station coordinates for processing were defined to be half-way between surveyed stations (i.e. station 1000 for processing is located at 1000.5 as surveyed).

CDP (common-depth-point) locations were also defined. For a horizontal reflector, the midpoint between a source and receiver pair lies vertically above the depth point (or reflecting point) for that pair, so that the CDP location is the same as the common midpoint (CMP) location. For dipping reflectors, this correspondence no longer holds, but the CDP terminology is so entrenched in seismic processing that it is used in place of the more correct term “common midpoint”. Note that the midpoint spacing along a straight line is half the receiver group interval.

Crooked line processing was used for both 01AGS-NY1 and 01AGS-NY3, and was essential for the former due to bends in the existing roads. In the crooked line case, the midpoints do not always lie along the line defined by the surveyed stations. The CDP line is defined as a smoother representation that follows the highest density of midpoints, while keeping as close as possible to the original line (Figure 2). Note that the CDP bins extend perpendicular to the CDP line as shown in Figure 2. For both lines, the CDP line was defined with a constant CDP interval (20 m for 01AGS-NY1 and 15 m for 01AGS-NY3). Since the CDP line is shorter than the line of stations, the CDP number will be less than twice the station number.

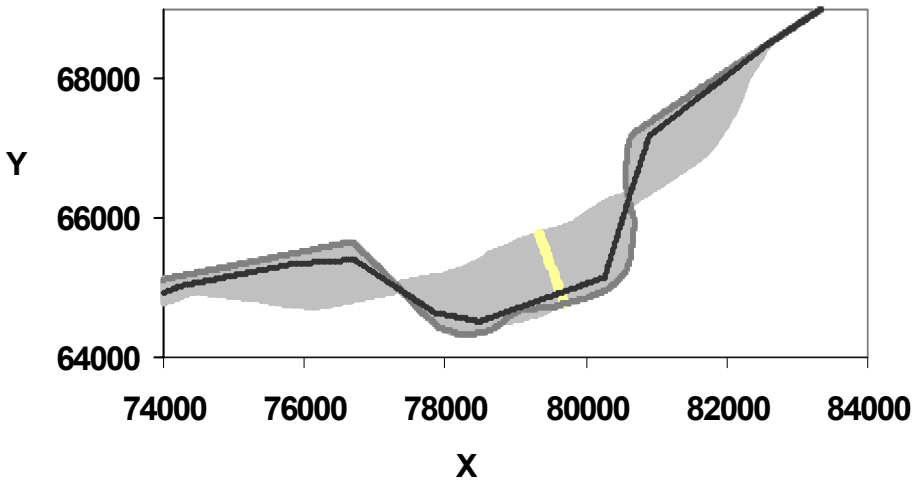

Figure 2. Crooked line geometry, with X and Y coordinates in m. Surveyed station line is shown in grey and CDP line in black. Shaded area shows midpoints. Light coloured strip perpendicular to the CDP line is a diagrammatic representation of a CDP bin, showing location of midpoints assigned to a particular CDP (actual strips 20 m wide).

For 01AGS-NY3, which was relatively straight, the CDP line was calculated automatically as a least-squares fit to the midpoints, with an inclusion radius equal to the length of the spread (7200 m). Typically the CDP line lay within 150 m (or closer) of the surveyed line. The CDP line for the more crooked 01AGS-NY1 was defined manually as a series of linear segments, in order to keep closer to the surveyed line than would be achieved by a least squares fit. In this case, the CDP line generally lay within 250 m of the surveyed line. The initial choice of CDP line was refined after assessing the distribution of midpoints into CDP bins and examining the quality of the brute stack.

During processing, a common midpoint (or CDP) sort gathered the data into ensembles of traces (CDP gathers) with midpoints in the same CDP bin. No restriction was placed on the perpendicular extent of the CDP bin, in order to keep the fold (traces per gather) as high as possible. Since the traces in a CDP gather would later be stacked to produce a seismic section, it is the CDP line, rather than the line of stations, that should be used for reference in geological interpretation.

Edits

Documentation of manual trace edits began during field QC. Problems included shot records contaminated by coincidental mine blasts, channels intentionally left open for roads, receivers accidentally disconnected and occasional equipment malfunctions. Problem traces were omitted during processing. The two closest traces to each vibration point were also excluded because of source generated noise.

Random noise trains also occurred, mainly due to vehicle movement along the line. An automatic edit was designed to zero such traces, based on anomalously high amplitudes prior to the first arrival of seismic energy. This was used successfully to eliminate noisy traces from the automatic first break picking routine. However, a judgement was made not to use automatic editing of vehicle noise in the final processing flow because the noise trains are not vertical and at later times good data would be removed instead of noise. Other processes such as alpha-trimmed mean stack would be more effective.

Refraction statics and datums

Statics corrections are needed to remove variability in seismic travel times due to surface topography and variations in regolith thickness and velocity. The travel times of refracted waves, recorded as the first arrivals in seismic reflection data, are analysed to obtain a model of the main refracting interface, that is, the boundary between near-surface low velocity and deeper high velocity material, usually the regolith/bedrock boundary. The first breaks (first arrivals) were picked on 2 s subsets of the original 2 ms shot records, using a combination of manual and supervised automatic picking. Apart from amplitude balance and automatic edits, no pre-processing was done. The first strong peak on the seismic trace was interpreted as the first arrival, since the cross-correlation of the recorded trace and the vibrator reference sweep should be zero phase.

The method of Taner et al. (1998) was used to separate the spatial variation of the refraction statics into a long wavelength component due to gradual change in surface and refractor topography and a short wavelength component attributed to more rapid near surface variations in seismic velocity. The smoothing radius chosen to separate the statics was 160 m for 01AGS-NY1 and 120 m for 01AGS-NY3 (4 times the receiver group interval), based on parameter tests. A two-refractor model was chosen for line 01AGS-NY3, in view of the smaller group interval of 30 m. For 01AGS-NY1, the larger group interval of 40 m and the much thinner regolith towards the west resulted in too few picks to robustly define an additional near surface layer. For both lines, the main refractor (second for 01AGS-NY3) was interpreted as base of regolith, although in the poor data area on 01AGS-NY3 it is probable that the refractor corresponds to an intermediate interface, due to high attenuation of first arrivals at larger offsets.

Refraction statics were calculated by subtracting the vertical travel time calculated for the lower velocity regolith, and adding the vertical travel time calculated from datum to bedrock at a higher replacement velocity. For both lines 01AGS-NY1 and 01AGS-NY3, a datum of 350 m (Australian Height Datum) was used. For 01AGS-NY3, the replacement velocity was 4000 m/s. Since 01AGS-NY1 crossed the boundary between Archaean craton (bedrock velocity ~6000 m/s) and Proterozoic/Palaeozoic basins (bedrock velocity ~4500 m/s), a variable replacement velocity was required: 5500 m/s for stations 992 to 9500, and 4500 m/s for stations 10200 to 10592, with linear interpolation between stations 9500 and 10200.

The results of the refraction statics analysis are presented in Figure 3 for part of the eastern end of line 01AGS-NY1. Receiver statics only are shown in Figure 3a, as the shot statics are virtually identical due to the surface consistent approach. The long wavelength static is the major component with the short wavelength static limited to +/- 5 ms in general. Figure 3b illustrates the refractor model, showing both surface and refraction elevation. Note that refractor topography contributes more to the refraction statics than does surface elevation in this region and that the regolith is more than 200 m thick. Figure 3c shows the value of refractor (bedrock) velocity, which was used to choose replacement velocity and can also provide an indication of lithology. There is a marked decrease in seismic velocity from 6000 m/s to just under 4500 m/s over a distance of 28 km, indicating the edge of subcrop of the Yilgarn Craton.

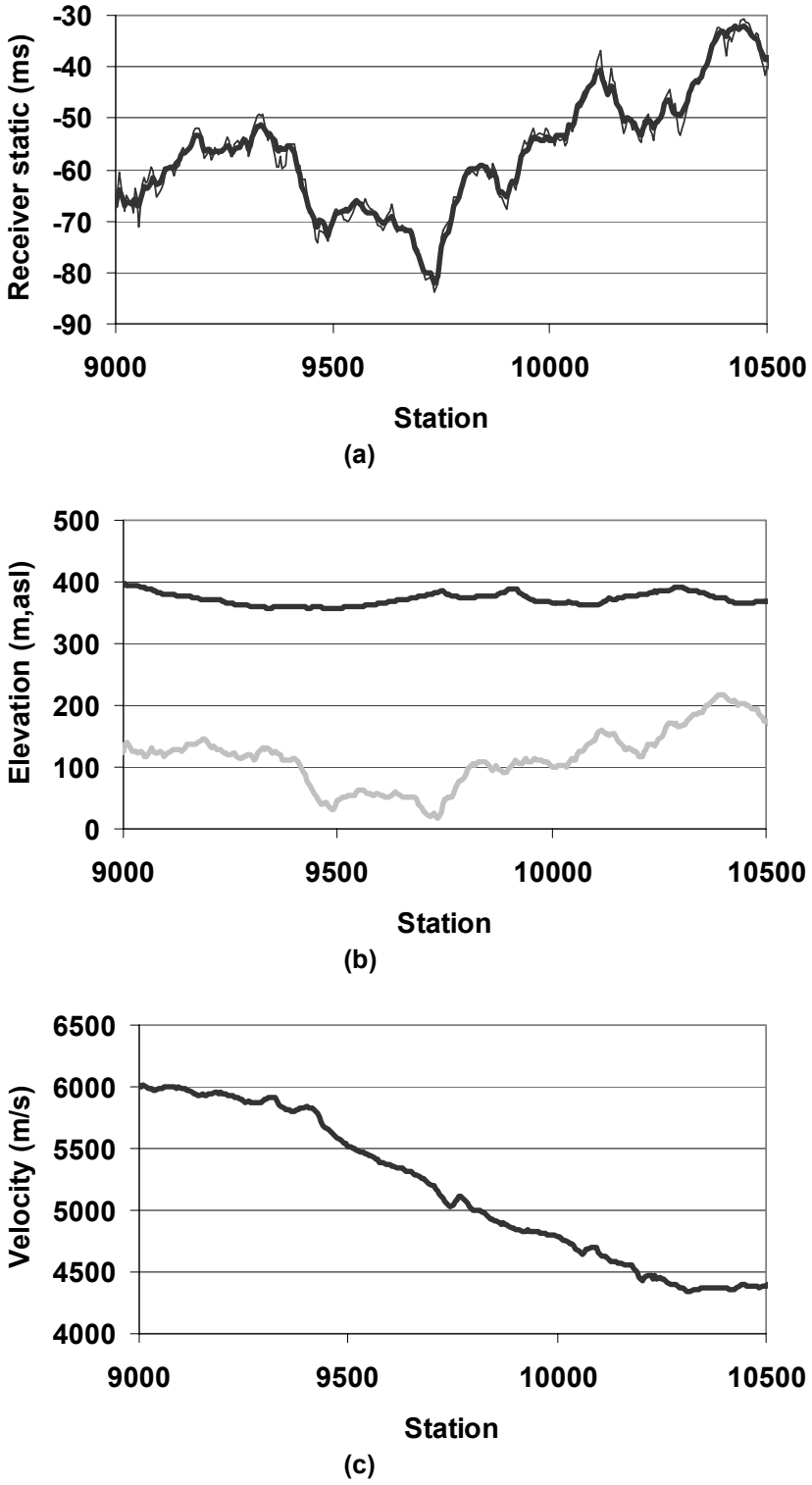

Figure 3. Refraction statics results for line 01AGS-NY1 from station 9000 to 10500 (east to west). (a) Receiver refraction statics with long wavelength as thick black line and total (long plus short wavelength) as fine black line. (b) Elevation in m of surface (black) and refractor (grey). Datum is at 350 m. (c) Refractor (P-wave) velocity in m/s.

Note that a bulk shift of +100 ms was applied prior to application of statics. This was done to prevent loss of shallow information and to keep the processing approximately surface referenced (average two way static is of the order 100 ms). Thus 100 ms on the processed seismic data corresponds to the 350 m datum.

The effect of refraction statics corrections is shown in Figure 4 for stack data in the vicinity of the Yamarna Tectonic Zone. For comparison purposes, all other processing steps and parameters are identical, except for application of refraction statics. Statics corrections result in much better definition of reflectors, particularly in the shallow section.

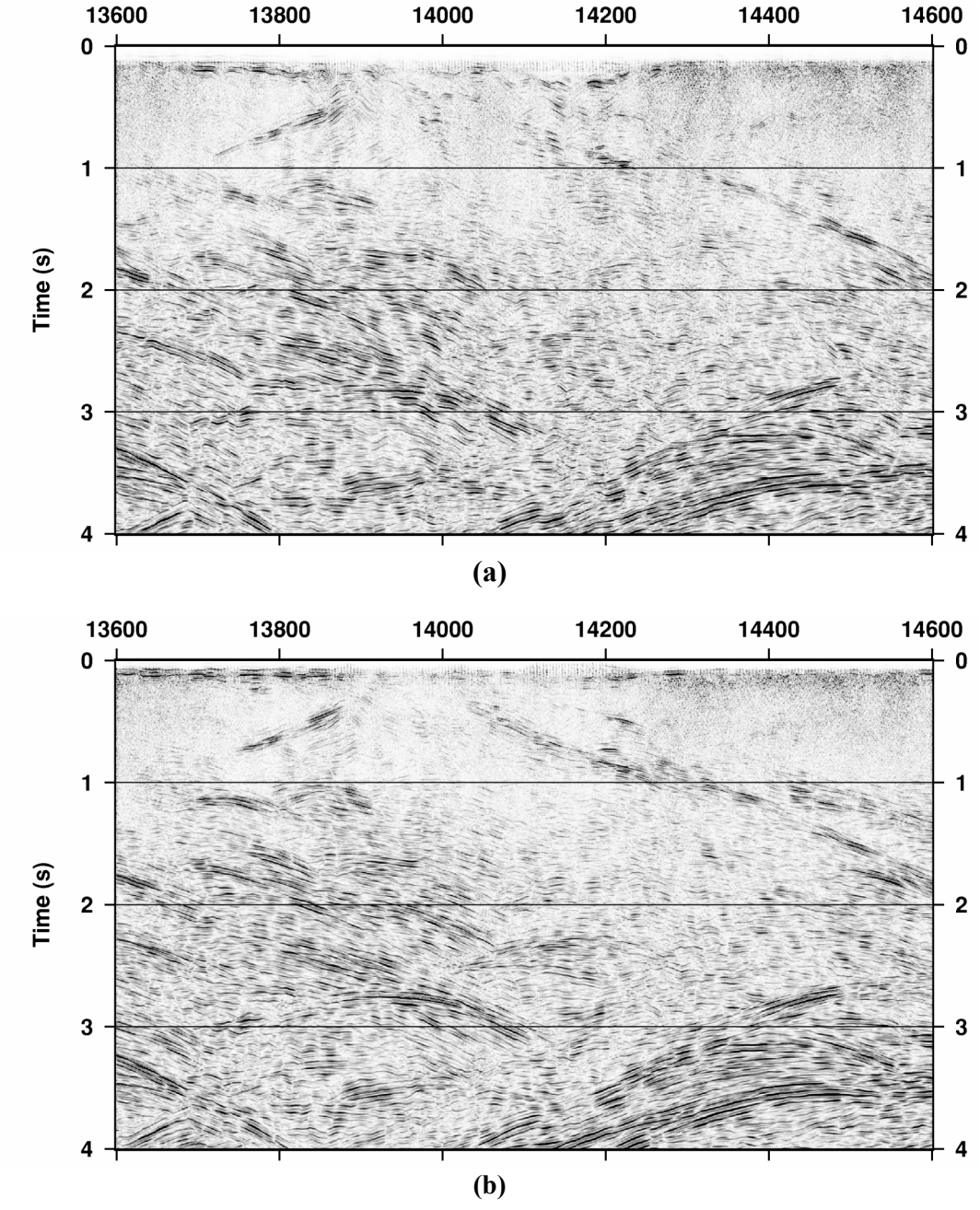

Figure 4. Stack for line 01AGS-NY1 from CDP 13600 to 14600 and 0 to 4 s TWT at V/H=1.
(a) No statics applied. (b) Refraction statics only applied.

Spectral equalisation and filtering

Spectral equalisation is a key processing step which minimises contamination by low-frequency source-generated noise, such as ground roll and direct waves, plus random noise such as traffic noise. This step is particularly important at shallow depths where the fold is lower and where source generated noise interferes with reflections. Spectral equalisation employs a zero-phase deconvolution operator to perform spectrum balancing or whitening across the range of signal bandwidth, as shown in Figure 5. The AGC (automatic gain control), included in the spectral balancing algorithm, was removed in order to preserve amplitudes for later processing steps, particularly migration.

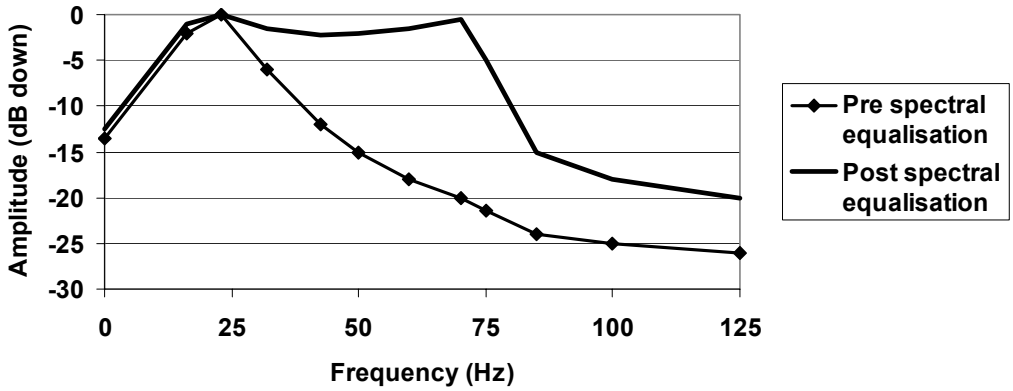

Figure 5. Frequency spectrum for shot 4539 on line 01AGS-NY1 from 0 to 2 s, before and after spectral equalisation.

The spectrum balancing is carried out using a number of user designed frequency gates, with an option to shape the output spectrum. The final spectral equalisation design consisted of overlapping frequency gates beginning with (8-12-16-20) Hz (outer values are 50% and inner values 100% amplitude). Five additional gates of the same form were used with the gates overlapping at the 50% amplitude values. These parameters were suitable for both the deep data and the shallow section, in combination with a temporally varying frequency filter.

The record for shot 4539 on line 01AGS-NY1 (Figure 6a) is a typical example of a raw shot record in the vicinity of Lake Yeo (Figure 1), where the regolith is thicker. Linear dipping bands of coherent low-frequency source-generated noise dominate the record, although there is a hint of a reflection hyperbola between 0.5 and 1 s TWT (two-way time). The corresponding spectrum (Figure 5) is dominated by energy in the range 20-25 Hz. Application of spectral equalisation to enhance high frequencies relative to lower frequencies (Figure 5) results in the appearance of several reflection hyperbolas above 1 s, even above 0.5 s (Figure 6b). An offset hyperbola, indicative of a dipping reflector, is now very obvious, with the apex just above 1.5 s.

The same reflections can be seen around CDP 19900 on the stacked sections in Figure 7, which demonstrate the effectiveness of spectral equalisation in the processing sequence. All other processing is identical. Spectral equalisation has suppressed the low frequency noise (particularly between 1 and 2 s TWT) and resulted in much better vertical resolution and continuity of shallow reflections. Spectral equalisation applied to shot data early in the processing sequence also improves the estimation of automatic statics and stacking velocity, which depend on stack quality for evaluation.

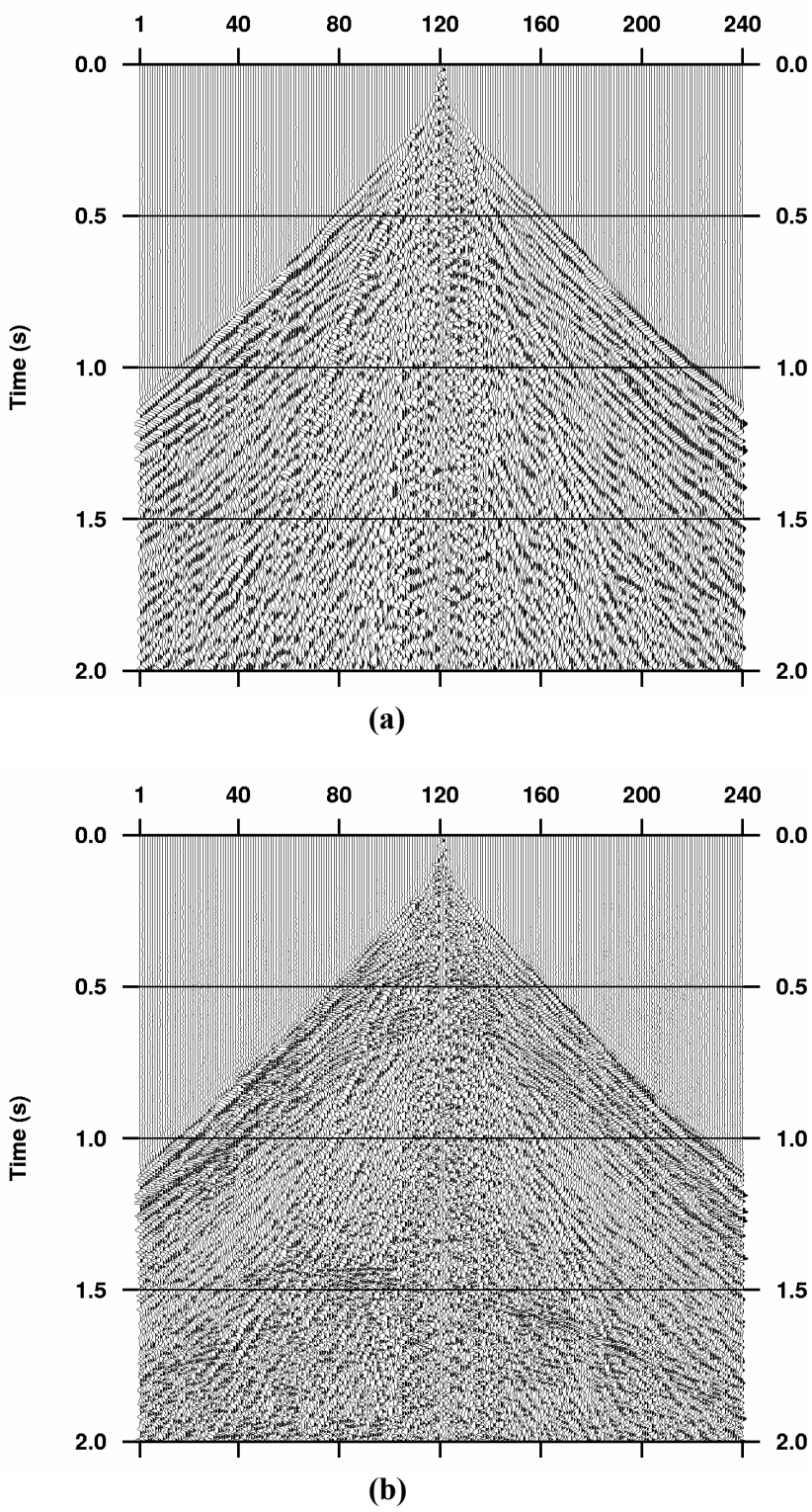

Figure 6. Record for shot 4539 at station 10106 on line 01AGS-NY1 displayed from 0 to 2 s. An AGC has been applied for display purposes. (a) Raw shot with no spectral equalisation. (b) Processed shot after application of spectral equalisation. Reflection hyperbolas are now visible around 0.5 s and 1.5 s.

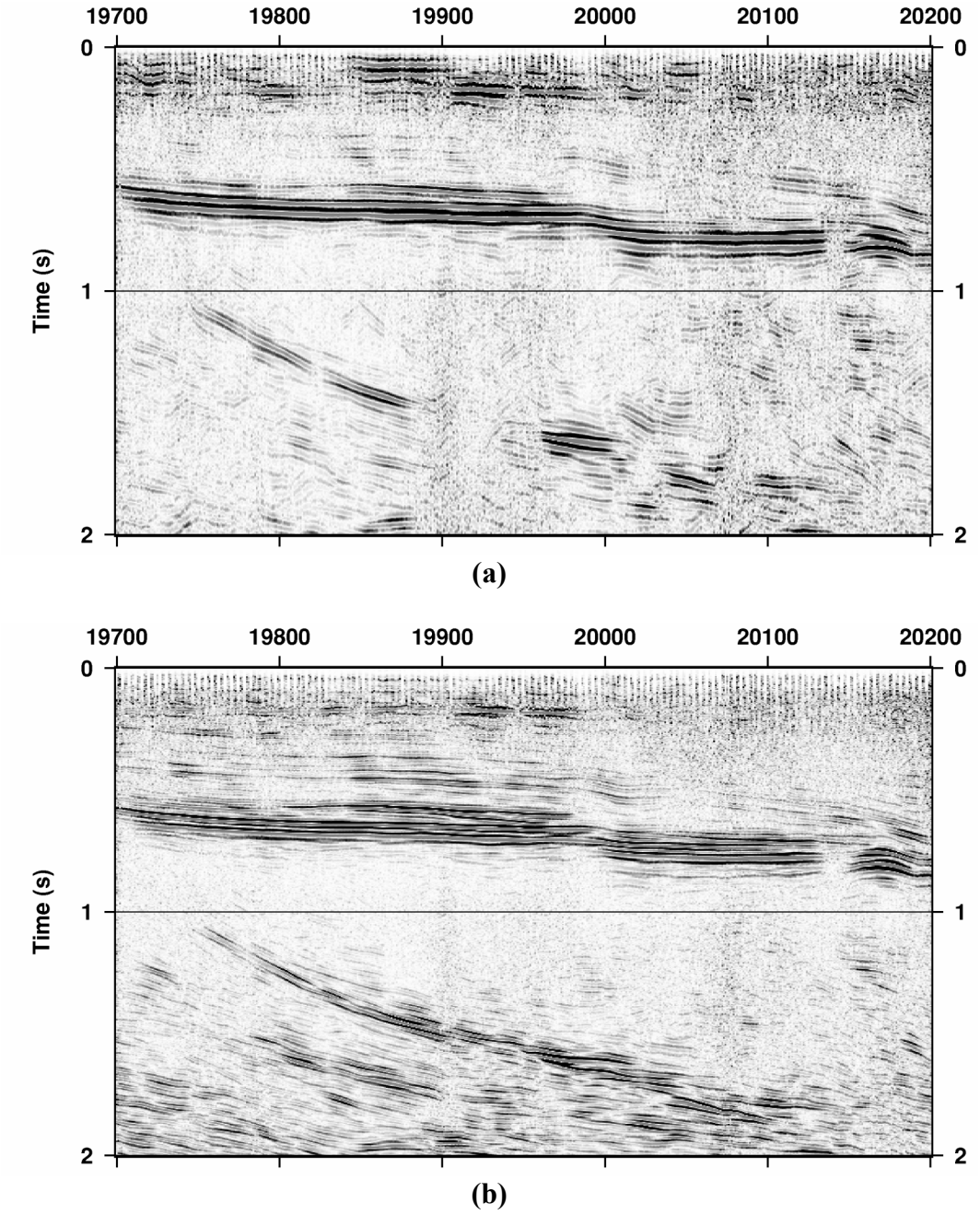

Figure 7. Stack for line 01AGS-NY1 from CDP 19700 to 20200 and 0 to 2 s TWT at V/H=1. (a) Without spectral equalisation in processing sequence. (b) With spectral equalisation in processing sequence. Shot 4539 (Figure 6) is located near CDP 19900.

For the western half of line 01AGS-NY1, spectral equalisation did not effect such dramatic improvement in the quality of the data. This is probably because bedrock was closer to the surface and source generated noise was not a major problem on the shot records. However, vertical resolution of reflectors was improved by the higher frequencies resulting from spectral equalisation.

Bandpass filters were also used to suppress high and low frequency noise. Prior to final display, a bandpass filter with a more limited frequency pass range at later TWT was applied

to improve appearance of deeper reflections which would have lost any true high frequency due to attenuation in the earth.

Gain recovery and amplitude balance

Corrections were made for amplitude loss with increasing time due to spherical divergence and intrinsic attenuation. All traces were multiplied by a time varying scalar of the form C*VelocityV*TimeT, with C=1, V=2 and T=1. Velocity refers to the velocity function used in the calculation. The stacking velocity function (see below) was used, or in the case of line 01AGS-NY1, a smoothed version of it.

Instead of using an AGC, amplitude balancing was performed across a number of user defined gates, with the aim of preserving true amplitudes. The lower gates extended from 2.5-4 s, 4-6 s, 7-9 s, 11-12 s, 13-15 s and (15-17 s). The uppermost gate was tailored according to the offset of the traces, in order to exclude times prior to the first arrival of seismic energy.

Stacking velocity analysis

Another critical processing step is the correction of seismic data for the offset dependence of travel time, the normal moveout (NMO) correction, which depends (inversely) on seismic velocity and two-way travel time. With the appropriate choice of velocity for NMO correction, a reflection event will add constructively when the traces of a common-midpoint gather are stacked. In the shallow section (less than 1 to 2 s TWT), the quality of the stack is quite sensitive to changes in the stacking velocity, but becomes progressively less so for the deeper data.

Stacking velocity analysis was carried out using a velocity estimation and plotting module that applied a series of normal moveout corrections to designated CDP gathers according to user specified velocity functions. Velocity picks for reflections were made on the basis of maxima in coherency, flattening across the CDP gather and the quality of narrow stack panels. An effort was made to stack both horizontal and dipping reflectors where possible. Several passes were made, including initial estimates of velocity, plus more detailed analysis after application of refraction statics and again after application of automatic residual statics. The final stacking velocity functions are listed in Appendix A for both lines.

As expected, the stacking velocity functions were quite different for the hard rock areas of the Yilgarn Craton compared with the Palaeozoic/Proterozoic Basins (Figure 8). Generally the velocity picks were consistent above 2 s, with deviations explained by the need to stack dipping reflectors. Stacking velocity decreases towards the east, demonstrating the effect of increasing sedimentary cover. The implications for depth conversion are that using 6 km/s for the Yilgarn Craton is a good approximation, but in the sedimentary basins, a more rigorous analysis using Dix interval velocities would be required.

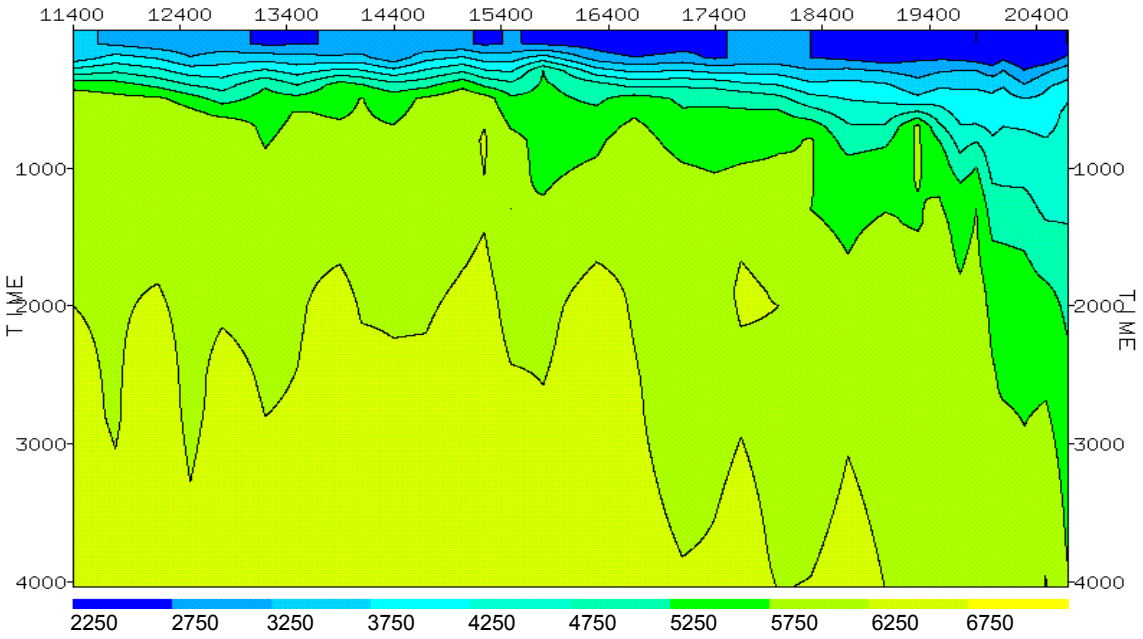

Figure 8. Stacking velocities for the eastern half of line 01AGS-NY1 from CDP 11400 to 20700. Display is from 0 to 4 s TWT. Contours are every 500 m/s from 2250 to 6750 m/s.

Common mid-point stack and stretch mute

Prior to stack, a 15% stretch mute was applied to zero those parts of traces distorted beyond 15% by NMO correction. This mute was used instead of a specific front end mute, as it satisfactorily removed most of the first arrival energy train. The mute is velocity dependent and is more severe for lower stacking velocities. Since the stretch mute used the final stacking velocity functions, it was more severe at the eastern end of the survey, which was appropriate, as the first arrivals and noise trains extended to later times because of the lower velocity in the sedimentary basins.

Stacking seismic traces after NMO correction improves the signal to random noise ratio by $\sqrt{n}$, where n is the fold. An improved technique for suppressing large bursts of non-Gaussian noise, such as vehicle noise, is a type of median stack. The alpha trimmed mean stack examines trace amplitudes at each sample time, and omits a designated percentage of the highest and lowest amplitudes from the stack, in this case 15% at each end.

This stacking option was also useful in suppressing noise generated at the end of the sweep below 8 or 12 s. For the shallow section, with lower fold, a minimum of 6 traces was retained in the stack. The stacked trace amplitude was normalised by dividing by the number of (live) traces in the stack at each sample time.

Automatic residual statics

Automatic residual statics were calculated in order to fine-tune the stack. This process operates on unstacked CDP gathers with normal moveout and refraction statics applied and calculates the additional time shifts (residual statics) necessary to maximise correlation across the gather in a selected time gate, such that shot and receiver surface consistency is

maintained. An iterative technique is used to apply the static before the next calculation, with the number of iterations specified by the user.

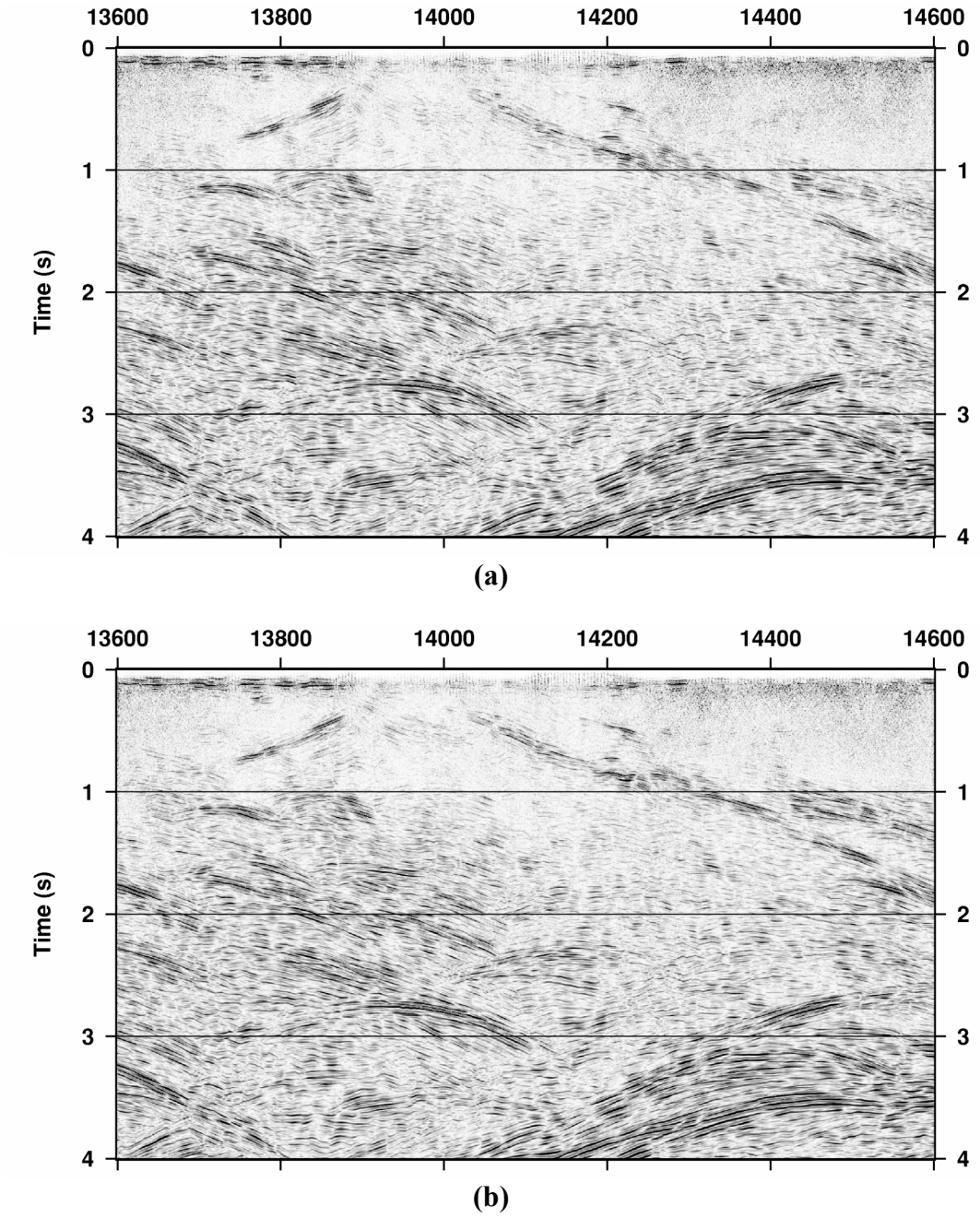

Figure 9. Stack for line 01AGS-NY1 from CDP 13600 to 14600 and 0 to 4 s TWT at V/H=1. (a) Refraction statics only. (b) Both refraction and automatic residual statics.

For line 01AGS-NY3, two gates were used. One gate bracketed the top of Yilgarn reflector, which gradually deepened from 1.25 s to 1.9 s TWT along the length of the line. The corresponding gate width varied from 400 to 800 ms. A second deep gate, 2 s wide and centred on 5 s TWT, was chosen from CDP 4400 to the end of the line. This was done to better constrain the calculation in the poor data area using visible deeper reflectors. A maximum time shift of 10 ms was allowed, being half the period of a 50 Hz wavelet. Automatic residual statics generally lay within +/- 3 ms, with much better consistency in the good data areas.

A single gate was used for the entire length of line 01AGS-NY1. It was chosen from 1.75 s to 4.5 s TWT because of good reflector strength and continuity and because at later TWT the calculation is not as sensitive to NMO correction.. Again the maximum time shift was restricted to 10 ms. Automatic residual statics generally lay within +/- 5 ms.

Technically, a single broad gate with reflectors of different dip should not work, as structure should be flattened before the residual statics calculation. However, within the chosen gate, the overall structural grain on average is horizontal, and the approach is vindicated by the results in the shallow section above the user defined gate. The effect of automatic statics on the stack is shown in Figure 9, again in the vicinity of the Yamarna Tectonic Zone. There is a definite improvement in reflector continuity and amplitude compared with using refraction statics only, particularly around 1 s TWT from CDP 14200 to 14600.

Migration

On an unmigrated final stack section with V/H=1, the apparent dip of dipping reflectors will never exceed 45°. Migration is the process of moving the recorded reflections into their true spatial locations. Thus dipping reflectors will be steepened, shortened and moved up dip. Diffractions from discontinuities, such as reflector terminations at faults, are collapsed in the process (see Jones et al., this volume, for a fuller discussion of migration).

A finite difference migration algorithm was used that allowed a spatially varying velocity function. Dip-corrected stacking velocities were used as the migration velocities. At selected locations on line 01AGS-NY1, DMO (dip moveout) processing was carried out to remove the dip dependence of stacking velocity prior to further velocity analysis. This resulted in a more smoothly varying velocity function along the line. For line 01AGS-NY3, migration was carried out using 90% of the stacking velocity. A layer thickness of 40 ms TWT was used for migration and the maximum dip specified exceeded dips observed along the line.

Prior to migration, a linear gain function was applied (with negative gains) to progressively decrease trace amplitudes towards the edge of the section for the first and last 50 traces. After migration, the linear gain function was re-applied (with positive gains) to boost amplitudes back almost to the original values. This was done in order to suppress migration artefacts at the edge of the sections.

Migrated sections (hard copy and digital) were the end product of the processing stream. The successful application of migration is attributed to the continuity of reflectors and preservation of amplitudes resulting from earlier stages of processing.

Coherency enhancement

A signal enhancement algorithm (digistack) was applied for final display only to the stacked or migrated data. Digistack enhances events that are coherent across several traces, thus making reflections stand out better against background noise.

This process determines the coherency of linear events for all dips within a specified range and outputs a second set of seismic traces that is essentially a coherency section. A weighted sum is then made of the coherency section and the actual seismic section, such that a weight of zero reproduces the input seismic data and a weight of one gives the coherency section. For

final display, weights of 0.8 or 0.85 were used. For the stack data, dips up to 50° were enhanced, while for the migrated data the range was extended to 70°.

Display parameters and archive

The main differences between the 4 s and 16 or 18 s stack and migrated data lie in the display parameters. The 4 s data is displayed as variable area wiggle trace and the 16/18 s as variable area. In addition, trace amplitude scaling was applied using an AGC where the scale factor was calculated with 50% contribution from amplitude in the gate and 50% from the whole trace amplitude. The gate length was 500 ms for the 4 s data and 1000 ms for the 16/18 s data. A linear gain was also applied on the final displays to boost amplitudes in the shallow section on the 16 and 18 s data.

The digital versions of the data archived in SEG-Y format have had coherency enhancement and trace amplitude scaling applied. For both the 4 s and 16/18 s stack and migrated data in SEG-Y format, substantial information has been entered in the trace headers, while the EBCDIC reel header contains a complete summary of acquisition and processing parameters. Sample EBCDIC headers are given in Appendix B.

Conclusion

Processing of the regional seismic reflection data for the 2001 Northeastern Yilgarn Seismic Survey has resulted in seismic sections that facilitate interpretation of regional geological structure from the near surface to the Moho. Good results were achieved by a combination of processing steps, in particular spectral equalisation, statics corrections and detailed stacking velocity analysis. Further processing in selected areas to enhance particular features of interest may be of benefit at some future date.

Acknowledgements

Ed Chudyk is thanked for his contribution in picking first arrivals and stacking velocities for the western half of line 01AGS-NY1 and part of line 01AGS-NY3. This paper is published with the permission of the Chief Executive Officer, Geoscience Australia and the Chief Executive Officer, Predictive Mineral Discovery Cooperative Research Centre.

References

Barbour, S., 2001. Final Operations Report, North Yilgarn Seismic Survey, Western Australia.

Dynamic Satellite Surveys, 2001. Report 01-66, Final Operations Report on the AGSO 2001 Yilgarn 2D Seismic Survey for Trace Energy Services Pty, Ltd, July-August 2001.

Jones, L. E. A., Goleby, B. R. and Drummond, B. J., this volume, Capabilities and limitations of the seismic reflection method in hard rock terranes.

Taner, M. T., Wagner, D.E., Baysal, E. and Lee, L., 1998. A unified method for 2-D and 3-D refraction statics. Geophysics, 63, 260-274.

APPENDIX A – STACKING VELOCITY FUNCTIONS

Stacking velocity functions are listed as time-velocity pairs for CDP locations where velocity analysis was performed. Time is given in ms and velocity in m s-1. Note that refraction and automatic residual statics and the bulk shift of +100 ms were applied prior to final velocity determination.

01AGS-NY1

2263		**2413**		**2563**		**2963**	
100	3000	150	2917	150	2917	150	3154
200	3350	450	4150	750	5477	475	5000
300	3900	750	5900	950	5762	650	5100
450	4572	900	6195	1150	5859	1150	6250
1150	6250	1150	6250	3000	6700	2950	6700
3000	6700	3000	6700	16000	7350	16000	7350
16000	7350	16000	7350				

3113		**3213**		**3363**		**3493**	
100	3066	150	3520	200	4287	150	3818
300	5000	400	5600	500	5550	500	5500
400	5363	1000	5650	1500	6100	1000	5615
550	5750	1250	5729	2275	6430	2200	6567
950	5900	2275	6430	2900	6600	2900	6800
1450	6100	2900	6700	16000	7350	16000	7350
2950	6700	16000	7350				
16000	7350						

3538		**3563**		**3663**		**3713**	
200	3645	150	3461	150	3453	100	3066
475	5500	500	5600	450	5409	150	4030
800	5965	900	6074	1000	6070	400	5400
1050	6376	1100	6100	1300	6254	1450	6066
1900	6600	1800	6500	1900	6500	1900	6500
2900	6700	2900	6700	2900	6650	2900	6600
16000	7350	16000	7350	16000	7350	16000	7350

3763		**3863**		**4513**		**4539**	
150	3464	150	3464	150	3717	150	3717
300	4600	300	4600	300	4500	300	4500
500	5600	500	5212	800	5735	550	5824
900	6000	1000	5965	1050	6161	1050	6250
1200	6250	1200	6250	1200	6250	1200	6250
1700	6450	1700	6450	1700	6450	1700	6450
2500	6500	2500	6500	2500	6650	2500	6650
16000	7350	16000	7350	16000	7350	16000	7350

4914		**4976**		**5763**		**6413**	
100	3219	100	3219	100	3219	150	3891
350	5146	400	4800	400	4800	400	5300
500	5550	500	5650	550	5628	1000	6000
800	6000	750	6150	800	5968	1500	6400
1200	6450	1200	6450	950	6129	16000	7350
1700	6550	1700	6550	1100	6396		
2500	6650	2500	6650	1700	6550		
16000	7350	16000	7350	2500	6650		

				16000	7350		

6550		**7013**		**7388**		**8353**	
150	3891	100	3250	150	3935	100	2975
400	5600	200	4000	500	6000	400	5500
1000	6200	550	5800	1000	6400	600	5969
1500	6400	750	6150	2400	6600	1000	6379
16000	7350	1200	6250	16000	7350	1700	6550
		1700	6450			3100	6700
		2500	6650			16000	7350
		16000	7350				

8388		**8663**		**8938**		**9113**	
150	3370	150	3529	100	4000	200	3500
400	5600	400	5350	400	5121	400	5350
1500	6600	500	6051	600	5900	900	6100
3100	6750	800	6145	1050	6050	1400	6400
16000	7350	1050	6292	1550	6100	1700	6550
		1950	6332	1950	6332	3100	6700
		3100	6700	3100	6700	16000	7350
		16000	7350	16000	7350		

9213		**9313**		**9413**		**9513**	
100	3219	100	3219	100	3219	100	3300
450	5345	450	5345	450	5345	300	4751
900	6050	900	6450	900	6450	750	5800
1700	6550	1700	6550	1700	6550	1200	6250
3100	6700	3100	6750	3100	6750	1850	6275
16000	7350	16000	7350	16000	7350	2500	6300
						3100	6750
						16000	7350

10413		**10513**		**10613**		**10713**	
100	3400	100	3400	150	3400	150	3779
300	4751	300	4751	400	4914	300	5044
750	5765	750	5765	700	6086	700	5765
1200	6150	1200	6150	1250	6250	1500	6050
1850	6194	1850	6194	2050	6275	1850	6100
2500	6225	2500	6225	2500	6300	2500	6225
3100	6750	3100	6750	3100	6750	3100	6750
16000	7350	16000	7350	16000	7350	16000	7350

11400		**11800**		**12200**		**12500**	
0	3400	0	3150	0	2950	0	2900
200	3400	100	3150	100	2950	150	2900
450	6100	450	5850	550	6200	550	5850
1000	6000	700	6100	1450	6150	1200	6200
2000	6250	1050	5900	1850	6250	1800	6100
3300	6500	1750	6200	2600	6550	2700	6100
6500	7000	2800	6200	6500	7000	3850	6400
16000	7000	3500	6350	18000	7000	6500	7000
		6500	7000			18000	7000
		18000	7000				

12800		**13200**		**13500**		**13900**	
0	2950	0	2650	0	2700	0	2800
100	2950	100	2650	100	2700	150	2800
700	6100	400	5200	550	5750	400	5500

1150	6200	550	5550	900	5950	1000	6100
1700	6050	1250	6000	1450	6150	1400	6100
2500	6400	1950	6100	2950	6300	2000	6400
6500	7000	2800	6250	6500	7000	2750	6450
18000	7000	6500	7000	18000	7000	6500	7000
		18000	7000			18000	7000

14100		**14400**		**14700**		**15050**	
0	2900	0	2900	0	2800	0	2850
150	2900	200	2900	100	2800	100	2850
450	5750	450	5450	500	5850	450	6100
1600	6100	850	5950	1050	6200	1400	6100
2300	6300	1150	6100	1700	6000	1750	6250
6500	7000	1950	6200	2200	6250	2100	6500
18000	7000	6500	7000	6500	7000	6500	7000
		18000	7000	18000	7000	18000	7000

15250		**15500**		**15800**		**16300**	
0	2650	0	2800	0	2650	0	2500
100	2650	100	2800	100	2650	150	2500
500	6000	450	5250	300	5250	400	4950
750	6300	800	5900	900	5650	750	5650
1350	6200	1300	5750	1350	5800	1350	6000
1950	6450	2650	6350	2050	6150	1950	6450
6500	7000	6500	7000	6500	7000	2650	6450
18000	7000	18000	7000	18000	7000	6500	7000
						18000	7000

16650		**17100**		**17400**		**17650**	
0	2300	0	2500	0	2650	0	2850
150	2300	150	2500	200	2650	200	2850
500	5500	450	5100	450	5100	500	5150
750	5950	950	5750	700	5450	850	5650
1950	6200	1200	5950	1150	5850	1450	6150
3600	6450	1950	5850	2000	6000	1900	6350
6500	7000	2500	6000	2600	6100	2400	6150
18000	7000	2850	5950	3550	6250	3500	6350
		4300	6400	6500	6750	6500	6750
		6500	6750	18000	6750	18000	6750
		18000	6750				

18000		**18300**		**18650**		**19000**	
0	2900	0	2750	0	2600	0	2400
200	2900	200	2750	200	2600	200	2400
550	5250	750	5800	350	3800	350	3650
900	5750	1300	5750	700	4800	850	5300
1450	6000	1800	6000	1050	5550	1100	5600
2000	6250	2950	6050	2050	5900	1550	5900
2700	6100	6500	6750	2750	6200	2350	5850
3850	6200	18000	6750	6500	6750	3100	6150
6500	6750			18000	6750	6500	6500
18000	6750					18000	6500

19300		**19500**		**19700**		**19850**	
0	2650	0	2350	0	2300	0	2250
200	2650	150	2350	150	2300	175	2250
500	3850	275	3100	350	3600	275	3150
700	5850	400	3650	600	4050	400	3700

1400	5700	850	5450	1150	5350	650	4100
1750	6000	1450	5950	1550	5650	900	5100
2700	6000	2100	5850	2200	5950	1300	5750
3450	6100	2800	5950	2700	6000	2150	6000
6500	6500	6500	6500	6500	6500	3200	6000
18000	6500	18000	6500	18000	6500	6500	6500
						18000	6500

20000		**20100**		**20300**		**20500**	
0	2350	0	2300	0	2300	0	2300
200	2350	150	2300	200	2300	200	2300
400	3650	350	3600	550	4000	350	3600
700	4150	600	4150	900	4500	600	4000
1250	4950	800	4350	1150	4750	1000	4550
1850	5600	1800	5550	1650	5300	1250	4600
2550	5800	2600	5700	2400	5550	1950	5400
3650	6000	3100	6000	2850	5750	2600	5700
6500	6500	6500	6500	6500	6500	3450	6200
18000	6500	18000	6500	18000	6500	6500	6500
						18000	6500

20700	
0	2250
150	2250
250	3400
550	4350
1000	4450
1950	5150
2600	5400
6500	6500
18000	6500

01AGS-NY3

2200		**2400**		**2600**		**2800**	
0	2150	0	2150	0	2100	0	1950
150	2150	150	2150	175	2100	150	1950
375	3400	400	3500	300	3000	475	3650
550	3950	500	3850	650	3900	650	4050
1200	4450	850	4400	1300	4600	1000	4500
1500	4550	1200	4650	2000	5150	1300	4750
2150	5200	1800	5100	6000	6500	2500	5500
6000	6500	2250	5250			6000	6500
		6000	6500				

3000		**3400**		**3600**		**3800**	
0	1900	0	2000	0	2000	0	2100
150	1900	150	2000	150	2000	200	2100
300	3050	500	3850	700	4550	650	4350
600	4150	700	4500	850	4600	1050	4400
1300	4750	850	4700	1350	5000	1250	4550
2200	5100	1250	4800	2000	5350	1550	4900
6000	6500	1650	5150	6000	6500	6000	6500
		6000	6500				

4000		**4080**		**4200**		**4400**	
0	2600	0	2100	0	2000	0	2000
250	2600	200	2100	200	2000	200	2000
400	3800	400	3600	300	2850	500	3950
650	4300	750	4300	650	4400	650	4100
850	4700	1150	4500	1450	5050	1600	4700
1150	4800	1550	4850	1800	5100	1950	4900
1500	5000	6000	6500	6000	6500	6000	6500
6000	6500						

4600		**5250**	
0	2200	0	2000
300	2600	200	2000
750	4050	350	3100
1100	4450	1450	4700
1650	5050	1950	4950
6000	6100	6000	6100

APPENDIX B – EBCDIC REEL HEADER FOR SEG-Y PROCESSED DATA

Table B1: Listing of EBCDIC reel header for 18 s migrated data for 01AGS-NY1

```
C1  ACQUIRED BY ANSIR FOR GEOSCIENCE AUSTRALIA, GSWA and pmd*CRC
C2  SURVEY NAME : NORTHERN YILGARN 2001 SURVEY NO.        : L154
C3  LINE NO.    : 01AGS-NY1                  SEGY FILE PRODUCED : JUNE 2002
          C3  LINE NO        : 01AGS-NY1              SEGY TAPE PRODUCED : JUNE 2002
C4  1ST SHOT NO.: 3 WEST                     LAST SHOT NO.      : 4782 EAST
C5         RECORDING PARAMETERS
C6  SYSTEM       : ARAM24                    DATE RECORDED      : AUG 2001
C7  NO. CHANNELS  : 240                                VP INTERVAL       : 80 METRES
C8  SOURCE TYPE   : 3 IVI HEMI-60 VIBE   VIBE CONFIG: 15M PAD-PAD 15M MOVEUP
C9  SWEEP TYPE             : 3 X 12 S VARISWEEPS 7-56 Hz, 12-80 Hz, 8-72 Hz
C10 RECORDING FILTERS : LOW-CUT 3 HZ, HIGH-CUT 205 HZ, NOTCH OUT
C11 GROUP PATTERN : 12 IN-LINE @ 3.33M  GROUP INTERVAL     : 40 METRES
C12 CMP SPACING   : 20 METRES                          COVERAGE (NOMINAL) : 60-FOLD
C13 SPREAD PATTERN : -4780....-20*20....4780 M  (1....120*121....240) (W->E)
C14 SAMPLE RATE   : 2 MS                     RECORD LENGTH      : 16 and 18 S
C15 DATA RECORDING FORMAT - SEGY ON 3490E and EXABYTE
C16   STATION RANGE : 992 - 10592 (W->E)CDP RANGE : 1984 - 20862
C17   ORIGINAL FIELD TAPE NOS: L15401003-L15401027 and L15401036-L15401068
C18
C19   PROCESSING SEQUENCE : Migration (18 s, 4 ms)
C20 [1] crooked line geometry definition [2] segy to 'disco' format, resamp 4 ms
C21 [3] qc displays and trace edits      [4] spectral equalisation (AGC removed)
C22 [5] cmp sort (wide bin fixed CDP int)[6] spherical divergence correction
C23 [7] trace amplitude balance              [8] surgical air wave mute
C24 [9] bulk shift + 100 ms            [10] refraction statics (refsol)
C25[11] autostatics                          [12] bandpass filter
C26[13] velocity analysis (velex), 1st pass after [10], 2nd pass after [11]
C27[14] NMO (15% stretch mute)               [15] cmp stack (alpha trimmed mean)
C28[16] trace amplitude balance              [17] finite difference migration
C29[18] bandpass filter                  [19] coherency enhancement (digistack)
C30[20] trace amplitude scaling designed for display of whole section
C31
C32  HEADER ENTRIES AS PER SEGY STANDARD. REFER TO AGSO RECORD 1991/98 FOR
C33  DESCRIPTIONS OF EXTRA HEADER ENTRIES. RFR-XXX ENTRIES REFER TO REFRACTOR
C34  ELEVATION, VELOCITY, DELAY AND TOTAL RECEIVER STATIC KEYED TO CDP POSITION.
C35  (2 BYTES INT) CDP-STAT 183,SHT-STAT 185, REC-STAT 187,SHOT 189,SHRSTAT 207,
          C35  RCRSTAT 209,CDPELEV 211,DMXSHT 213,SHIFT 215,
C36  RCRSTAT 209,CDPELEV 211,RFR-ELEV 217,RFR-VEL 219,RFR-DLY 221,RFR-TST 223,
C37  SHIFT 215. (4 BYTES IBMFP) CDP-X 191,CDP-Y 195,AIRMAG 199,GRAVITY 203.
C38  NOTE: X and Y ARE RELATIVE COORDINATES.
C39
C40  COPYRIGHT RESERVED COMMONWEALTH OF AUSTRALIA 2002
```

Table B2: Listing of EBCDIC reel header for 16 s migrated data for 01AGS-NY3

```
C1  ACQUIRED BY ANSIR FOR GEOSCIENCE AUSTRALIA, GSWA and pmd*CRC
C2  SURVEY NAME : NORTHERN YILGARN 2001 SURVEY NO.        : L154
C3  LINE NO.    : 01AGS-NY3                SEGY FILE PRODUCED : JUNE 2002
          C3  LINE NO        : 01AGS-NY3              SEGY TAPE PRODUCED : JUNE 2002
C4  1ST SHOT NO.: 1 SOUTHWEST                         LAST SHOT NO.      : 1226 NORTHEAST
C5        RECORDING PARAMETERS
C6  SYSTEM       : ARAM24                 DATE RECORDED     : AUG-SEP 2001
C7  NO. CHANNELS  : 240                               VP INTERVAL       : 30 and 60 METRES
C8  SOURCE TYPE   : 3 IVI HEMI-60 VIBE   VIBE CONFIG: 15M PAD-PAD 10M MOVEUP
C9  SWEEP TYPE            : 3 X 8 S VARISWEEPS  8-72 Hz, 12-100 Hz, 6-80 Hz
C10 RECORDING FILTERS : LOW-CUT 3 HZ, HIGH-CUT 205 HZ, NOTCH OUT
C11 GROUP PATTERN : 12 IN-LINE @ 2.5M   GROUP INTERVAL    : 30 METRES
C12 CMP SPACING   : 15 METRES                         COVERAGE (NOMINAL) : 60 and 100-
FOLD
C13 SPREAD PATTERN : -3585....-15*15....3585 M  (1....120*121....240) (SW->NE)
C14 SAMPLE RATE   : 2 MS                  RECORD LENGTH     : 16 S
C15 DATA RECORDING FORMAT - SEGY ON 3490E and EXABYTE
C16   STATION RANGE : 1040 - 2794 (SW->NE) CDP RANGE : 2080 - 5509
C17   ORIGINAL FIELD TAPE NOS: L15401069-L15401082
C18
C19   PROCESSING SEQUENCE : Migration (16 s, 4 ms)
C20 [1] crooked line geometry definition [2] segy to 'disco' format, resamp 4 ms
C21 [3] qc displays and trace edits      [4] spectral equalisation (AGC removed)
C22 [5] cmp sort (wide bin fixed CDP int)[6] spherical divergence correction
C23 [7] trace amplitude balance              [8] surgical air wave mute
C24 [9] bulk shift + 100 ms           [10] refraction statics (refsol)
C25[11] autostatics                          [12] bandpass filter
C26[13] velocity analysis (velex), 1st pass after [10], 2nd pass after [11]
C27[14] NMO (15% stretch mute)               [15] cmp stack (alpha trimmed mean)
C28[16] trace amplitude balance              [17] finite difference migration
C29[18] bandpass filter                 [19] coherency enhancement (digistack)
C30[20] trace amplitude scaling designed for display of whole section
C31
C32  HEADER ENTRIES AS PER SEGY STANDARD. REFER TO AGSO RECORD 1991/98 FOR
C33  DESCRIPTIONS OF EXTRA HEADER ENTRIES. RFR-XXX ENTRIES REFER TO
REFRACTOR
C34  ELEVATION, VELOCITY, DELAY AND TOTAL RECEIVER STATIC KEYED TO CDP
POSITION.
C35  (2 BYTES INT) CDP-STAT 183,SHT-STAT 185, REC-STAT 187,SHOT 189,SHRSTAT 207,
          C35  RCRSTAT 209,CDPELEV 211,DMXSHT 213,SHIFT 215,
C36  RCRSTAT 209,CDPELEV 211,RFR-ELEV 217,RFR-VEL 219,RFR-DLY 221,RFR-TST 223,
C37  SHIFT 215. (4 BYTES IBMFP) CDP-X 191,CDP-Y 195,AIRMAG 199,GRAVITY 203.
C38  NOTE: X and Y ARE RELATIVE COORDINATES.
C39
C40  COPYRIGHT RESERVED COMMONWEALTH OF AUSTRALIA 2002
```


APPLICATION OF POTENTIAL FIELD DATA IN THE OFFICER BASIN AREA

S. I. Shevchenko
Geological Survey of Western Australia,
100 Plain St, East Perth, W. A. 6004

Introduction

The Geological Survey of Western Australia (GSWA) Morton Craig semi-detailed gravity survey was carried out in the southwestern part of the Officer Basin (Figure 1). The new gravity data and existing magnetic data were integrated to assist with the structural interpretation of the area around seismic line 03AGSNY03. Previously acquired airborne magnetic and reconnaissance 11 × 11 km gravity data (Figure 2) were also used for a regional structural interpretation.

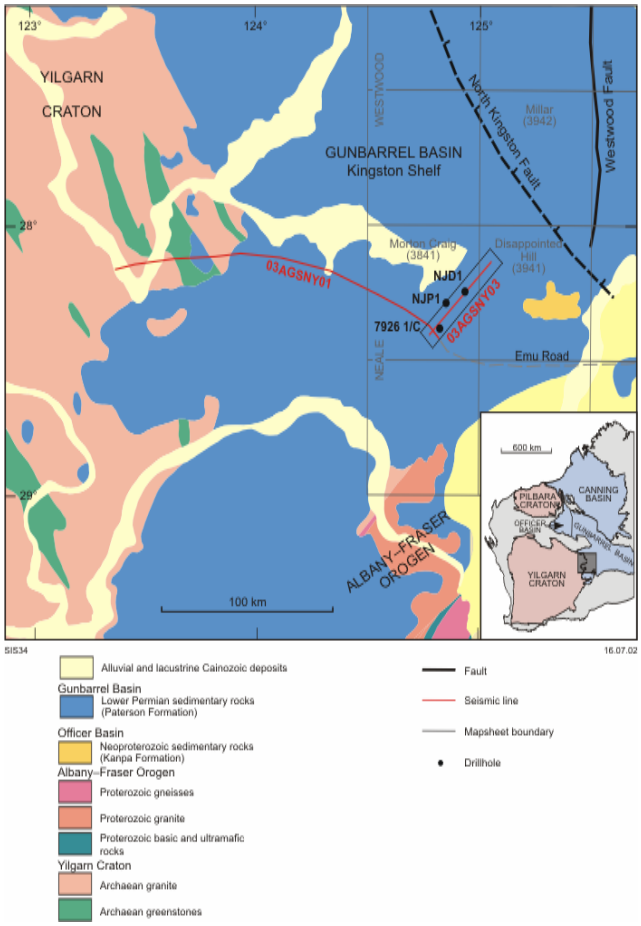

Figure 1. Simplified geology of the eastern Yilgarn Craton region. The Morton Craig gravity survey is outlined in black.

The regional gravity data and the geology of the eastern Yilgarn Craton margin region are also discussed. The details of acquisition and processing of the new gravity data is described in Shevchenko (2002).

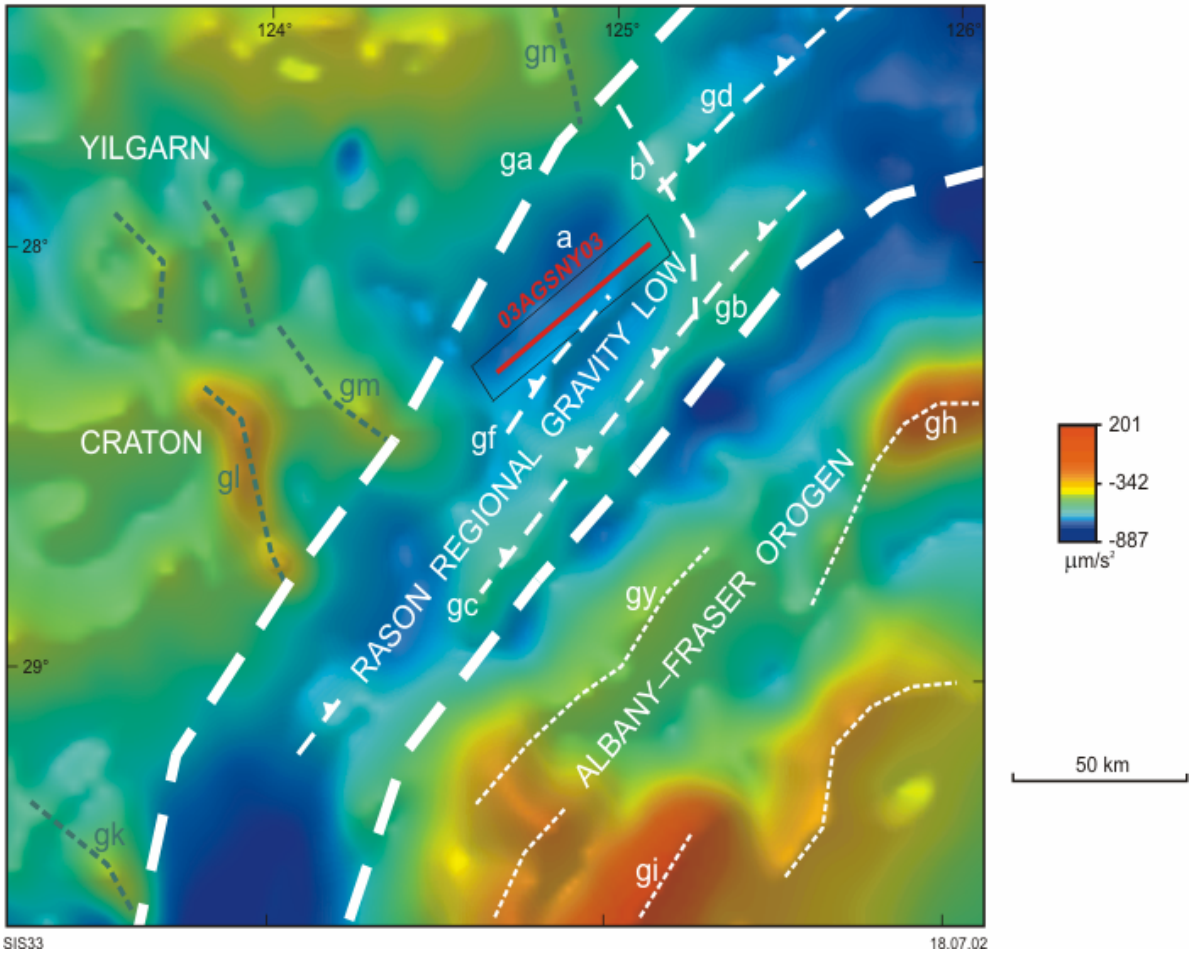

Figure 2. Regional Bouguer gravity of the eastern Yilgarn Craton region, showing the intermediate geophysical province between the Yilgarn Craton (*ga*) and the Albany–Fraser Orogen (*gb*). The Morton Craig gravity survey is outlined in black. Interpreted high-density granulite rocks of the Fraser Complex labelled *gh*, *gi* and *gy*. Anomalies related to greenstones shown labelled *gk* to *gn*. a = regional gravity low; b = interpreted as major regional structure boundary. *gc* to *gf* interpreted as thrust faults. The Bouguer gravity image was created using the Geoscience Australia national gravity database.

Geological Setting

The Morton Craig gravity survey covers parts of the Kingston Shelf of the Gunbarrel Basin (Hocking, 1994; Perincek, 1996), which overlies the Westwood Shelf of the Officer Basin (Iasky, 1990, Hocking, 1994; Perincek, 1996). The northeastern edge of the Kingston Shelf is the western edge of the Officer Basin, and is in part a faulted contact along the North Kingston Fault (Perincek, 1996; Figure 1). The area is poorly explored, with limited outcrop, and geological investigations are limited to the early mapping of the Neale (van de Graaff and Bunting, 1975) and Westwood (Kennewell, 1977) 1:250 000-scale map sheets. The area is mostly covered by Quaternary eolian sands, colluvium, and minor alluvium, with clay, silt, and sand deposits marginal to salt lakes (van de Graaff and Bunting, 1975).

Scattered poor exposures of Lower Permian sedimentary rocks (Paterson Formation) in the southern part of the area consist mainly of claystone, sandstone, and poorly sorted conglomerate. The Paterson Formation is flat lying and considered to be a glacially influenced deposit lying unconformably on generally flat lying Neoproterozoic to ?Cambrian siliciclastic and calcareous sedimentary rocks. These rocks are regarded as equivalents of the Kanpa Formation (formerly 'Babbagoola Beds'; Grey, K., 2002, written comm.) and were intersected in Western Mining Corporation's (WMC's) diamond hole NJD 1, which was drilled to 517 m (Figure 1) as part of a base metals exploration program (Western Mining Corporation Limited, 1981). Outcrops mapped as Neale Beds in the central part of the Neale 1:250 000 sheet are also now included in the Kanpa Formation (Grey, K., 2002, written comm.).

The NJD 1 drillhole contains Cainozoic, and possibly some Permian or Cretaceous, rocks overlying a Neoproterozoic succession above a Mesoproterozoic succession. The Neoproterozoic succession in NJD 1 contains almost all of the Officer Basin succession, from the Kanpa Formation down to the Townsend Quartzite (Hocking, R. M., et al., 2002, in press.). Two nearby drillholes, NJP 1 drilled by WMC and 7926 1/C (Figure 1) drilled by Seltrust Mining Corporation Ltd, reached granitic basement at 57 and 76 m respectively. However, the 'basement' may have been large glacial erratics.

Gravity data

Previous gravity surveys

As part of their regional gravity surveys across parts of Western Australia, the Bureau of Mineral Resources (now Geoscience Australia) covered the eastern Yilgarn Craton area with an 11 × 11 km reconnaissance survey in 1969–70 (Fraser and Pettifer, 1980). Due to the relatively poor accuracy, these data and the regional 11 × 11 km gravity data were not incorporated with the new data for detailed interpretation, and were only used to produce a regional gravity image around the new detailed survey (Figures 2 and 3).

New gravity survey

In November–December 2001 GSWA conducted a vehicle-supported gravity survey, which covered an area of 60 × 10 km over seismic line 03AGSNY03, on a regular 1 × 2 km grid (Figure 3). Gravity meters and dual-frequency global positioning system (DGPS) units were provided by the Geoscience Australia (GA) under the National Mapping Agreement (NMA). The final accuracy of the survey is estimated to be ±0.8 $\mu m/s^2$ with the accuracy of the elevations for the gravity stations ±0.15 m.

Magnetic surveys

Regional airborne magnetic surveys with east–west oriented lines spaced 3000 m apart, with a 150 m flying height, for which the average sample interval is 60 m were flown over the Neale and Westwood 1:250 000 sheets by the Bureau of Mineral Resources between 1976 and 1978 (Figure 4).

CRA Exploration Ltd flew a magnetic survey with north–south oriented lines spaced 300 m apart, with an 80 m flying height, over most of the western part of the Officer Basin in 1981. The data from this survey were used for interpretation (Figure 5), but are not publicly available.

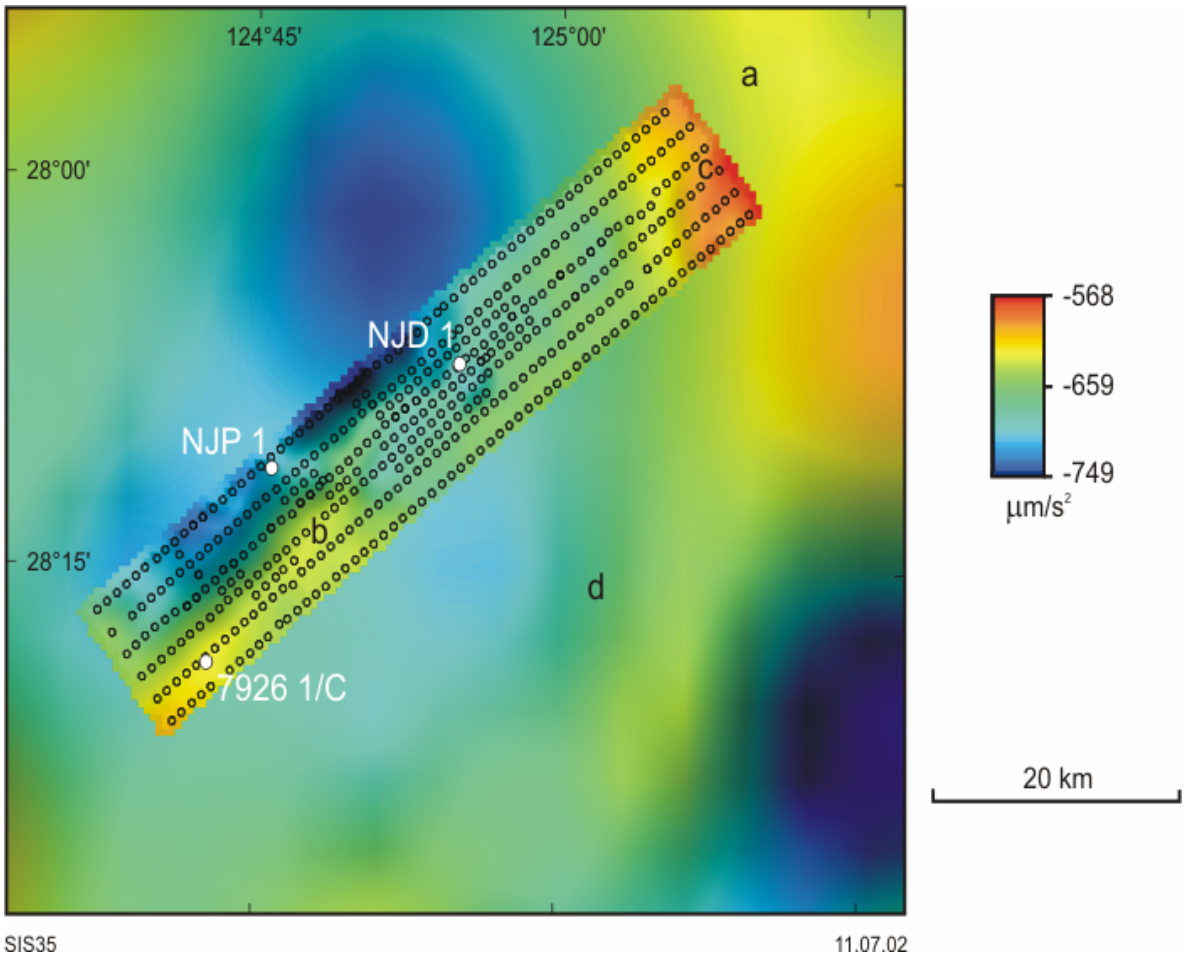

Figure 3. Bouguer gravity image of the Morton Craig gravity survey. The image is a mosaic of the detailed 1× 2 km Morton Craig gravity survey and the regional 11 × 11 km gravity data. Gravity station are shown as black circles. The northerly trending gradient d is interpreted as regional fault; (a to c = gravity highs, discussed in text).

Geophysical signatures

Interpretation of regional data

The gravity survey is in the Rason Regional Gravity Low Province defined by Fraser and Pettifer (1980; Figure 2). The regional gravity low is probably due to thicker crust resulting from continent–continent collision of the Yilgarn Craton margin with east Antarctica, between 1345 and 1140 Ma (Clark et al., 2000).

Based on the gravity and magnetic fields the area within the gravity low can be described as an intermediate or transitional province between the Yilgarn Craton to the west and the Albany–Fraser Orogen to the east. The western border of this province is marked by gravity lineament *ga* (Figure 2). It separates northwest-trending, positive, high-intensity, gravity

anomalies *gk*, *gl*, *gm*, and *gn* (Figure 2), related to high-density greenstones within the Yilgarn Craton, from the subtle northeast-trending elongated anomalies southeast of *ga* (Figure 2). These anomalies (*gc*, *gd*, and *gf*) are up to 150 km long and 15 to 25 km wide. They may relate to high-density, mafic layered bodies within basement or, more likely, faults in both the Proterozoic sedimentary section and the underlying Yilgarn Craton resulting from compression from the southeast.

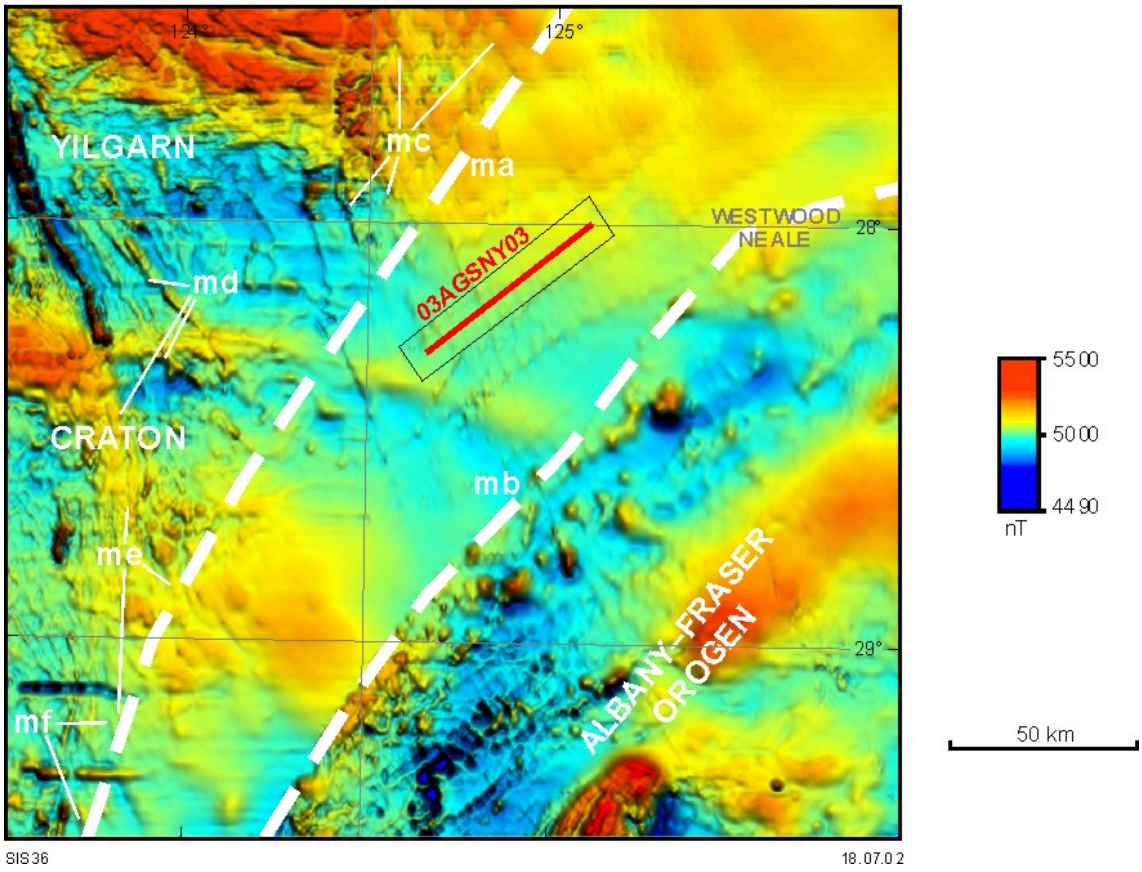

Figure 4. Total magnetic intensity image of the eastern Yilgarn Craton region, showing the intermediate geophysical province between the Yilgarn Craton (ma) and the Albany–Fraser Orogen (mb); mc to mf = magnetic anomalies, discussed in text.

The high-intensity, north-northwest-trending, long, sinuous magnetic anomalies (such as *mc*, *md*, *me*, and *mf* — Figure 4) relating to greenstone belts of the Yilgarn Craton, attenuate and disappear at the magnetic boundary ma (Figure 4). This boundary generally coincides with gravity lineament ga (Figure 2). Whitaker (2001) interpreted the *ma* lineament as a demagnetization boundary in the Yilgarn Craton, similar to the area between the Yilgarn Craton and the western part of the Albany–Fraser Orogen in the Albany Province where deformation is attributed to tectonic interaction between the orogen and the Yilgarn Craton (Whitaker, 1994).

The eastern border of the transitional zone between the Yilgarn Craton and the Albany–Fraser Orogen is interpreted along magnetic lineament *mb* (Figure 4) and gravity lineament *gb* (Figure 2). The northeast-trending, high-intensity magnetic anomalies east of *mb* are probably related to layered mafic gneiss of the Fraser Complex, with the high-intensity positive gravity anomalies *gh*, *gy*, and *gi* (Figure 2) related to high-density granulite rocks of the orogen (Shevchenko, 2000).

The intermediate province or zone between lineaments *ma* and *ga* and *mb* and *gb* is characterized by a smooth magnetic field with scattered, high-frequency 500–600 m-wide linear magnetic anomalies related to near-surface mafic dykes. The trend of these anomalies is random in the west of the province and predominantly northeasterly in the east. The absence of northwest-trending magnetic anomalies east of lineament ma (Figure 4) could be explained by attenuation due to a thickening sedimentary section. However, in the southwestern part of the province, where there is no thick sedimentary cover, the southeast-trending magnetic features still attenuate, suggesting that demagnetization is the more likely explanation (Whitaker, 2001).

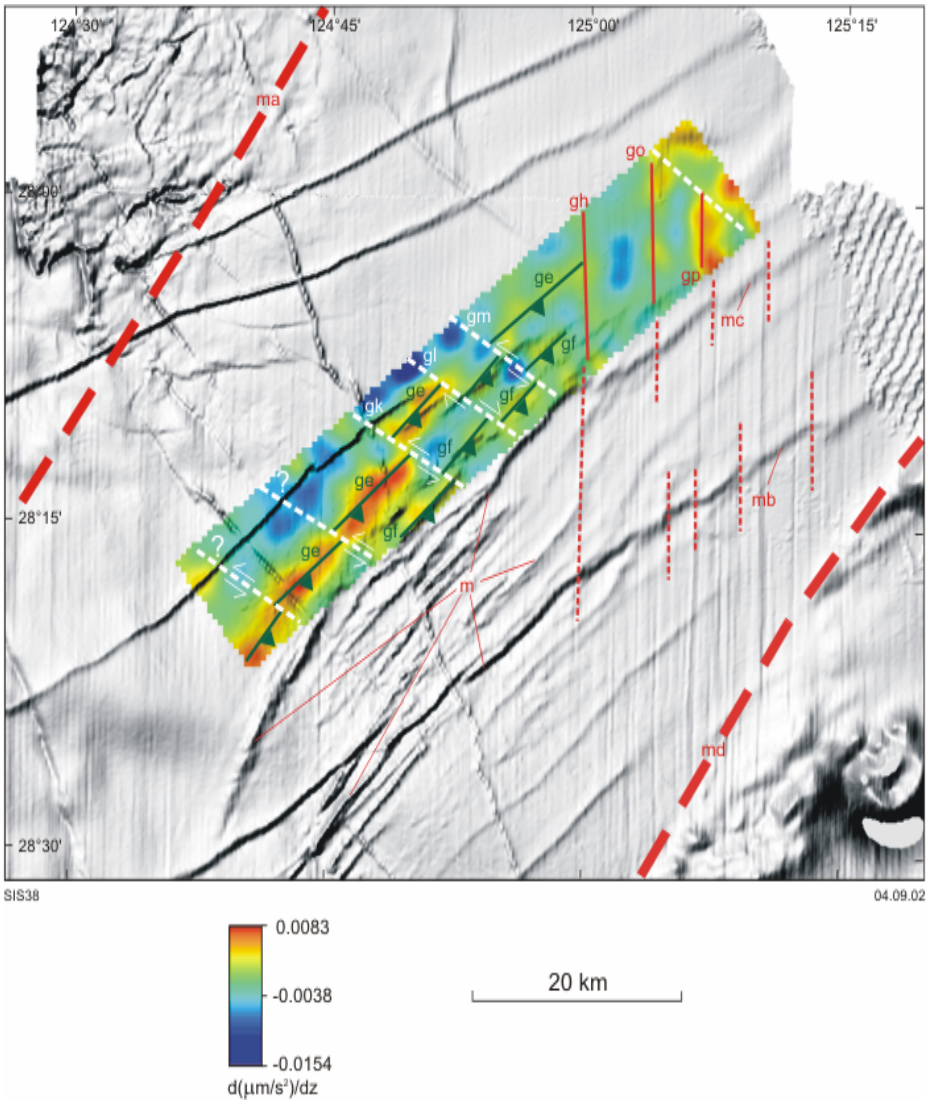

Figure 5. Detailed Morton Craig gravity pseudo-colours image draped over CRA Exploration Ltd total magnetic intensity image. Published with permission of Rio Tinto. Gravity lineaments *ge*, *gt* interpreted as thrust faults, *ge*, *gl*, *gm* — strike-slip faults and *gh*, *go*, *gp* — series of faults; *m* to *md* = magnetic anomalies, interpreted as related to near-surface mafic dykes.

Interpretation of new data

The Morton Craig gravity survey is in a regional gravity low (a in Figure 2) of 100 µm/s^2. This suggests thickening of the Permian and Proterozoic sedimentary section overlying the eastern margin of the Yilgarn Craton outlined by the gravity low. Using a bulk density

contrast of -0.2 t/m^3, the thickness of the sedimentary section in the area of the survey is estimated at 1200–1500 m.

Three major structural trends are interpreted from the new gravity data:

1. Northeast-elongated, narrow gravity anomalies *ge* and *gf* on the first vertical derivative of the Bouguer gravity image (Figure 6) have the same trend as regional anomalies *gd*, *gf*, and *gc* (Figure 2), and are interpreted as thrust faults resulting from tectonism associated with the Albany–Fraser Orogen. The structure *ge* (Figure 6) may be associated with a thrust fault C on 03AGSNY01 (Figure 7). This thrust has probably produced a large-scale fold of package A in a fold. These structures may result from southeast directed compression and the fold may be enhanced by a salt flow within sedimentary unit B (Apak and Tyler, 2002). The positive anomaly b on the Bouguer gravity image (Figure 3) indicates a zone of higher density, related to the upthrown side of the thrust. The northeasterly trending swarm of arcuate magnetic anomalies (labelled with m; Figure 5), immediately east of ge, may also indicate a high degree of shearing and deformation in this area, and may comprise mafic material injected as dykes into the sedimentary section along the shear zones.
2. Northwest-trending gravity lineaments *gk*, *gl*, *gm* (Figure 6) displace the *ge* and *gf* gravity anomalies by about 2 to 2.5 km. These lineaments are interpreted as strike-slip faults, also resulting from the tectonism associated with the Albany–Fraser Orogen. On 03AGSNY03 (Figure 7) faults D, E, F are related to *gk*, *gl* and *gm* (Figure 6) respectively.
3. Distinctive gravity lineaments *gh*, *go*, and *gp* (Figures 5 and 6) in the northeastern part of the area are interpreted as a series of northerly trending faults. These faults correlate with the poor reflection seismic data at the northeastern end of 03AGSNY03 (Figure 7). The regional gravity gradient also trends north (*d* on Figure 3) and is probably a continuation of a regional fault structure to the south. The northeasterly trending high-frequency magnetic anomalies *mc* and *mb* (Figure 5) attributed to mafic dykes appear to be offset by the northerly trending faults *gh*, *go*, and *gp* (Figure 6), and these are probably related to the regional northerly trending fault. The regional structure has the same trend as the post-Miocene Westwood Fault (Townson, 1985) and is possibly of the same tectonic origin and age. The large-amplitude Bouguer gravity anomaly c (Figure 3) in the northeastern part of the study area continues as a 40–50 km-wide, north-northwesterly trending gravity high (as a on Figure 3 and b on Figure 2). This anomaly may indicate a lateral change in density of the sedimentary section, which may be related to possible upthrown granitic basement in the area. The gravity data indicates a major regional structural boundary, which is characterized by extensive faulting and possible lateral changes of lithology in the sedimentary section.

Rotary percussion drillholes 7926 1/C (Seltrust Mining Corporation Proprietary Limited, 1981) and NJP 1 (Western Mining Corporation Limited, 1981) reportedly reached granitic basement at 76 m and 57 m respectively (Figure 3). This interpretation is inconsistent with the new gravity and preliminary seismic data. Assuming that crystalline basement is at 76 m in 7926 1/C, and that gravity high b (Figure 3; a gravity anomaly of -45 μm/s^2) is produced by shallower basement, the depth to basement in the area of NJD 1 can be calculated to be 500 to 600 m using the infinite slab equation (Dobrin, 1976) with a density contrast of -0.2 t/m^2. However, preliminary interpretation of seismic section 03AGSNY03 indicates high-amplitude reflections interpreted as the crystalline basement at a minimum depth of 1000 to 1500 m in the area of NJD 1 (Figure 7).

In the area near drillhole NJP 1 (Figure 3) the Bouguer gravity is lower than around NJD 1. The basement was not reached at the total depth of 517 m in NJD 1 (Western Mining Corporation Limited, 1981), suggesting that basement would also not be encountered in the

presumed deeper basinal area at NJP 1. Hence the report of granitic basement at 57 m at NJP 1 (Western Mining Corporation Limited, 1981) may be explained by large granitic boulders in the glacigene Permian Paterson Formation being misinterpreted as granitic basement (Hocking, R., 2002, written comm.).

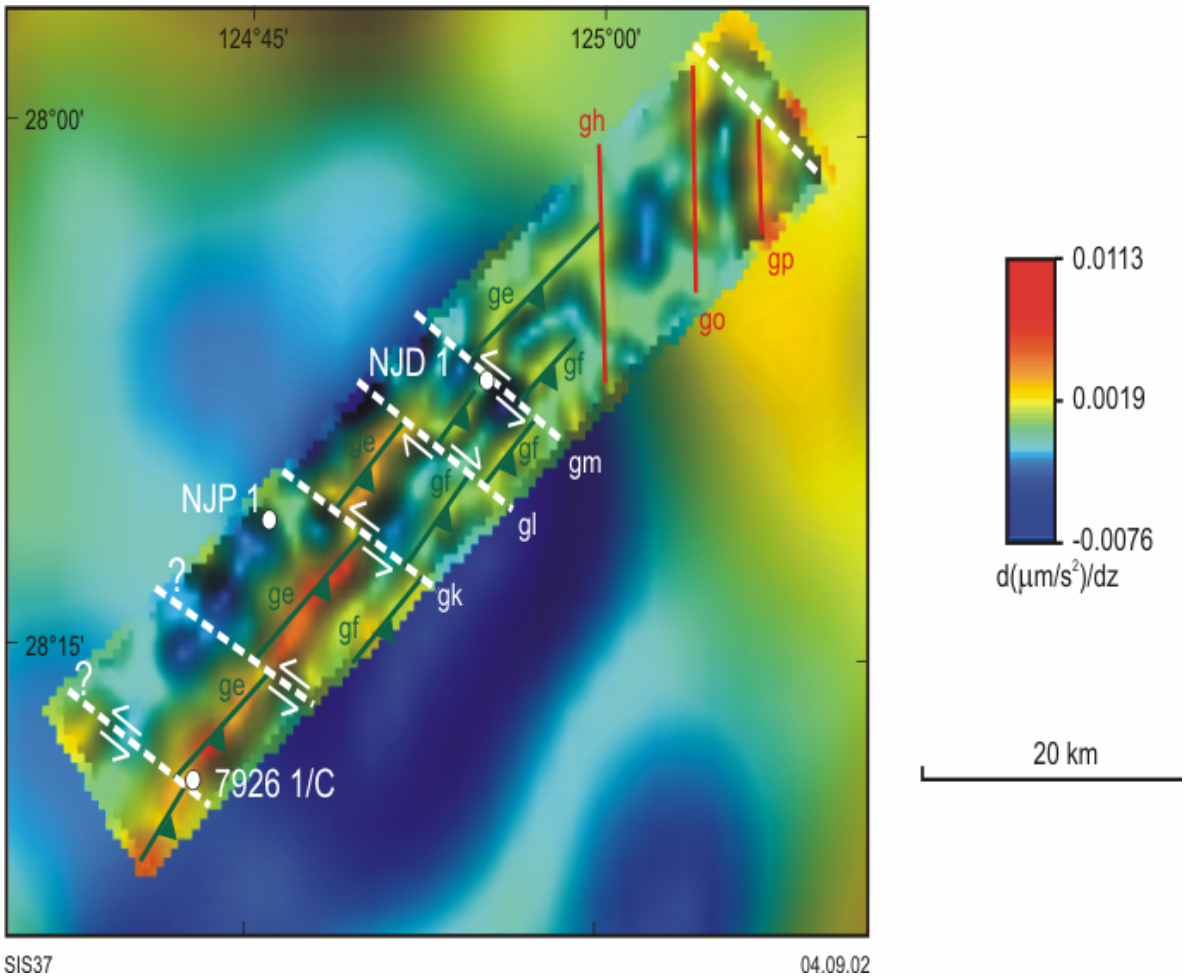

Figure 6. Image of first vertical derivative of Bouguer gravity, showing interpreted features. The image is a mosaic of detailed Morton Craig and regional gravity surveys. Gravity lineaments *ge*, *gf* interpreted as thrust faults, *ge*, *gl*, *gm* — strike-slip faults, and *gh*, *go*, *gp* — series of faults.

Conclusions

The area of the Morton Craig survey is in the southwestern part of the Officer Basin on the Kingston Shelf, which is interpreted as a structural terrace of the Yilgarn Craton. It is within the intermediate geophysical province between the Yilgarn Craton and the Albany–Fraser Orogen.

In the survey area the sedimentary section consists of a thick Mesoproterozoic succession underlying a thin Neoproterozoic succession, with a thin cover of local Permian, and possibly Cretaceous and Cainozoic, rocks. The thickness of sedimentary rock is estimated at 1200–1500 m from gravity and preliminary seismic data.

Three major structural trends are interpreted. Northeasterly elongated gravity anomalies and northwesterly lineaments, interpreted as thrust faults and strike-slip faults respectively,

probably resulted from compression from the southeast associated with tectonism in the Albany–Fraser Orogen. South-trending lineaments in the northeastern part of the area are interpreted as faults, probably representing a major regional lithologic and tectonic boundary.

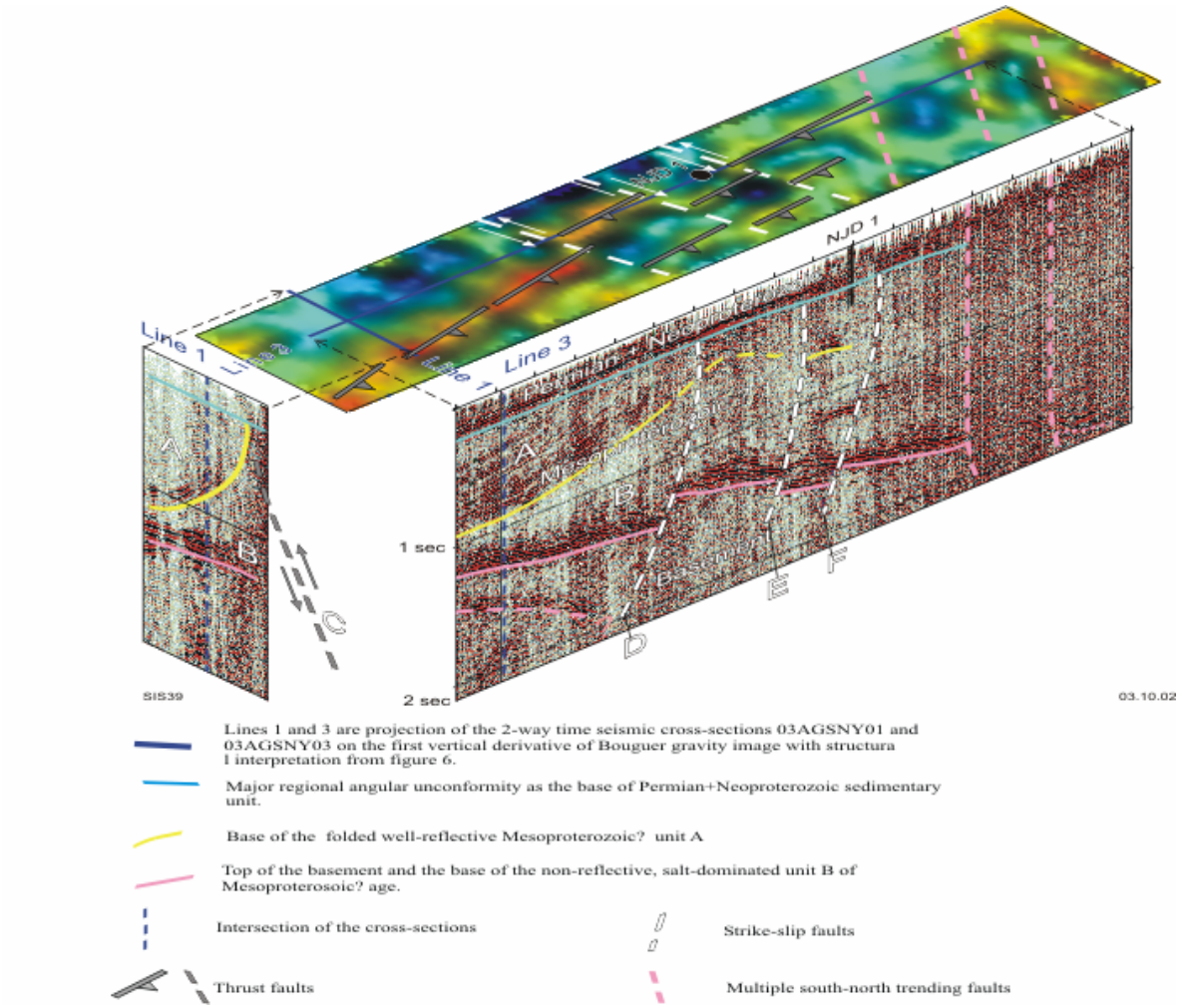

Figure 7. Correlation of the structural interpretation with seismic data (pers. comm. G. Carlsen) shown as a 3D composite view.

References

Apak, S.N. and Tyler, I.M., 2002. Regional geology and seismic interpretation of the sedimentary basins, Western Australia: Northeastern Yilgarn Workshop, *Geoscience Australia*, Workshops Notes, 49–52.

Clark, D.J. Hensen, B.J. and Kinny, P.D., 2000. Geochronological constrains for a two-stage history of the Albany–Fraser Orogen, Western Australia. *Precambrian Research*, **102**, 155–183.

Darby, F., 1970. Barometric heighting — an assessment of the accuracy achieved during reconnaissance gravity survey in Australia. *Australia Bureau of Mineral Resources, Geology and Geophysics, Record* **1970/89**, 7p.

Dobrin, M.B., 1976. *Introduction to geophysical prospecting*. U.S.A., McGraw-Hill Inc., p. 377.

Fraser, A.R. and Pettifer, G.R., 1980. Reconnaissance gravity surveys in WA and SA, 1969–1972. *Australia Bureau of Mineral Resources, Geology and Geophysics, Bulletin* **196**, 60p.

Hocking, R.M., 1994. Subdivisions of Western Australian Neoproterozoic and Phanerozoic sedimentary basins. *Western Australia Geological Survey, Record* **1994/4**, 84p.

Hocking, R.M., Ghori, K.A.R., Pirajno, F., Grey, K., Stevens, M.K. and Carlsen, G.M., 2002. Geology of drillhole WMC NGD 1, Western Officer Basin, *Western Australia: Western Australian Geological Survey, Record* (in press.).

Howard, S.H.D. and Shevchenko, S.I., 2000. Operations and processing methodology used in GSWA regional gravity surveys 1997–1999. *Western Australian Geological Survey, Record* **2000/6**, 12p.

Iasky, R.P., 1990. Officer Basin, in Geology and mineral resources of Western Australia. *Western Australian Geological Survey, Memoir* **3**, 362–380.

Kennewell, P.J., 1977. Westwood, W.A. *Western Australia Geological Survey, 1:250 000 Geological Series Explanatory Notes*, 14p.

Perincek, D., 1996. A compilation and review of data pertaining to the hydrocarbon prospectivity of the Officer Basin: *Western Australia Geological Survey, Record* **1997/6**, 209p.

SELTRUST MINING CORPORATION PROPRIETARY LIMITED, 1981. Neale Area, WA TRs 7925H to 7928H, Final report: *Western Australia Geological Survey, Statutory mineral exploration report*, Item 1376 A10838 (unpublished).

Shevchenko, S.I., 2002. Morton Craig gravity survey, southwestern Officer Basin, Western Australia. *Western Australian Geological Survey, Record* **2002/16**.

Shevchenko, S.I., 2000. Gravity data — Fraser Range region, Western Australia. *Western Australian Geological Survey, Record* **2000/15**, 25p.

Townson, W.G., 1985. The subsurface geology of the western Officer Basin — results of Shell's 1980–1984 petroleum exploration campaign. *APEA Journal*, **25 (1)**, 34–51.

Van de Graaff, W.J.E. and Bunting, J.A., 1975. Neale, W.A.. *Western Australia Geological Survey, 1:250 000 Geological Series Explanatory Notes*, 25p.

WESTERN MINING CORPORATION LIMITED, 1981. Terminal report on the Neale Temporary Reserves 8165H to 8169H. *Western Australia Geological Survey, Statutory mineral exploration report*, Item 1305 A10540 (unpublished).

Whitaker, A.J., 1994. Integrated geological and geophysical mapping of southwestern Western Australia: *Australian Geological Survey Organisation, Journal of Australian Geology and Geophysics*, **15 (3)**, 313–328.

Whitaker, A.J., 2001. Components and structure of the Yilgarn Craton, as interpreted from aeromagnetic data, in 4th International Archaean Symposium, Perth, W.A., 2001, Extended Abstracts: *AGSO–Geoscience Australia, Record* **2001/37**, 542p.

Seismic interpretation of ?Mesoproterozoic to Palaeozoic sedimentary basins imaged at the eastern end of 01AGSNY1 and in 01AGSNY3

S. N. Apak and I. M. Tyler
Geological Survey of Western Australia, East Perth WA 6004
Email: neil.apak@mpr.wa.gov.au

Introduction

The Neoproterozic Officer Basin and the Palaeozoic Gunbarrel Basin unconformably overlie the eastern margin of the Yilgarn Craton (Tyler and Hocking, 2002; Tyler, 2002). The succession of sedimentary rocks deposited within the Officer Basin in Western Australia can be divided into three unconformity-bounded supersequences (SS1, SS3 and SS4 on Figure 1) (Walter and Gorter, 1994). Available well and seismic data (Apak and Moors, 2000, 2001; Moors and Apak, 2002) indicate that the Officer Basin succession thins towards its southeastern margin.

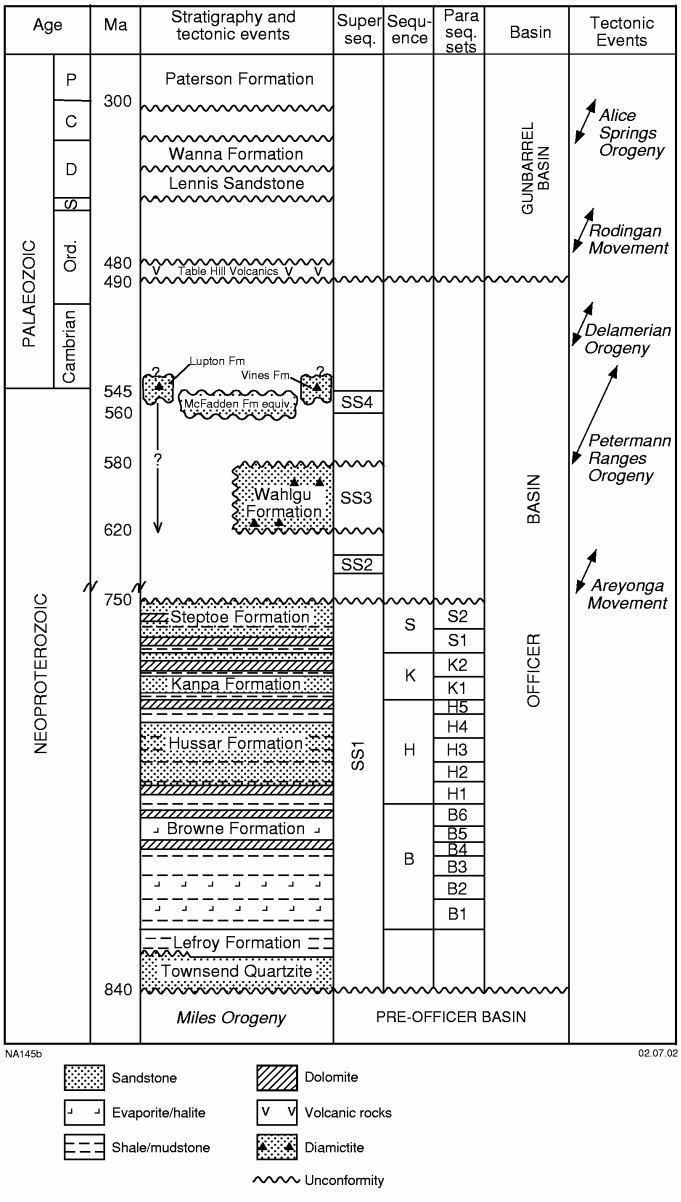

Figure 1. Stratigraphy of the Officer Basin

Geology

Apak and Moors (2000, 2001) and Moors and Apak (2002) could not recognise the basin sub-divisions of the Officer Basin (cf Tyler and Hocking, 2002), which were based on potential field data. These sub-divisions were interpreted as representing older, underlying, sedimentary sequences.

An unconformity between the Officer Basin succession and underlying strata has been recognised in available seismic data, but is not a prominent reflector.

Overlying massive salt within the Officer Basin succession commonly masks the basal unconformity and, in part the contact with underlying strata

is disconformable. However where the contact is angular the horizon can be picked with some confidence (Moors and Apak, 2002).

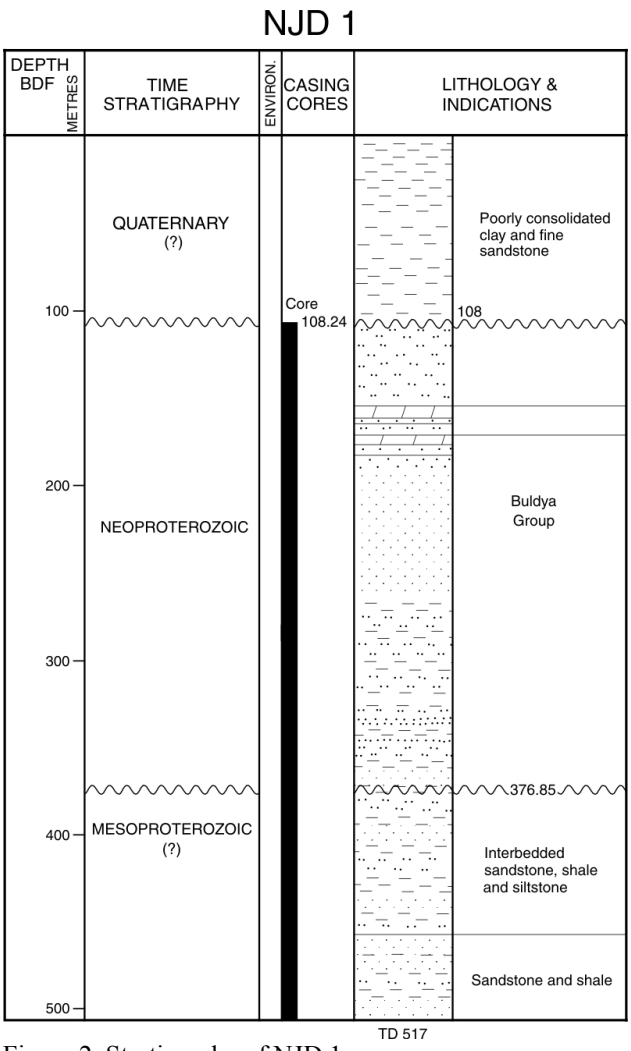

Figure 2. Stratigraphy of NJD 1

The mineral exploration drillhole NJD-1, drilled by Western Mining Corporation on the Westwood Shelf in the western Officer Basin, is located on the joint GA/GSWA deep seismic line 01AGSNY3 near shot point 2040 (Figure 2). A major unconformity is present at 376.85 m between the Officer Basin and underlying rocks (Hocking et al., in prep.). A recent reassessment of the core from NJD-1 by Hocking et al. (in prep.) indicates that the section above 376.85m contains mostly sub horizontal and unmetamorphosed sedimentary rocks of the Buldya Group (SS 1) of the Officer Basin (Figures 1 and 2). The section below 376.85 m is low-grade metamorphosed sedimentary rocks with dips of up to 70 degrees.

On line 01AGSNY3 and 01AGSNY1 an unconformity at 200 msecs may well correspond the angular unconformity at the base of the Officer Basin (Figs 3 and 4). Below this unconformity a thick-bedded succession is folded, and is truncated beneath the basal Officer Basin unconformity. A non-reflective section at the eastern end of line 01AGSNY may be a salt-dominated unit as interpreted by comparison with other seismic data from the overlying Officer Basin. Below the salt-dominated unit, a major reflective package dipping from 1 to 2 seconds may be the basal sedimentary section of a succession of metasedimentary rocks that lies between the Officer Basin and the top of the Yilgarn Craton. This succession is cut by normal faults that overlie deep-seated basement thrust faults. Reactivation of the existing normal faults at later stage resulted in minor displacement of the basal Officer Basin unconformity.

The age of the metasedimentary succession underlying the Officer Basin is uncertain, and a number of post-Archaean – pre-Neoproterozoic sedimentary basins marginal to the Yilgarn Craton could be correlatives (Earaheedy Basin, Edmund Basin, Collier Basin; Tyler and Hocking, 2002). If the thrust faults recognised in the Yilgarn Craton basement are related to the development of Stage II of the Albany-Fraser Orogeny, then the basin should be younger than c. 1150 Ma (Clark et al., 2000). Basalt at the bottom of the Empress 1 and 1A drillhole, which has been interpreted as representing basement to the Officer Basin succession, gave a K-Ar age of 1058 ± 13 Ma (Stevens and Apak, 1999). The basin concealed by the Officer Basin could correlate with Collier Basin to the north of the Yilgarn Craton (which is intruded by c. 1080 Ma mafic sills; Wingate, 2002), and could also be related to the Mission Group, and the c. 1080 Ma Tollu Volcanics of the Musgrave Complex (Glickson et al., 1996; Jackson and van de Graaff, 1981).

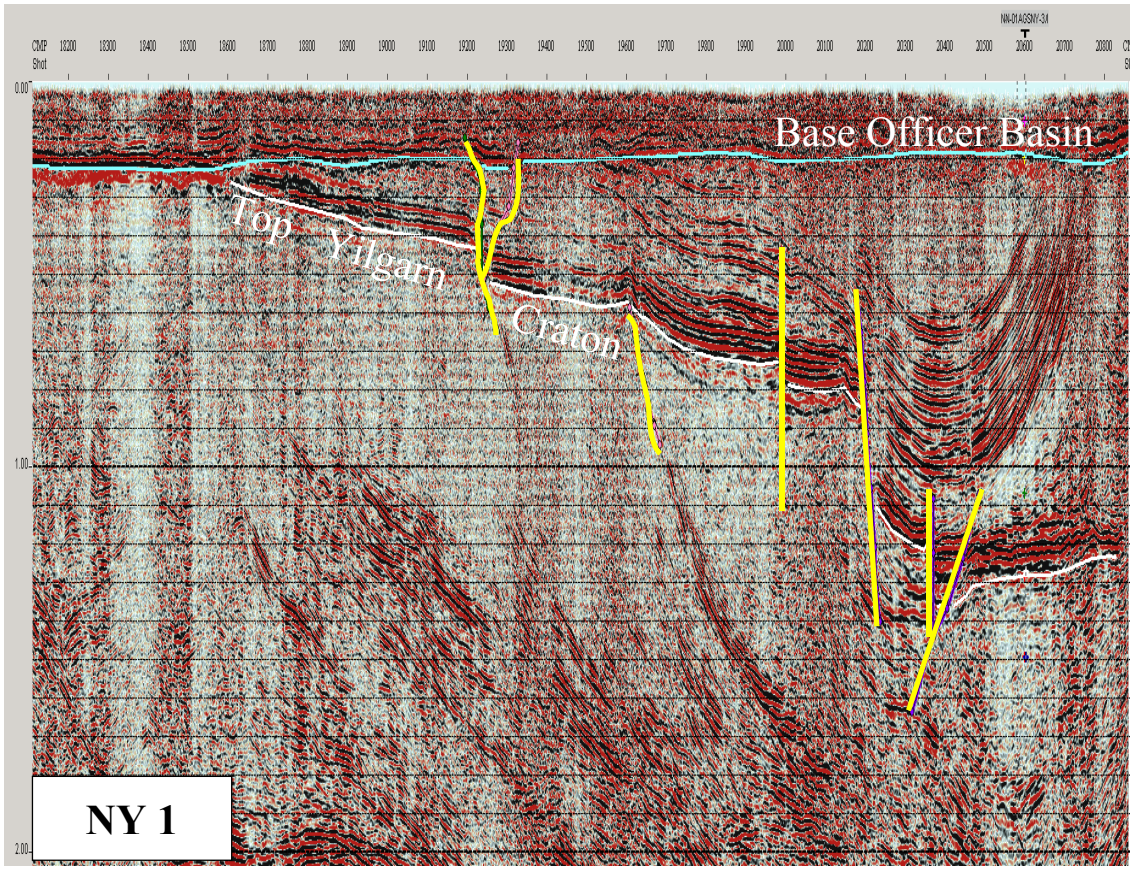

Figure 3. Seismic line 01AGSNY1

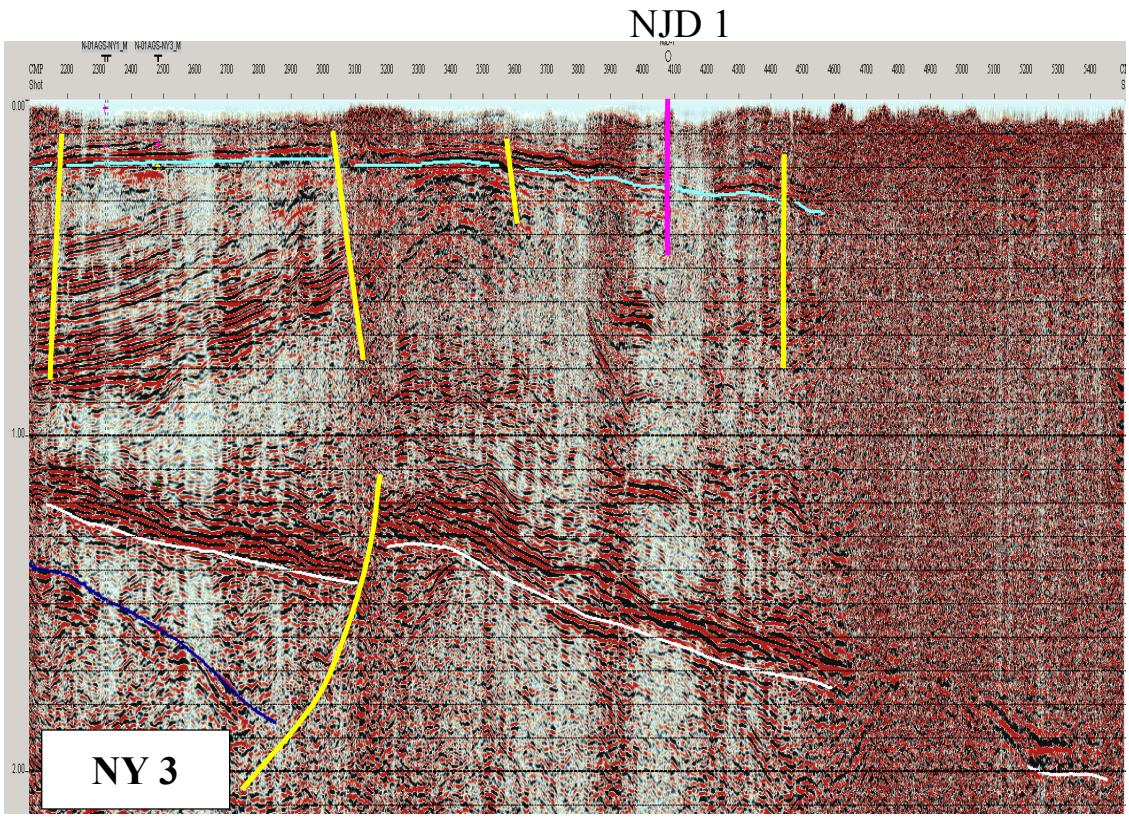

Figure 4. Seismic line 01AGSNY3

References

Apak, S.N. and Moors, H.T., 2000, Basin development and petroleum exploration potential of the Yowalga area, Officer Basin, Western Australia. *Western Australia Geological Survey, Report,* **76**, 61p.

Apak, S.N. and Moors, H.T., 2001, Basin development and petroleum exploration potential of the Lennis area, Officer Basin, Western Australia. *Western Australia Geological Survey, Report*, **77**, 42p.

Clark, D.J., Hensen, B.J. and Kinny, P.D., 2000. Geochronological constraints for a two stage history of the Albany-Fraser Orogen, Western Australia. *Precambrian Research*, **102**, 155-183.

Glikson, A.Y., Stewart, A.J., Ballhaus, C.G., Clarke, G.L., Feeken, E.H. J., Leven, J.H., Sheraton, J.W. and Sun, S-S., 1996. Geology of the western Musgrave Block, central Australia, with particular reference to the mafic-ultramafic Giles Complex. *Australian Geological Survey Organisation, Bulletin*, **239**, 206p.

Hocking, R.M., Ghori, K. A. R., Pirajno, F., Grey, K., Stevens, M.K. and Carlsen, G.M., 2003. Geology of drillhole WMC NJD 1, Western Officer Basin, Western Australia. *Western Australia Geological Survey, Record*, (in prep).

Jackson, M.J. and van der Graaff, W.J.E., 1981. Geology of the Officer Basin, W.A., Australia. *BMR, Geology and Geophysics, Bulletin*, **206**, 102p.

Moors, H.T. and Apak, S.N., 2002. Basin development and petroleum exploration potential of the Gibson area, Western Officer Basin, Western Australia. *Western Australia Geological Survey, Report*, **80**, 42p.

Stevens, M.K. and APAK, S.N., 1999. GSWA Empress 1 and 1A well completion report, Yowalga Sub-basin, Officer Basin, Western Australia. *Western Australia Geological Survey, Record*, **1999/4**, 110p.

Tyler, I.M. and Hocking, R.M., 2002. A revision of the tectonic units of Western Australia. *Western Australia Geological Survey, Annual Review 2000-01*, 33-44.

Tyler, I. M., 2002. Tectonic setting of the 2001 "northeast Yilgarn" deep seismic reflection survey, eastern Yilgarn Craton and adjacent Officer and Gunbarrel Basins: GA-GSWA northeastern Yilgarn Workshop – Notes, p. 97-101.

Walter, M.R. and Gorter, J., 1994. The Neoproterozoic Centralian Superbasin in Western Australia: the Savory and Officer Basins, *in* Purcell, P.G. and Purcell, R.R., eds.,The sedimentary basins of Western Australia. *Petroleum Exploration Society of Australia, Symposium, Perth, W.A. 1994, Proceedings*, 851-864.

Wingate, M.T.D, 2002. Age and palaeomagnetism of dolerite sills intruded into the Bangemall Supergroup on the EDMUND 1:250 000 map sheet, Western Australia. *Western Australia Geological Survey, Record*, **2002/4**, 48p.

GEOLOGY OF THE EASTERN GOLDFIELDS AND AN OVERVIEW OF TECTONIC MODELS

P.B. Groenewald[1], P. A. Morris[2], and D. C. Champion[3]
[1]Geological Survey of Western Australia, P.O. Box 1664, Kalgoorlie, W.A. 6433
[2] Geological Survey of Western Australia, 100 Plain St, East Perth, W. A. 6004
[3]Geoscience Australia, GPO Box 378, Canberra, A. C. T., 2601

Introduction

The Yilgarn Craton is one of the world's largest Archaean granite–greenstone assemblages and comprises several tectonostratigraphic subdivisions (Figure 1). The principal factors that allow the broad scale subdivision are the age and nature of dominant rock types and structural style. Granitic gneiss and granitoid rocks make up about 80 % of the craton, with the remainder made up of metamorphosed sedimentary and volcanic rocks in arcuate greenstone belts. These belts are of limited extent in the western parts of the craton, and are particularly abundant in the Eastern Goldfields.

The economic importance of the Eastern Goldfields as a producer of gold, nickel and other metals for more than a century has made it the most extensively studied part of the craton. Outcrop of Archaean rocks is limited, with about 80 % of the craton covered by regolith or locally by small outliers of Proterozoic or younger rocks. Comprehensive drillhole and aeromagnetic data generated during mineral exploration have delineated the distribution of Precambrian rock types and, where supplemented by locally detailed gravity studies, some three dimensional understanding of the geology has been possible. However, the complex structural history involving multiple deformational events, has hindered both three dimensional interpretations and a detailed understanding of the tectonic history. A 213 km-long reflection seismic survey line extending from west to east across the southern Eastern Goldfields (91EGF1 in Figure 1) in 1991 allowed significant advances in subsurface interpretation, albeit essentially in 2-dimensions (Goleby et al. 1993). This was followed by further work in the Kalgoorlie region with a grid of five more lines (99AGSY1–5 in Figure 1) expanding the study into a 3-dimensional interpretation (Goleby et al., in press).

Assuming an accretionary history, Myers (1990, 1995, 1997) argued for subdivision of the Yilgarn Craton into "fault-bounded composite rafts of sialic crust", making up the Eastern Goldfields and Southern Cross Superterranes, the Murchison and Narryer terranes, and the Southwest Composite terrane. This subdivision was used in a revised form by Tyler and Hocking (2002) to define tectonic units in Western Australia (Figure 1). The initial use of tectonostratigraphic terranes in modelling of Western Australian crustal evolution by Myers (1990) coincided with an interpretation of the southwest Eastern Goldfields that introduced subdivision into terranes (Swager and Griffin, 1990; Swager et al., 1990). This was expanded upon with identification of several more terranes further east by Swager (1995). Plate tectonic related subdivision of the Eastern Goldfields into an eastern volcanic arc and western marginal basin was proposed by Barley et al. (1989), on the grounds that the Kalgoorlie area was dominated by a komatiite–tholeiite association (back-arc), whereas the area further east comprised a tholeiite–calc alkaline (arc) association. These interpretations complemented the extensional ensialic basin models (Archibald et al., 1981; Hallberg, 1986; Hammond and Nisbet, 1993), and the mantle plume tectonics model of Campbell and Hill (1988).

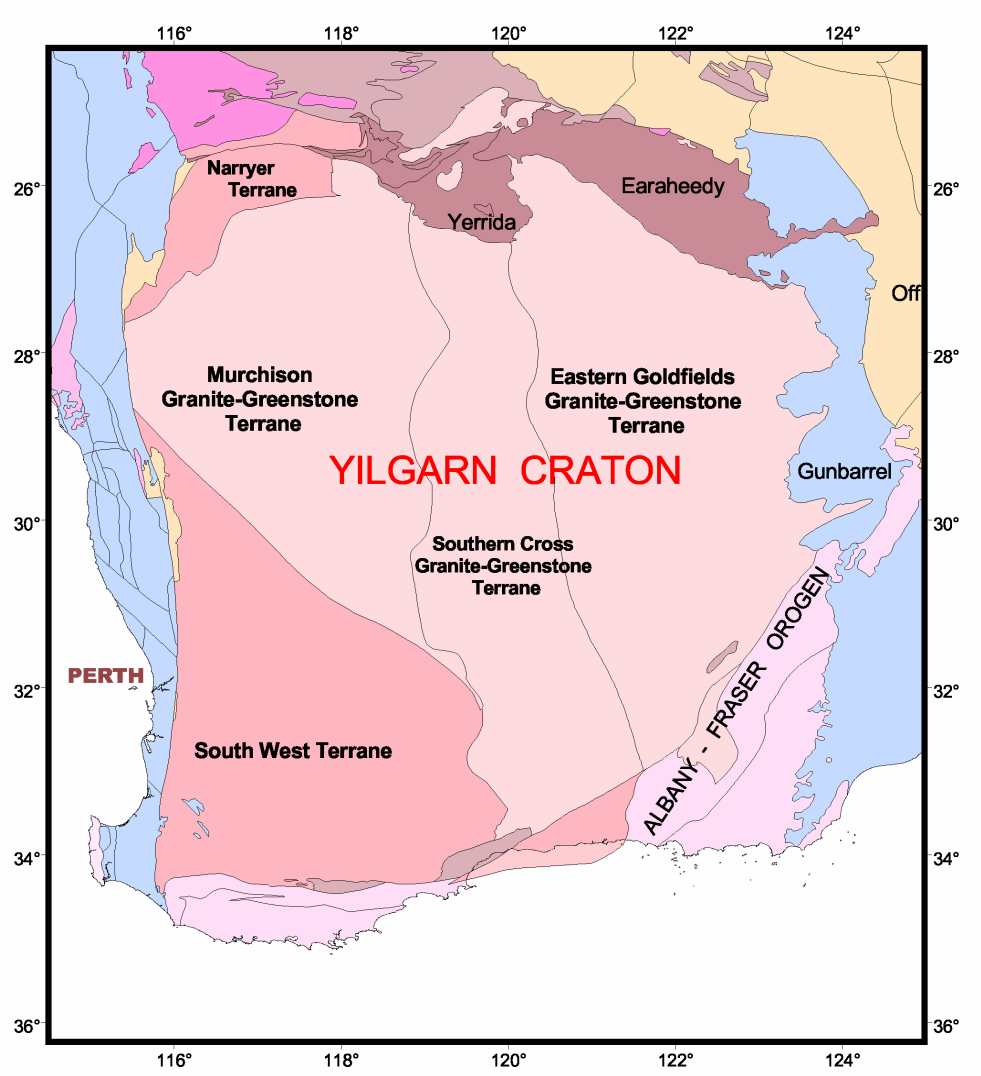

Figure 1: The Yilgarn Craton in Western Australia, divided into tectonic units by Tyler and Hocking (2002).

These orogenic "terranes" of the Eastern Goldfields require confirmation1. As noted by Nelson (1997), isotopic ages show that much of the Eastern Goldfields evolved contemporaneously prior to deformation, and Swager (1997) considered the "terranes" in the south to have been segments of a single extensive basin. The Ida Fault, an inferred major structural boundary between the Southern Cross and Eastern Goldfields Grnite-Greenstone Terranes, is recognized as a crustal-scale extensional fault on which normal downthrow to the east postdated metamorphism and most other tectonic history (Goleby, 1993; Swager et al., 1997), characteristics atypical of a terrane boundary or suture. In a detailed study of the structure of another proposed terrane boundary, the Keith–Kilkenny fault zone (Figure 3), Passchier (1994, p.61) concluded that *"A plate tectonic model for events in the Yilgarn is unsatisfactory since no relics of oceanic crust, accretionary complexes or molasse basins have been recognized"*. He also argued that the craton-wide contemporaneity of igneous, metamorphic and deformational activity is unlike anything recognized in modern convergent plate tectonic settings.

[1] terranes, by definition, are ".. fault-bounded geological entities of regional extent, each characterized by a geological history different from the histories of contiguous terranes" (Jones et al. 1983). Even in terranes so metamorphosed that original stratigraphical relations are obscure, demonstrable protolithic contrasts with adjacent terranes are required (Jones et al. 1986). Implicit in the definition is the allochthonous nature and plate tectonic assembly of collages of these entities.

This presentation provides an overview of the geology of the Eastern Goldfields together with an outline of the petrogenetic constraints on the settings in which the supracrustal assemblages were deposited. For the purpose of presentation, the "terranes" will be retained as this provides a useful geographical subdivision, without the implying that a model of accretionary tectonics involving allochthonous, exotic crustal fragments is favoured.

Regional geology of the Eastern Goldfields

Identification of greenstone lithostratigraphy, and variations in such stratigraphy between greenstone belts are important in interpreting the regional extent of depositional environments, regional structures, and tectonic settings of the Eastern Goldfields. The spatial relationships between these supracrustal rocks are obscured by a lack of stratigraphic markers, meaning that the identification of cogenetic volcanic and sedimentary deposits remains only partly understood. However, major lineaments on detailed aeromagnetic maps, interpreted as faults, allow subdivision into separate terranes bounded by a northwest to northeast trending series of anastomosing regional faults (Figure2).

No basal contact to the greenstones has been established. Although complexly deformed gneisses were regarded as basement remnants (Archibald and Bettenay, 1977), SHRIMP zircon U-Pb studies revealed that these gneisses were probably derived from felsic intrusions into the greenstone sequence (Nelson, 1997a) and demonstrated that relative ages based on apparently more complex deformation history are unreliable for the gneisses, granites and greenstones of the Eastern Goldfields.

Nonetheless, there is evidence that a felsic basement did predate the greenstones, as follows:

- Contamination of komatiite and basalt by crustal material (Arndt and Jenner, 1986; Barley, 1986; Morris, 1993)
- xenocrystic zircons up to c.3.1 Ga in both granites and greenstones (Compston et al., 1986; Campbell and Hill, 1988, Claoué-Long et al., 1988, Hill et al. 1989)
- regional granite geochemistry requires a substantial and evolved lower crustal source (Hill et al., 1992; Champion and Sheraton, 1993; Wyborn, 1993)
- early felsic volcanism predating and contemporaneous with the early mafic to ultramafic greenstones has been identified (Nelson, 1995, 1997).

Regional mapping has identified lithostratigraphic sequences only in the Kalgoorlie and Norseman terranes. These areas differ in lithological characteristics , and also in age, with the latter being significantly older (2930 Ma) than the former (2720 to 2660 Ma).

The Norseman Terrane

The Norseman terrane, a 27 x 60 km lens in the southernmost part of the Eastern Goldfields (Figure 2), has an apparently well-defined, west-younging stratigraphy. The Penneshaw Formation, at the deepest level, consists mainly of amphibolites and massive to pillowed

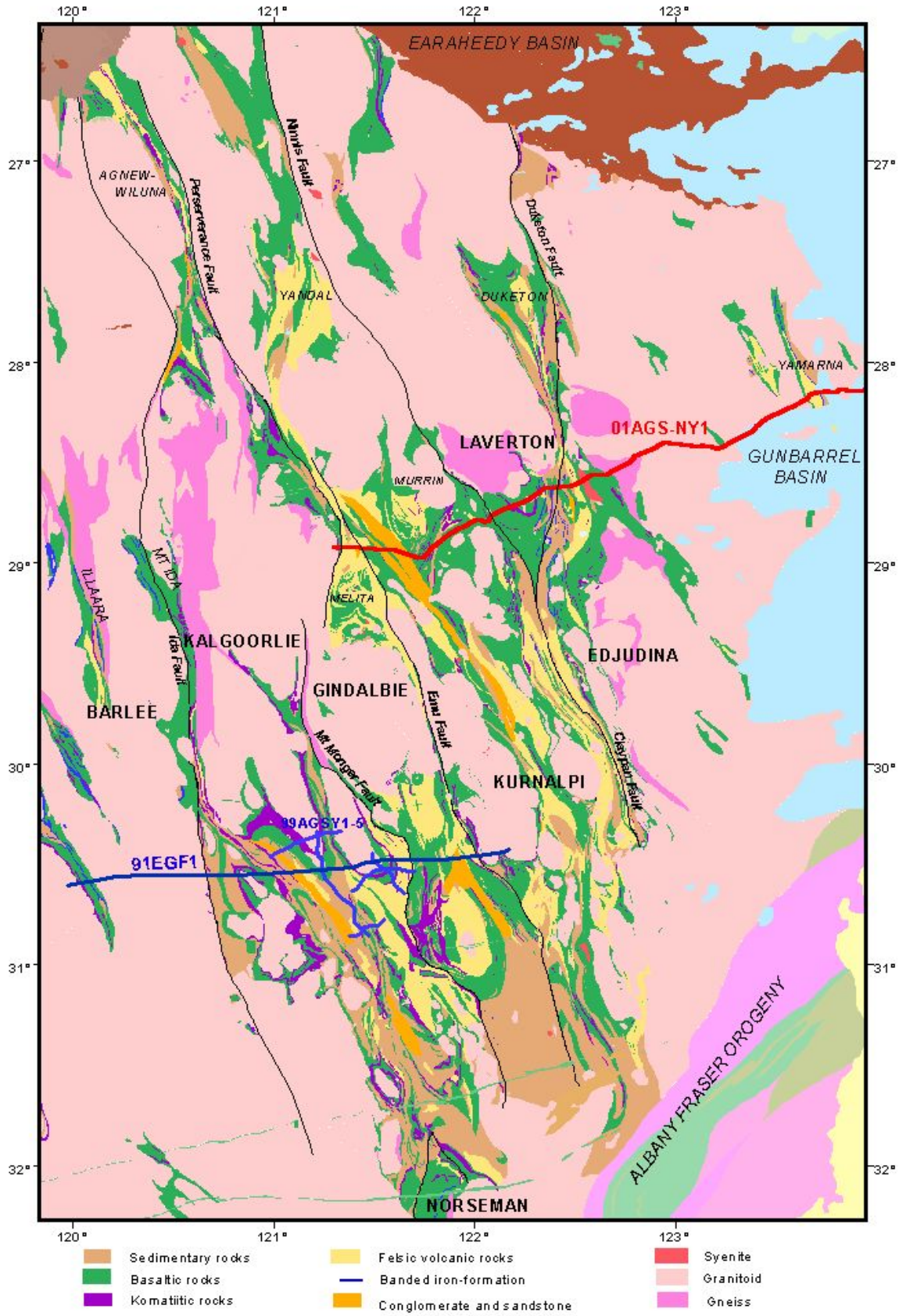

Figure 2: Simplified basement geology of the Eastern Goldfields Granite - Greenstone Terrane. The subdivision into terranes is based on Myers (1997); geological map from GSWA database compilation.

basalts, with minor felsic volcanic rocks. Nelson (1995) obtained an age2 of 2930 ± 4 Ma for rhyolite in the Penneshaw Formation, confirming an age of 2938 ±10 Ma reported earlier (Campbell and Hill, 1988; Hill et al., 1989). The rhyolite contains clustered xenocryst populations of 2977 ± 9 Ma and 3106 ± 13 Ma (Nelson, 1985), with single grains having ages as great as c. 3450 Ma (Hill et al., 1989).

The overlying Noganyer Formation is characterized by persistent BIF layers within clastic sedimentary rocks, and is intruded by gabbro sills. This followed by Woolyeenyer Formation, a monotonous sequence of massive basalt flows with a minor ultramafic component. Hill et al. (1992) obtained a minimum age on a fractionated intrusion of 2714 ± 5 Ma. Although this sequence is apparently 10 km thick in total, shear zones may represent thrust faults and hence stratigraphic duplication.

The Kalgoorlie Terrane

The sequence in the Kalgoorlie terrane is best developed locally in areas such as Kambalda and Ora Banda, but lithological and chronological similarities between the southern (Kalgoorlie) and northern (Agnew-Wiluna) parts have been noted. In the most complete occurrences, the sequence consists broadly of lower basalts, overlain by a komatiite unit, in turn overlain by an upper basalt unit, followed by felsic volcanic and sedimentary rocks. It includes layered and differentiated mafic sills at various stratigraphic levels.

The lower basalt unit consists of greenschist to amphibolite facies rocks, with weak to intense penetrative foliation partly obscuring primary features such as pillow lavas, flow-top breccias and amygdales. An upwards change in character from komatiitic to tholeiitic was documented by Redman and Keays (1985). Felsic volcaniclastic rocks interfinger with the basalts at several places.

This unit is overlain by a prominent and regionally extensive sequence of komatiites (up to several kilometres thick) that locally preserves original mineralogy and textures. Olivine spinifex textured komatiite is the dominant rock type in lower parts, while the upper part consists of variolitic komatiitic basalt. The komatiite flows range from 2 to >100 m thick, locally separated by thin (<5 m) fine-grained metasedimentary beds. In the Ora Banda, Kurrajong, Mount Pleasant and Mount Keith areas, the komatiites include distinctive thick dunitic and peridotitic units, interpreted by Hill et al. (1987, 1995) as cumulates in inflated lava flows.

An upper basalt unit overlying the komatiites in the Ora Banda and Kambalda areas comprises both tholeiitic and komatiitic basalts. Some thick differentiated flows or sub-volcanic sills have been identified. Compositional diversity in these rocks was found to be the result of assimilation, by komatiitic lavas, of up to 25% granitic crustal material (Arndt and Jenner, 1986).

The Black Flag Group is a felsic volcanic–sedimentary package that overlies the mafic-ultramafic volcanic succession unconformably. Thickness is poorly constrained, but 450 to 3000 m is suggested by outcrop mapping. These rocks are mostly volcaniclastic tuffs, agglomerates and debris flows, but lava flows are recognized locally. They are closely interbedded with siltstone and sandstone, that have quartzo-feldspathic compositions consistent with derivation from the associated volcanic rocks. Oligomictic conglomerates at

[2] All dates are from Sensitive High-Resolution Ion Microprobe (SHRIMP) U-Pb analysis of zircon, as detailed in Nelson, 1997a, unless stated otherwise.

numerous levels in the sequence are dominated by feldspar-quartz porphyry clasts. The association of fine grained sedimentary units with conglomeratic horizons suggest a tranquil submarine environment, subjected to periodic influxes of large scale debris flows. Minor polymictic conglomerate units with felsic to ultramafic lithic clasts in a chloritic matrix suggest that proximal tectonic exhumation occurred during deposition. The overall characteristics suggest accumulation in an environment of ongoing volcanism, intermittent extension, with deep water conditions and a considerable influx of sedimentary debris.

The uppermost units in the Kalgoorlie terrane are the Kurrawang and Merougil conglomerates that lie within locally fault-bounded synclines parallel to the regional tectonic trend. These consist of coarse sandstone and polymictic conglomerates deposited in an alluvial environment.

The Gindalbie Terrane

The Gindalbie terrane is situated east of the Kalgoorlie terrane between the Mount Monger and Emu Faults (Figure 2). The Gindalbie terrane was separated on the basis that it has both bimodal (basalt-rhyolite) and calc-alkaline intermediate to silicic volcanic successions, as well as the komatiitic rocks typical of the Kalgoorlie terrane. In the Gindalbie area, these three greenstone successions are separated by regional, early (D1), low-angle thrust faults, further complicated by subsequent refolding and faulting. The structurally lowermost calc-alkaline succession, ranging from basaltic andesite to rhyolite in composition, has an age of 2672 ± 12 Ma (Nelson, 1995). A second succession, an ultramafic/mafic association, dated at 2705 ± 4 Ma (Nelson, 1995), is older than the underlying felsic rocks, supporting a map interpretation of thrust faulting (Ahmat, 1995). The third, uppermost, succession is a bimodal suite with dacite dated at 2681 ± 5 Ma (Nelson, 1995). The northern extremity of the Gindalbie terrane includes the Melita Complex, also a bimodal volcanic suite dated at 2683 ± 3 Ma (Nelson, 1997a). Although lithologically different from the adjacent Kalgoorlie terrane, sequences in both terranes accumulated synchronously and have very similar structural histories.

The Kurnalpi Terrane

The Kurnalpi terrane lies between the Emu Fault and the Clay Pan Fault (Figure 2). The lateral extent of this domain is substantial in that in extends from the northern limit of the Yandal Belt to the southern margin east of Norseman.

The southwesternmost greenstones in this terrane, dipping and facing to the west, are mainly basalt, with several marker units of komatiite. Lateral changes from basalt-dominated to felsic epiclastic-dominated packages are interpreted as original depositional features(Swager, 1995). Nelson (1995) dated a felsic volcanic unit between two komatiite layers at 2706 ± 3 Ma, effectively equivalent to similar associations in the Kalgoorlie terrane.

To the east and north of this are several east-facing mafic–felsic volcanic and volcaniclastic packages that show substantial lateral variations in mafic versus felsic rock volumes. A major shear zone in this area separates upper rocks with an age of 2684 ± 3 Ma (Nelson, 1995) from a lower felsic fragmental unit with an age of 2708 ± 7 Ma (Nelson, 1997). Further north, in the Yilgangi area, are tholeiitic basalt and minor komatiite, interleaved with and overlain by felsic volcanic and epiclastic rocks. Ultramafic rock types are dominantly olivine-cumulate peridotites, with minor gabbro, komatiitic basalt and some olivine-spinifex flows.

The Murrin sector of the Kurnalpi terrane is located east and northeast of Leonora The major south–plunging Benalla anticline comprises a thick sequence of basaltic, andesitic and rhyolitic volcanic rocks. In the core of this anticline is the Welcome Well Complex, a sequence of subalkaline to intermediate volcanic rocks and associated epiclastic rock (Brown et al., 2001). The sequence comprises predominantly andesitic volcaniclastic rocks, with subordinate andesites, overlain by pillow basalts with substantial hyaloclastite interlayers that may indicate some emergence. Layered mafic to ultramafic complexes of the Rio Tinto and Kilkenny synclines southeast of the Benalla anticline consist of olivine adcumulates, orthocumulates and gabbro, associated with pyroxene spinifex-textured komatiitic basalts.

The Laverton Terrane

The Laverton terrane, east of the Kurnalpi terrane, is a triangular area between the Ninnis and Duketon faults (Figure 2). In the south it includes the Margaret anticline, the Mount Korong and Mount Windarra greenstones. The northern parts include the Duketon and Dingo Well greenstones. The Margaret anticline consists almost entirely of mafic rocks, dominated by basalt, komatiitic basalt, dolerite and gabbro, with less substantial komatiitic units. The lowermost part of the stratigraphy is preserved at Mount Windarra and South Windarra, where basal BIF is overlain by ultramafic schist and basalt.

The Duketon greenstone belt contains mafic and ultramafic rocks, felsic volcanic and volcaniclastic rocks, chert, shale, sandstone, and conglomerate. Poor exposure, deep weathering, lack of younging indicators, and structural complexity have prevented recognition of any well-constrained lithostratigraphy. Mafic rocks make up about half of the greenstone area and are mostly tholeiitic basalts, komatiitic basalts, and gabbros, but metamorphism and weathering prevent detailed interpretation. Similarly, considerable felsic volcanic, volcaniclastic and sedimentary rocks are present, but the only possible markers are BIF units. In the central, possibly uppermost, part of the belt, the exposed greenstones are exclusively felsic volcanic and volcaniclastic rocks. Conglomerates with felsic volcanic and granitic clasts near the western margin may represent a similar setting to the Jones Creek Conglomerate in the Agnew–Wiluna greenstone belt.

Hallberg (1985) interpreted the lithostratigraphy of the Laverton area as an earlier association than that present immediately to the west in the Murrin area. His argument was based largely upon the presence of komatiites, substantial BIF and quartz-rich sediments in the Laverton area and the apparent lack thereof further west. Subsequent classification of the Murrin Murrin igneous complex as komatiitic, and the presence of substantial chert units equivalent in stratigraphic position relative to the komatiites in the west (i.e., an iron-poor lateral facies equivalent?) may be contrary to this interpretation. Geochronology is required to elucidate the lithostratigraphic validity of this boundary.

The Edjudina Terrane

South and east of the Laverton terrane, is the Edjudina terrane (Figure 2) chracterised by the abundance of BIF near and Lake Carey. The BIF units occur in intensely deformed sequences of siltstone to fine grained sandstone, some of which are possibly of volcaniclastic origin. Several andesitic volcanic complexes and laterally extensive belts of epiclastic debris occur together with tholeiitic and minor komatiitic basalts. Little is known about the internal structure and age relations in this terrane.

A narrow selvage of greenstones at the southeasternmost extremity of the Edjudina terrane is notable. This greenstone association includes tholeiitic basalt, komatiite with substantial komatiitic basalt, and felsic volcaniclastic sequences that appear to young to the west.

Deformation history and structural architecture

The pronounced north northwesterly structural trend of the Eastern Goldfields is defined by the regional fault pattern and elongate granitoid bodies that separate the greenstone belts and control their general strike. The regional-scale faults appear to form an anastomosing network, leading to an apparent lensoid subdivision of the area.

Many of the interpretations of regional deformation history were summarised by Swager (1997). Broadly, the recognized deformation involved early D_1 recumbent folding and thrusting, followed by east-west shortening through large-scale upright D_2 folding, then a period of strike-slip D_3 faulting with associated folding, followed by continued regional D_4 transpressive oblique and reverse faulting (Table 1). Early, intermediate and late periods of extension have been proposed by some authors. Deformation sequences established in various areas are not entirely consistent, probably because of the difficulty of unravelling the later deformation to elucidate early history in a region of generally poor exposure.

The possibility that the earliest deformation may have been extensional has been very difficult to elucidate. Hammond and Nisbet (1992, 1993) proposed that early extension predated D_1 thrusting and may represent the last stages of development of the actual basin in which the greenstones accumulated. Detailed work in the Leonora area led Passchier (1994) to suggest that the D_1 recumbent folds may have formed in an extensional setting. However, the D_1 event did result in some large-scale stratigraphic repetition, as in a regional-scale thrust duplex structure that extends from Kambalda to Kalgoorlie and duplicates stratigraphy significantly (Swager and Griffin, 1990). Early recumbent folds occur within the sedimentary pile and are clearly refolded by upright F_2 folds (Archibald, 1987; Griffin, 1990).

Subsequent D_2 folding involved considerable (ENE–WSW) crustal shortening to produce major regional–scale upright F_2 folds. Anticlines are best preserved and can be traced over long distances, commonly with doubly plunging to horizontal fold axes. Synclines are commonly more complex fault-related structures. The widespread subvertical penetrative foliation is interpreted in most cases as a composite $S_1 + S_2$ fabric, particularly outside the main shear zones.

Continued regional shortening (D_3) is particularly evident in the major mining centres. At Kalgoorlie, Swager (1989) described late-stage foliations and sets of reverse strike faults compatible with continued shortening after D_3 sinistral shearing. Prominent, oblique faults, that crosscut and offset these late-stage structures, and interpreted as a separate D_4 event by Mueller et al. (1988), could be attributed to a small rotation in the main shortening direction. The en echelon F_3 folds may show very steep plunges because they formed in already steeply tilted sequences.

Crustal scale, extensional faulting is recognized in the Mount Ida fault only through an abrupt eastward change in metamorphic grade across and the reflection seismic data that reveal about 5 km of downthrow to the east. The age constraint on this fault provided by cross-cutting granitoids (Table 1) places it at before 2640±8 Ma but after peak metamorphism at around 2650 Ma. The orientation of this fault parallel to the D_2 compressional structures suggests a

relationship to the main orogenic activity, and the extension probably represents post-orogenic collapse.

Table 1: Summary of proposed regional deformation events in the Eastern Goldfields Province, with age constraints provided by inferred magmatic crystallization dates.

Event	*Structures*	*Locality or example*	*Timing constraint*
?D_e Ma	Low angle shear on granite–greenstone contacts; N–S movement; synvolcanic granites[a]; polydirectional extension, Local recumbent folding[b]	Lawlers; Mount Malcolm (central Eastern Goldfields)	Felsic ash interbedded in komatiites c. 2705 Ma[n]; early granites c.2680
D_1 D_{1c}	Low-angle thrust faults and recumbent folds;[c,d,j] ?shear on early granitoid–greenstones contacts; late synvolcanic slides caused by uplift? [a,b]	Between Kalgoorlie and Democrat (south of Kambalda)	Felsic volcanic rocks 2681 ± 5 Ma, 2675 ± 3 Ma [n] maximum age constraint; 2674 ± 6 Ma post-D_1 felsic porphyry dyke[q]
D_{1e}	Deformed contacts between early granitoid complexes and greenstones; N–S lineations in contact zone; recumbent folds in overlying greenstones[e]	Jeedamya–Kookynie area	
D_e	Roll-over anticlines and E–W extension leading to clastic infill of synclinal basins[f,g]	Kurrawang, Penny Dam, Merougil conglomerates	Post-D1 and pre-D2 felsic porphyry; 2674 ± 6 Ma[q]
D_2	Upright folds with shallowly plunging, NNW fold axes[c,e,h]	Kambalda Anticline, Goongarrie – Mount Pleasant anticline, Kurrawang syncline	Minimum: 2660 ± 3 Ma[n] (post-D2 monzogranite)
De	Local extension in final uplift of granite domes[i]	Barret Well (Yabboo)	Maximum: 2675 ± 2 Ma[i] (post-D1 monzogranite)
D_3	Tightening of F2 folds[k,l]; NW to NNW sinistral strike-slip faults and shear zones; N to NNE dextral strike-slip faults and shear zones	Boorara–Menzies Fault;[e,k] Boulder–Lefroy Fault;[l,c] Butchers Flat Fault[e]	Minimum: 2658 ± 13 Ma (Brady Well Monzogranite); 2640 ± 8 Ma (Clark Well Monzogranite)
	Transpression on NNW faults, with compressional jogs and fold axes trending N to NNE[m]	Laverton, Yandal (central and northeast Eastern Goldfields)	
Late D_3	Steeply plunging lineations on strike-slip faults Steeply dipping reverse faults	Goongarrie, Bardoc Tectonic Zone;[e] Melita, Niagara[e]	
D_e	Post-metamorphic orogenic collapse[r]	Ida Fault	Late-tectonic granite c. 2640 Ma
D_4	NW to WNW oblique sinistral[e] faults; NE to ENE oblique dextral/reverse faults [e,j]	Paddington area; Mount Charlotte (Kalgoorlie); Black Flag Fault (Mount Pleasant)	2638 ± 26 Ma[o]; 2651 ± 5 Ma[p] alkaline granites, post-tectonic

SOURCES:

(a) Hammond and Nisbet (1992)
(b) Passchier (1994)
(c) Swager and Griffin (1990b)
(d) Gresham and Loftus-Hills (1981)
(e) Witt (1994)
(f) Williams (1993)
(g) Swager (1997)
(h) Hunter (1993)
(i) Swager and Nelson (1997)
(j) Archibald et al. (1981)
(k) Swager et al. (1995)
(l) Swager (1989b)
(m) Chen et al. (in press)
(n) Nelson (1997a)
(o) Hill et al. (1992)
(p) Nelson (1995)
(q) Kent and McDougall (1995)
(r) Goleby et al. (1993)

Wide zones of intense shear, with associated widespread carbonate alteration, are recognized in outcrop, but rarely give direct evidence of the. Regional aeromagnetic data reveal large-scale disruption of the greenstone successions with lineaments of great lateral extent truncating those that represent lithostratigraphic units; apparent drag structures on the lesser lineaments close to the truncation may indicate the sense of displacement. These major lineaments have been interpreted as the major subdivisions of the greenstone stratigraphy, that

is, as domain or terrane boundaries, albeit that displacements on these inferred shear zones are unknown and their continuity poorly constrained.

It has been argued that all major shear zones may be long-lived structures, initiated in an extensional regime during deposition and repeatedly reactivated by subsequent complex compressional and transcurrent movements during the regional deformation (Chen et al., 2001; Hallberg, 1985). The total amount of displacement is impossible to determine, but the similarity of greenstone geology on either side of, for example, the Emu Fault precludes craton-scale displacements juxtaposing entirely different tectonic units. Furthermore, the horizontal shortening during D_2 would have reoriented any pre-existing planar structures into the same general northward direction, with much steepening of the original fault planes likely.

Previous seismic interpretations

Interpretations of seismic reflection profiling (Goleby et al., 1993; Swager et al., 1997) suggested that the greenstones rest upon a sub-horizontal detachment which truncates complex fold structures within the greenstones. The underlying crust is dominated by subhorizontal tectonic fabrics and sheets of granitoid rocks. These interpretations in combination suggested that the greenstones may be allochthonous relative to the underlying sialic crust. Although some crust below the greenstones includes younger intrusive granitic sheets, the extensive sharp truncation of the complex greenstone structures is better explained as some sort of detachment at a historical brittle-ductile boundary.

The continental crust beneath the Eastern Goldfields region appears to comprise three major layers (Goleby et al., 1993; Swager et al., 1997):

1. An upper crustal layer, extending to a depth of 4 to 7 km, comprising the Eastern Goldfields Granite-Greenstone terrane, characterized by folded, thrust-stacked greenstones with steep tectonic structures.
2. A middle crustal layer, between depths of 7 and 28 km, comprising an east-dipping imbricate stack of quartzo-feldspathic gneiss, below the flat-lying detachment that forms the base of the Eastern Goldfields greenstones, and above a major flat-lying zone of ductile deformation that may be an extension of the Ida Fault.
3. A lower crustal layer between depths of 28 and 38 km, dominated by quartzo-feldspathic gneiss that may represent an imbricated former margin of the Southern Cross Granite-Greenstone terrane.

Granitoids

Granitoids and granitic gneisses form approximately 70 % of the surface area in the Eastern Goldfields part of the Yilgarn Craton. Although mainly biotite(±hornblende) monzogranite and lesser granodiorite, trondhjemite and syenogranite, minor quartz diorite, tonalite, monzonite, two-mica(–garnet) syenogranite, and syenite intrusions are also recognized.

Two different styles of intrusion have long been recognised, i.e.:

1. numerous plutons of limited extent, pods and dykes that are entirely surrounded by or marginal to greenstones, the internal granites of Sofoulis (1964) and Perring et al. (1989), and
2. extensive composite batholiths (external granites of Sofoulis (1964) and Perring et al. (1989)) which build the typically fault-bounded arches separating the greenstone belts.

Other workers have suggested a classification scheme based on structural events with subdivision into gneisses, and pre-, syn- and post-kinematic granites (e.g., Bettenay, 1977), although the recognition of the age of emplacement relative to deformation stages has proved difficult to apply. Witt and Swager (1989) attempted to separate granitoids into pre- to syn-D_2, post- to syn-D_3, and post-tectonic classes. However, the poor quality of outcrop precludes detailed examination of structures in many granitoids. For the purposes of their geochemical study, Witt and Davy (1997) recognized two main groups: pre-regional folding granitoid (pre-RFG) complexes that commonly form composite cores to F_2 anticlines; and circular to ovoid post-RFG plutons. Noting the considerable overlap in geochemical characteristics of granites with very different structural characteristics, Champion and Sheraton (1997) argued that the complexity of deformation over a protracted period of granite generation renders subdivision using field characteristics equivocal. This is supported by on-going SHRIMP isotope studies of the granites (e.g., Hill et al., 1992; Nelson, 1995-2000; Fletcher et al., 2001, in prep; Black et al., 2002), which indicate that granite magmatism was essentially continuous between 2.72 and 2.63 Ga but with the great bulk emplaced between 2.68 and 2.65 Ga, a 30 Ma year range spanning previous estimates of the timing of both D_1 and D_2 (Table 1). Late plugs and dykes of alkaline granitoids which commonly yield emplacement ages between 2635–2650 Ma, have been considered to be post-tectonic, providing a minimum age for the regional deformation. This, however, has also been recently questioned, given the current debate over the actual timing of the main deformation (D_2), e.g., Krapez et al. (2000) have suggested that D_2 may be as young as ca 2640 Ma, versus ca 2665-2660 Ma of previous workers (e.g., Swager, 1997).

More recent classification schemes have concentrated solely or partly on geochemistry and petrologic characteristics (e.g., Champion and Sheraton, 1993, 1997; Witt and Davy, 1997). The geochemical classification scheme utilised by Champion and co-workers (e.g., Champion and Sheraton, 1993, 1997; Champion and Cassidy, 2002), in combination with available SHRIMP zircon geochronology appears to better constrain the actual timing of the major deformation and provide important constraints on tectonic development of the region. Champion and Sheraton (1993, 1997) broadly subdivided the granites and gneisses of the eastern Yilgarn into two major (High-Ca, Low-Ca) and three minor (High-HFSE, Mafic and Syenitic) granite groups (Table 2, see Champion and Cassidy (2002) for a detailed discussion of the granite groups and their geochemistry). The growing geochronological database for these granites clearly shows that there were distinct time periods characterised by specific granite magmatism (Champion and Cassidy, 2002). In particular, there is a pronounced change in type and style of magmatism at ca 2655 Ma, from voluminous dominantly High-Ca to less voluminous but widespread Low-Ca granites. This change must reflect a significant corresponding change in the tectonic environment at this time and Champion and Cassidy (2002) have speculated it may indicate a change from an arc-related environment to one dominated by extension or post-tectonic relaxation.

Geochemical characteristics of the Eastern Goldfields granites are generally typical of I-type granites, though the syenitic rocks are clearly A-types. The great bulk of the granites (the pre 2655 Ma High-Ca group of Champion and Sheraton, 1997) have geochemistry consistent with being a LILE-enriched variant of the typical Archaean tonalite-trondhjemite-granodiorite (TTG) suite. Such rocks, the transitional TTGs of Champion and Smithies (2001), were most likely derived by high pressure melting (garnet in the source) of a broadly basaltic precursor (e.g. Martin, 1994), either within thickened crust or a subducting slab, with an additional significant crustal input, though Witt and Davy (1997) alternatively suggested hydrous melting of tonalite, granodiorite and monzogranite in a layered lower crust to generate such granitoids. The subordinate later granites (post 2655 Ma Low-Ca granites of Champion and

Sheraton, 1997) were most probably derived by melting of a more uniform tonalitic to granodioritic mid-crustal source.

Table 2: Characteristics of granite groups in the Eastern Goldfields (after Champion and Sheraton, 1997; Champion and Cassidy, 2002).

Group Abundance	**Lithologies**	**Geochemistry**	**Petrogenesis**
High-Ca *> 60 %*	Monzogranite, granodiorite, trondhjemite	High Na_2O; low Th, LREE, Zr; Rb/Sr low; mostly Y-depleted *SiO_2 68-77 wt%*	Deep crustal (garnet stable) or slab melting with assimilation of crust and fractionation; older crust essential
Low-Ca *>20%*	Syenogranite, monzogranite, minor granodiorite	Low Al_2O_3, CaO, Na_2O and Sr; higher HFSE and LILE, than High-Ca group *SiO_2 70-76 wt%*	Reworked crustal source – Archaean TTG; variable partial melts by dehydration; high temperatures at moderate crustal depth
High-HFSE *5 - 10 %*	Syenogranite, monzogranite, minor granodiorite; associated with felsic volcanic centre	Enriched in TiO_2, MgO, total FeO, Y, Zr, and Nb. CaO, K_2O contents similar to the Low-Ca group; LILE moderate to low *SiO_2 >74 wt%*	Pre-existing crustal rocks at moderate depth; possible partial melt of tholeiitic source or crustally contaminated fractionated tholeeite magmas
Mafic *5 -10%*	Diorite, grano-diorite, tonalite, monzogranite, trondhjemite	Variable silica content, subdivided by variations in the LILE and LREE contents *SiO_2 50 -70 wt%*	Crustal and mantle - derived sources required
Syenite < 5 %	Syenite, monzonite, quartz syenite, alkali feldspar syenite	High alkali content, abundance of other elements varies; –ve Nb, Ti anomalies *SiO_2 55-73 wt%*	Dominantly crustal origin? Possible metasomatised mantle source with crustal contribution.

Witt and Davy (1997) also invoked fractional crystallisation of biotite, feldspars and, in the more mafic magmas, hornblende, as the cause of some compositional variations within the granites. There are some rare metal-enriched pegmatites which probably represent incompatible element enrichment of the final magmatic phase in the granitoids, but the general characteristics do not favour the formation of genetically related metalliferous deposits. The most likely orthomagmatic deposits (apart from pegmatites) are small Mo, W and base-metal (Cu, Pb, Zn) concentrations associated with fractionated post-RFG plutons.

There is also evidence that the regional and temporal variations in granite geochemistry reflect variations in the basement, both in space and time. Wyborn (1993) showed that many granites have trace element patterns which require garnet in their source rocks, whilst others have characteristics indicating stable plagioclase. Champion and Sheraton (1997) found that progressive changes in Nd isotope ratios of the granites reflect variations in the age of their source, increasing in age to the west, while Smithies and Witt (1997) suggested the presence

of a distinct basement terrane in the south-east Eastern Goldfields, on the basis of the granite chemistry in that region. Similarly, the predominantly I-type compositions of the Eastern Goldfields granitoids probably reflects an absence of large sedimentary accumulations from the middle to lower crust.

Tectonic constraints imposed by greenstones

Acceptable petrogenetic models must explain greenstone stratigraphy (e.g. basalt – komatiite – basalt – felsic volcanic rocks in the Kambalda – Kalgoorlie area), and the spatial relationship of greenstone belts. Early petrogenetic models focussed on the Kambalda area, where the greenstone stratigraphy was well known through drilling related to nickel and gold exploration (Woodall, 1965; Gresham and Loftus-Hills, 1981). The basalt unit (Lunnon Basalt) beneath the komatiite hosting nickel mineralization, has typical tholeiite chemistry, with flat to slightly depleted light rare earth element (LREE) patterns, and $\varepsilon Nd > 0$. In contrast, the mafic rocks overlying the komatiite unit were more Mg-rich, with elevated LREE contents and more variable εNd (> 0 and < 0; Arndt and Jenner, 1986; Morris, 1993; Chauvel et al., 1985; Claoue-Long et al., 1984; Bateman et al., 2001). The chemistry of basaltic rocks overlying the komatiite unit, and parts of the komatiite unit itself (Lesher and Arndt, 1990) result from assimilation of crustal material by komatiite magma combined with fractional crystallisation (AFC of De Paolo, 1981), although the nature of the contaminant and the extent of contamination are still debated (Arndt and Jenner, 1986; Lesher and Arndt, 1985; Morris, 1993; Bateman et al., 2001; Jochum et al., 1991). A crustal contamination model is independently supported by the occurrence of zircon xenocrysts in basaltic rocks from Kambalda (Compston et al., 1986). Brown et al. (2001) have argued that Woolyeenyer Formation basalt in the Norseman terrane, dated at 2714 ± 5 Ma (Hill et al., 1992), is the correlative of the Lunnon Basalt, although Morris (1993) noted compositional differences between the two units, and the precise age of the Lunnon Basalt is unclear. Mafic volcanic rocks of the Penneshaw Formation in the Norseman area have no correlatives in the Kambalda – Kalgoorlie area.

Morris (1998) and Morris and Witt (1997) discussed the chemistry of the felsic upper part of the greenstone sequence in and adjacent to the Kalgoorlie – Kambalda area. They argued that the steep and smooth REE patterns with depleted heavy rare earth elements (HREE), and high Sr/Y of these rocks were similar to those described from convergent margins where young and hot lithosphere was being subducted at a shallow angle, resulting in melting of the subducting plate rather than the overlying mantle wedge (Drummond and Defant, 1990). In contrast, felsic volcanic rocks from the adjacent Gindalbie terrane and lithologically similar units extending north as far as Teutonic Bore had flat REE patterns with well developed negative Eu anomalies and relatively low Sr/Y, indicative of crustal melts (see also Witt et al., 1996).

Major advances in understanding the spatial relationships of greenstone belts (in particular felsic volcanic and related sedimentary successions) in terms of petrogenetic models have been made recently, as summarised in Brown et al. (2001), largely due to detailed studies in the Eastern Goldfields, coupled with an increasing amount of precise U/Pb geochronology (as discussed by Krapez et al., 2000). They discuss three felsic volcanic and associated sedimentary rock associations, identified on the basis of chemistry, volcanology, and age. Andesitic volcanic rocks and associated sedimentary rocks of their subalkaline intermediate association, some of which were discussed by Hallberg (1985) and Hallberg and Giles (1986), are found as volcanic centres south and west of Laverton in the Kurnalpi and Edjudina terranes of Swager (1995). They form locally emergent, subaqueous successions dominated

by andesitic rocks, with HFSE depletion and LIL and LREE enrichment characteristic of subduction-related magmatism (Barley et al., 1989). Associated rhyolites are probably derived from andesites by fractional crystallisation.

The second association (high-Na and Sr association, discussed in relation to the Black Flag Group by Morris and Witt (1997) and Morris (1998), is largely confined to the upper stratigraphic levels of the Kalgoorlie area, although similar rocks have been reported by Messenger (2000) from the Yandal greenstone belt, and by Bateman et al. (2000) and Brown et al. (2001) from within the komatiite succession. As discussed previously, their steep REE patterns, HREE depletion lacking a Eu anomaly, elevated Sr/Y ratios, and $Na_2O/K_2O > 1$ (Morris and Witt, 1997) are similar to rocks found at modern convergent margins where slab melting takes place, although melting of a mafic underplate has been proposed as a suitable mechanism (Atherton and Petford, 1993), and this may be more consistent with coexistence of high-Sr and Na association volcanics with komatiites in the Kalgoorlie area.

The third association is a bimodal basalt-rhyolite succession forming a thin belt between the subalkaline intermediate association, and the basalt komatiite association typical of the Kalgoorlie area to the west. This succession includes well-exposed volcanic rocks at Melita (near Leonora) and the Spring Well complex in the Yandal Greenstone belt. Unlike the high-Na and Sr association, felsic rocks of this association are characterised by flat REE patterns with well-developed negative Eu anomalies, low Sr and high Y (hence low Sr/Y), with K2O/Na2O usually > 1. Witt et al. (1996) and Morris and Witt (1997) have argued that this chemistry is typical of magmas generated by melting of felsic crust.

Tectonic settings and models

Interpretation of Archaean crustal evolution has led to a large number of models invoking arguments that plate tectonics operated (de Wit, 1998) and were impossible (Hamilton, 1998). Three main types of model for the origin of the Yilgarn Craton in general and the Eastern Goldfields in particular: rifting and plume tectonics (e.g. Campbell and Hill, 1988; Campbell, et al., 1989), convergent margin processes (Barley et al., 1989; Morris, 1993; Morris and Witt, 1997), and accretionary tectonics (e.g. Myers, 1995; Krapez et al., 2000). In each case, different aspects of petrogenesis, possible tectonic settings, and realistic development scenarios must be considered in evaluating the most appropriate tectonic setting. The general agreement from trace element and isotopic work is the greenstones were erupted through older sialic crust. This is also consistent with the geochemistry and Sm-Nd isotopic signatures of spatially associated granites which clearly indicate the presence of pre-existing felsic crust (Champion and Sheraton, 1997). Recent granite geochronology is further confirming this with the discovery of older (>2750 Ma) greenstones and granitoids across the Eastern Goldfields (see summary in Cassidy and Champion, 2002).

Komatiitic magmas with up to 32 wt.% MgO, as are typical of the Kalgoorlie Terrane, indicate extensive partial melting of the mantle that would require elevated thermal anomalies at depths greater than 200 to 250 kilometres (cf. Arndt et al., 1997). In addition, chronological constraints (reviewed above) restrict the volcanic flow fields recognised in an area of >100 000 km^2 to a large igneous episode of short duration. The basalt-komatiite-basalt-felsic volcanic sequence recognised in the Kalgoorlie Terrane also preserves evidence of intermittent felsic volcanism during the dominantly mafic and ultramafic episode. These data led to a model attributing much of the development in the Eastern Goldfields to a mantle plume (Hill et al. 1992; Griffiths and Campbell, 1990; Campbell et al., 1989; Campbell and Hill, 1988).

This data led to a model attributing much of the development in the Eastern Goldfields to a mantle plume (Hill et al. 1992; Griffiths and Campbell, 1990; Campbell et al., 1989; Campbell and Hill, 1988).

Mantle plumes are recognised as generating effects over large areas, up to 2000 km in diameter, ranging from continental rifting and huge magmatic events in the form of continental flood basalts to widespread dynamic uplift, extension and thermal anomalies (White and McKenzie, 1989). In the East Yilgarn model of Campbell et al. (1989) and Hill et al. (1992), a 600-800 km diameter komatiite plume initiated at the core-mantle boundary, ascended through thermal buoyancy. As the plume head and thermal anomaly approached the lower lithosphere boundary, melting ensued to produce basaltic magma while the plume mushroomed to a diameter of 2000 km. The first basalts produced the tholeiitic lower basalt unit, followed by eruption of komatiite magma comprising the plume axis. Assimilation of crustal material by the waning plume axis, coupled with fractional crystallisation, produced the komatiitic basalts of the overlying mafic unit. Felsic volcanism represents melting of the continental crust by the rising plume.

It is possible that the Yilgarn proto-continent moved across the plume, allowing propagation of the extension and magmatism along a path central to the Eastern Goldfields (Passchier, 1994). The relatively short duration of plume-sourced magmatic events has been recognised in numerous large igneous provinces through much of the geological record (White and McKenzie, 1989), but the disturbance of crustal and lithospheric geotherms may last much longer (Hill et al., 1992). Using numerical modelling, Campbell and Hill (1988) found that granite plutonism could commence about 15 Ma after the end of plume volcanism. Time-distance analysis of conduction predicted voluminous felsic volcanism about 27 Ma after the initiation through plume arrival at the lithosphere, with on-going granite magmatism through remelting of precurory granitoids at different levels in the crust for as long as 50 million years. (Hill et al., 1992). Bateman et al. (2001) also favoured a plume model, and argued against a convergent margin model based on the lack of features typical of convergent margins (ophiolites, paired metamorphic belts, and zonation in granite chemistry away from the postulated trench position).

Although the plume model explains the eruption, first of basalt then komatiite, it fails to address the widespread occurrence of felsic volcanic rocks and associated sedimentary rocks that are coeval and, in parts, interbedded with mafic and ultramafic volcanic rocks. It is also difficult to account for the relative abundance of calc-alkaline volcanic rocks in the eastern parts of the Eastern Goldfields using only the plume model. Morris (1993) pointed out that the plume model cannot account for parts of the greenstone stratigraphy north of Kalgoorlie, and the occurrence of felsic volcanic rocks throughout the mafic and komatiite sequence. Instead, he argued for the Kambalda-Kalgoorlie sequence being deposited in a back-arc basin, followed by the eruption of convergent margin volcanic rocks represented by the upper part of the greenstone sequence. He argued for a fan-shaped opening of the back-arc, analogous to that of the Japan Sea (Otofuji et al., 1985). The plume model also has difficulty explaining the age profile of the voluminous spike in granite magmatism from ca 2680 to 2655 Ma, which appear to show two overlapping but separate peaks at ca 2675 and 2665 Ma (Champion and Cassidy, 2002).

A convergent plate-margin model for the Eastern Goldfields was proposed by Barley et al. (1989). They recognised two lithostratigraphic associations in the Norseman-Wiluna area: a tholeiite–calc alkaline volcanic association with felsic sedimentary rocks to the east (Kurnalpi terrane) and a tholeiite–komatiite assemblage with fine-grained siliceous sedimentary rocks to

the west (Kalgoorlie terrane). They inferred that the eastern association corresponds to a volcanic arc succession, whereas the western association represents a marginal basin (back-arc) sequence.

An interpretation based on stratigraphic sequence mapping in the East Yilgarn was presented by Krapez et al. (1997; 2000). Despite the considerable difficulty of determining large-scale stratigraphy from structurally abbreviated sections in the sedimentary and volcanic successions, these authors postulated five tectonic settings: (i) intra-arc rift-basin; (ii) back-arc spreading basin; (iii) arc related basin; (iv) deep-marine stage of remnant-ocean basin; and (v) non-marine stage of remnant-ocean basin. On the basis of these settings, a western Pacific style of multiple marginal basin formation was proposed for the East Yilgarn, with the Eastern Goldfields in an intra arc frame.

Archibald (1998) extended the intra-arc setting to a model of continental collision, suggesting obduction of a mafic and ultramafic lava assemblage generated in a back-arc spreading basin setting over hot continental crust. On-going komatiitic magmatism during the closure of the basin produced the suite of contaminated compositions found in the upper basalt unit in the Kalgoorlie terrane. Arc-related volcanism followed, producing a considerable sequence of volcaniclastic deposits in an intra-arc setting. This evolved into major granitoid emplacement and then a shift of the decoupling plane from the base of the greenstones to the lower crust–middle crust boundary. Archibald (1998) attributed the onset of post-orogenic gold mineralization to fluid flow focussing in deep crustal shears in the post-collisional stage.

Brown et al. (2001) argued that there is little evidence for crustal contamination in greenstones from the Kurnalpi terrane. Volcanological and sedimentological evidence shows that greenstones were deposited in a subaqueous environment, with precise U/Pb zircon dating allowing identification of subtle differences in the timing of volcanic activity in different terranes. This, coupled with the differences in petrology of greenstones (particularly felsic volcanic rocks) in these domains, points to variations in the polarity of greenstones that is best explained by convergent margin processes (Brown et al., 2001). From west to east, the bimodal volcanic rocks of the Kalgoorlie terrane represent eruption of mafic and ultramafic magma in a back-arc environment. Felsic volcanic rocks of the high-Na and Sr association found within these eruptives and forming the upper part of the greenstone sequence result from melting of a mafic underplate and/or a subducting oceanic plate (Atherton and Petford, 1993; Morris and Witt, 1997). Forming a thin belt to the east of this association are greenstones dominated by bimodal (basalt-rhyolite) of the Gindalbie terrane, whose chemistry is indicative of crustal melts, which Brown et al. (2001) have suggested can be found in a rifted arc or back-arc environment. The third association (subalkaline intermediate) is found to the east of the bimodal basalt-rhyolite association in the Kurnalpi terrane, where andesites and subordinate dacites and rhyolites preserve subduction-zone chemistry (ie high LILE/HFSE and LREE/HFSE).

Closing remarks

The considerable extent of the Eastern Goldfields volcanic and sedimentary rocks that accumulated in a geologically brief period, and the enormous extent of granitoid rocks generated during and immediately after this development, is likely to provide greater insight to Archaean crustal evolution. The deep crustal structure must provide significant constraints to the modelling, an aspect not yet addressed in any detail in the models formulated to date. Three dimensional modelling using seismic studies in conjunction with gravity and magnetic data will no doubt make an important contribution.

References

Archibald, N. J., 1987, Geology of the Norseman-Kambalda area, in Second Eastern Goldfields Geological Field Conference. Geological Society of Australia (W. A. Division); Eastern Goldfields Geological Field Conference, 2nd, Kalgoorlie, W. A., 1987, Abstracts and Excursion Guide, p. 13-14.

Archibald, N. J., 1998, An allochthonous model for the greenstone belt evolution in the Menzies–Norseman area, Eastern Goldfields Province: implications for gold mineralisation: http://www.agcrc.csiro.au/publications/yilgarn98/abstracts/archibald1.html, p. 5.

Archibald, N. J. and Bettenay, L. F., 1977, Indirect evidence for tectonic reactivation of a pre-greenstone sialic basement in Western Australia. Earth and Planetary Science Letters, v. 33, p. 370-378.

Archibald, N. J., Bettenay, L. F., Bickle, M. J. and Groves, D. I., 1981. Evolution of Archaean crust in the Eastern Goldfields Province of the Yilgarn Block. Special Publication Geological Society of Australia 7, p. 491-504.

Arndt, H. T., and Jenner, G. A., 1986, Crustally contaminated komatiites and basalts from Kambalda, Western Australia. Chemical Geology, v. 56, p. 229-255.

Arndt, H. T., Kerr, A. C., and Tarney, J., 1997, Dynamic melting in plume heads: the formation of Gorgona komatiites and basalts. Earth and Planetary Science Letters, v. 146, p. 289-301.

Atherton, M. P., and Petford, N., 1993, Generation of sodium-rich magmas from newly underplated basaltic crust. Nature, v. 362, p. 144-146.

Barley, M. E., 1986, Incompatible-element enrichment in Archean basalts: a consequence of contamination by older sialic crust rather than mantle heterogeneity. Geology, v. 14,p. 947-950.

Barley, M. E., Eisenlohr, B. N., Groves, D. I, Perring, C. S., and Vearncombe, J. R., 1989, Late Archean convergent margin tectonics and gold mineralization: a new look at the Norseman-Wiluna belt, Western Australia. Geology, v. 17, p. 826-829.

Bateman, R., Costa, S., Swe, T., and Lambert, D., 2001, Archaean mafic magmatism in the Kalgoorlie area of the Yilgarn Craton, Western Australia: a geochemical and Nd isotopic study of the petrogenetic and tectonic evolution of a greenstone belt. . Precambrian Research, v. 108, p. 75-112.

Bettenay, L. F., 1977, Regional geology and petrogenesis of Archaean granitoids in the southeastern Yilgarn Block. University of Western Australia, PhD thesis, 328p.

Black, L. P., Champion, D. C., and Cassidy, K. F., 2002, Compilation of SHRIMP U–Pb geochronology data, Yilgarn Craton, Western Australia, 1997–2000. Geoscience Australia Record.

Brown, S. J. A., Krapez, B, Beresford, S. W., Cassidy, K. F., Champion, D.C, Barley, M. E., and Cas, R. A. F., 2001, Archaean volcanic and sedimentary environments of the Eastern Goldfields Province, Western Australia — a field guide. Western Australia Geological Survey, Record 2001/13, 66p.

Campbell, I. H., and Hill, R. I., 1988, A two-stage model for the formation of the granite-greenstone terrains of the Kalgoorlie–Norseman area, Western Australia. Earth and Planetary Science Letters, v. 90, p. 11-25.

Campbell, I. H., Griffiths, R. W., and Hill, R. I., 1989, Melting in an Archaean mantle plum: heads it's basalts, tails it's komatiites. Nature, v. 339, p. 697-699.

Cassidy, K. F., Champion, D. C., Fletcher, I. R., Dunphy, J. M ., Black, L. P., and Claoue-long, J. C., 2002, Geochronological constraints on the Leonora-Laverton transect area, north eastern Yilgarn Craton. Geoscience Australia Record 2002/18, p. 37-58.

Champion, D. C., and Sheraton, J. W., 1993, Geochemistry of granitoids of the Leonora-Laverton region, Eastern Goldfields Province, *in* Kalgoorlie 93 - an international conference on crustal evolution, metallogeny, and exploration of the Eastern Goldfields compiled by P.R. Williams and J.A. Haldane. *Australian Geological Survey Organisation, Record* **1993/54**, 39-46.

Champion, D. C. and Sheraton, J. W., 1997. Geochemistry and Nd isotope systematics of Archaean granites of the Eastern Goldfields, Yilgarn Craton, Australia: implications for crustal growth processes. *Precambrian Research*, **83**, 109-132.

Champion, D. C. and Cassidy, K. F., 2002. Granites in the Leonora-Laverton transect area, northeastern Yilgarn Craton. Geoscience Australia Record 2002/18, p. 13-35.

Champion, D. C. and Smithies, R. H., 2001, Archaean granites of the Yilgarn and Pilbara cratons, Western Australia, in 4th International Archaean Symposium 2001, Extended Abstracts. *AGSO-Geoscience Australia, Record* **2001/37**, 134–136.

Chauvel, C., Dupre, B. and Jenner, G. A., 1965. The Sm-Nd age of Kambalda volcanics is 500 Ma too old! *Earth and Planetary Science Letters*, **74**, 315-324.

Chen, S. F., Witt, W. and Liu, S. F., 2001. Transpressional and restraining jogs in the northeastern Yilgarn Craton, Western Australia. *Precambrian Research*, **106**, 309–328.

Claoué-Long, J. C., Compston, W. and Cowden A., 1988. The age of the Kambalda greenstones resolved by ion-microprobe: implications for Archaean dating methods. *Earth and Planetary Science Letters*, **89**, 239-259.

Compston, W., Williams, I. S., Campbell, I. H. and Gresham, J. J., 1986. Zircon xenocrysts from the Kambalda volcanics: age constraints and direct evidence for older continental crust below the Kambalda–Norseman greenstones. *Earth and Planetary Science Letters*, **76**, 299–301.

De Paolo, D. J., 1981. Trace elements and isotopic effects of combined wallrock assimilation and fractional crystallisation. *Earth and Planetary Science Letters*, **53**, 189-202.

De Wit, M. J., 1998. On Archaean granites, greenstones, cratons and tectonics: does the evidence demand a verdict? *Precambrian Research*, **91**, 181-226.

Drummond, M. S. and Defant, M. J., 1990. A model for trondjemite-tonalite-dacite genesis and crustal growth via slab melting — Archaean to modern comparisons. *Journal of Geophysical Research*, 95, 21503–21521.

Fletcher, I. R., Dunphy, J. M., Champion, D. C. and Cassidy, K. F., 2001. Compilation of SHRIMP U–Pb geochronology data, Yilgarn Craton, Western Australia, 2000-2001. *Geoscience Australia Record*

Goleby, B. R., Rattenbury, M. S., Swager, C. P., Drummond, B. J., Williams, P. R., Sheraton, J. E. and Heinrich, C. A., 1993. Archaean crustal structure from seismic reflection profiling, Eastern Goldfields, Western Australia. *AGSO, Record* **1993/15**, 54p.

Goleby, B. R., Korsch, R. J., Fomin, T., Bell, B., Nicoll, M. G., Drummond, B. J. and Owen, A. J., 2002. A 3D interpretation of the Kalgoorlie region, Eastern Goldfields, Western Australia, from deep seismic reflection and potential field data. *Australian Journal of Earth Sciences*.

Gresham, J. J. and Loftus-Hills, G. D., 1981. The geology of the Kambalda nickel field, Western Australia. *Economic Geology*, **76**, 1373–1416.

Griffin, T. J., 1990. Geology of the granite-greenstone terrane of the Lake Lefroy and Cowan 1:100 000 sheets, Western Australia. *Western Australia Geological Survey, Report* **32**, 53p.

Griffiths, R. W. and Campbell, I. H., 1990. Stirring and structure in mantle plumes. *Earth and Planetary Science Letters*, **99**, 66-78.

Hallberg, J. A., 1985. *Geology and mineral deposits of the Leonora–Laverton area, northeastern Yilgarn Block, Western Australia*. Hesperian Press, Perth, Western Australia, 140p.

Hallberg, J. A., 1986. Archaean basin development and crustal extension in the northeastern Yilgarn Block, Western Australia. *Precambrian Research*, **31**, 133–156.

Hallberg, J. A. and Giles, C. W., 1986. Archaean felsic volcanism in the northeastern Yilgarn Block, Western Australia. *Australian Journal of Earth Sciences*, **33**, 413-427.

Hamilton, W. B., 1998. Archaean magmatism and deformation were not products of plate tectonics. *Precambrian Research*, **91**, 143-179.

Hammond, R. L. and Nisbet, B. W., 1992. Towards a structural and tectonic framework for the Norseman-Wiluna Greenstone Belt, Western Australia, *in* Glover, J.E. and Ho, S.E., eds., *The Archaean Terrains, processes and metallogeny*, University of Western Australia, Geology Department and University Extension, Publication **22**, 39-50.

Hammond, R. L. and Nisbet, B. W., 1993. Archaean crustal processes as indicated by the structural geology, Eastern Goldfields Province of Western Australia, *in* Williams, P.R. and Haldane, J.A., eds., K*algoorlie 93 - an international conference on crustal evolution, metallogeny, and exploration of the Eastern Goldfields*, Australian Geological Survey Organisation, Record **1993/54**, 105–114.

Hill, R. E. T., Barnes, S. J., Gole, M. J. and Dowling, S. J., 1995. The volcanology of komatiites as deduced from field relationships in the Norseman–Wiluna greenstone belt, Western Australia. *Lithos*, **34**, 159–188.

Hill R. E. T., Barnes, S. J. and Perring, C. S., 1996. Komatiite volcanology and the volcanogenic setting of associated nickel deposits, *in* Grimsby, E.J. and Nuess, I., eds., *Nickel'96 – Mineral to Market*, Australian Institute of Mining and Metallurgy, Publication Series **6/96**, 91-95.

Hill, R. E. T., Gole, M. J. and Barnes, S. J., 1989. Olivine adcumulates in the Norseman-Wiluna greenstone belt, Western Australia: implications for the volcanology of komatiites, *in* Prendergast, M.D. and Jones, M.J., eds., *Magmatic sulphides- the Zimbabwe Volume*, The Institute of Mining and Metallurgy, London, 189-206.

Hill, R. I., Campbell, I. H. and Compston, W., 1989. Age and origin of granitic rocks in the Kalgoorlie-Norseman region of Western Australia: implications for the origin of the Archaean crust. *Geochimica et Cosmochimica Acta*, **53**, 1259-1275.

Hill, R. I., Chappell, B. W. and Campbell, I. H., 1992. Late Archaean granites of the southeastern Yilgarn Block, Western Australia: age, geochemistry and origin. *Royal Society Edinburgh, Transactions*, **83**, 211-226.

Hunter, W. M., 1993. The geology of the granite-greenstone terrane of the Kalgoorlie and Yilmia 1:100 000 sheets, Western Australia. *Western Australia Geological Survey, Report* **35**, 80p.

Jochum, K.P., Arndt, N.T. and Hofmann, A. W., 1991. Nb-Th-La in komatiites and basalts: constraints on komatiite petrogenesis and mantle evolution. *Earth and Planetary Science Letters*, **107**, 272-289.

Jones, D.L., Howell, D.G., Coney, P.J. and Monger, J.W.H., 1983. Recognition, character, and analysis of tectonostratigraphic terranes in western North America, *in* Hashimoto, M. and Uyeda, S., eds., *Accretion tectonics in the Circum-Pacific regions: Tokyo, Japan*, Terra Scientific Publishing Company, 21–35.

Jones, D.L., Silberling, N.J. and Coney, P.J., 1986. Collision tectonics in the Cordillera of western North America; examples from Alaska, *in* Coward, M.P. and Ries, A.C., eds., *Collision Tectonics*. Geological Society of London Special Publication **19**, 367–387.

Kent, A.J.R. and McDougall, I., 1995. 40Ar–39Ar and U–Pb age constraints on the timing of gold mineralization in the Kalgoorlie Gold Field, Western Australia. *Economic Geology*, **90**, 845-859.

Krapez, B., Brown, S.J.A., Hand, J., Barley, M.E. and Cas, R.A.F., 2000. Age constraints on recycled crustal and supracrustal sources of Archaean metasedimentary sequences,

Eastern Goldfields Province, Western Australia. Evidence from SHRIMP zircon dating. *Tectonophysics*, **322**, 89–133.

Lesher, C.M. and Arndt, N.T., 1995. REE and Nd isotope geochemistry, petrogenesis and volcanic evolution of contaminated komatiites at Kambakda, Western Australia. *Lithos*, **34**, 127-157.

Martin, H., 1994. The Archaean grey gneisses and the genesis of continental crust, *in* Condie, K.C., ed., *Archaean Crustal Evolution*, Elsevier, Amsterdam, 205–259.

Messenger, P.R., 2000. Igneous geochemistry and base metal potential of the Yandal belt, *in* Phillips, G.N. and Anand, R.R., eds., *Yandal greenstone belt: regolith, geology and mineralization*, Australian Institute of Geoscientists, Bulletin **32**, 69–71.

Morris, P.A., 1993. Archaean mafic and ultramafic volcanic rocks, Menzies to Norseman, Western Australia. *Western Australia Geological Survey, Report* **36**, 107p.

Morris, P.A., 1998. Archaean felsic volcanism in the Eastern Goldfields Province, Western Australia. *Western Australia Geological Survey, Report* **55**, 80p.

Morris, P.A. and Witt, W.K., 1997. Geochemistry and tectonic setting of two contrasting Archaean felsic volcanic associations in the Eastern Goldfields, Western Australia. *Precambrian Research*, **83**, 83–107.

Mueller, A.G., Harris, L.B. and Lungan, A. 1988. Structural control of greenstone-hosted gold mineralization by transcurrent shearing: a new interpretation of the Kalgoorlie mining district, Western Australia. *Ore Geology Reviews*, **3**, 359-387.

Myers, J.S., 1990b, Precambrian tectonic evolution of part of Gondwana, southwestern Australia. *Geology*, **18**, 537–540.

Myers, J.S., 1995.The generation and assembly of an Archaean supercontinent. Evidence from the Yilgarn craton, Western Australia, *in* Coward, M.P. and Ries, A.C., eds., *Early Precambrian Processes*, Geological Society Special Publication **95**, 143-154.

Myers, J.S., 1997.Preface. Archaean geology of the Eastern Goldfields of Western Australia—a regional overview. *Precambrian Research*, **83**, 1-10.

Nelson, D.R., 1995.Compilation of SHRIMP U–Pb zircon geochronology data, 1994. *Western Australia Geological. Survey, Record* **1995/3**, 244p.

Nelson, D.R., 1996.Compilation of SHRIMP U–Pb zircon geochronology data, 1995. Western *Australia Geological. Survey, Record* **1995/3**, 168p.

Nelson, D.R., 1997a. Evolution of the Archaean granite-greenstone terranes of the Eastern Goldfields, Western Australia: SHRIMP U-Pb zircon constraints. *Precambrian Research*, **83**, 57-81.

Nelson, D.R., 1997b. Compilation of SHRIMP U–Pb zircon geochronology data, 1996. *Western Australia Geological Survey, Record* **1996/2**, 189p.

Otofuji, Y., Matsuda, T. and Nohda, S., 1985. Opening mode of the Japan Sea inferred from the paleomagnetism of the Japan Arc. *Nature*, **317**, 603-604.

Passchier, C.W., 1994. Structural geology across a proposed Archaean terrane boundary in the eastern Yilgarn craton, Western Australia. *Precambrian Research*, **68**, 43-64.

Perring, C.S., Barley, M.E., Cassidy, K.F., Groves, D.I., McNaughton, N.J., Rock, N.M.S., Bettenay, L.F., Golding, S.D. and Hallberg, J.A., 1989. The association of linear orogenic belts, mantle–crustal magmatism and Archaean gold mineralisation in the Eastern Yilgarn Block of Western Australia. *Economic Geology*, Monograph **6**, 571–585.

Redman, B.A. and Keays, R.R., 1985. Archaean basic volcanism in the Eastern Goldfields Province, Yilgarn Block, Western Australia. *Precambrian Research*, **30**, 113-152.

Ross, A.A., Barley, M.E., Ridley, J.R. and McNaughton, N.J., 2001. Two generations of gold mineralisation at the Kanowna Belle gold mine, Yilgarn Craton, *in* Cassidy, K.F. et al. eds., *4th International Archaean Symposium 2001, Extended Abstracts*, AGSO – Geoscience Australia, Record **2001/37**, 398-399.

Smithies, R.H. and Witt, W.K., 1997. Distinct basement terranes identified from granite geochemistry in late Archaean granite–greenstones, Yilgarn Craton, Western Australia, *Precambrian Research*, **83**, 185-201.

Sofoulis, J., 1963. Boorabin, W. A. *Western Australia Geological Survey*, 1:250 000 Geological Series Explanatory Note.

Swager, C.P., 1989. Structure of the Kalgoorlie greenstones regional deformation history and implications for the structural setting of gold deposits within the Golden Mile. *Western Australia Geological Survey, Report* **25**, 59-84.

Swager, C.P., 1995. Geology of the greenstone terranes in the Kurnalpi–Edjudina region, southeastern Yilgarn Craton. *Western Australia Geological Survey, Report* **47**, 31p.

Swager, C.P., 1997. Tectono-stratigraphy of late Archaean greenstone terranes in the southern Eastern Goldfields, Western Australia. *Precambrian Research*, **83**, 11-42.

Swager, C.P. and Griffin, T.J., 1990a. Geology of the Archaean Kalgoorlie Terrane (northern and southern sheets). *Western Australia Geological Survey*, 1:250 000 geological map.

Swager, C.P. and Griffin, T.J., 1990b. An early thrust duplex in the Kalgoorlie-Kambalda greenstone belt, Eastern Goldfields Province, Western Australia. *Precambrian Research*, **48**, 63-73.

Swager, C.P. and Nelson, D.R., 1997. Extensional emplacement of a high-grade granite gneiss complex into low grade granite greenstones, Eastern Goldfields, Western Australia. *Precambrian Research*, **83**, 203-209.

Swager, C.P., Goleby, B.R., Drummond, B.J., Rattenbury, M.S. and Williams, P.R., 1997. Crustal structure of the granite-greenstone terranes in the Eastern Goldfields, Yilgarn Craton, as revealed by seismic reflection profiling. *Precambrian Research*, **83**, 43-56.

Swager, C.P., Griffin, T.J., Witt, W.K., Wyche, S., Ahmat, A.L., Hunter, W.M. and McGoldrick, P.J., 1990. Geology of the Archaean Kalgoorlie Terrane - an explanatory note. *Western Australia Geological Survey, Record* **1990/12**.

Swager, C.P., Griffin, T.J., Witt, W.K., Wyche, S., Ahmat, A.L., Hunter, W.M. and McGoldrick, P.J., 1995. Geology of the Archaean Kalgoorlie Terrane - an explanatory note. *Western Australia Geological Survey, Report* **48**, 26p.

Swager, C.P., Witt, W.K.,Griffin, T.J., Ahmat, A.L., Hunter, W.M., McGoldrick, P.J. and Wyche, S., 1992. Late Archaean granite-greenstone of the Kalgoorlie Terrane, Yilgarn Craton, Western Australia: *in* Glover, J.E. and Ho. S.E., eds., *The Archaean. Terrains, processes and metallogeny*, University of Western Australia, Geology Department and University Extension, Publication Number **22**, 107-122.

Tyler, I.M. and Hocking, R.M., 2002. A revision of the tectonic units of Western Australia. *Western Australia Geological Survey*, Annual Review 2000–2001, 33–44.

White, R., and McKenzie, D., 1989. Magmatism at rift zones: the generation of volcanic continental margins and flood basalts: *Journal of Geophysical Research*, **94/B6**, 7685-7729.

Williams, P.R., 1993. A new hypothesis for the evolution of the Eastern Goldfields Province, in Kalgoorlie 93, *in* Williams, J.A. and Haldane, J.A., eds., *An international conference on crustal evolution, metallogeny, and exploration in the Eastern Goldfields*, Australian Geological Survey Organization, Record **1993/54**, 77-84.

Witt, W.K., 1994. Geology of the Bardoc 1: 100 000 sheet. *Western Australia Geological Survey, 1:100 000 Geological Series Explanatory Notes*, (a preliminary edition of these notes was published in 1990 as Record 1990/14).

Witt, W.K. and Davy, R., 1997. Geology and geochemistry of Archaean granites in the Kalgoorlie region of the Eastern Goldfields, Western Australia: a syn-collisional tectonic setting. *Precambrian Research*, **83**, 133-183.

Witt, W.K., Swager, C.P. and Nelson, D.R., 1996. 40Ar/39Ar and U-Pb constraints on the timing of gold mineralization in the Kalgoorlie gold field, Western Australia —A discussion. *Economic Geology*, **91**, 792-795.

Woodall, R., 1965. Structure of the Kalgoorlie Goldfield. *in* McAndrew, J., ed., *Geology of Australian Ore Deposits* (2nd ed.), Commonwealth Mining and Metallurgical Conference, **1**, 71-79.

Wyborn, L.A.I., 1993. Constraints on interpretations of lower crustal structure, tectonic setting and metallogeny of the Eastern Goldfields and Southern Cross Provinces provided by granite geochemistry. *Ore Geology Reviews*, **8**, 125–140.

SEISMIC INTERPRETATION OF THE NORTHEASTERN YILGARN CRATON SEISMIC DATA

B.R. Goleby[1], R. Blewett[1], B. Groenewald[2], K. Cassidy[1], D. Champion[1], R.J. Korsch[1], A. Whitaker[1], L.E.A. Jones[1], B. Bell[1], and G. Carlson[3].

[1] Predictive Mineral Discovery Cooperative Research Centre, Geoscience Australia, P.O. Box 378, Canberra, ACT, 2601, Australia

[2] Kalgoorlie Regional Office, Geological Survey of Western Australia, P.O. Box 1664, Kalgoorlie, W.A., 6430.

[3] Geological Survey of Western Australia, Minerals House, 100 Plain Street, East Perth, W.A., 6004

An overview of the seismic traverse

The crustal architecture of the mineralised northeastern Yilgarn Craton is poorly understood. In addition, the relationship between the northeastern Yilgarn Craton and the overlying Proterozoic and Phanerozoic sedimentary basins to the east is also poorly understood but is of interest to both the mineral and petroleum exploration industries. Geoscience Australia (GA) and the Geological Survey of Western Australia (GSWA), in conjunction with the Predictive Mineral Discovery Cooperative Research Centre (*pmd**CRC), acquired over 430 km of deep seismic reflection data in the northeastern part of the Yilgarn Craton in Western Australia in 2001 (Figure 1).

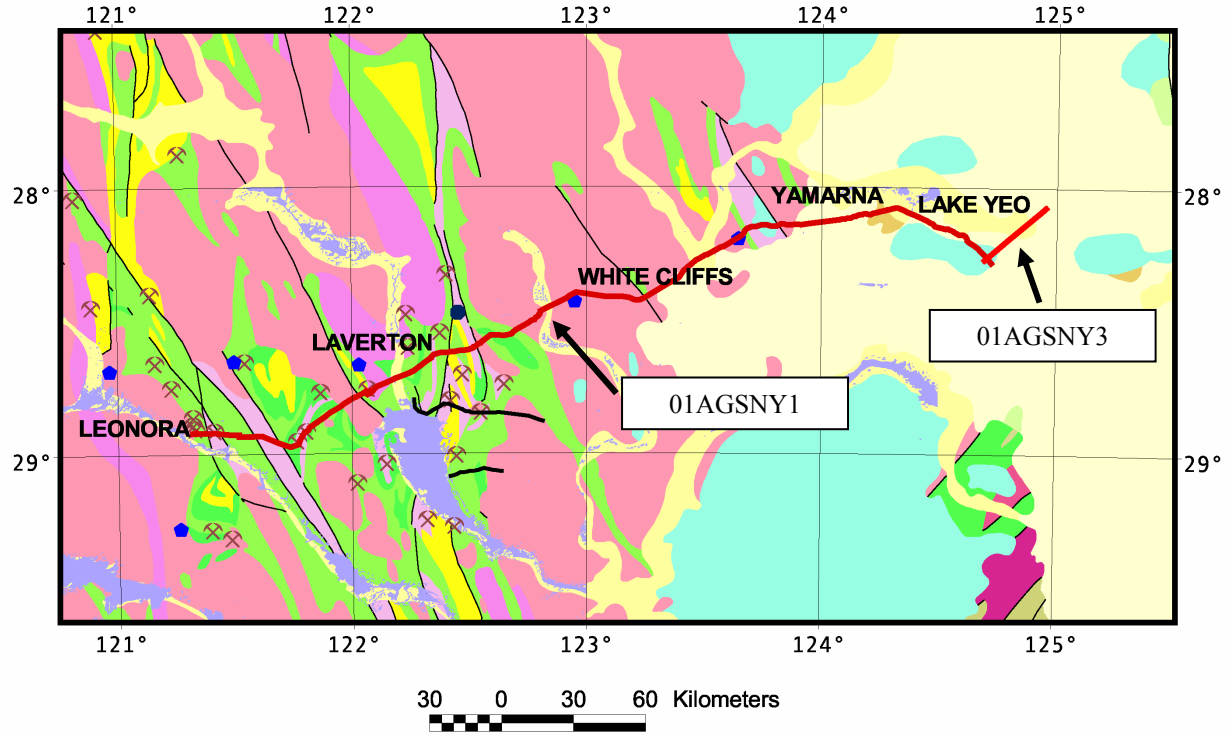

Figure 1: Location of the 2001 Northeastern Yilgarn deep seismic reflection traverse in the Eastern Goldfields region of the Northern Yilgarn. The background is taken from the 1:5m Geology Map of Australia. The deep seismic reflection traverse is shown in red. The blue dots are broadband instrument locations, positioned to determine receiver function values for this area.

Deep seismic reflection data were collected along an east-west traverse, made up of two traverses, 01AGSNY1 and 01AGSNY3 (Figure 1). Jones et al. (this volume) described the acquisition and processing of the data. The 384km long regional traverse, 01AGSNY1, had its western end within the Sons of Gwalia gold mine lease near Leonora and extended eastwards past Laverton and Yamarna before finishing in the Officer Basin to the east of Lake Yeo. Traverse 01AGSNY3 was 52 km long. It trended northeast from the eastern end of 01AGSNY1, passing over the mineral exploration drill hole NJD1 and continued further into the Officer Basin.

For the purposes of interpreting the two deep seismic sections, we treat both sections as part of one continuous regional profile.

The following descriptions are based on our initial interpretation of the seismic data. The interpretations are consistent with the forward modelled gravity and magnetic profiles along the seismic traverse and the known geological data. In several places however there are several interpretations that are plausible and further information is required before a final interpretation can be made.

Throughout this paper we use the term granite as a general term to indicate intrusive rocks ranging in composition from quartz diorite through to syenogranite. We also use the term greenstone succession to refer to the package of ultramafic and mafic rocks that also contain felsic volcanic units, sediments and younger conglomerates. We use the term mafic to refer to both ultramafic and mafic rocks and the term felsic to represent any rock that has a low density (up to 2.7 gm/cm^3). Thus the term felsic can refer to a sedimentary, granitic, gneissic or non-mafic volcanic rock.

Interpretation Methodology

The methodology used to interpret the deep seismic reflection data was as follows:

- Identify prominent trends in the seismic reflectivity by highlighting the main trends defined by the stronger reflections,
- Identify angular relationships between different reflective packages, that indicate an inferred discontinuity in geology,
- Draw boundaries around regions of similar reflectivity and/or between regions of different reflectivity to create packages or domains of consistent reflectivity. To be consistent, the tops of highly reflective zones were used to define the boundary to the domain (here we used similarities in the amplitude, coherency and dip of the seismic reflections to define the regions),
- Identify major large-scale trends in reflectivity, for example, reflectivity that extends over large distances, either as dipping bands or sub-horizontal bands (e.g. the Moho),
- Using the known surface geology, project the geological units and mapped faults to depth along previously defined reflective zones or boundaries between the reflection zones respectively,
- Identify the presence kinematic indicators (eg reflection truncations showing a sense of relative movement) that suggest movement directions or sense of displacement,
- Extend the surface geological and structural information to depth and link this geometry to the major large-scale trends and package or domain boundaries interpreted in the deeper crust to create a crustal structure that is consistent with the geology and the seismic data,
- Where features have been mapped at the surface but have not been imaged by the seismic data, investigate likely depth extents possible within the seismic reflectivity constraints

and then complete the upper geological succession. It is assumed that these structures or units are non-reflective,

- Add interpretations to the section to account for areas of strong reflectivity that do not correlate to known geological structures of units,
- The seismic interpretation was then cross-checked against known geology and against other geological and geophysical data sets (eg drill hole information), and finally
- The seismic interpretation was forward modelled using both gravity and magnetic data to test for consistency.

Scale is very important. All sections were plotted at a V/H ratio equal to 1, assuming an average crustal velocity of 6 km/s. Detailed seismic sections were plotted at 1:25 000 scale to approximately 12 km depth. These were used to interpret the greenstone succession geology and structure on the seismic data and relate it to the known surface geology. Smaller scaled seismic sections were plotted at 1:100 000 scale to approximately 54 km depth (18 s) and were used to interpret the larger structures and to check continuity of reflectivity through the crust. Even smaller scaled sections plotted at 1:250 000 and 1:500 000 (at V/H=2) were used to investigate the deeper structure.

The seismic traverse had several significant changes in direction (Figure 1). These allowed a partial three-dimensional view of the crust in places.

In several areas, unusual looking reflections, including reflection with opposing dips that crossed over each other, were regarded as suspect. In these cases, small portions of the seismic data were reprocessed to check the effects of this suspect data. In most cases the suspect reflections were inferred to be from surfaces 'out-of-the-plane' of the seismic section.

Seismic Characteristics

The seismic data quality is very good, with a good range of frequencies recorded, indicating that the attenuation of the bedrock is low. The coherency of the returned seismic signal is variable, with some areas showing continuity of reflections for a distance of over 4 km near the surface and longer with depth. The complex deformation in the granite-greenstone succession, however, has destroyed any large continuous reflectivity and made interpretation more difficult.

The major cause of the reflectivity throughout the section is interpreted to represent shear zones. There are only two areas where lithological reflections have been interpreted, in the Welcome Domain and in the Laverton Tectonic Zone. According to the potential field modelling, the higher amplitude reflectivity is found in areas that are low in density. This suggests that these areas consist of foliated gneiss, sheared gneiss or even mylonite, with the reflectivity caused by the summation of seismic signal reflected from the tops and bases of the zones of varying mineral assemblages within these rocks. The areas where there are large volumes of mafic material are less reflective and have lower amplitude reflections than expected.

Finally it should be pointed out that the seismic method tends to image more horizontal and straighter structures than folded or deformed structures. There is a preference to image the latest deformation over the older more deformed surfaces. Late structures are imaged better because they cut across and deform earlier structures.

Main seismic features of the Northeastern Yilgarn seismic transect

The Northeastern Yilgarn deep seismic reflection transect is characterised by several prominent features (Figure 2), which are related to the seismic characteristics of the crust. These features are:

- a change in the thickness of the crust across the Northeastern Yilgarn Craton,
- a subdivision of the crust into three broad layers,
- a prominent east dip to the majority of the reflections, and
- three east dipping crustal-penetrating shear zones.

The crust is approximately 40 km thick in the Leonora-Laverton region, and thickens eastwards towards the Albany-Fraser Province; a feature also noted on the Eastern Goldfields seismic data (Goleby *et al*., 2000). There is a prominent sub horizontal thin band of reflections that we interpret as the Moho and which defines the seismic base of the crust. There is no refraction data in the region to confirm that this boundary is the Moho, however, refraction to the southwest indicates that the Moho is at a similar depth. The Moho's seismic character and its position is similar, although a bit deeper, to that interpreted on the regional Eastern Goldfields Traverse 91EGF01 (Goleby *et al*., 2000). The Moho is interpreted to be at about 13.5 s (40 km) beneath the town of Leonora, deepening to about 15.5 s (46 km) at the eastern end of the traverse. This deepening of the Moho is achieved by a series of ramps and flats, with the Moho generally sub-horizontal for long sections, and then it ramps down over a short distance. This is similar to that seen in the regional Eastern Goldfields Traverse 91EGF01.

Based on the overall seismic characteristics seen in the section, the crust is subdivided into three sub horizontal layers. The lowest layer is considered to be a ductile lower crustal unit. There are only two instances where dipping reflections are seen in this layer and they both relate to the deep penetrating shears. The upper surface of this sub horizontal layer is defined by a sudden change in reflection character to a zone where large packages of dipping reflectivity are the norm. The seismic reflectivity in this middle level is characterised by numerous prominent east-dipping reflections that can be subdivided into large units that have similar seismic character, producing large-scale, lozenge-like, mid-crustal bodies. The boundary between the middle and upper layers is diffuse and irregular in geometry. The upper layer is far more complex and variable in its seismic character.

There is a very pronounced dip to the east for the majority of the reflectivity seen along the seismic traverse, both in the middle and upper levels of the crust. West-dipping features are also imaged, but these are restricted to only a few locations. These will be discussed in detail below. The east-dipping reflections generally have a shallow dip, typically around 30°.

Within this east-dipping fabric, there are three prominent east-dipping zones of reflectivity that cut deep into the crust. These three deep penetrating shear zones divide the Northeastern Yilgarn Craton into four distinct domains, and are interpreted to represent the Mount George Shear Zone, the Laverton Shear Zone and the Yamarna Shear Zone. The Yamarna Shear Zone dips at about 30° and is wider at the surface that at depth. The shears can be traced from the surface to the lower crust and in two cases to the Moho. The Laverton and the Yamarna Shear Zones are the more clearly defined, whereas the Mount George Shear Zone appears to have been intruded by later granite emplacement or subsequent deformation. All three deep penetrating shear zones have a complex geometry, suggesting that these zones have seen several episodes of deformation. The domains defined by these crustal penetrating shear zones are the region from the Ida Fault (to the west of the seismic section) to the Mt George Shear

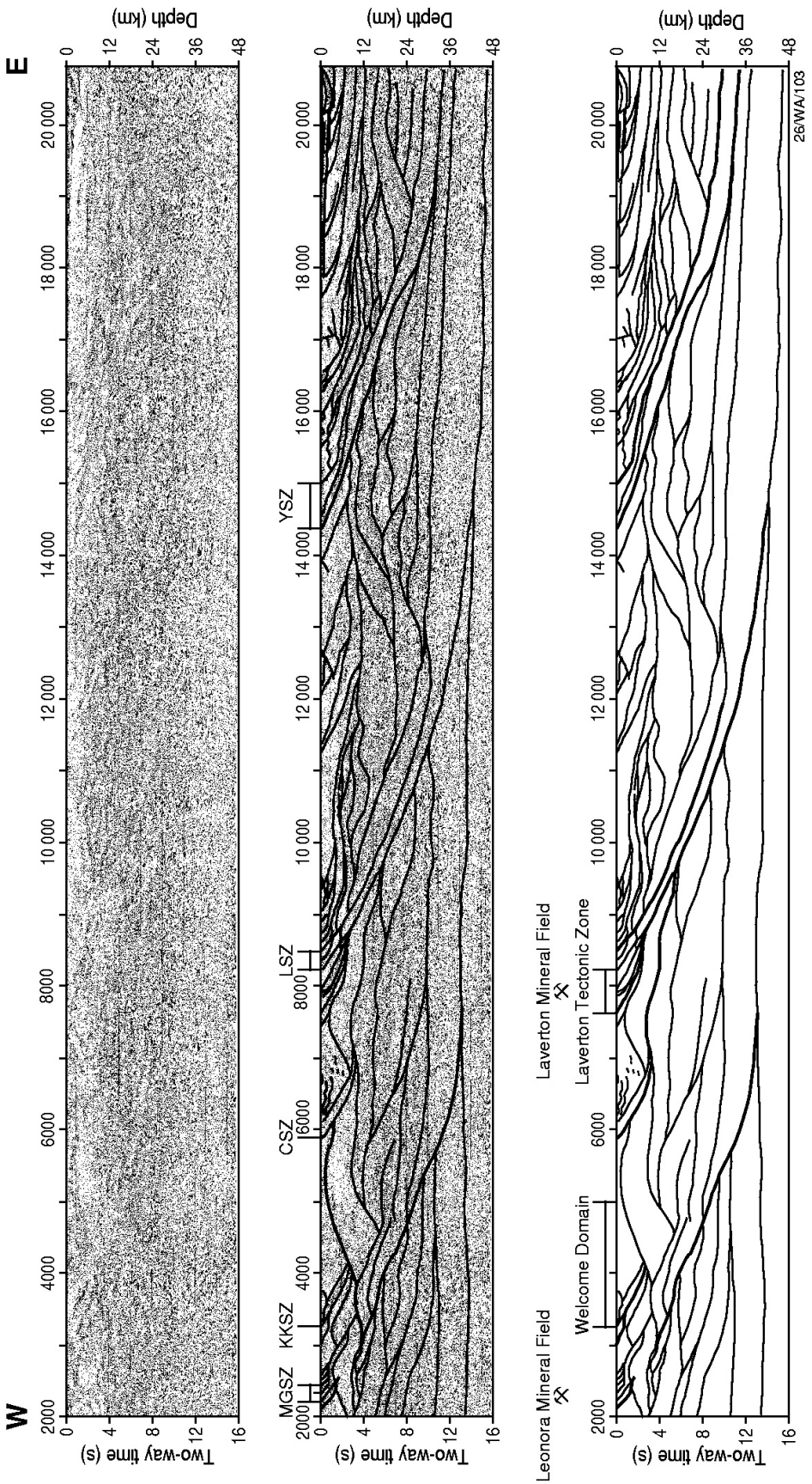

Figure 2: Northern Yilgarn deep seismic data. a) uninterpreted seismic reflection section, b) interpreted seismic reflection section and c) Interpretation only. MGSZ = Mt George Shear Zone, LSZ = Laverton Shear Zone, YSZ = Yamarna Shear Zone, CF = Celia Fault and KKF = Keith-Kilkenny Fault.

Zone, the Leonora to Laverton region between the Mt George and Laverton Shear Zone which contains abundant greenstone, the Laverton Shear Zone to the Yamarna Shear Zone and the Yamarna Shear Zone to the Albany-Fraser region. At the western end of the seismic section, there are sets of east dipping reflective bands (at approximately 6 s to 9 s two-way travel time). Assuming their dip does not change westwards, these project to the surface in the approximate positions of the Menzies and Ballard Faults. The Ida Fault lies farther to the west and is not imaged by this section.

In addition to the dominant seismic features described above, there are a range of features that are important in the interpretation of the seismic data. These are either restricted to one region of the crust or are observations based on similarities between these data and the earlier 91EGF01 seismic traverse.

Compared to the "detachment" recorded in the deep seismic data from the Kalgoorlie region (Goleby *et al*., 2000), there is no single detachment surface that has been imaged within the Northeastern Yilgarn region. There are several areas where a "detachment" is interpreted to be present, but in many places it appears that there could be two or more sub-horizontal shear zones. Rather than use the term 'detachment', we now use the term "low angle shear zones" to refer to such structures.

West dipping structures are rare. They occur as either small structures that are restricted to the uppermost crust and interpreted to represent faults, or as larger bodies defined by coherent west-dipping reflectivity that are seen in several areas within the middle to upper crust. The latter larger bodies are confined to regions close to the major deep penetrating shear zones.

A key feature of the Kalgoorlie area is the 'Y-front' structure formed by the Ida Fault and the Bardoc-Boorara Shear (Drummond and Goleby, 1998; Hall, 1998). In the northeastern Yilgarn seismic data, there is also no clear evidence for a similar 'Y-front'; although the series of west-dipping reflections discussed above may be some structural variation on the 'Y-front'. It is interesting to note that each of these west-dipping packages are wider but shorter, in contrast to the Kalgoorlie region where the major west-dipping structure, the Bardoc Fault, extends from the surface to the Ida Fault.

There is also the suggestion that numerous faults or shear zones have subdivided the upper crustal layer into different packages of material. These packages have been grouped into regions displaying similar reflectivity and presumably indicating similar geology. The seismic reflectivity in this layer has a larger variation in amplitude and even greater variation in continuity and frequency. These variations in seismic characteristic do not appear to be caused by near-surface effects but reflect actual geological variations within the sub-surface.

Two of these shear zones are the Celia Fault and the Keith-Kilkenny Fault (Figure 2). They are interpreted to sole into shear zones within the upper crust, which in turn link to the one of the major crustal penetrating shear zones. This geometry gives the impression of significant amounts of crustal contraction during the last major deformational episode.

Between the Leonora and the Laverton region, there is an undulating contact between the granitoid-greenstone succession and the inferred felsic basement material. This contact is interpreted to be a low angle shear zone because of the marked difference in seismic character of the material above and below it. In addition, there is evidence of an angular relationship between material above and below the contact to the contact itself.

Where 01AGSNY1 ties with 01AGSNY3, there is an approximately 90° angle between the lines (Figure 1). This provides an excellent opportunity to obtain a three-dimensional image of the deeper crust and provide some constraints on the shape of the interpreted deeper bodies. The lozenges interpreted at depth are also lozenge shaped in cross section. This shape reflects the patterns seen on the surface maps. Therefore, the geometries shown by the geological maps are repeated in the third dimension in both the strike and dip directions.

There is a shallow dip to the unconformity between Archaean Northeastern Yilgarn basement and the Proterozoic and younger sedimentary rocks. This unconformity surface and another unconformity surface within the sedimentary rocks of the Neoproterozoic Officer Basin are planar, but appear to be cut by numerous faults. These faults may originally be Archaean in age but the latest movement is interpreted to be post-Mesoproterozoic, especially at the eastern margin of the traverse. It is uncertain as to how far this deformational event extends westwards into the Yilgarn Craton.

There is a correlation between the surface outcrops of the major crustal penetrating shear zones with the regions where the major mineral fields are located. The Leonora mineral field is located close to the Mt George Shear Zone and the Laverton mineral field is located close to the Laverton Shear Zone.

In summary, there are at least three major crustal penetrating east dipping shear zones with the Eastern Yilgarn Province of the Northeastern Yilgarn. These shear zones divide the region into four domains. Each shear zone has a similar geometry to the other (Figure 3). In the hanging wall of the shear, there is evidence of increased deformation, which decreases eastwards away from the shear. There is evidence for a low angle shear zone or detachment surface at depth in the hanging wall of each shear. In the footwall, the seismic character shows a large body of non-reflective material, suggesting the presence of a large granite intrusion or a zone of massive leaching and homogenisation. At depth, there is commonly a west-dipping package of reflectivity.

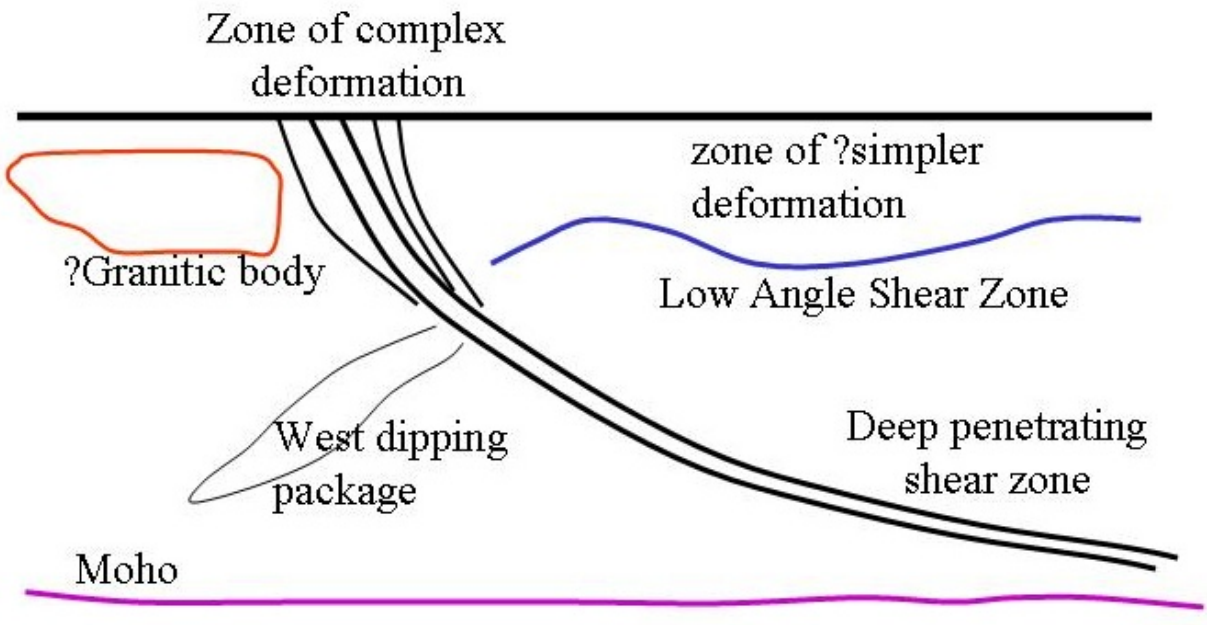

Figure 3: Schematic representation of the features associated with the three major crustal penetrating shear zones.

The Western Portion - Leonora to Laverton

The western part of the seismic reflection profile images a marked partitioning of the crust into three broad domains. The three domains are divided by the Mt George Shear Zone and the Laverton Shear Zone (Figure 2). Between these shear zones the upper crust is characterised by broad open flat structures see (Figure 2). This style is partly a function of the oblique section of the profile with respect to regional strike. However, this style is considered to be real because few major faults transect the area, and the known surface geology (Murrin Domain and western Laverton Domain) contains some of the most complete stratigraphic succession of the profile area. In contrast, to the west of the Kilkenny Shear Zone, and to the east of the Laverton Shear Zone, the geometry of the upper crust is characterised by thrust? imbricates, with abundant well-developed seismic reflections and roll-over anticlines developed in the hanging wall of major faults. In these areas, major faults transect the upper and middle crust, and the surface geology is coincident with numerous shear zones and disruption of stratigraphy.

The following section reports on the detail of the geometry of, and possible timing relationships between, the major features imaged by the seismic reflection data between the western end of the seismic profile to just east of Laverton.

Mt George Shear Zone **(Figure 4)**

- The Mt George Shear Zone is a major structure in the Leonora-Laverton transect area.
- The Mt George Shear Zone is an east-dipping planar structure, dips around 30°, and transects the entire crust, and possibly the Moho.
- The edge of the Raeside Batholith is sheared, with a series of parallel reflections merging with the Mt George Shear Zone, marking the deformed batholith margin.
- Below the Raeside Batholith is a strong band of west-dipping reflections that are transected by the Mt George Shear Zone.
- An upper crustal mostly non-reflective zone above the Mt George Shear Zone is interpreted as granite-gneiss. This zone is bounded above by an open antiform that is defined by high amplitude reflections that are transected by the Mt George Shear Zone further west.
- A few strong reflections are evident in the interpreted granitic areas, possibly marking shears or faults.

Melita-Emu Shear Zone **(Figure 5)**

- The Melita-Emu Shear Zone has a thrust geometry with a well-developed hanging wall anticline developed above the thrust plane.
- The sense of movement is east over west in this plane of section.
- The Melita-Emu Shear Zone is a planar structure that dips approximately 30° to the east
- The Melita-Emu Shear Zone is cut by the Yundamindra LASH1 at a depth of approximately 10 km (3.5 secs TWT).

[1] LASH is an acronym for low-angle shear [zone] and is distinguished from ‘detachment’ because of the genetic connotations of the latter.

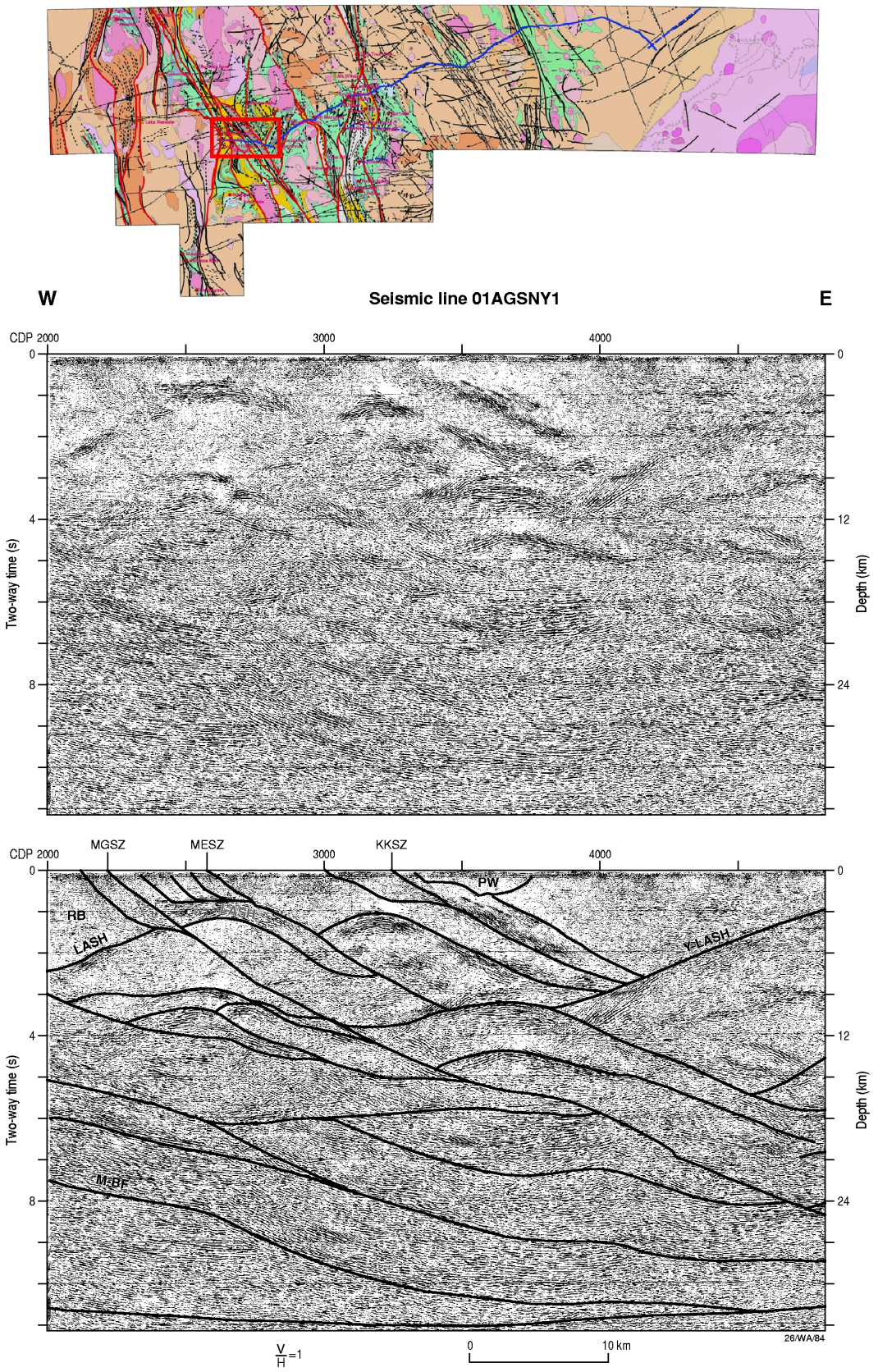

Figure 4. General view of the seismic line (data and interpretation) from the Raeside Batholith (RB) to east of the Pig Well sequence (PW). Note prominent east-dipping reflections in the upper crust and the thrust-duplex geometry. MGSZ = Mt George Shear Zone, MESZ = Melita-Emu Shear Zone, KKSZ = Keith Kilkenny Shear Zone, YLASH = Yundamindra (Low-Angle) Shear Zone, LASH = Low-Angle Shear Zone.

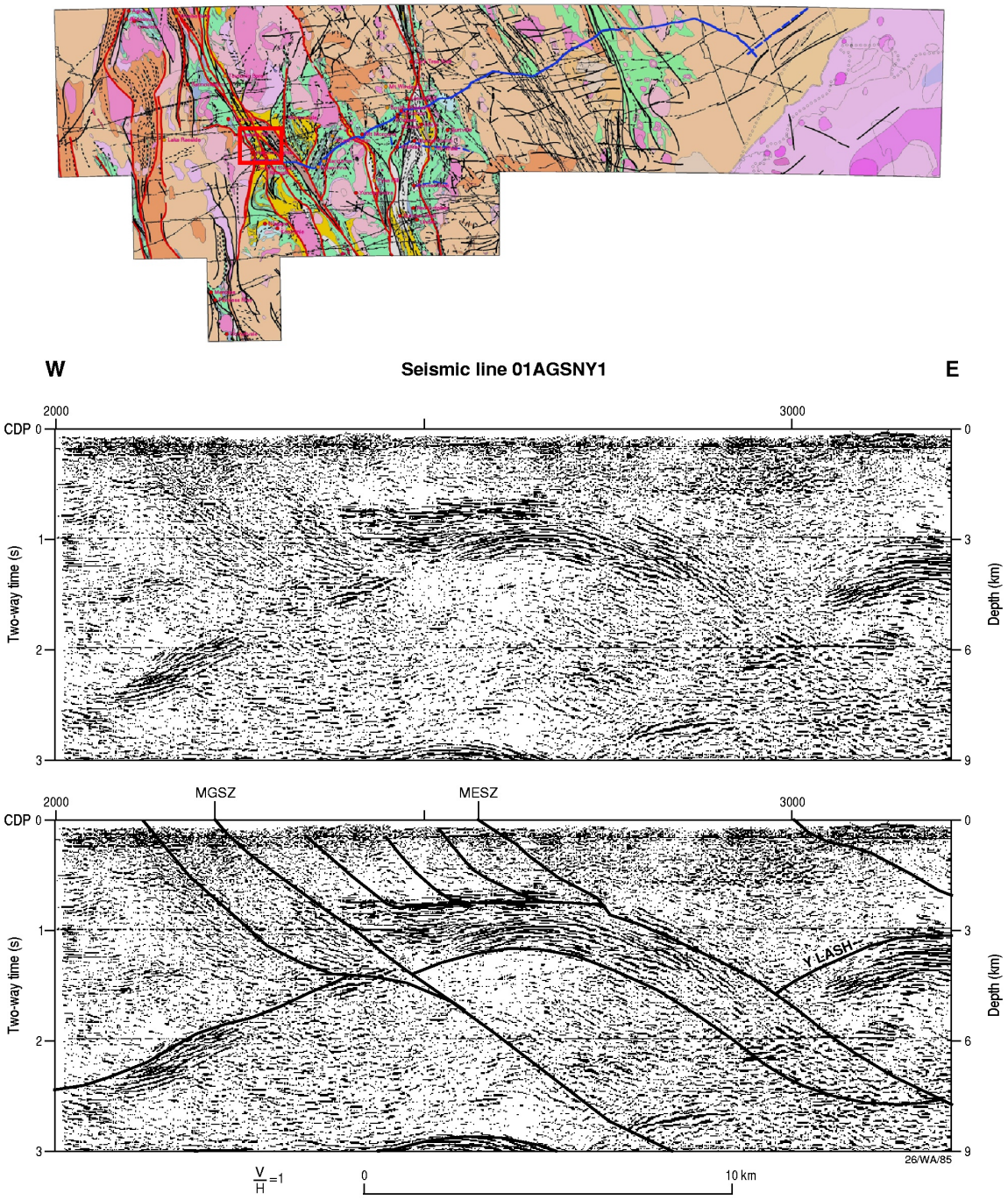

Figure 5. Detailed view of the seismic line (data and interpretation) of the Mt George Shear Zone (MGSZ) and Melita-Emu Shear Zone (MESZ). YLASH = Yundamindra (Low-Angle) Shear Zone.

Kilkenny Shear Zone **(Figure 6)**

- The Kilkenny Shear Zone is difficult to precisely locate on the seismic reflection data. In this interpretation, it is located at the base of a series of high-amplitude parallel reflections that dip to the east at approximately 30° under the Pig Well sequence.
- The high-amplitude reflections may represent stratigraphy or lithology as opposed to structural discontinuities.
- The Kilkenny Shear Zone bounds an 8 km thick section in its hanging wall to the west, and is cut by the Yundamindra LASH.

- The Pig Well sequence appears to have truncations of east-dipping reflections at a depth of no more than 1.2 km.
- This interpretation differs from that presented by Blewett et al. (2002), where the Kilkenny Shear Zone is interpreted as a deeper structure that cuts the Yundamindra LASH.
- A strong set of reflections located at the intersection of the Kilkenny Shear Zone and the Yundamindra LASH are interpreted here as out of plane artefacts.

Alternative interpretations to the above include:

- The Kilkenny Shear Zone cuts the Yundamindra LASH and is a deep penetrating structure (cf. Blewett et al., 2002).
- The Kilkenny Shear Zone is a splay off the Yundamindra LASH (which is cut by the Celia Shear Zone to the east). However, the Yundamindra LASH almost approaches the surface between the two major structures, suggesting that intersection between the Kilkenny and Celia Shear Zones was close to this section. The two shear zones converge to the southeast.
- The Kilkenny Shear Zone dips west, and has nothing to do with the Pig Well sequence or the Yundamindra LASH. All the surface geology indicate moderate east dips however, and the geometry of the inward converging antiformal reflections on both side of the fault is geologically unreasonable.

Yundamindra (Low-Angle) Shear Zone **(Figure 7)**

- Along the line of section, the Yundamindra LASH is a broad arched (antiformal) structure defined by a series of well-developed high amplitude reflections.
- The crest of the Yundamindra LASH is at approximately 1.5 km depth and 'limbs' extend to a depth of approximately 10 km (in the west) and to a depth of approximately 4 km (in the east).
- The Yundamindra LASH has a strike length of 45 km from its intersection with the Kilkenny Shear Zone in the west, to the Celia Shear Zone in the east.
- The section is partially parallel to the strike of the Yundamindra LASH, and the surface probably dips to the north.
- The Yundamindra LASH bounds a pronounced non-reflective area (granite?), suggesting that the base of the greenstone is very thin under the antiformal crest.
- At a depth of 10 km and extending to the lower crust there are a series of probable thrust(?) duplexes. These suggest that the Yundamindra LASH might be a roof thrust, or a hangingwall culmination.
- Alternatively, the Yundamindra LASH may represent an extensional surface (collapse?) following earlier thrusting.
- In this interpretation, the Yundamindra LASH cuts the Kilkenny Shear Zone and is transected by the Celia Shear Zone.
- Minor vertical offsets of the Yundamindra LASH are locally evident.

Celia Shear Zone **(Figure 8)**

- The Celia Shear Zone is an east-dipping listric structure that soles out into a flat surface at about 9 km depth (3 secs). Below this, there is some upward bowing of the shear zone.
- The Celia Shear Zone merges with, or is truncated by, the Laverton Shear Zone at about 17 km (5.5 secs).
- The Celia Shear Zone cuts the Yundamindra LASH.
- The Celia Shear Zone forms a synformal 'floor' below the greenstone base along the section of the Mt Margaret Anticline.

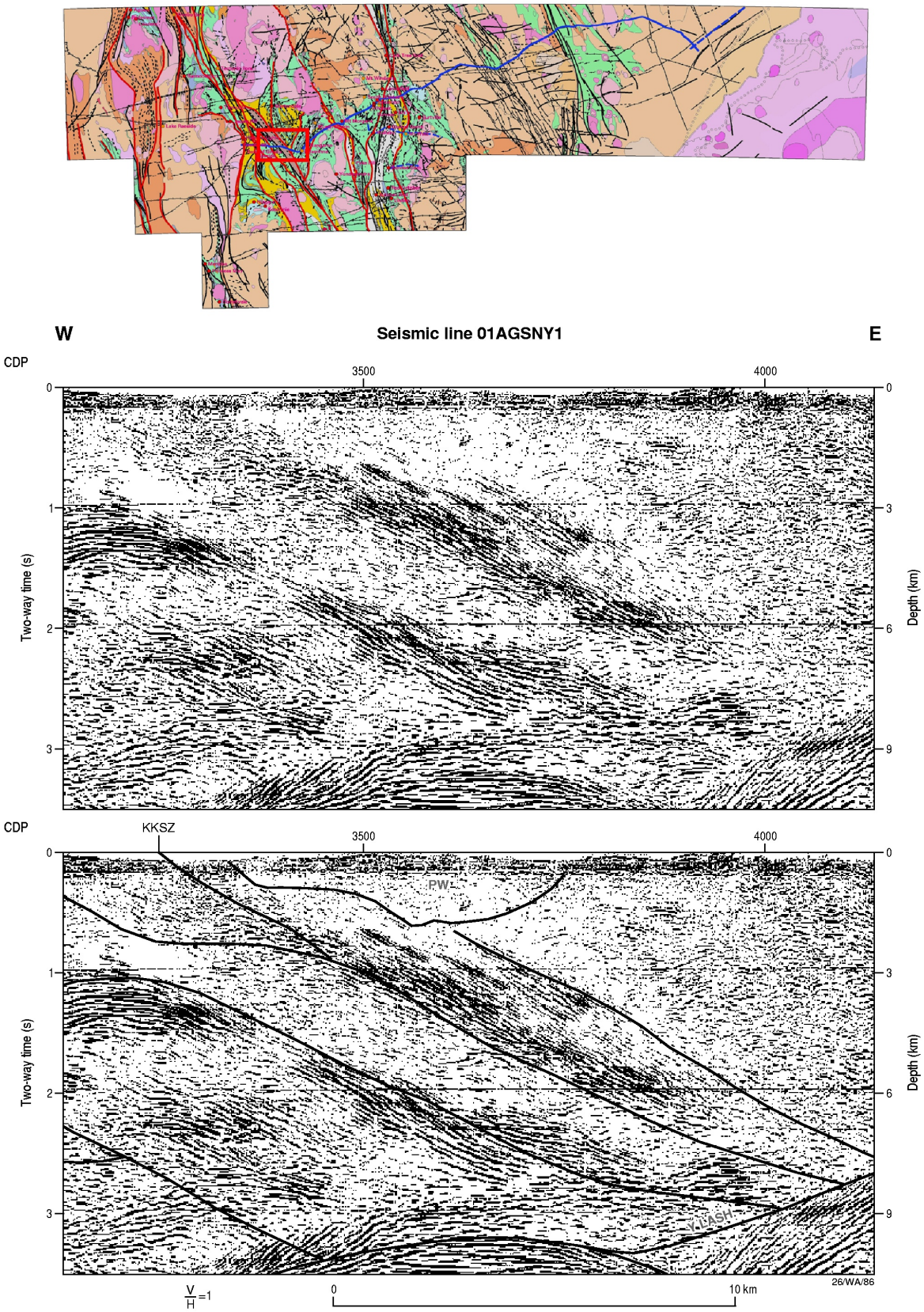

Figure 6. Detailed view of the seismic line (data and interpretation) of the Kilkenny Shear Zone. PW = Pig Well sequence, KKSZ = Keith Kilkenny Shear Zone, YLASH = Yundamindra (Low-Angle) Shear Zone.

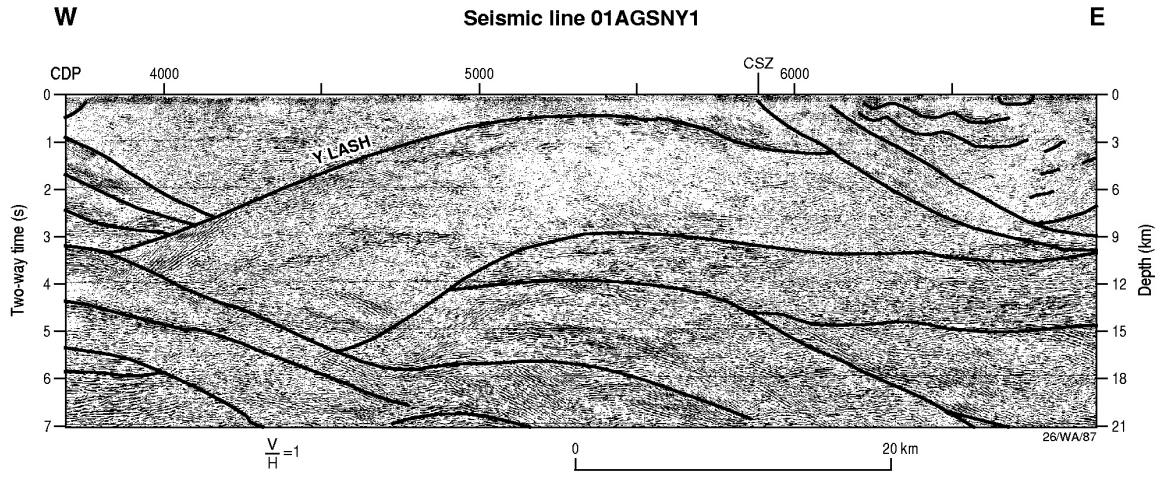

Figure 7. Detailed view of the seismic line (interpretation) of the Yundmindra LASH (YLASH). CSZ = Celia Shear Zone.

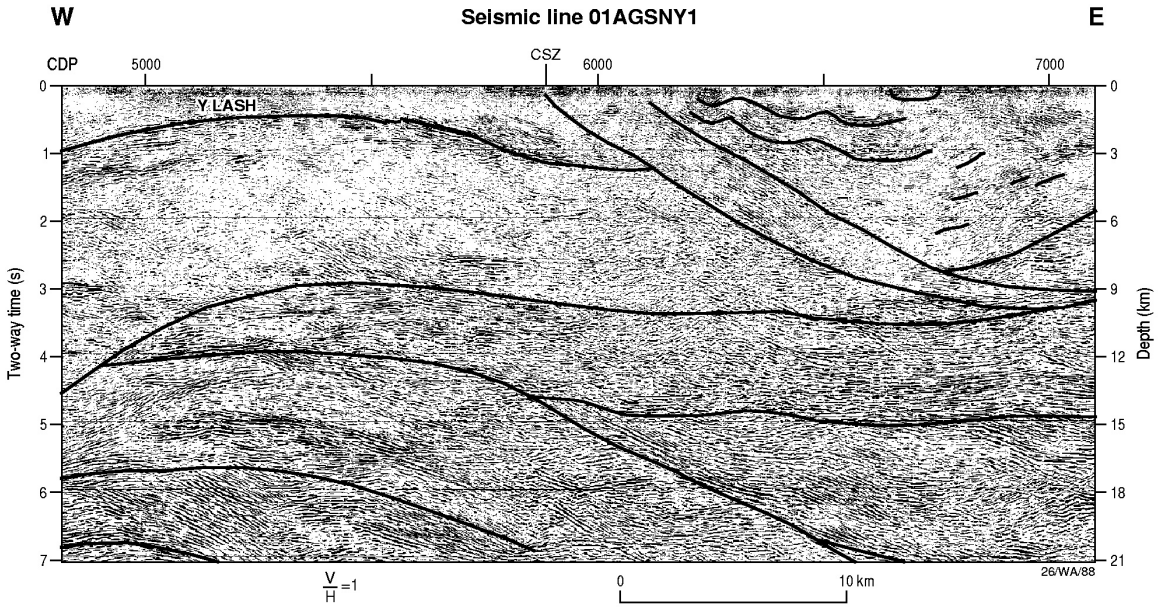

Figure 8. Detailed view of the seismic line (interpretation) of the Celia Shear Zone (CSZ). YLASH = Yundamindra (Low-Angle) Shear Zone.

- A series of undulating reflections below the footwall of the Celia Shear Zone are interpreted as folded gneiss.

Laverton Shear Zone **(Figure 9, Figure 10)**

- The Laverton Shear Zone is the most pronounced cross-cutting structure along the entire seismic section.
- The Shear Zone is imaged by a series of parallel reflections (deformation corridor?) that define a planar structure that dips about 30° to the east.
- Below the top of the lower crust, the Laverton Shear Zone flattens and soles into the Moho.
- The Laverton Shear Zone crosses the section for a total of 140 km (surface to Moho).

- Closer to the surface, the Laverton Shear Zone splays and may represent a master fault to a series of synthetic splays.
- The Laverton Shear Zone cuts, or merges with, the Celia Shear Zone at a depth of about 17 km (5.5 secs).
- A wedge-shaped mid to upper crustal block is defined by the intersection of a series of flat high-amplitude reflections in the hanging wall to the east and the more-steeply east-dipping Laverton Shear Zone.
- A series of high-amplitude reflections between 3 and 6 km depth (1-2 secs) may be caused by lithology rather than imposed structure (shears).

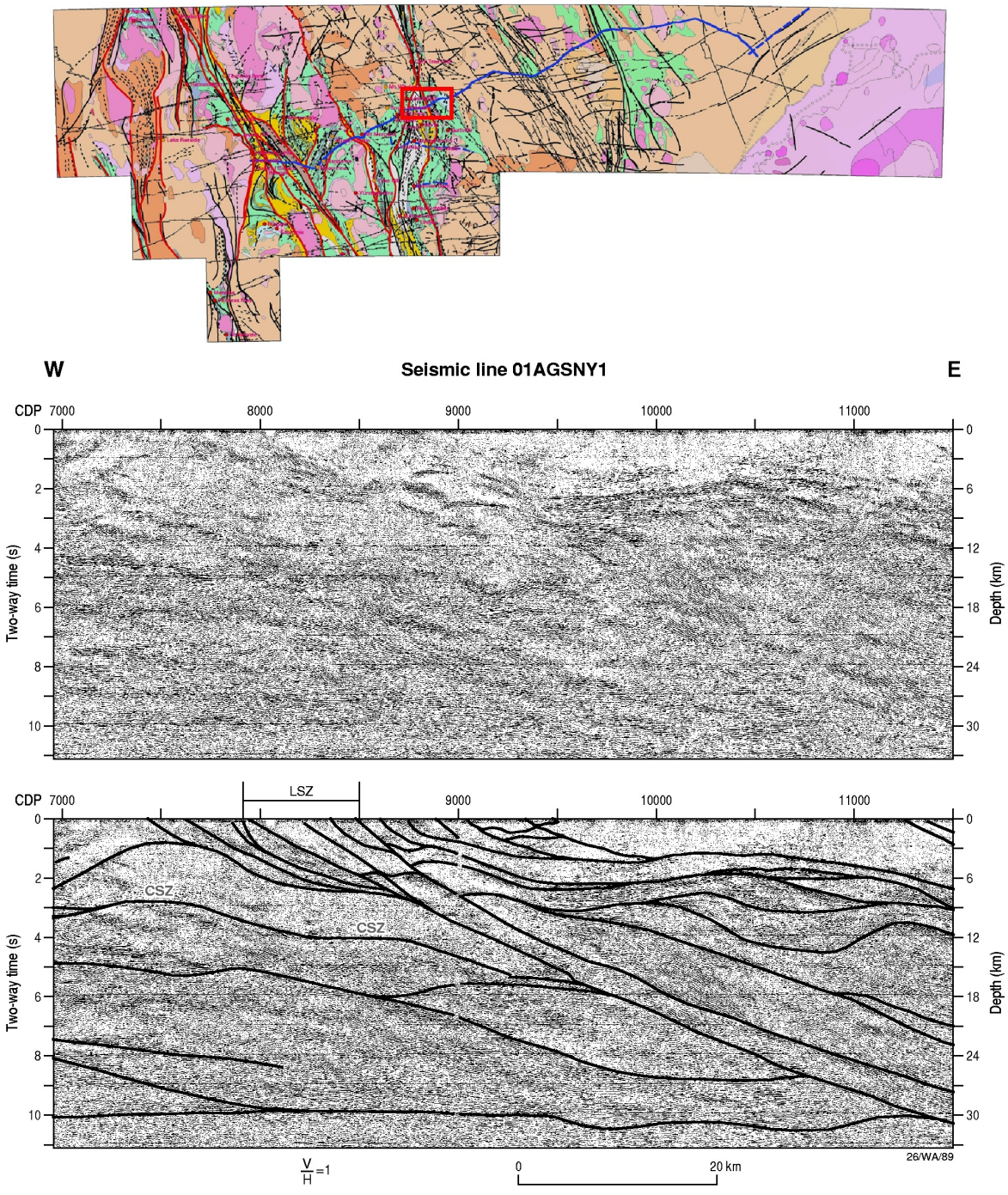

Figure 9. General view of the seismic line (data and interpretation) of the Laverton Shear zone. LSZ = Laverton Shear Zone, CSZ = Celia Shear Zone. V/H = 1 @ 6 km/s.

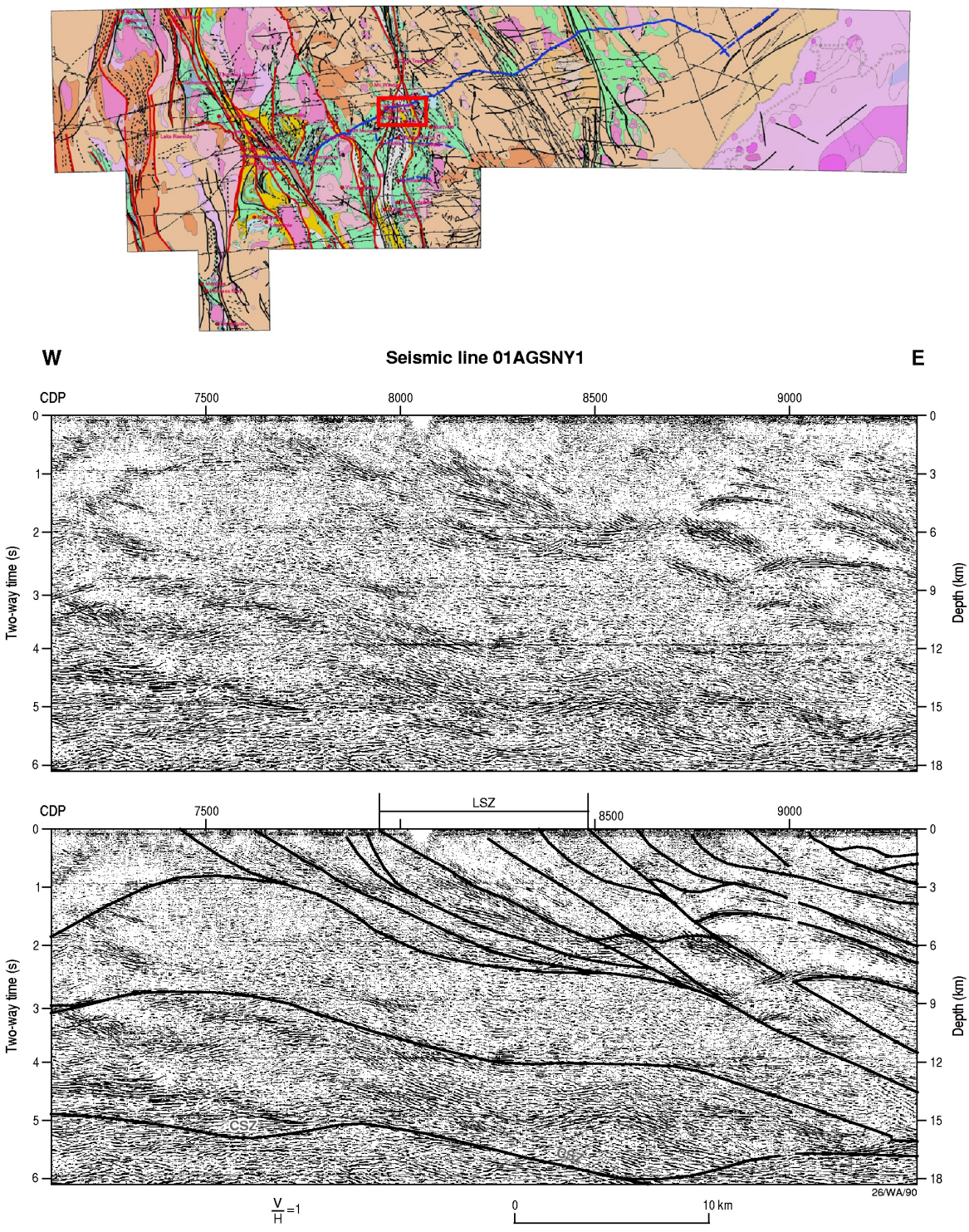

Figure 10. Detailed view of the seismic line (data and interpretation) of the Laverton shear zone. LSZ = Laverton Shear Zone, CSZ = Celia Shear Zone. V/H = 1 @ 6 km/s.

The Eastern Portion - Laverton to Lake Yeo and farther east

This section reports the geometry of, and possible timing relationships between, the major features imaged by the seismic reflection data between Diorite Hill and the end of line 01AGSNY1, as well as line 01AGSNY3. The seismic data for the eastern portion of 01AGSNY1 are shown in Figure 11 and the uninterpreted and interpreted 01AGSNY3 is shown in Figures 12 and 13 respectively.

The region is very poorly exposed, with outcrop restricted to minor Archaean granitoid and greenstone and overlying sedimentary rocks of the Officer and Gunbarrel basins. There is also abundant in situ and transported regolith. The region contains some greenstones, limited to the Mt Sefton and Yamarna greenstone belts, with granite, gneiss and migmatite in the regions between the greenstone belts.

Region of granite-gneiss-migmatite (Point Kidman domain) between Diorite Hill and Mt Sefton greenstone belt **(Figure 14)**

- The region is characterised by generally sub-horizontal to east dipping reflections in the middle and upper crust, with the upper crust containing numerous strong east-dipping reflections. East-dipping reflections in the mid- to lower crust are interpreted to represent the down-dip extension of the Laverton Shear Zone.
- The eastern end of the region contains the poorly exposed Mt Sefton greenstone belt, whose geometry cannot be resolved in the seismic data.
- At the western end of the region, there is a highly reflective sub horizontal package at 2-4 s TWT and dipping slightly to the west. The top of the package may represent a low-angle shear zone (LASH). This is illustrated on Figure 14.
- There is a steeply dipping to sub vertical structure on the western side of this reflective package. It is one of several potential splays off the hanging wall of the Laverton Shear Zone that steepen to the east. It may be a splay of the Laverton Shear Zone or, alternatively, the structure may be the loci for the Diorite Hill mafic magma.
- Above the package is a fairly homogeneous, non- to variably-reflective zone, possibly consisting of intrusive granitoids in a granite-gneiss-migmatite domain. The geometry of this material is unable to be determined, although velocity calculations suggest mainly felsic material in the top few seconds of data.
- There are a series of east-dipping faults in the region. One unnamed interpreted fault in this region is interpreted to project to the surface at CDP 12050. There is obvious disruption in the near surface reflectivity at this CDP, with stronger more continuous reflections from the overlying younger sediments in the hanging wall compared to much weaker, less continuous reflections in the footwall. This suggests late, late Proterozoic or early Palaeozoic movement on the fault.

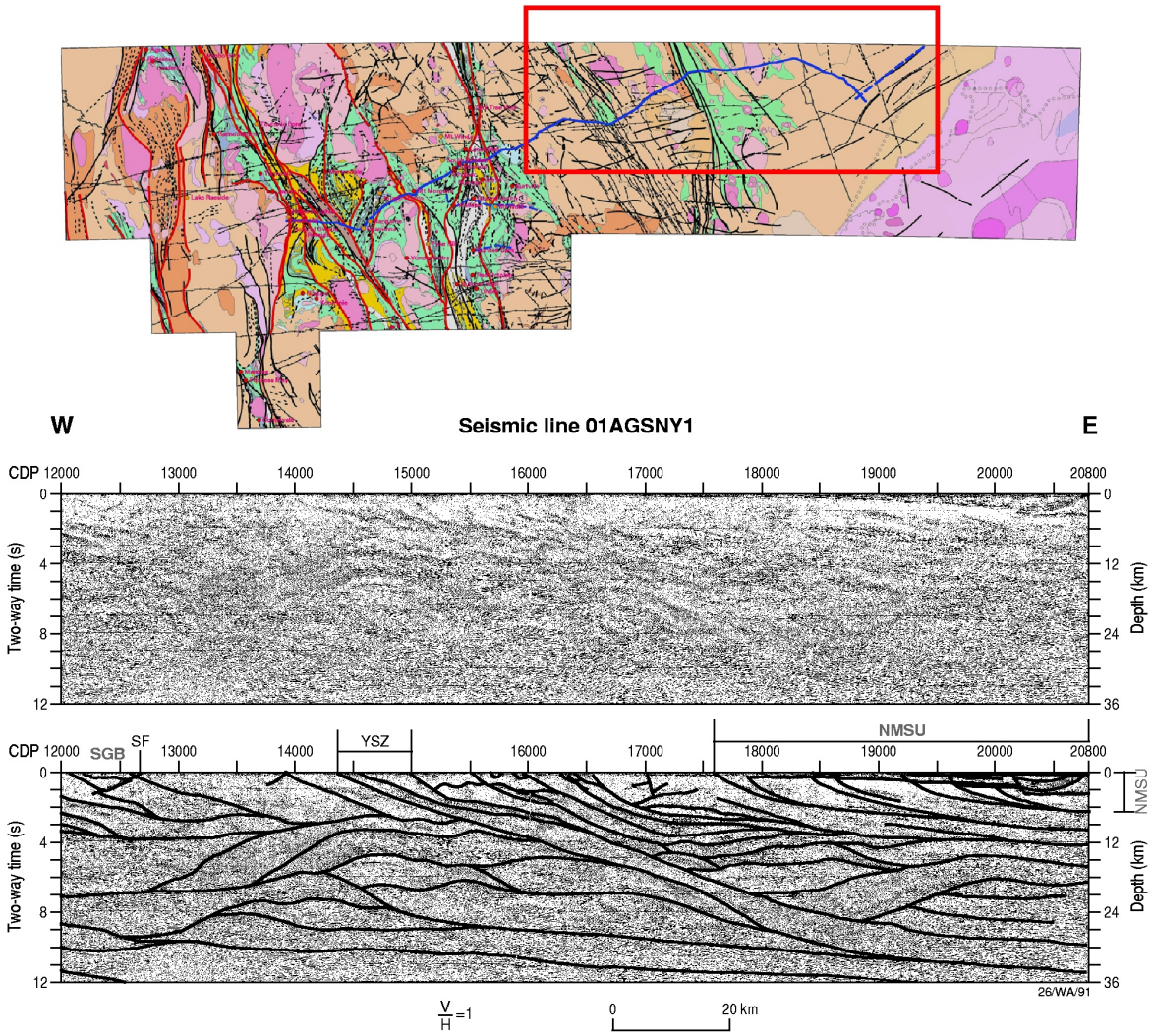

Figure 11. Eastern portion of 01AGSNY1. SGB = Sefton Greenstone Belt, SF = Sefton Fault, NMSU = Neo-Mesoproterozoic Sedimentary Units, YSZ = Yamarna Shear Zone.

- Similar east-dipping faults also occur to the west of this fault. These appear to project to the surface, although it is difficult to interpret them as reaching the surface as there is not the variation in the near-surface that was seen for the fault at CDP 12050. One fault projects to the surface near CDP 11620, and another at about CDP 11250. Although there is no clear evidence, we interpret them as reaching the surface. They can be traced from depths of around 2-3 km to at least 300 m beneath the surface. It is unclear if they are reactivated Archaean, Proterozoic or even later structures. To the north and northeast of the region, post-Earaheedy Basin faults (ie post Mesoproterozoic) can be traced into the Yilgarn (GSWA, unpublished data). In addition, the region (11800-12500 CDP) contains numerous NNW-trending dykes.

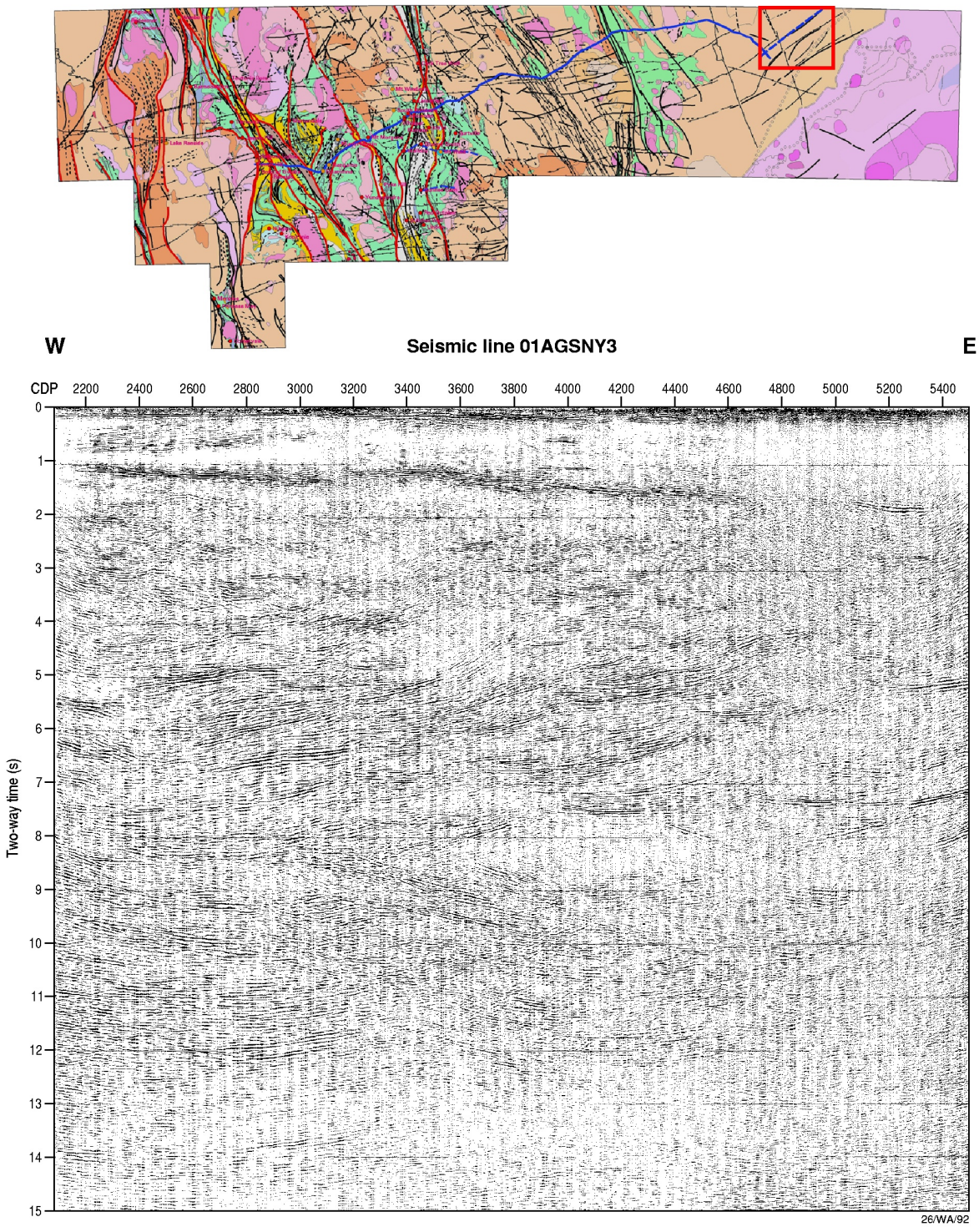

Figure 12. Uninterpreted migrated section for seismic line 01AGSNY3.

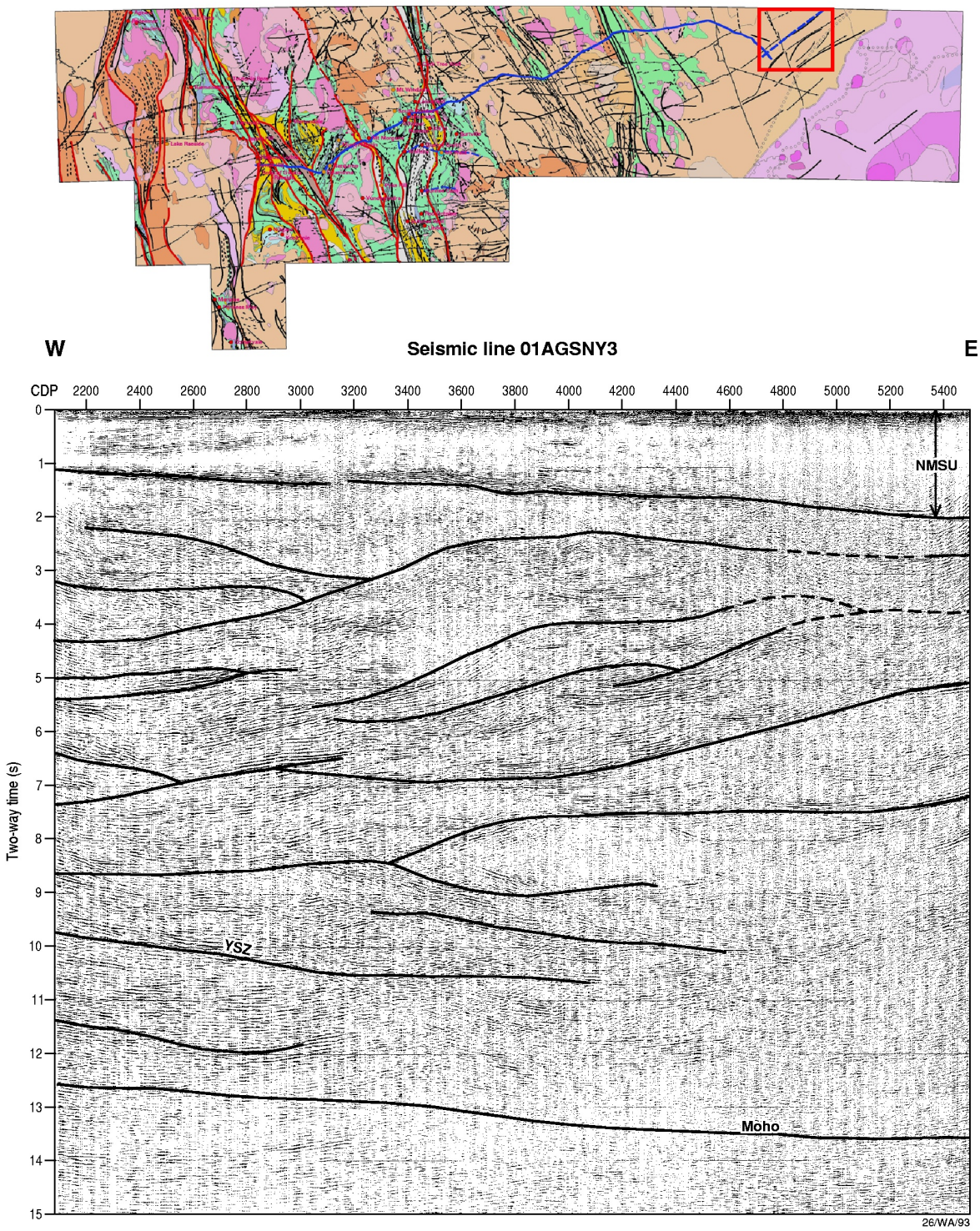

Figure 13. Interpreted migrated section for seismic line 01AGSNY3. NMSU = Neo- Mesoproterozoic Sedimentary Units, YSZ = Yamarna Shear Zone.

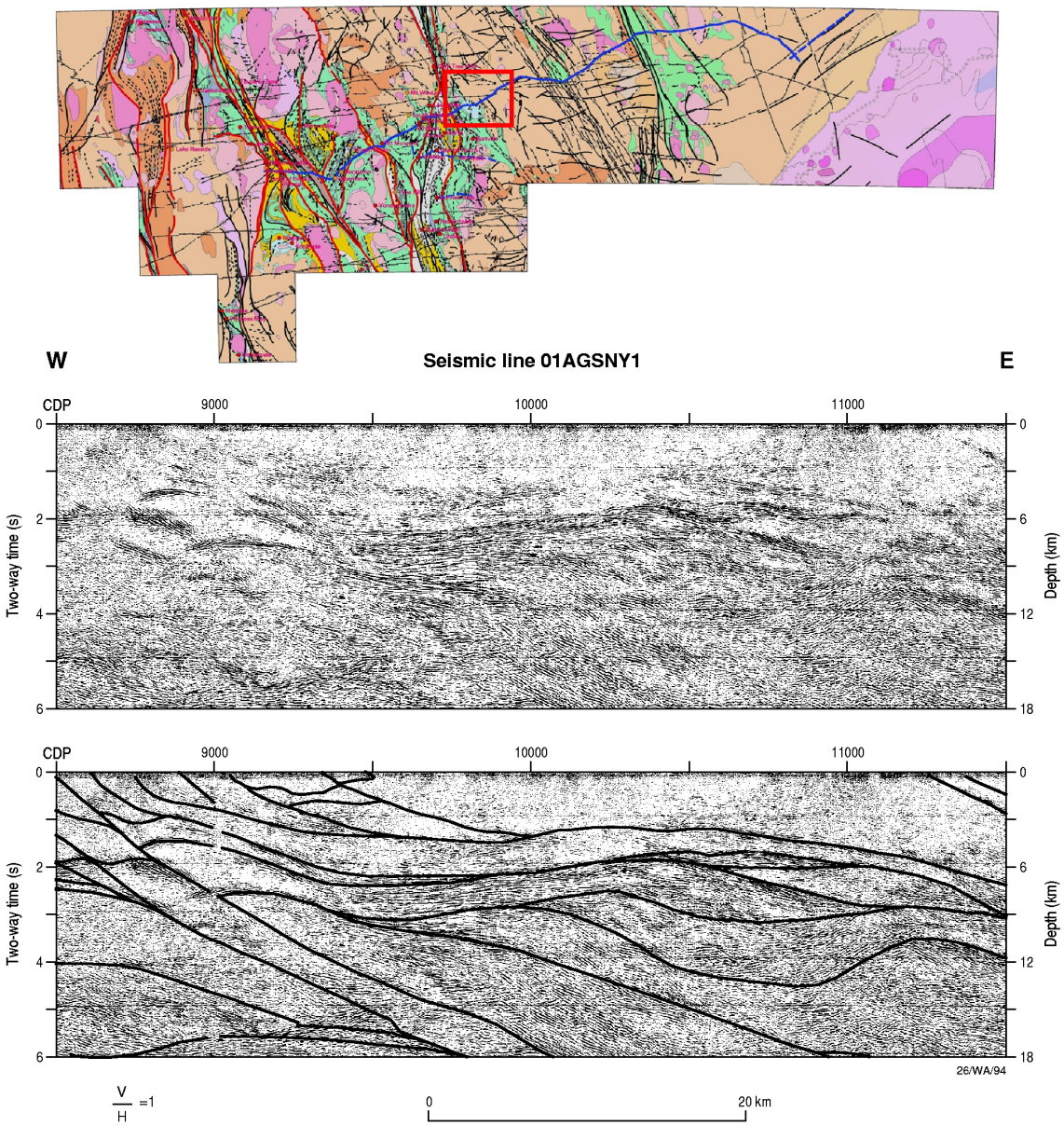

Figure 14. Portion of seismic line 01AGSNY1 to east of the Laverton Tectonic Zone. Top section is uninterpreted migrated seismic section, bottom section is interpreted migrated section. V/H = 1.

Region of granite-gneiss-migmatite east of Mt Sefton greenstone belt and Yamarna greenstone belt **(Figure 15)**

- The region is characterised by dominantly east-dipping reflections in the upper crust (2-3 s TWT), and subhorizontal, east-dipping and west-dipping packages in the mid-crust.
- The mid-crust is dominated by a package of dominantly west-dipping reflections from approximately 3 s to approximately 7 s TWT over a width of 30-35 km. This package is one of only a few west-dipping packages throughout the whole profile. The width of the reflection package is about 7-8 km thick. The west-dipping package appears to sole into the top of the lower crust at about 8 s TWT. The west-dipping package changes to sub horizontal at about 14500 CDP, with the lower part of the package continuous at 4-5 s TWT between 14500 and 16300 CDP where is it cut by the lower part of the Yamarna Shear Zone. This is illustrated on Figure 15.
- The top 1 s of seismic data in dominantly granite-gneiss-migmatite and contains few reflections, with the exception being a few approximately 40º west -dipping reflections (eg CDP 13900, Figure 15) and that are imaged within the upper 3 km. These are unusual features in the seismic profile and are interpreted to be faults.
- One of these fault, the Sefton Fault (CDP 13900, Figure 15), correlates with the position of the eastern contact of the Mt Sefton greenstone belt, interpreted to be a faulted contact by Gower and Boegli (1977). The fault appears to truncate an east-dipping fault at about 1 s (described above), indicating a reverse component of movement on the Sefton Fault. The timing of the displacement is unknown, but in combination with the other west-dipping fault and the inferred timing of the east-dipping structures immediately to the west, the west-dipping faults are definitely post-Archaean, probably post-Proterozoic and possibly even post-Permian.
- The eastern fault is more listric in form, dipping approximately 45º near surface and soling out at about 1 s. The fault may define and/or control the occurrence and preservation of Permian (Gunbarrel Basin) sediments deposited on the Yilgarn Craton. It is interpreted that this west-dipping structure is either Permian or was reactivated since the Permian. The bright near-surface reflections may correspond to outcropping Permian.

Yamarna Shear Zone **(Figure 15, Figure 16)**

- The Yamarna Shear Zone is a major deep, crustal-scale structure, and is one of only three very pronounced structures along the entire seismic profile.
- The shear zone is imaged by a series of parallel reflections that form a wide, highly-complex, structural corridor that defines a planar structure that dips about 30º to the east. The corridor is very similar in character to the Laverton Shear Zone.
- The structural corridor starts on the surface at approximately CDP 14300, dips eastwards to approximately CDP 19000, and then is sub horizontal until the end of the profile (01AGSNY1). This equates to a distance of over 80 km (surface to lower crust).
- The Yamarna Shear Zone appears to flatten or soles out at the base of the mid-crust at approximately 30-35 km depth (11 s TWT). This is probable due to a bend in the seismic traverse and the change in direction of the profile results in the shear zones becoming sub horizontal. The structural corridor is about approximately 3-6 km thick at mid-crustal levels.
- In the hanging wall of the Yamarna Shear Zone, a complex series of east-dipping structures (1-3 s) is consistent with a complex thrust package, and similar to the hanging wall of other crust-penetrating structures, in particular the Laverton Shear Zone.

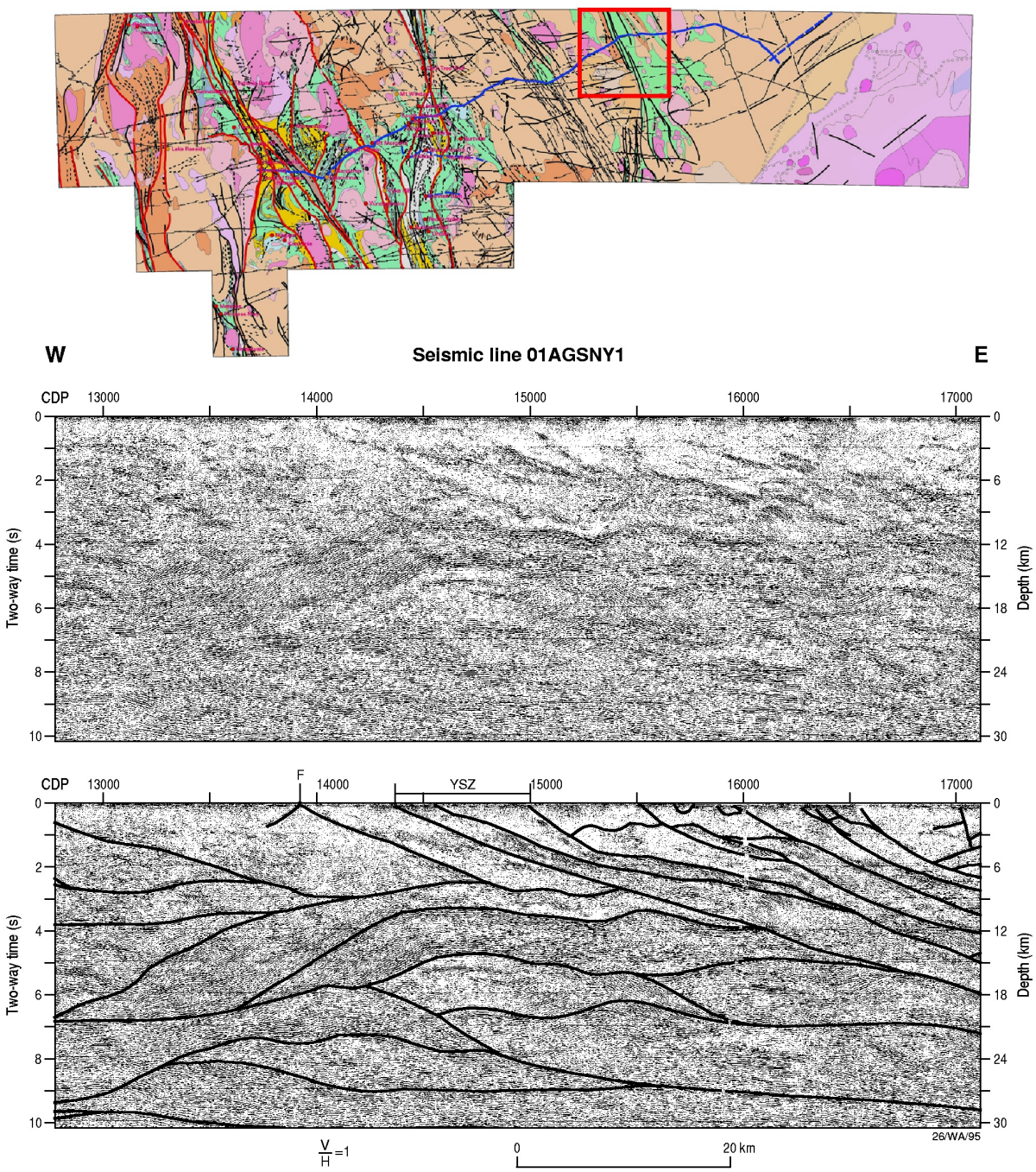

Figure 15. Portion of seismic line 01AGSNY1 showing the Yamarna Shear Zone. Top section is uninterpreted migrated seismic section; bottom section is interpreted migrated section. YSZ = Yamarna Shear Zone, F = west dipping Fault. V/H = 1.

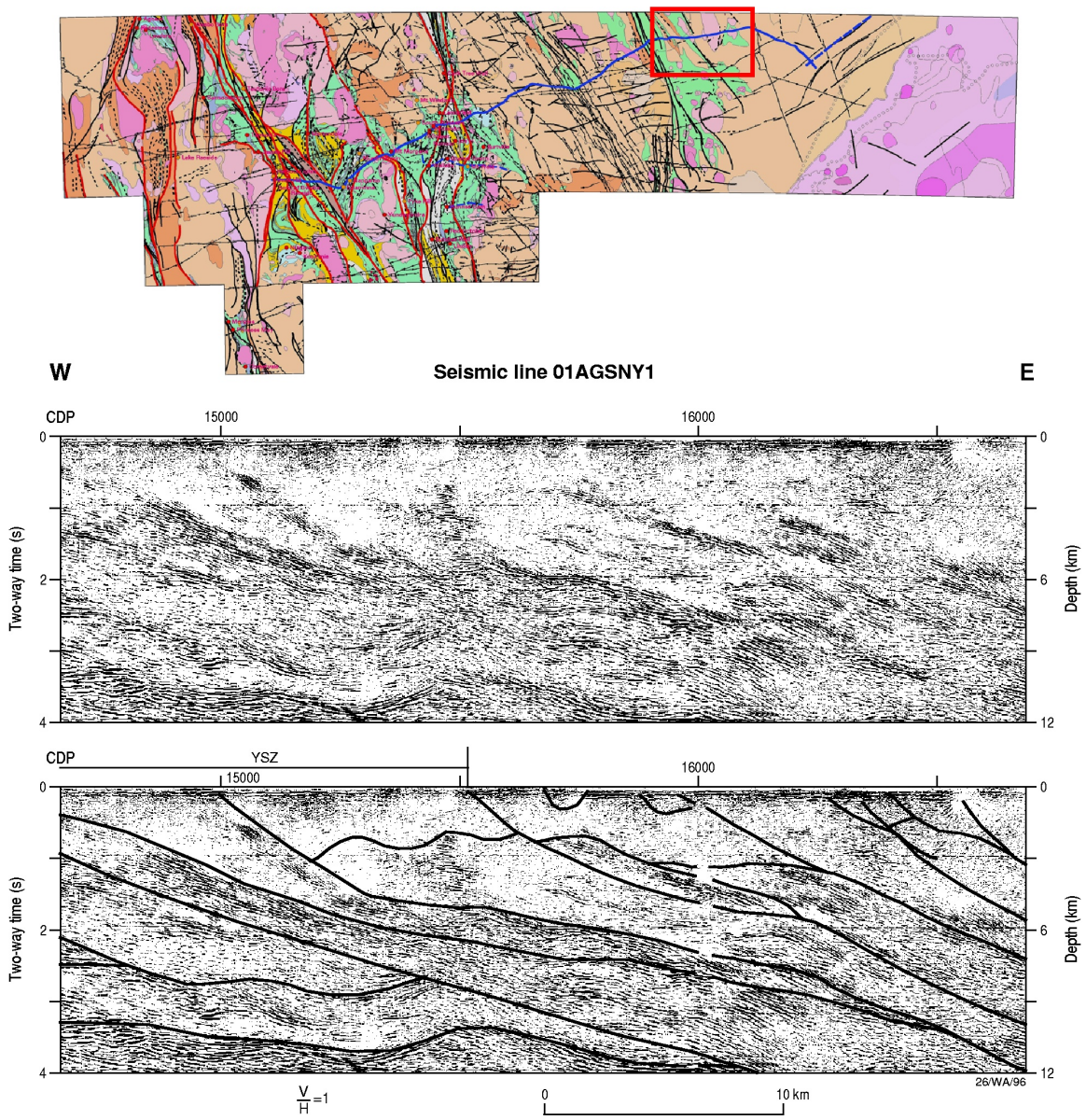

Figure 16. Detailed portion of seismic line 01AGSNY1 showing the Yamarna Shear Zone (YSZ). Top section is uninterpreted migrated seismic section; bottom section is interpreted migrated section. V/H = 1.

- The surface expression of the complex approximately 30 km wide Yamarna structural corridor, including the thrust package on the hanging wall of the Yamarna Shear Zone, is from CDP 14350 to CDP 16500 (Figure 15). Much of this zone is granite-gneiss-migmatite, with greenstones of the Yamarna greenstone belt from about CDP 15000 to CDP 15500, and minor greenstone at about CDP 15700 and about CDP 15900. Interpretation of aeromagnetic data by Whitaker (2002) indicates that the Yamarna greenstone belt widens to the south and contains numerous intrusive granitoids.
- West of the Yamarna Shear Zone, a series of east-dipping reflections are present in the top 2 s (approximately 6 km), and these sole onto the sub horizontal package in the upper mid-crust. It is possible that east-dipping reflections in the top 1 s between CDP 14100 and CDP 14200 may reflect late structures such as those present to the west of this zone, as well as present beneath the Proterozoic basins to the east.
- Beneath the Yamarna Shear Zone, the mid-crust is characterised by dominantly sub-horizontal and east- and west-dipping reflections, including the major west-dipping to sub horizontal package (described above) that appears to be truncated by the lower part of the Yamarna Shear Zone.
- The Moho ramps down from approximately 14 s to 15 s (approximately 42 to 45 km) over a short interval from CDP 15300 to CDP 15900. The down-dip projection of the Laverton Shear Zone coincides with the change in the Moho, and may indicate late extension of the Laverton Shear Zone (Figures 2 and 11).

Region of granite-gneiss-migmatite (Point Sunday domain) east of Yamarna greenstone belt **(Figure 17, Figure 18)**

- The region is dominantly granite-gneiss-migmatite with overlying Proterozoic and younger sedimentary successions (Apak and Taylor, this volume). This is illustrated on Figure 17.
- In the top 2-3 s TWT (6-8 km) of data there are a series of shallowly (<30º) east-dipping listric faults, that sole out at about 8-9 km. Some of these structures cut the lower parts of the Proterozoic successions. The fault at CDP 20200 shows an apparent 1 km displacement. The east-dipping faults may have partly controlled the deposition of the Proterozoic successions, at least the lowermost parts of the successions (Figure 18).
- Beneath this zone, the upper crust (to 4 s) is dominated by sub horizontal and variably east-dipping reflections.
- The mid-crust is dominated by a major west-dipping to sub horizontal reflection package that is about 6 km thick in the hanging wall of the Yamarna Shear Zone and extends east from CDP 18800 to the end of the profile.
- On top of this west-dipping package and below the upper crust are a series of thin west-dipping to sub horizontal packages that appear to also be truncated by the Yamarna Shear Zone. These packages thin and become sub horizontal to the east.
- The lower crust is dominated by the down-dip continuation of the Yamarna Shear Zone. The shear zone flattens or soles out at the base of the mid-crust at approximately 30-35 km (11 s TWT).

The eastern most part of the 01AGSNY1 profile changes orientation from east northeast to east southeast at approximately Lake Yeo homestead. The ENE-trending 01AGSNY3 profile ties with 01AGSNY1 near the easternmost part of 01AGSNY1, providing an opportunity to view some of the Yilgarn Craton structures in three dimensions. As indicated above, the Yamarna Shear Zone appears to flatten in the easternmost part of 01AGSNY1 with the change approximating the change in orientation of the line. In the east northeast-trending 01AGSNY3 profile, the sub horizontal reflection package ascribed to the Yamarna Shear

Zone appears to dip shallowly to the east into the lower crust. In combination, these indicate that the Yamarna Shear Zone is approximately east northeast-dipping and may indicate that further to the east it is crustal-penetrating and comparable to the Laverton Shear Zone.

Line 01AGSNY3

Line 01AGSNY3 is shown in Figures 12 and 13.

- The 01AGSNY3 seismic profile is 53 km long and is oriented east northeast. Acquisition parameters were designed to give higher resolution in the sedimentary rocks of the Officer Basin. The eastern end of 01AGSNY3 contains few discernible reflections and cannot be easily interpreted at depth.
- The Yilgarn Craton is unconformably overlain by Proterozoic and younger sedimentary successions along the extent of the 01AGSNY3 profile. The base of the sedimentary successions is characterised by a series of bright reflections at about 3 km at its deepest point.
- Beneath the unconformity, the upper crust (to 4 s) is characterised by sub horizontal to variably east- and west-dipping reflections, similar to much of the 01AGSNY1 profile.
- Many of the characteristics of the 01AGSNY1 profile can be traced onto the 01AGSNY3 profile.
- The mid-crust is dominated by sub horizontal to east-dipping reflections, with a shallowly east-dipping package at the mid-lower crust boundary interpreted to be the continuation of the Yamarna Shear Zone.

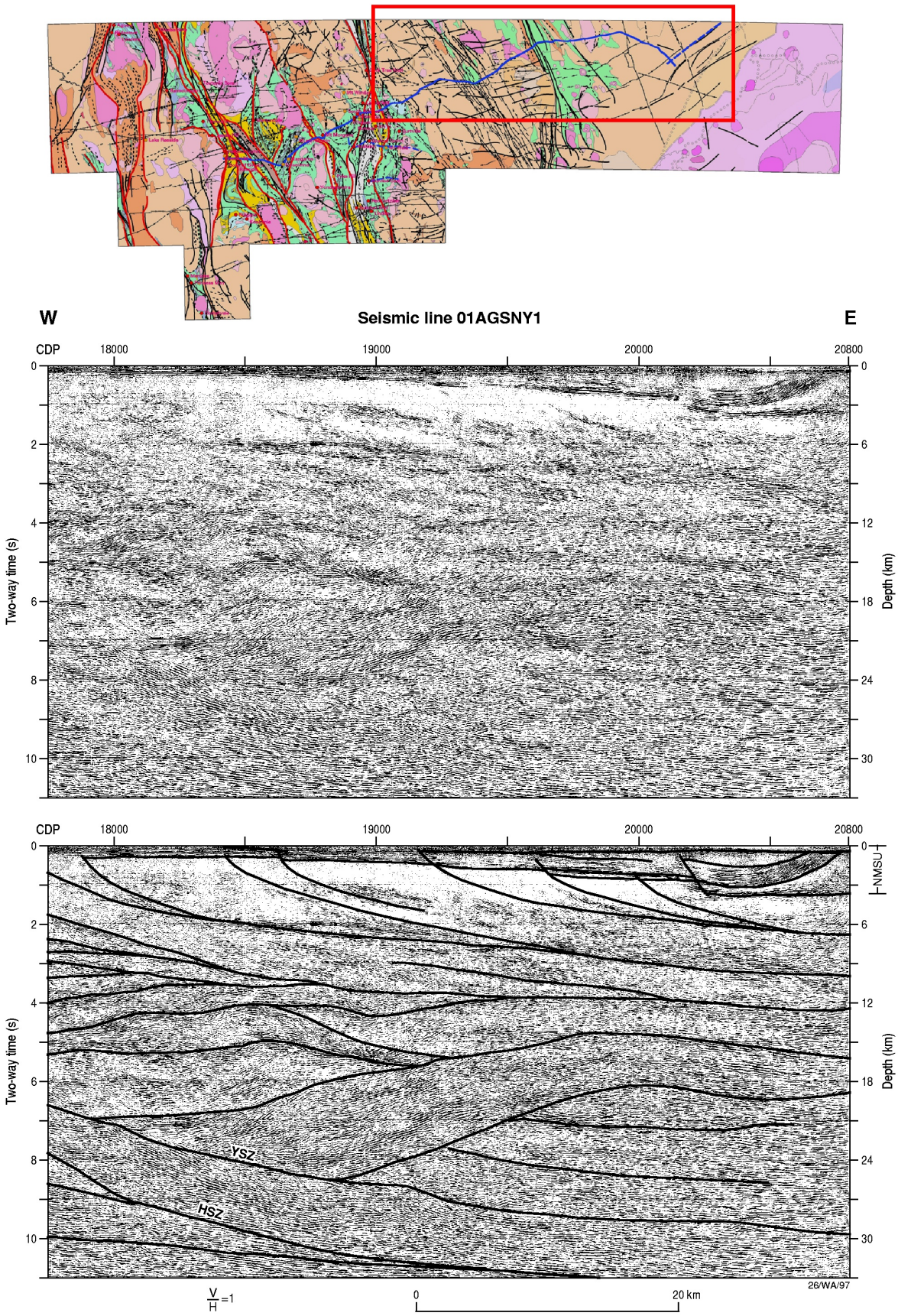

Figure 17. Uninterpreted and interpreted migrated sections for eastern most end of seismic line 01AGSNY1. NMSU = Neo- Mesoproterozoic Sedimentary Units, YSZ = Yamarna Shear Zone, HSZ = Lower Yamarna Shear.

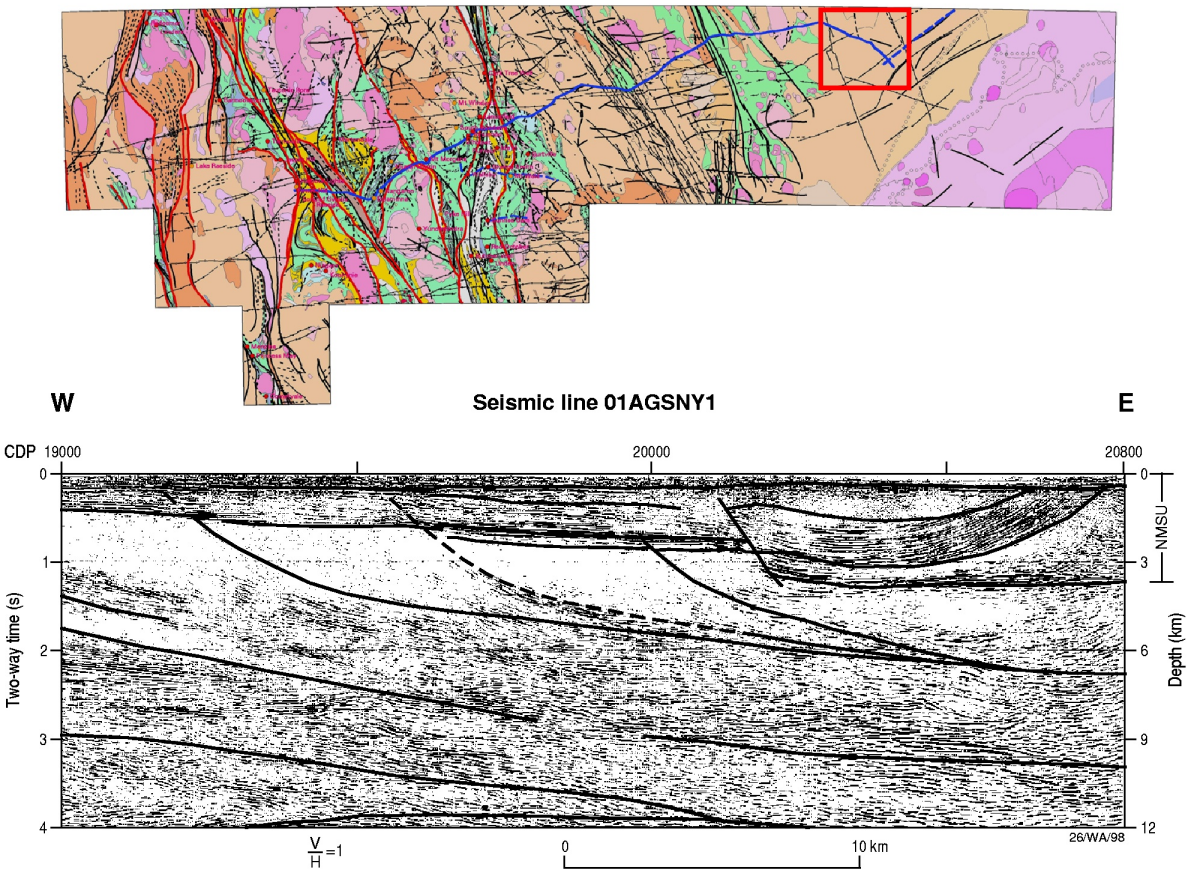

Figure 18. Detailed uninterpreted migrated sections for eastern most end of seismic line 01AGSNY1. NMSU = Neo- Mesoproterozoic Sedimentary Units.

References

Blewett, R.S., Champion, D.C., Whitaker, A.J., Bell, B., Nicoll, M., Goleby, B.R., Cassidy, K.F. and Groenewald, P.B., 2002. Three dimensional (3D) model of the Leonora-Laverton transect area: implications for Eastern Goldfields tectonics and mineralisation. *Geoscience Australia, Record*, **2002/18**, 83-100.

Drummond, B.J. and Goleby, B.R. 1998. Yilgarn crustal structure revealed in five seismic profiles. *in* Wood, S.E., ed., Geodynamics and Gold Exploration in the Yilgarn. Workshop Abstracts of Australian Geodynamics CRC Workshop, Perth, *Australian Geodynamics Cooperative Research Centre, Nedlands*, 23-32.

Goleby, B.R., Bell, B., Korsch, R.J., Sorjonen-Ward, P., Groenewald, P.B., Wyche, S., Bateman, R., Fomin, T., Witt, W., Walshe, J., Drummond, B.J. and Owen, A.J., 2000. Crustal structure and fluid flow in the Eastern Goldfields, Western Australia. *Australian Geological Survey Organisation, Record*, **2000/34**.

Gower, C.F. and Boegli, J.C., 1977. Rason, W.A. Sheet SH/51-3 International Index. *Western Australia Geological Survey, 1:250 000 Geological Series Explanatory Notes*, 17pp

Hall, G., 1998. Autochthonous Model fort Gold Metallogenus and Exploration in the Yilgarn. *in* Wood, S.E., ed., Geodynamics and Gold Exploration in the Yilgarn. Workshop Abstracts of Australian Geodynamics CRC Workshop, Perth, *Australian Geodynamics Cooperative Research Centre, Nedlands*, 32-35.

Jones, L.E.A., Goleby, B.R. and Barton, T.J., 2002. Seismic processing - 2001 Northeastern Yilgarn Seismic Reflection Survey (L154), *Northeastern Yilgarn Seismic Workshop*, Workshop Notes.

Whitaker, A.J., 2002. Aeromagnetic interpretation of the Yilgarn Craton with emphasis on the north eastern Yilgarn. *in* Cassidy K.F., ed., GA-GSWA North Eastern Yilgarn Workshop, *Geoscience Australia, Record*, **2002/18**, 1-6.

IMPLICATIONS OF THE NORTHEASTERN YILGARN SEISMIC TO LEONORA-LAVERTON 3D MAP

Richard Blewett[1,2], David Champion[1,2], Kevin Cassidy[1,2], Bruce Goleby[1,2], Ben Bell[1,2], Bruce Groenewald[3], Malcolm Nicoll[1,2], and Alan Whitaker[1,2]
[1] Minerals Division, Geoscience Australia
[2] *pmd**CRC, Predictive Mineral Discovery CRC
[3] Geological Survey of Western Australia

Introduction

Three dimensional (3D) maps are critical in understanding the structural architecture of a region. They help constrain a region's tectonics, and are clearly critical for predicting fluid flow in an orogenic mineral system such as gold. The Eastern Goldfields Province has a number of previously developed regional 3D maps. These include the Australian Geodynamics CRC model covering twelve 1:100 000 geological sheets from Norseman to Menzies (AGCRC, 1997), and a 3D map developed by Goleby *et al*. (2003) for the Kalgoorlie area. This latter 3D map built on the AGCRC model incorporating a number of new seismic lines acquired in 1999. There is, accordingly, a relatively good understanding of the third dimension in the southern part of the Eastern Goldfields.

A new 3D map, down to 15 km depth, was built for the Leonora-Laverton transect area in the central Eastern Goldfields Province of the Yilgarn Craton, straddling the western part of the recently acquired northeastern Yilgarn seismic traverse (line 01AGSNY1). The 3D map incorporates a transect of geology from eighteen 1:100 000 sheet areas, and is located north and northeast of the previously published models. The new 3D map area is bounded between 28ºS and 29.5ºS, and 120ºE and 123ºE, and includes the important mining centres of Agnew-Lawlers, Leonora, Laverton, Wallaby, and Sunrise (Figure 1).

This paper briefly documents the methodology and processes of how the new Leonora-Laverton 3D map was built. We also discuss the implications for Eastern Goldfields tectonics, and the new insights provided by the northeastern Yilgarn seismic traverse.

Building the 3D map

Building the 3D map was an iterative process that involved the integration of 1:100 000 scale outcrop and solid geology and point observations, images of aeromagnetic data, gravity data (horizontal gradient anomalies, grids and stations), combined magnetic/gravity images, existing cross sections, seismic reflection data in the area (line 01AGSNY1), and seismic reflection data along strike to the south.

The interpretation process began with the construction of a base geological layer. The underlying data for the base geological layer were a set of 1:100 000 scale solid geology maps that were derived from the interpretation of the gravity and magnetic data, and various combinations of both, and integrated with the 1:100 000 scale outcrop geology (fact) maps (Painter *et al*., 2002; Groenewald, 2002). These solid geology maps were simplified and

combined into a 1:250 000 scale solid geology map of the entire 3D map area (Whitaker and Blewett, 2002), providing the framework or base layer from which the 3D map was built. The resultant simplified map portrayed seven basic rock types, i.e., granite, gneiss, ultramafic rock, mafic greenstone (basalt, gabbro and dolerite), felsic greenstone, sedimentary rocks, and conglomerate or 'late' basins (Figure 1). These seven 'units' were chosen as they were the easiest to manage in terms of both their geometry in 3D, and potential field modelling to constrain the depths of the units (see Bell, 2002). The actual process of building the 3D map meant that the base map was critically reviewed and found wanting in some areas. In such cases changes were made to the base solid geology map.

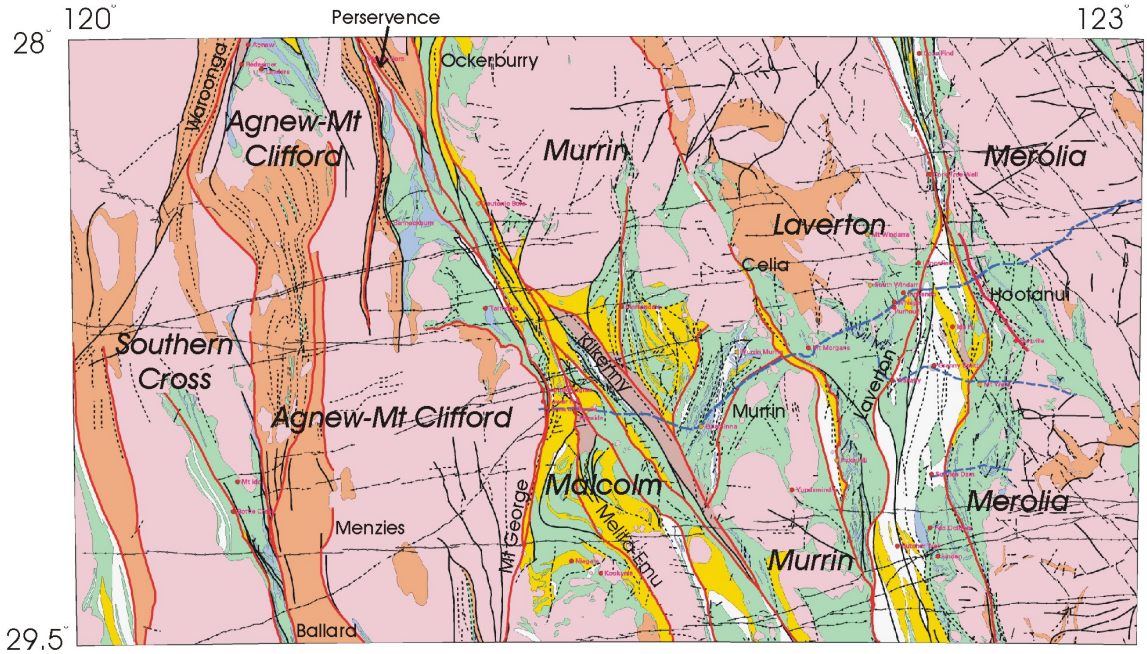

Figure 1: Solid geology map of Leonora-Laverton transect area with domains and their bounding structures

The third dimension of the 3D map was obtained by drawing and integrating a series of east-west serial cross sections every 20 km across the 3D map area. This process began before the seismic data were available for interpretation. The surface intercepts were obtained accurately from the GIS and the dips of lithological boundaries and structures estimated from structural readings on the geology maps, the horizontal gradient anomalies, and/or the gravity/magnetic anomaly patterns. Based on previous modelling (Drummond *et al*., 1997; Goleby *et al*., 2003) and the extrapolating from previous seismic surveys around the Kalgoorlie area (Swager *et al*., 1997), the greenstones depths were taken to be about 7 km. The 'style' of the sections also assumed a similar geometry to that from the Kalgoorlie area. For example, the early sections were drawn with ~7 km greenstone depths and the fault dips were shallowed out into a 'detachment' at this depth at the base of the greenstone (Figure 2). Some modifications were made to the greenstone depths based on gradient changes in the gravity images.

These early serial sections were subsequently modelled to constrain the depths and attitude of structures and boundaries (Bell, 2002). The sections were adjusted significantly following the potential field modelling. The team of geologists consistently overestimated both the thickness of greenstone, and the dips of structural surfaces (too steep).

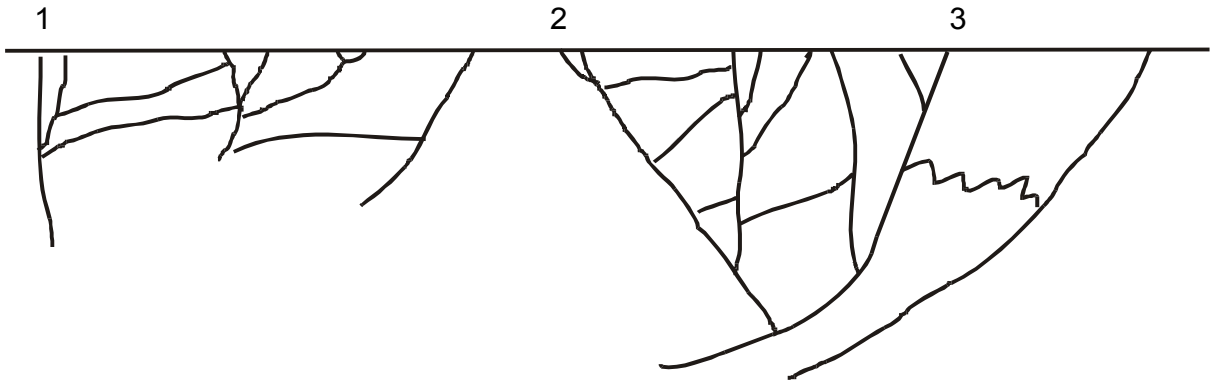

Figure 2: Example of the first iteration of the cross sections. Note the generally steep dips, and relatively deep greenstone (~7 km).

The result was a new set of sections (Figure 3) that were captured in GOCAD® and a skeleton 3D map was constructed.

One of the problems of the potential field data was the difficulty in constraining the geometry of structures below the base of the greenstones, or in the granite-gneiss-dominated areas, reflecting the lack of rock property contrasts in these areas. The seismic reflection data, therefore, was used to address this problem and to provide an independent test of the preliminary 3D map.

Figure 3: Example of the second iteration of the cross sections (same area as Figure 2). Note the generally steep dips, and shallowing of the greenstone.

In many cases the post-potential field modelled sections stood up to interpretations of the seismic data. The main area of difference in the serial cross sections was in the attitude of the structures. The seismic data are very good at imaging low-angle to moderately dipping structures. Most of us were surprised by the very shallow nature of the major bounding structures, and the enormous amount of 'structure' in the granite-gneiss domains.

A new set of serial sections was drawn to account for the more shallow dips, most flattening out to the east (Figure 4). The process focussed on the area where the seismic line crossed, or was close to, the serial section lines. As the seismic line trends northeast, it crossed three of the serial east-west section lines. New sections were drawn in parts and then extrapolated northwards and southwards to adjacent sections to maintain the continuity of structural style. The gravity data were reviewed in light of changing the dips on the bounding structures (and consequently their contained rock volumes) as this inevitably shifted mass eastwards.

The major bounding structures are modelled as surfaces. These surfaces were created from interpolation between the cross sectional lines. The geometry and style of the surface was maintained by sliding a template northwards and southwards to successive cross sections.

Attempting to pick the 'major structure' in successive lines was a test in itself. The earliest sections were not consistent and parallel faults were sometimes chosen as the main bounding structure.

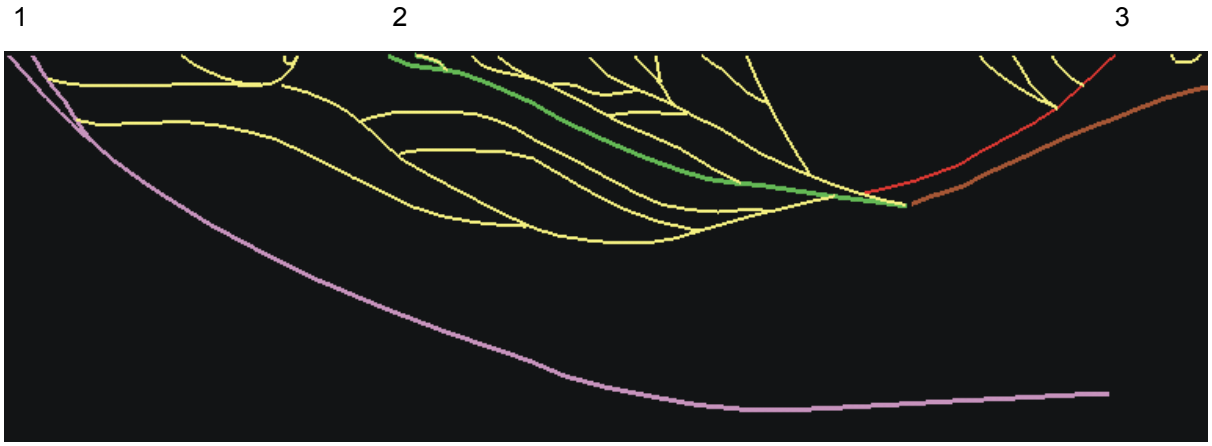

Figure 4: Example of the final iteration of the cross sections (same area as Figs. 3, 4), following input of seismic reflection geometry. Note the shallow dips, and relatively shallow greenstone. (1-Mt George shear zone, 2-Kilkenny shear zone, 3-Murrin fault).

Each successive section in itself becomes a test of the adjacent section. This is particularly true where the geology is elongate and linear as the same surface is represented on all ten sections. New information was commonly available along strike, such that earlier sections often needed to be revisited. The rigour of drawing serial sections tested assumptions about what structures were important, suggesting that this approach challenges the rigour of simply drawing a single section across a map in terms of representing the third dimension.

After the 3D map was built, subsequent reprocessing aimed at improving the seismic reflection data 'migrated' some anomalies. The result was a change in the interpretation of the seismic data and, therefore, the geometry of some of the major structures. It is interesting to note that most iterations of the seismic interpretation produced a very similar result. The areas of difference were invariably in the areas of ambiguity in the seismic data.

Features of the 3D map

The following is a list of the main features or observations of the 3D architecture of the Leonora-Laverton 3D map:

- domains defined on the basis of surface geology and structure coincide with differences in the reflectivity of the seismic data;
- gravity modelling show that the crust below the greenstones is essentially felsic, and may be equivalent to the gneiss-migmatite dominated domains (external granites);
- greenstones are mostly shallow (<6 km), some areas are <1 km thick above gneiss/granite substrate;
- the greenstone to underlying granite/gneiss interface is modelled as a low-angle surface that dips gently to the east, a feature confirmed by the seismic reflection data;
- the seismic data image a number of low-angle shears (LASH's), with several observed within the felsic crust below the greenstone base[1];

[1] The term low-angle shear zone is preferred to that of detachment, because of the genetic connotations of the latter.

- the LASH's have 'topography' and it is difficult to determine if these are openly folded or part of a mega S-C geometry,
- exposed 'internal' granites are modelled as windows through the greenstone base, and they show that the greenstone base is partly intrusive;
- however, the seismic data show that parts of the greenstone base are likely to be sheared by LASH's;
- forward modelling of the gravity data show that some of the 'internal' granites are thin sheets ('surfboards') in 3D;
- major domain-bounding shear zones dip to the east at <45° and flatten out at depth;
- the timing relationships between the major domain-bounding shear zones and the LASH's at depth is variable,
- there are few west-dipping structures, in the 3D map area;
- the dip of penetrative fabrics generally is mostly steep at the surface;
- the main superimposed fabric or regional strike across the 3D map is north-northwest;
- major domain-bounding shear zones in the east of the 3D map have late extension (transtension) following earlier west-directed thrusting (transpression);
- major extension post-dates earlier compression of the Pig Well succession;
- out of plane movement (strike-slip deformation) is not easily resolved with the compression-extension geometry.

The 3D geometry of domain-bounding shear zones

Below the base of greenstone, or in granite-gneiss domains, it is difficult to establish the geometry of the major structures. The eastern half of the 3D map has the benefit of the seismic reflection data to provide additional control, and it images many of the major domain-bounding shear zones as deep-penetrating structures. In the west of the 3D map, some of the major domain-bounding shear zones (e.g., Ballard-Ida Fault) are imaged along strike to the south (in seismic data reported by Swager *et al*., 1997), also as deep structures. The major faults or shear zones transect the 3D map area dividing the region into a series of domains (Figure 1). Most of these structures are high-strain zones that trend north-northwest. Some may separate different lithostratigraphic packages and may have been initiated as basin-bounding faults with a prolonged kinematic history (Hallberg, 1985).

Waroonga-Ballard Shear Zones

At the western side of the 3D map area, the Waroonga-Ballard Shear Zones strike mostly north-south and separate rocks of the Southern Cross Province to the west from Eastern Goldfields Province rocks to the east. The Waroonga-Ballard Shear Zones form the boundary between the Southern Cross Domain and the Agnew-Mt Clifford Domain (Figure 1).

The Waroonga Shear Zone dips steeply to the west, flattening out at about 10 km depth into a listric geometry. It appears to transect the Ballard Shear Zone which is a steeply east-dipping structure to the bottom of the 3D map at 15 km. The Waroonga Shear Zone and related faults record sinistral shear (Liu *et al*., 2002) along the northern arm, and dextral shear on the southern arm (Platt *et al*., 1978).

A blastomylonitic fabric in gneissic granite along the Ballard Shear Zone dips steeply to the east, hosts a gentle (<20°) south-plunging lineation, and records a dextral sense of shear on S-C planes. On the regional scale, the geometry of the Ballard Shear Zone is normal in the 3D

map, consistent with its along strike trace (the Ida Fault) to the west of Kalgoorlie (Swager *et al*., 1997). Slivers of amphibolite along the shear zone on the Wilbah 1:100 000 sheet area, record an additional steeper lineation and an earlier fabric. However, the steep lineation may be an intersection lineation between the two fabrics.

The Menzies Shear Zone

The Menzies Shear Zone is a wide zone of deformation with a prolonged movement history, separating different tectonostratigraphic terranes (Swager, 1994). On the basis of alignment of aeromagnetic features, the Menzies Shear Zone trends northwest from Menzies and forms the north-trending eastern margin of the Wilbah gneiss belt on the Wilbah 1:100 000 sheet area (the Ballard Shear forming the western margin). Swager (1994) describes sinistral west-block down movement on the Menzies Shear Zone to the south.

The 3D map considers the base of the Wilbah gneiss to be dipping to the west, with deeper levels of gneiss preserved in the east. The Menzies Shear Zone is overprinted by undated granite plutons. Under the town of Leonora, at a depth of about 20 km (6.5 seconds two-way travel time), the seismic reflection data image a set of strong reflectors that dip 20° to the east. These reflectors project to the surface at the Menzies Shear Zone some 60 km further west, and may represent the deep expression of this shear system.

The Moriaty-Mt George-Perseverance Shear Zones

The Mt George Shear Zone is the eastern splay of the Moriarty Shear Zone (Witt, 1994), and they separate the Agnew-Mt Clifford Domain from the Malcolm Domain. Witt (1994) described dextral shear on the Moriarty Shear Zone, and on the northeastern trace of the Mt George Shear Zone. Williams *et al*. (1989) described sinistral shear on the Mt George Shear Zone along the northwest trending segment to the north of Leonora.

In the 3D map, the Mt George Shear Zone is shown as a listric structure, dipping moderately to gently to the east, flattening out at about 17 km. *Further re-interpretation of the seismic reflection data (not shown in the 3D map), suggests that the Mt George Shear Zone is actually a planar east-dipping structure that possibly transects the Moho.* The Mt George Shear Zone is clearly a major structure.

The Perseverance Shear Zone is the name given to the northwest-trending segment of the Mt George Shear Zone to the north of Mt Clifford. Intensely foliated and lineated granite and greenstone rocks up to 1 km wide comprise the shear zone. Movement indicators are sinistral on steeply dipping mylonitic foliations (Liu *et al*., 2002). Eisenlohr (1992) described a steep south-southeast, and a gentle north-plunging lineation. The merging of relating faults into the Perseverance Shear Zone, and the asymmetry of folds, suggest that there was a component of west-directed thrusting across this structure (Liu *et al*., 2002).

The Melita-Emu Shear Zone

The north-northwest trending Melita-Emu Shear Zone runs through the central part of the Malcolm domain, before merging with the Kilkenny Shear Zone and forming the western boundary of the Murrin domain. In this interpretation the Melita-Emu Shear Zone represents either a splay of the Kilkenny Shear Zone or is, transected by it (Figure 1). The Emu Fault

was interpreted, in the Kalgoorlie 3D map area, to dip to the west (see Goleby *et al*., 1993; Swager *et al*., 1997). However, based on the coincidence of a pronounced gravity inflection and the shear zone across a granite-greenstone boundary in the southern part of the 3D map area, we suggest that the Melita-Emu Shear Zone actually dips to the east, and not west. Chen *et al*. (2001) recorded sinistral shear as well as a component of dip-slip movement on the Melita-Emu Shear Zone. *Further re-interpretation of the seismic reflection data, however, suggests that the Melita-Emu Shear Zone has a thrust geometry with a hangingwall anticline developed to the east.*

The Kilkenny and Ockerburry Shear Zones

The Kilkenny Shear Zone, separating the Malcolm and Murrin Domains (Figure 1), is a prominent north-northwest linear zone of deformation that controls the present day topography. In the 3D map area it contains and deforms the Pig Well sequence, which comprises canyon-fill conglomerate and coarse clastic metasedimentary rocks (Hallberg, 1985). Rocks considered equivalent to these have been dated elsewhere at <2665 Ma (Krapez *et al*., 2000). Early movements on the fault may have been important in controlling sedimentation of the Pig Well sequence, either as an extensional growth fault, or as a piggy back basin during foreland-directed thrusting. The Kilkenny Shear Zone marks a significant gravity low that is at a high angle to a gravity high located in the Welcome Well area to the east (Northern Murrin Domain). This gravity low is not simply due to thick accumulations of Pig Well metasediments, because the underlying basement is locally exposed, suggesting that significant older felsic greenstone (i.e., low-density rock) is incorporated into the Kilkenny Shear Zone at depth. Chen *et al*. (2001) described sinistral strike-slip movements that overprint an earlier phase of dip-slip movement. In the 3D map, the Kilkenny Shear Zone dips 35-40° to the east, and is more planar than other major faults in 3D. *Additional re-interpretation of the seismic reflection data (not shown on the 3D map), indicates that the Kilkenny Shear Zone is a planar structure that is transected by the Yundamindra LASH at about 8 km depth.*

The Kilkenny Shear Zone wraps around the western margin of the Mertondale Batholith, and merges with its interpreted northern trace the Ockerburry Shear Zone (Figure 1). Both sinistral and dextral movement senses have been observed along the Ockerburry Shear Zone (Vearncombe 1998, Chen *et al*. 2001). However, the overall architecture of the fault zone shows a Z-sigmoidal pattern, consistent with sinistral shearing (Chen *et al*., 2001). Lineations are mostly shallow plunging, indicative of strike-slip movements. An alternative model is to link the Ockerburry Shear Zone with the Mt George Shear Zone, thereby transecting the Kilkenny Shear Zone (see Whitaker *et al*., 2002).

The Yundamindra LASH

The Yundamindra LASH is imaged as an upward bowed set of bright reflectors that transect east-dipping rock packages from east of the Mt George Shear Zone, including the Murrin Fault and all rocks of the Murrin Domain. The relationship between the Yundamindra LASH and the Mt George Shear Zone is unclear in the seismic data, but it is likely that the latter cuts the LASH.

The Yundamindra LASH is a relatively late structure, and has an overall extensional geometry. The shear zone is interpreted to not intersect the present day land surface, and is, therefore, an overall flat structure. *Re-interpretation of the seismic reflection data (not shown*

in the 3D map), suggests that the Yundamindra LASH may actually transect, and hence postdate, the Kilkenny Shear Zone, although the seismic data appears to be complicated in this region by out-of-plane reflections. The re-interpretation also confirms that the Yundamindra LASH is transected by, and hence, predates the last movement on the Mt George Shear Zone.

The Murrin Fault

The Murrin Fault separates the Murrin Domain into north and south subdomains (Figure 1), and trends northeast between the younger Kilkenny and Celia Shear Zones. The seismic reflection line was acquired parallel to the Murrin Fault, however the fault is interpreted to dip northwestward and be truncated by structures parallel to the Kilkenny Shear Zone. The Murrin Fault is one of the few structures that dip with an apparent attitude to the west in the 3D map.

The Murrin Fault marks the southeastern extent of the geology ascribed to the Mt Kilkenny-Welcome Well area by Chen *et al*. (2001). To the southeast of the Murrin Fault, in southern Murrin Domain, granites intrude the basalts.

The Celia Shear Zone

The Celia Shear Zone is another strike continuous north-northwest trending structure, with a pronounced aeromagnetic pattern reflecting a wide high-strain zone. The Celia Shear Zone dips moderately to gently to the east (30°), and cuts the Murrin Fault. Its last movements are interpreted as extensional as thick greenstone is preserved above the eastern footwall (Laverton Domain), reflecting higher structural levels than the greenstone to the west (Murrin Domain). Chen *et al*. (2001) described predominantly sinistral shear kinematics for some of the later movements. Swager (1995) inferred earlier thrusting and repetition of stratigraphy on the Celia Shear Zone, an interpretation supported by shallow-plunging folds and steeply-plunging lineations (Chen *et al*., 2001). *Following re-interpretation of the seismic reflection data, the Celia Shear Zone is now interpreted as a listric structure flattening out at 9 km (3 secs), steepening to the east and being cut by the Laverton Shear Zone (further east) at a depth of about 17 km (5.5 secs). An alternative model, also consistent with this re-interpretation, is that the Celia Shear Zone may form a splay, at depth, off the Laverton Shear Zone.*

The Laverton Shear Zone

The Laverton Shear Zone is an east-dipping structure with an extensional (normal) geometry (on the base of the greenstones). Imbrication of Western Merolia Domain rocks during thrusting has been more than offset by a greater extensional reactivation (assuming the base of the greenstone is a reliable marker surface). In the 3D map, the Laverton Shear Zone is a splay of the Celia Shear Zone. *Following re-interpretation of the seismic reflection data, the Laverton Shear Zone is now interpreted to be a planar structure with a 30o dip to the east. The shear zone extends from the surface for ~140 km eastwards where it soles into the Moho. The Laverton Shear Zone cuts the Celia Shear Zone or the latter splays off the former. There is a marked change in reflectivity to the east of the Laverton Shear Zone.*

The Hootanui Shear Zone

The north-northwest trending Hootanui Shear Zone (Chen *et al*., 2001) dips gently to the east, and on the surface is marked by highly deformed (mylonitic) syenites that are dated at 2664 Ma (Black *et al*., 2002). Kinematic indicators in the mylonites record early sinistral shear overprinted by a reworking of the fabric by dextral shearing. In both cases, lineations are gently dipping on moderately to steeply east-dipping mylonitic fabrics. Chen *et al*. (2001) also recorded earlier dip-slip movements. The Hootanui Shear Zone is a splay from a series of apparent west-directed thrusts deeper in the crust.

Geological-tectonic implications of the 3D map

The 3D map provides a geometrical framework for the distribution of granites and greenstones, as well as the major domain-bounding shear zones for the Leonora-Laverton transect area. This framework when combined with structural, stratigraphic, geochemical, and isotopic (age) constraints provides a powerful starting point for the geological restoration of the area. However, most of the geometry and architecture of the 3D map, and structures in the seismic reflection data, are recording the latest events.

Regional structural studies generally describe a D_e, D_1, D_2, D_3 structural history for the Eastern Goldfields Province, and the Leonora-Laverton transect area (Archibald *et al*., 1978; Swager, 1989; Hammond and Nesbitt, 1992; Williams and Whitaker, 1993; Chen *et al*., 2001) The successive phases of deformation are generally characterised by:

- D_e - low angle extension, top down to the southeast;
- D_1 – top to the north thrusting;
- D_2 – upright folding and thrusting due to east-north oriented compression;
- D_3 and younger – a series of strike-slip faults and shearing.

The following discussion considers the 3D map in terms of this regional deformation framework (Table 1). The earliest geological events are recorded by the discovery of old (>2750 Ma) greenstone and granite/gneiss across a number of the domains mainly to the north of the Leonora-Laverton transect area at Wiluna, Dingo Range, and Duketon, but also west and south-west of Leonora (Fletcher *et al*., 2001, in press; Black *et al*., 2002). The relationship between these old fragments, their deformation/metamorphic history, and the Kalgoorlie-based stratigraphy (and its deformation/metamorphic history), is unclear. The presence of 2755 Ma Au mineralisation in the Leonora area (Witt, 2001) reflects deformation/metamorphism and fluid movement at least 50 Ma before much of the Kalgoorlie stratigraphy was deposited.

A major komatiite event at ca. 2705 Ma (age from Nelson, 1997) reflects a major extensional event across the Eastern Goldfields Province. The komatiites were erupted with thick basalt flows, and intruded by gabbro and dolerite. Interflow sedimentary rocks, including fine-grained clastics, epiclastics, and cherts, were also deposited. Evidence for an extensional event at this time occurred in the Laverton Domain (see Williams and Whitaker, 1993), and at Lawlers in the Agnew-Mt Clifford Domain (Hammond and Nesbit, 1992), and is best preserved along granite-greenstone contacts (lags). This event is variably defined as D_e, and involved top to the southeast movement. Variable extension resulted in the development of a series of basins, with movement accommodated by northwest-southeast transfer faults.

D_1 shortening from the north or south inverted the greenstone basins, with thrusting to the north on previous extensional shear zones, and macroscale folding about east-west axes. The D_e transfer faults were reactivated as lateral ramps.

D_2 shortening from the east resulted in macroscale refolding of F_1 folds in a number of areas, prior to the so-called late basins (e.g., Pig Well sequence). Associated with the east-west shortening was the reactivation of D_1 lateral ramps into frontal ramps of major west-directed thrust faults, resulting in duplicated stratigraphy and the west-directed vergence.

The late-stage sediments may have been deposited in intermontane basins during piggy-back thrusting, or in roll-over anticlines (Swager, 1997). Alternatively, extension occurred and these basins were developed on reactivated thrusts. Davis *et al*. (2001) describe a hiatus in east-west compression at Mulgarrie (to the south of the Leonora-Laverton transect area), perhaps reflecting this event. Compression continued/renewed and inverted and deformed the late-stage basins.

D_3 strike-slip was mostly sinistral on the major domain-bounding faults, followed by dextral shearing (Swager, 1997; Chen *et al*., 2001). Hammond and Nesbit (1992) point out that many of the so-called D_3 sinistral strike-slip faults are D_2 tilted D_1 thrusts, and that the apparent sinistral movement is consistent with earlier flat lying south over north thrusting. This may be partly true, however, sinistral shear zones cut ca. 2640 Ma Low-Ca granites in the 3D map area, indicating, at least some of, these structures are late.

Table 1-Event chronology in Leonora-Laverton transect area.

Age Ma	Regional Event	Event Characteristics	Gst	Grt	Au
		Basement developed and deformed (thrusted?)[1], only remnants preserved	↕	↕	
2760					Leonora[1] ↕
		Extension? In an arc/backarc setting?? Welcome Well? and other sequences below regional komatiite marker eg Kurnalpi domain	↕	↕	
~2705	De	Mantle upwelling (plume); N-S extension (core-complex) [3]; develop N-S transfer structures; juxtaposition of 'external' gneiss and greenstone; [2]komatiite, basalt, and high Mg basalt/komatiite	↕	↕	
	D1 ↕	N-S compression develop E-W folds, equivalent to N-directed thrusting[4]			
		Extension? regional 'tilt' down to SW (preservation of BFG to Kalgoorlie Domain); erosion not too base of greenstone as few granite clasts in Late Basins			
>2665	D2 ↕	ENE compression, major folding, imbrication of structurally lower (older?) west over structurally higher (younger?) packages in east; develop main NNW fabric	⋮		[7]Jundee? ↕
<2655[5]		Late Basins (Pig Well) in inter-montane or piggy back basins	↕		
<2665	D3 ↕	Sinistral strike-slip (NNW) followed by dextral strike-slip; dextral strike-slip (N and NE); transpression[6]		↕	
2640					Main Au ↕
		Inferred extension (collapse?) down to east, inferred from base of greenstone offset and greenstone thickness changes		⋮	
~2400		E-W sinistral shearing rotated entire Goldfields ~15° anticlockwise; E-W dykes			

Sources: [1]Witt, 2001; [2]Nelson, 1997; [3]Williams and Whitaker, 1993; [4]Swager, 1997; [5]Krapez *et al*., 2000; [6]Chen *et al*., 2001; [7]Yeats *et al*., 2001. (Gst-greenstone; Grt-granite).

One of the main new findings of this study is the suggestion of significant late extension/transtension, which resulted in the reactivation of a number of deep penetrating faults. This extension may reflect an orogenic (gravity?) collapse, and be associated with exhumation of the orogen. What influence this had on the fluid pathways of the orogenic gold system is unknown, but if true, adds a new dimension to our understanding of the mineral system.

The last event was a rotation of the entire area, manifest by the development of numerous small offset (sinistral) east-west brittle faults (Whitaker and Blewett, 2002).

Conclusions

The 3D map provides a geometrical framework for the distribution of granites and greenstones, as well as the major domain-bounding shear zones for the Leonora-Laverton area. This framework when combined with structural, stratigraphic, geochemical, and isotopic (age) constraints provides a powerful starting point for understanding the tectonic evolution of the Eastern Yilgarn Craton. The 3D map highlights gaps in the geological understanding and identifies and focuses on the key issues that need to be further addressed in order to resolve the tectonic and metallogenic history of the region. The 3D map needs to be updated with the new understanding from the reinterpretation of the seismic reflection data. The major changes are on the geometry of the Mt George, Celia, and Laverton Shear Zones at depths below about 8 km. These principal structures will have to be modified for all the serial cross sections in the 3D map, and the 3D map rebuilt. The 3D map will also benefit from extending the sections to the full depth of the crust, and extending eastwards to incorporate the entire seismic reflection line.

Acknowledgements

We would like to thank Tania Fomin, and Leonie Jones for their processing of the seismic reflection data. Terry Brennan and David Beard provided unfailing GIS and cartographic support in the development of this paper. Russell Hay converted the GOCAD 3D map into vrml for web delivery. This paper is a contribution to the *pmd**CRC.

References

AGCRC, 1997. 4-DGM. http://www.agcrc.csiro.au/4dgm/yilgarn/#3DgeologyModel.

Archibald, N.J., Bettenay, L.F., Binns, R.A., Groves, D.I. and Gunthorpe, R.J., 1978. The evolution of Archaean greenstone terrains, Eastern Goldfields Province, Western Australia. *Precambrian Research*, **6**, 103-131.

Bell, B., 2002. Application of potential field data to constrain three-dimensional geological modelling in the Leonora-Laverton transect area. *in* Cassidy, K.F., ed., GA-GSWA North Eastern Yilgarn Workshop, *Geoscience Australia, Record*, **2002/18**, 67-74.

Black, L.P., Champion, D.C. and Cassidy, K.F., 2002. Compilation of SHRIMP U-Pb geochronology data, Yilgarn Craton, W, 1998-2000. *Geoscience Australia Record*.

Chen, S.F, Witt, W.K. and Liu, S., 2001. Transpression and restraining jogs in the northeastern Yilgarn Craton, Western Australia. *Precambrian Research*, **106**, 309-328.

Davis, B.K., Hickey, K.A. and Rose, S., 2001. Superposition of gold mineralisation on pre-existing carbonate alteration: structural evidence from the Mulgarrie gold deposit, Yilgarn Craton. *Australian Journal of Earth Sciences*, **48**, 131-150.

Drummond, B.J., Goleby, B.R. and Swager, C.P., 1997. Crustal signature of the major tectonic episodes in the Yilgarn Block, WA: evidence from deep seismic sounding. *Australian Geological Survey Organisation, Record*, **1997/41**, 15-20.

Eisenlohr, B.N., 1992. Contrasting deformation styles in superimposed greenstone belts in the northern sector of the Norseman–Wiluna belt, Western Australia, *in* Glover, J.E. and Ho, S.E., eds., The Archaean: Terrains, Processes and Metallogeny, *Geology Department (Key Centre) and University Extension, University of Western Australia, Publication*, **22**, 191–202.

Fletcher, I.R., Dunphy, J.M., Cassidy, K.F. and Champion, D.C., 2001. Compilation of SHRIMP U-Pb geochronology data, Yilgarn Craton, Western Australia, 2000-01. *Geoscience Australia, Record*, **2001/47**, 110p.

Groenewald, P.B., 2002. Outcrop Geology in the Leonora-Lacerton region from the East Yilgarn Geoscience Database. *in* Cassidy K.F., ed., GA-GSWA North Eastern Yilgarn Workshop, *Geoscience Australia, Record*, **2002/18**, 7-12.

Goleby, B.R., Drummond, B.J., Swager, C.P., Williams, P.R. and Rattenbury, M.S., 1993. Constraints from seismic data on the regional and district scale structure of the Eastern Goldfields Province. *Australian Geological Survey Organisation, Record* **1993/54**, 85-90.

Goleby, B.R., Bell, B., Korsch, R.J., Sorjonen-Ward, P., Groenewald, P.B., Wyche, S., Bateman, R., Fomin, T., Witt, W., Walsh, J., Drummond, B.J. and Owen, A.J., 2000. Crustal structure and fluid flow in the Eastern Goldfields, Western Australia: results from the Australian Geodynamics Cooperative Research Centre's (AGCRC) Yilgarn deep seismic reflection survey and fluid flow modelling projects. *Australian Geological Survey Organisation, Record*, **2000/34**, 109p.

Goleby, B.R., Korsch, R.J., Fomin, T., Drummond, B.J, Bell, B., Nicoll, M. and Owen, A., 2002. A 3D interpretation of the Kalgoorlie Region, Eastern Goldfields, Western Australia: from Deep Seismic and Potential Field Data and its visualisation as a 3D model. *in* Korsch, R.J., ed., Geodynamics of Australia and its Mineral Systems, **2**, Thematic Issue, *Australian Journal of Earth Sciences*.

Hallberg, J.A., 1985. *Geology and mineral deposits of the Leonora–Laverton area, northeastern Yilgarn Block, Western Australia*. Hesperian Press, Perth, 140p.

Hammond, R.L. and Nesbit, B.W., 1992. Towards a structural and tectonic framework for the central Norseman-Wiluna Greenstone Belt, Western Australia. *in* Glover, J.E. and Ho, S.E., eds., The Archaean: terrains, processes and metallogeny*, University of Western Australia Publication*, **22**, 39-49.

Krapez, B., Brown, S.J.A., Hand, J., Barley, M.E. and Cas, R.A.F., 2000. Age constraints on recycled crustal and supracrustal sources of Archaean metasedimentary sequences, Eastern Goldfields Province, Western Australia: evidence from SHRIMP zircon dating. *Precambrian Research*, **322**, 89-133.

Lui, D.C., Champion, D.C. and Cassidy, K.F., 2002. Geology of the Sir Samuel 1:250 000 sheet area, Western Australia. *Geoscience Australia* **2002/14**.

Nelson, D.R., 1997. Evolution of the Archaean granite-greenstone terranes of the Eastern Goldfields, Western Australia: SHRIMP U-Pb zircon constraints. *Precambrian Research*, **83**, 57-81.

Painter, M.G.M., Groenewald, P.B. and McCabe, M., 2002. East Yilgarn Geoscience Database:1:100000 geology of the Leonora-Laverton region, Eastern Goldfields granite-greenstone terrane. *Western Australia Geological Survey*.

Platt, J.P., Allchurch, P.D. and Rutland, R.R., 1978. Archaean tectonics in the Agnew supracrustal belt, Western Australia. *Precambrian Research*, **7**, 3–30.

Swager, C.P., 1989. Structure of Kalgoorlie greenstones; regional deformation history and implications for the structural setting of the Golden Mile gold deposits. *Geological Survey of Western Australia, Report*.

Swager, C.P., 1994. Geology of the Menzies 1:100000 sheet and adjacent Ghost Rocks area. *Geological Survey of Western Australia*, Perth, 31p.

Swager, C.P., 1995. Geology of the greenstone terranes in the Kurnalpi-Edjudina region, southeastern Yilgarn Craton. *Geological Survey of Western Australia, Report*, **47**, 31p.

Swager, C.P., 1997, Tectono-stratigraphy of late Archaean greenstone terranes in the southern Eastern Goldfields, Western Australia. *Precambrian Research*, **83**, 11-42.

Swager, C.P., Goleby, B.R., Drummond, B.J., Rattenbury, M.S. and Williams, P.R., 1997. Crustal structure of granite-greenstone terranes in the Eastern Goldfields, Yilgarn Craton, as revealed by seismic reflection profiling. *Precambrian Research*, **83**, 43-56.

Vearncombe, J.R., 1998. Shear zones, fault networks and Archaean gold. *Geology*, **26**, 855–858.

Whitaker, A.J, Blewett, R.S. and Fokker, M., 2002. Laverton-Leonora Solid Geology. *in* Cassidy, K.F., ed., GA-GSWA North Eastern Yilgarn Workshop. *Geoscience Australia, Record*, **2002/18**, 51-66.

Williams, P.R., Nisbet, B.W. and Etheridge, M.A., 1989. Shear zones, gold mineralization and structural history in the Leonora district, Eastern Goldfields Province, Western Australia. *Australian Journal of Earth Sciences*, **36(3)**, 383-403.

Williams, P R. and Whitaker, A J., 1993. Gneiss domes and extensional deformation in the highly mineralised Archaean Eastern Goldfields Province, Western Australia. *Ore Geology Reviews*, **8**, 141-162.

Witt, W.K., 1994. Melita, W.A. (1st edition). *Western Australia Geological Survey, 1:100000 Geological Series Explanatory Notes*.

Witt, W.K., 2001. Tower Hill gold deposit, Western Australia: an atypical, multiply deformed Archaean gold-quartz vein deposit. *Australian Journal of Earth Sciences*, **48**, 81-99.

Yeats, C.J., Kohler, E.A., McNaughton, N.J. and Tkatchyk, L.J., 2001. Geological setting and SHRIMP U-Pb geochronological evidence for ca. 2680-2660 Ma lode-Au mineralisation at Jundee-Nimary in the Yilgarn Craton, Western Australia. *Mineralium Deposita*, **36**, 125-136.

NORTHEASTERN YILGARN SEISMIC REFLECTION SURVEY: IMPLICATIONS FOR OROGENIC AU SYSTEMS

K.F. Cassidy, R.S. Blewett, D.C. Champion and B.R. Goleby
Predictive Mineral Discovery Cooperative Research Centre and Minerals Division,
Geoscience Australia, GPO Box 378, Canberra, A.C.T., 2601, Australia

Introduction

Mineralising systems are generally defined in terms of (i) the scale and architecture of the system, (ii) the geodynamic framework, including the evolution of P-T conditions over time, (iii) the architecture of fluid pathways, including discharge zones, (iv) the nature of fluids reservoirs, as well as the source and characteristics of mineralising fluids, and, and (v) the nature of depositional mechanisms and processes at the site of mineralisation (see Hagemann and Cassidy, 2000, for an overview as applied to orogenic Au systems; Figure 1).

Understanding the architecture of a mineralising system is, therefore, one of the fundamental steps in any systems analysis. Major hydrothermal ore deposits, such as orogenic Au deposits, are commonly associated with faults or shear zones that can be traced for tens to hundreds of kilometres (Eisenlohr *et al*., 1989; Groves *et al*., 2000; Goldfarb *et al*., 2001). According to Cox (1999) localization of fluid flow along relatively limited linked networks of active faults and shear zones is a fundamental aspect in the development of the crustal-scale hydrothermal systems that produce orogenic Au deposits.

At a greenstone belt-scale, Archaean orogenic Au deposits are generally spatially related to large-scale (>100 km in length), transcrustal deformation zones. Economically significant, gold-associated fault zones in the Abitibi greenstone belt of the Superior Province include the Destor-Porcupine and Larder Lake-Cadillac fault zones that are spatially close to the world-class Timmins and Val d'Or gold camps, respectively. In most transcrustal fault zones, however, significant (>100 t) gold mineralisation is scarce, or is extremely localised. Orogenic Au deposits are generally within 5 km of major structures and associated with subsidiary or second- or higher-order structures (Hodgson, 1989; Eisenlohr *et al*., 1989). On a camp-scale, second- and third-order structures are considered to be more favorable dilational sites for gold deposition (Kerrich, 1989; Eisenlohr *et al*. 1989; Robert, 1990). For instance, in the Yilgarn Craton, highly-mineralised gold camps, such as the Golden Mile and Kambalda-St Ives camps, lie in second or higher order splays off the Bardoc-Boorara Shear and its southwards lateral continuation. Based on empirical observations (e.g., Eisenlohr *et al*., 1989; Hodgson, 1989; Robert, 1990), as well as chemical studies (Neumayr and Hagemann, 2002), transcrustal fault zones are considered to be the main conduits for gold-bearing, hydrothermal fluids that are subsequently channelled into the second- and third-order faults.

The third dimension of mineralising systems centred on such structures, however, is still poorly understood. Seismic surveys, in combination with a range of other geological, geophysical and structural studies, provide key constraints on the size and architecture of mineralising systems and have been successively employed in Archaean terranes (e.g., Yilgarn: Goleby *et al*. 1997; Abitibi: Wyman *et al*., 1999), as well as younger terranes (e.g., European Alps: de Boorder *et al*., 1998).

Increasingly, seismic and gravity studies are identifying crustal-scale structures that transect the crust (e.g., Ida Fault: Drummond and Goleby, 1993). Crustal seismic reflections are attributed to a range of causes including compositional layering, mafic intrusions, shear zones, anisotropy (resulting from preferred orientation of minerals), and fluid-filled faults and fractures (e.g., Jones and Nur, 1982; Ganchin *et al*., 1998). A combination of these factors may contribute to a specific reflection group, as has been demonstrated from seismic studies of the superdeep Kola and KTB scientific boreholes (Smithson *et al*., 2000). Shear zones have been demonstrated to cause reflections by seismic profiling over exposed shear zones and imaging of the zone at depth (Hurich *et al*., 1985) and may be the best crustal reflectors because of their high reflectivity and continuity (e.g., Cook *et al*., 1981; Jones and Nur, 1982; Drummond and Goleby, 1993). Shear zone reflectivity is generally the combined effect of compositional layering, anisotropy and fluid-filled fractures (Smithson *et al*., 2000).

Shallow-angle thrust zones and normal faults generally provide good images in that they present anomalies in seismicity, rheology and reflectivity. High-angle shear zones are generally poorly imaged in reflection profiles, and indirect evidence for their existence is used, such as vertical offsets of reflectors, zones of complete absence of continuous reflections, or the appearance of diffraction clusters (Meissner *et al*., 1991).

The use of crustal-scale seismic reflection data in tectonic analysis implicitly assumes a connection between patterns of reflectivity and tectonic processes. Beaumont and Quinlan (1994) indicate that two end-member situations can be envisaged. At one end of the spectrum, all reflectors are inherited from earlier tectonic episodes and only translated or rotated during orogenic deformation. At the other end, all reflectors are created by strain associated with orogenic deformation through mechanisms such as those mentioned above. Any orogenic belt, therefore, is likely to contain examples of each of these end-members as well as intermediate cases of inherited reflectors disrupted and rearranged by orogenic deformation.

Quinlan *et al*. (1993) demonstrated that many compressional orogens have a similar pattern of crustal reflections, leading Beaumont and Quinlan (1994) to suggest that a significant proportion of seismic reflectivity results from the tectonic processes by which the orogens were constructed. Smithson *et al*. (2000) note that the general dip in the Kola and KTB superdeep boreholes is moderate to steep whereas horizontal to subhorizontal reflections are found around both boreholes, and suggest that the seismic reflections can be attributed to a combination of factors, in particular fluid-filled fracture zones and potentially shear zones. In combination, these support the premise that seismic reflectivity results from tectonic processes related to orogeny rather than being inherited from rock-forming or early deformation processes. This is generally corroborated by specific examples in which the reflectivity fabric corresponds to the dip projection of faults and shear zones exposed at the surface (e.g., Hurich *et al*., 1985; Goleby *et al*., 1989; Calvert and Ludden, 1999). Furthermore, it is inferred that many of processes suggested to produce reflectivity are the result of strain and so for the most part patterns of seismic reflectivity records patterns of strain developed as a consequence of the later stages of compressional deformation (see Beaumont and Quinlan, 1994). Any pre-existing reflectivity that is caught up in high-strain zones is likely to be overprinted to an extent that it is not discernible as a separate pattern. Seismic profiles, therefore, tend to preserve features related to later major deformation events that have affected a terrane, in particular compressional events.

Seismic reflectivity patterns are also used to determine a relative chronology of events as well as development of a seismically based tectonic model (Beaumont and Quinlan, 1994). Drummond *et al*. (2000) suggest that regional seismic data through the Kalgoorlie region

show that crustal reflections attributed to crustal shortening have overprinted seismic signatures related to earlier events. This is largely based on the correlation of crustal reflections with known surface features related to specific deformation events. These, in turn, are overprinted by crustal reflections related to strike-slip faulting in and out of the plane of the profile and possibly later extensional movement on major faults. It is worth noting, however, that regions where some amount of post-orogenic extension is demonstrable (e.g., Appalachians: Quinlan *et al*., 1992) the overall reflectivity pattern retains the character attributed to the compressional events. Seismic reflectivity patterns, therefore, allow definition of the relative ages for some structures in the Kalgoorlie profile and provide evidence that the deformation mapped in the surface geology affected the whole crust, albeit on different scales at different depths and by different means. The association of orogenic Au mineralizing systems with major deformation zones that were active late during the tectonic development of a terrane (e.g., Robert, 1990; Goldfarb *et al*., 2001) further implies that structures important to the development of the mineralizing system may be preserved on seismic profiles and the architecture of the mineralizing system may be constrained using seismic profiling.

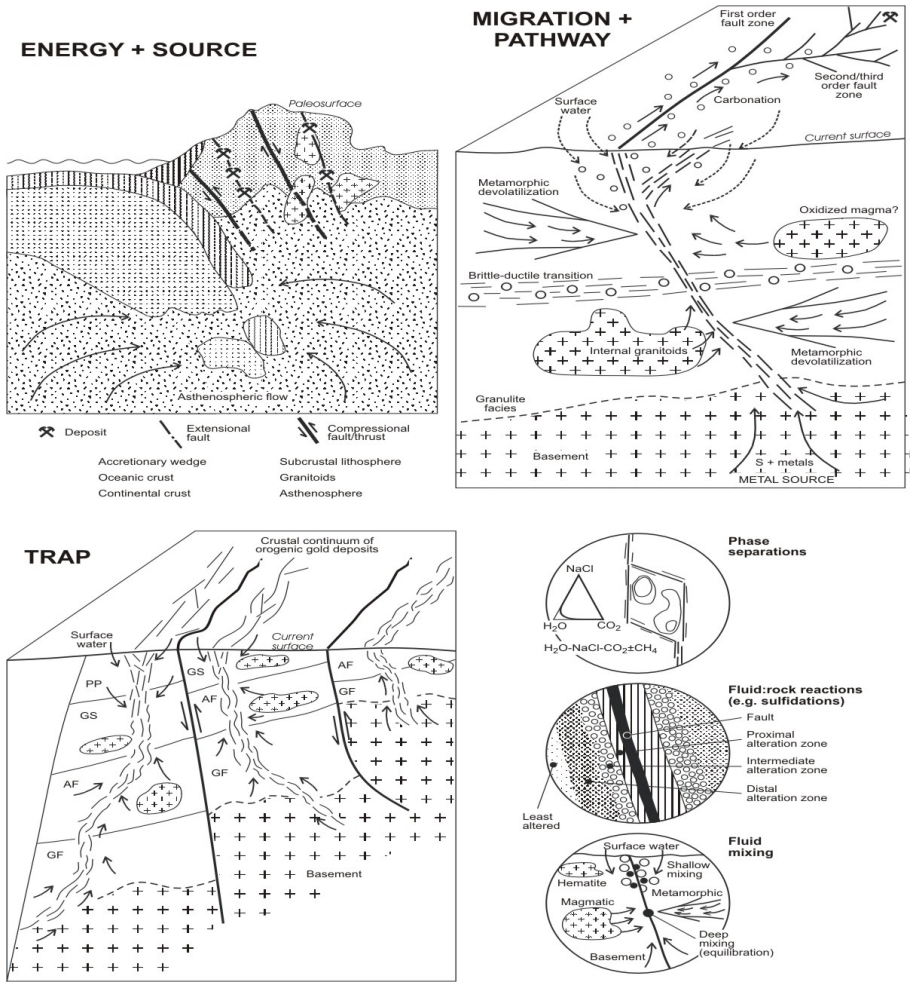

Figure 1. The mineral system concept as applied to Archaean orogenic Au deposits. (modified from Hagemann and Cassidy, 2000)

The northeastern Yilgarn Craton is an important metallogenic region and contains a variety of mineral systems, including orogenic Au, magmatic Cu-Ni-sulfide and lateritic Ni-Co, and possibly intrusion-related Mo-Au mineralisation. In recent years, the region has been the centre of mineral exploration that has led to the discovery of several major gold deposits

(Gwalia Deeps, Sunrise-Cleo, Wallaby) and development of the world-class Murrin Murrin lateritic Ni deposit. The vast majority of orogenic Au deposits are spatially associated with structures and the largest deposits in the northeastern Yilgarn are associated with structures within the Laverton tectonic zone (e.g., Sunrise-Cleo, Wallaby, Granny Smith). Acquisition of deep seismic reflection profiles (Jones *et al*., 2003), in combination with geological, geochronological and structural studies, have important implications for the development of conceptual models for various mineral systems, in particular orogenic Au systems, for this region. In particular, the seismic data provide information on the architecture and role of basement structures, the geometry of potential fluid reservoirs within the crust and possible pathways to allow for fluid ingression, mixing and metals deposition. Orogenic Au mineralising systems in the northeastern Yilgarn are generally associated with late stages of deformation (e.g., Groves *et al*., 2000; Davis, 2001) and, therefore, there is likely to be a link between structures preserved on seismic profiles and the development of the mineralising systems.

Crustal structure in the Kalgoorlie region and implications for orogenic Au systems

The Kalgoorlie region in the southeastern Yilgarn Craton is one of the most highly mineralised Archaean terranes in the world, containing the giant Golden Mile gold deposit, and several other world-class gold camps (e.g., Kanowna-Belle, Kambalda-St Ives, Mt Pleasant), as well as the world-class nickel deposit at Kambalda. Successive seismic surveys (1991, 1997, 1999) have been undertaken in the Kalgoorlie region to provide additional constraints and improve understanding of the geodynamics and mineral systems in this region. The first survey in 1991 imaged the detailed structure in the granite-greenstone belts and its relationship to the deeper crust (Goleby *et al*., 1993; Drummond *et al*., 2000). In 1997, several shorter profiles were acquired to determine the orientation of several key structures and placing these structures in the regional context. The 1999 survey acquired a grid of 2D data surrounding the earlier profiles to provide constraints on the 3D geometry of a well-documented greenstone belt over an area of 50 x 50 km (Figure 2; e.g., Goleby *et al*., 2000, 2002; Korsch *et al*., 2001). These studies have been used by academia and industry to develop geodynamic models of the region to understand how and why giant ore deposits form within this portion of the Yilgarn Craton (e.g., Goleby *et al*., 1997; Hall, 1998; Sorjonen-Ward *et al*., 2002).

Many of the current models for the development of orogenic Au systems in the Yilgarn Craton use the deep seismic reflection data acquired in the Kalgoorlie region as an integral component for their development. Some of the features of the seismic reflections in the Kalgoorlie region, based on interpretation of the 1991, 1997 and 1999 seismic reflections profiles (Swager *et al*., 1997; Drummond *et al*., 2000; Goleby *et al*., 2000, 2002; Korsch *et al*., 2001) relevant to orogenic Au systems include:

- Other prominent structures are two W-dipping shear zones. One is the Bardoc-Boorara Shear that is apparently displaced by, and displaces the basal decollement, and links at depth with the Ida Fault. The W-dipping nature of the Bardoc-Boorara Shear is unusual on a regional scale, where E-dipping structures predominate. The other is interpreted to be the Avoca fault to the east of the Kalgoorlie region.
- A number of moderately- to steeply-dipping district-scale faults (Zuleika Shear, Boulder-Lefroy Fault, Mount Hunt Fault, Abattoir Shear and Kanowna Shear) are not very reflective and are difficult to resolve on the majority of seismic reflection profiles. Their locations, however, are identified by either truncation of reflections or by the structure that subdivides the seismic section into discrete domains. They are all interpreted to link into

the basal decollement of the greenstones, although evidence for this in the seismic profiles is limited.

- The crust can be subdivided into a mostly non-reflective upper crust, a middle crust containing numerous thrust duplexes, and a lower crust containing the bases of the duplexes.
- The greenstones and their intrusive granitoid plutons form a 4 to 7 km thick layer in the upper part of the crust.
- The greenstone sequence is underlain by a regional, subhorizontal reflector, which is interpreted as a regional detachment surface. The detachment surface is deeper beneath two regional granitoid domes (Goongarrie-Mt Pleasant, Scotia-Kanowna), and also appears to be deeper in the hanging wall of the Bardoc-Boorara Shear, suggesting the possibility of extensional movement for this shear. Many of the terrane and internal domain faults are shallow east or west dipping structures that terminate against this detachment.

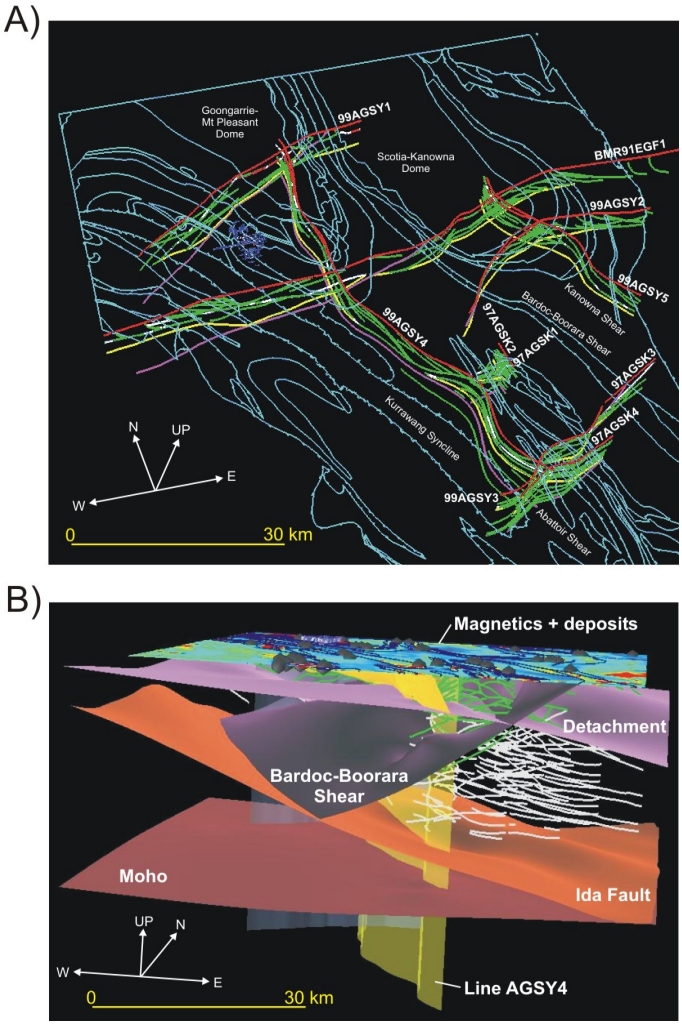

Figure 2. (A) Three dimensional 'wire' diagram of the Kalgoorlie region showing regional geological boundaries (blue) and the linework from the interpretation of the seismic profiles. Red = surface, yellow = detachment, purple = main faults, green = other boundaries interpreted on the seismic profiles. (B) View of the three-dimensional model of the Kalgoorlie region. This view looks northwards and shows the main features that defines the model. These are, from the bottom upwards, the Moho, the east-dipping Ida Fault, and the west-dipping Bardoc-Boorara Shear that soles onto the Ida Fault, the regional detachment beneath the granite-greenstone succession and the present day surface draped with aeromagnetic data. (modified from Goleby et al., 2002)

- The most prominent structure is the Ida Fault, which is an E-dipping, deep crustal structure. The Ida Fault has normal displacement, probably throughout the entire crust, as evidenced by an apparent deepening of the Moho from west of the Ida Fault to farther east, suggesting late stage extensional displacement across this structure.
- The middle- to lower crust beneath the Bardoc-Boorara Shear appears to be anomalous. It is mostly non-reflective, except for some weak, sub-horizontal reflections interpreted as late sills, and E-dipping linear reflections.
- The Moho can be traced continuously from west to east under this anomalous zone, but it deepens by approximately 5 kms towards the eastern part of the EGF1 seismic reflection profile.

The interpreted seismic reflection profiles indicate that there are elements consistent with both thrust-stacking and upright folding within the Kalgoorlie region. There is considerable evidence for extensive thrust stacking within the middle crust and in portions of the granite-greenstone succession, particularly beneath the granitoid domes. Archibald (1998) suggests that early structures (related to north-directed thrusting) appear bounded by the detachment at the base of the greenstones. The Ida Fault and Bardoc-Boorara Shear are examples of later structures that transect the detachment and appear related to deeper crustal decoupling around the lower crust-middle crust boundary. The importance of extensional movements in the deformation of the greenstones is now believed to be far greater than previously thought (Korsch *et al*., 2001).

In the Kalgoorlie region, orogenic Au deposits show a spatial proximity with some of the crustal-scale structures (e.g. Bardoc-Boorara Shear). Seismic reflection profiling discriminates between fault zones with no intrinsic reflectivity from those where strong fault zone reflectivity probably results from alteration caused by fluids that flux along the faults. In the Kalgoorlie region seismic images, the reflective fault systems appear linked and provide connecting pathways for hydrothermal fluids to move from lower crustal source regions up to sites of deposition (Drummond and Goleby, 1993). Linking of faults is important for fluid focussing and effective transport (Oliver, 2001). Provided fluids remain effectively channelled during transport to higher crustal-levels, camp- and deposit-scale structural focussing and associated local gold precipitation mechanisms may result in development of economic mineralisation at a variety of trap sites.

The Kalgoorlie region seismic images also record a region of anomalous reflectivity below the Bardoc-Boorara Shear, which is a consistent regional footwall feature to the highly mineralized Kalgoorlie-Kambalda corridor (Goleby *et al*., 1997; Drummond and Goleby, 1998). This mid-crustal region is mostly non-reflective except for some short sub-horizontal reflections. The Moho can be traced continuously underneath this anomalous zone indicating that the lack of reflectivity can be attributed to a lack of coherent reflectors. There are several ways to explain the anomalous reflectivity: (i) the crust may never have contained reflecting surfaces, (ii) the lack of reflections might be an indication that the region has been largely dehydrated during an episode of metamorphism, or (iii) the rocks in the region may have been largely homogenized through alteration by fluxing fluids (Drummond and Goleby, 1998). If the anomalous reflectivity is attributed to the fluxing of fluids, the region may have been the source of hydrothermal fluids that contributed to the development of the mineralizing systems. The Bardoc-Boorara Shear overlies the non-reflective region of the crust and may have acted as a conduit for the fluxing fluids to be transported to the surface. The development of gold mineralizing systems in the Kalgoorlie region, therefore, may be the result of large volumes of fluids being channelled from deeper within the crust into the overlying greenstone succession through linked crustal fluid pathways. At high crustal levels,

the role of secondary mixing of other fluid sources (e.g., meteoric water, high-level felsic magmas) with deeper mineralizing fluids potentially becomes important.

This linked fluid pathway model was tested and generally supported by numerical modelling of fluid flow (Upton *et al*., 1997) based on the structures defined by the 1991 EGF1 seismic transect across the Kalgoorlie region (Drummond and Goleby, 1993) and formed the basis of a generic fluid flow model ('Y-front' model; Figure 3) for the Kalgoorlie region (Hall, 1998). Fundamental to the Y-front model are transcrustal fault zones that penetrate and link entire crustal sections; in particular, the interpretation of the seismic profile indicating that the east-dipping Ida Fault intersects the west-dipping Bardoc-Boorara Shear in the mid-crust in a Y-like fashion. Thermal and fluid flow modelling for the 55 km section between the two faults suggest an early convection system involving the entire crust (Figure 3), possibly mobilizing metals from the lower crust to the mantle. Thermal modelling suggests both downward fluid flow in the upper crustal section and upward flow in the lower crustal section of the Ida Fault. Upward flow is indicated along the Bardoc-Boorara Shear from its intersection with the Ida Fault below the greenstone belt (Figure 3). This convection cell has the potential to mix mantle fluids and a myriad of metamorphic, magmatic (from "blind" stocks) and meteoric fluids, and to direct this "mixed" fluid along the Bardoc-Boorara Shear that acts as a focused discharge zone. The coupled deformation and fluid flow modelling predicted subsidiary (D_4) faults in the vicinity of known ore deposits and produces focused fluid flow into associated east-dipping shear zones. The study predicted higher prospectivity for gold along the Bardoc-Boorara, Zuleika, and to a lesser extent the Ida faults, with lower prospectivity along the other regional faults in the region (Goleby *et al*., 1997).

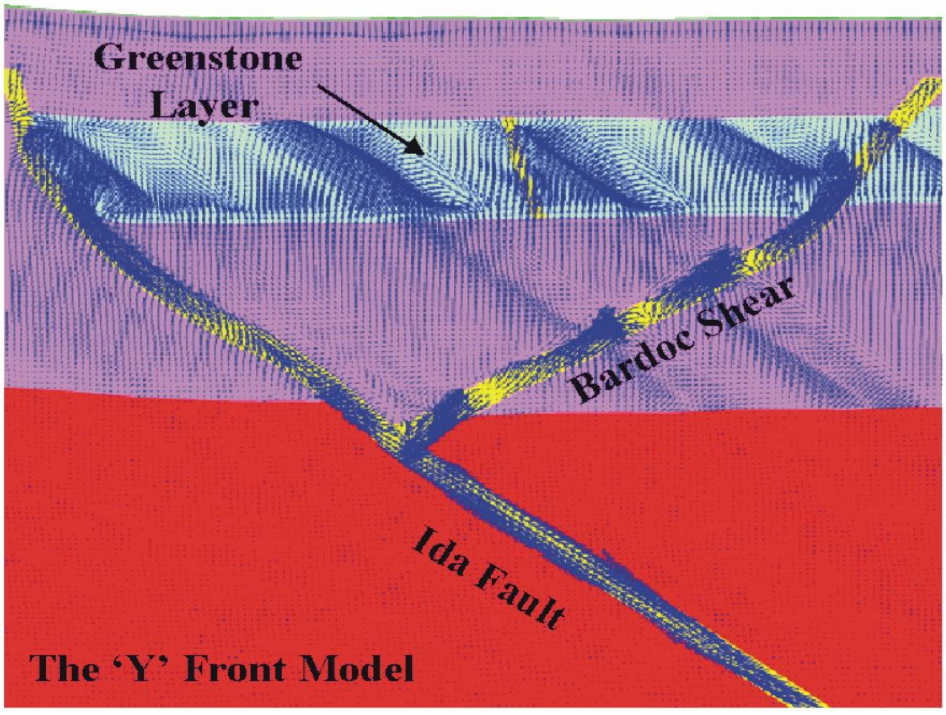

Figure 3. Fluid flow modelling of the interpreted EGF1 deep seismic reflection profile, Kalgoorlie region. The arrows represent fluid flow direction, their length representing the volume of fluid flow. The 'Y-front' model predicts increased fluid flow within the greenstone package along several major structures. (modified from Upton et al., 1997).

Subsequent numerical modelling of fluid flow and thermal convection by Sorjonen-Ward *et al* (2002) also focussed on the Kalgoorlie region and again used a simplified interpreted section

along part of the EGF1 deep seismic reflection profile. Sorjonen-Ward *et al*. (2002) suggest that the geometry of the interpreted seismic reflection profile is similar to tectonic wedges described in relation to backthrusting in thrust and fold belts and doubly vergent orogens (Figure 4; e.g., Jamison, 1993; Beaumont and Quinlan, 1994). The modelling illustrates the potential for fluid focussing and mixing in shear zones, lateral fluid flow driven by topographic elevation and upwards flow of fluids derived from melting and metamorphism in the deep crust (Figure 5; Sorjonen-Ward *et al*., 2002). The models highlight that tectonic wedging within a layered crust and diverging thrust systems that generate pop-up wedges may be important to drive fluid flow during uplift, whereas topographic differences tends to promote lateral fluid flow (Sorjonen-Ward *et al*., 2002). Similar conclusions were reached independently by Strayer *et al*. (2001), and highlight the importance of focussed fluid flow within fault zones.

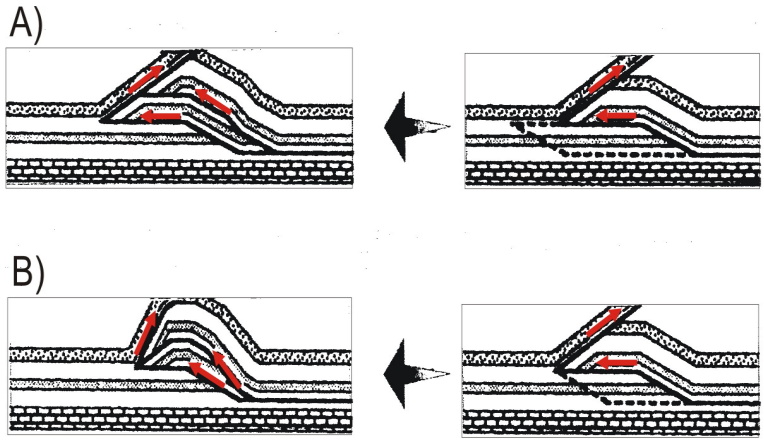

Figure 4. Tectonic wedging concept for a westward migrating thrust system beneath an east-vergent backthrust (modified from Jamison, 1993). Comparison of the antiformal stacks in (A) with (B) suggests that footwall rheology controls duplex propagation rate and amplification of the stack beneath the backthrust

Sorjonen-Ward *et al*. (2002) also modelled the effects of thermal convection and fluid-fluid interaction. The modelling identified two generic sites that are favourable for fluid mixing; these are hanging wall and footwall environments in major shear zones (e.g., Bardoc-Boorara Shear) and within broad antiformal structures such as the Goongarrie-Mt Pleasant dome.

In the above Kalgoorlie region case history, the broad geological framework is likely to have controlled both the distribution of the fluid sources and their migration pathways. These are key elements in one of the mineral systems models for gold in this region, and point to differing prospectivity across the region. Furthermore, knowing where fluids have moved through a province can further refine the areas of likely high prospectivity, with large deposits unlikely to occur where little or no fluids have been present. Knowledge of how the broad geological framework has affected the distribution of both fluid sources and migration pathways, therefore, has a profound effect on defining a region's prospectivity. It is important to note, however, that camp-, deposit- and ore shoot-scale fluid focussing mechanisms and depositional processes at these and even smaller scales are necessary for the development of economic mineralisation.

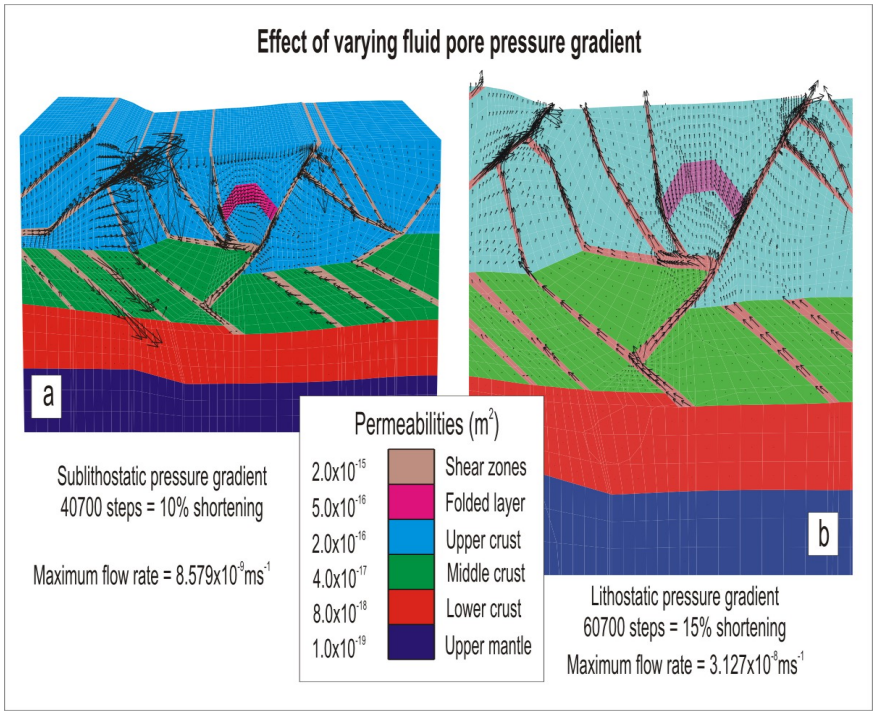

Figure 5. Numerical modelling of the interpreted EGF1 deep seismic reflection profile, Kalgoorlie region, showing incremental effect of pore pressure gradient on fluid flow and comparisons at different stages of deformation (modified from Sorjonen-Ward et al., 2002). (A) model is deformed by 10% shortening with fluid flow vectors superimposed on section and pore pressure gradient equivalent to 15% greater than hydrostatic. (B) model is deformed by 15% shortening and initial lithostatic pore pressure gradient throughout. Models illustrate fluid flow is focussed through shear zones, with some lateral flow

Major features of the Northeastern Yilgarn (01AGS-NY1 and 01AGS-NY3) seismic reflection profiles

Some of the major features of the Northeastern Yilgarn (01AGS-NY1 and 01AGS-NY3) deep seismic reflection profiles relevant to orogenic Au systems include:

- The crust can be subdivided into three layers; an upper crust that contains a complex arrangement of reflectivity, from areas that are non-reflective to areas that contain numerous high amplitude reflections, a middle crust containing numerous thrust duplexes, and a lower crust that contains predominantly sub-horizontal reflectors.
- The Moho can be traced continuously from west to east, although it deepens by approximately 5 kms towards the eastern part of the 01AGS-NY1 seismic profile. There is one prominent change where the Moho ramps down 2-3 kms over a short distance.
- The greenstones and their intrusive granitoid plutons form a 4 to 7 km thick layer in the upper part of the crust.
- The 01AGS-NY1 seismic reflection profile is characterised by abundant apparent E-dipping and sub-horizontal reflectors. In contrast, there are only a few apparent W-dipping reflectors along the profile. As most of the seismic reflection profile is across strike, the dips seen on the profiles are probably close to true values.
- The 01AGS-NY1 seismic reflection profile is dominated by three prominent E-dipping, deep crustal structures that penetrate the lower crust and possibly the mantle. They coincide, from west to east, with the down-dip extensions of the Mt George, Laverton and Yamarna shear zones. Each structure is a deformation corridor (up to several kilometres

wide) of sub-parallel reflectors that define a planar structure that dips about 30º to the east, and is characterised by a series of complex thrusts and shear zone splays in the hanging wall of the corridor (Figures 6, 7). The Laverton and Yamarna shear zones also have splays in the footwall of each structure; the Celia may be a splay or may form a basal structure to the Laverton shear zone. The Mt George shear zone is not as prominent as the other major structures and alternative interpretations are also possible for this structure (see Blewett *et al*., this volume).

- The Laverton and Yamarna shear zones are characterised by a wedge-shaped mid- to upper-crustal block defined by the intersection of a series of sub-horizontal high amplitude reflectors in the hanging wall to the east of each structure (Figure 7).
- The geometry of the Yamarna shear zone is determined through the changing orientation of the eastern end of 01AGS-NY1 and the intersection of 01AGS-NY1 with 01AGS-NY3 and indicates that the Yamarna shear zone is approximately ENE-dipping and approximately planar over significant length.
- As discussed by Blewett *et al*. (2002; this volume), the upper-crust is characterised by a series of LASH's (i.e., low-angle shears; e.g., Yundamindera LASH). These structures may be roof thrusts or represent extensional surfaces following earlier thrusting. TheYundamindera LASH is interpreted to predate the last movement on the Mt George shear zone (Blewett *et al*., this volume).
- Other shear zones prominent on the surface (e.g., Melita-Emu, Kilkenny and Celia shear zones) appear to be cut by the LASH's, although alternative interpretations for the Kilkenny shear zone have also been suggested (Blewett *et al*., 2002; this volume).
- Along the eastern end of the 01AGS-NY1 seismic reflection profile are two large, discrete W-dipping packages in the mid-crust. Analysis of their geometry along 01AGS-NY1 and 01AGS-NY3 suggests that they may be planar packages that have an apparent north dip. It is possible they are remnant D1 structures preserved in the mid-crust.
- Along the eastern end of the 01AGS-NY1 seismic reflection profile are several E- and W-dipping structures present in the top few kilometres of the crust. These structures are interpreted to reflect post-Archaean, and even post-Proterozoic deformation.

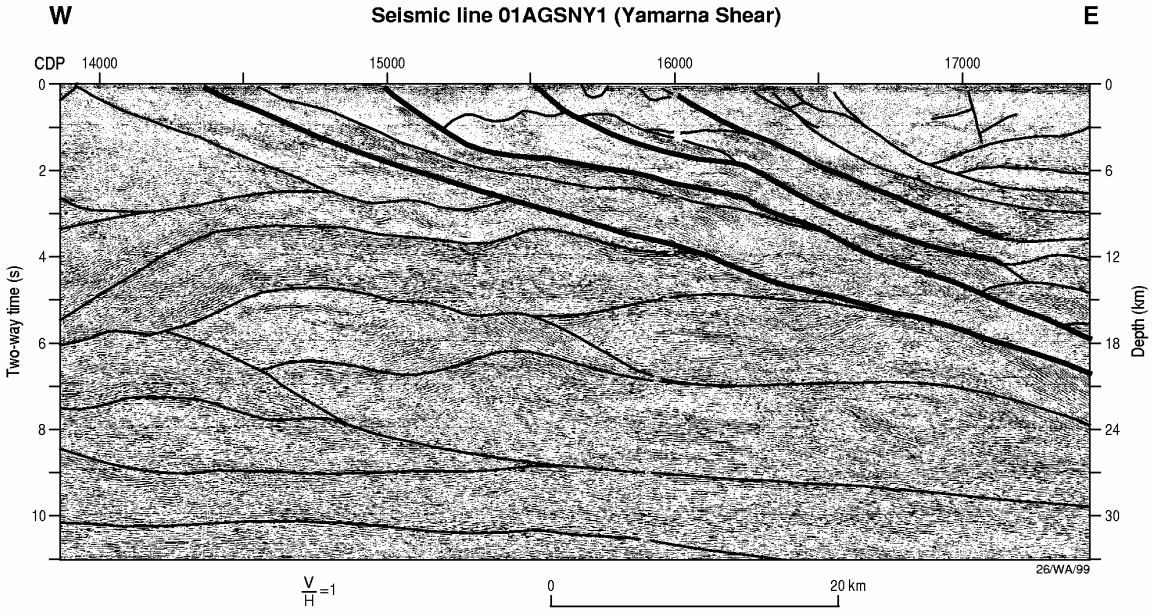

Figure 6. Section of the 01AGSNY1 deep seismic reflection profile showing the moderately E-Dipping Yamarna shear zone. Note also the subhorizontal reflectors in the hangingwall, and the sub-horizontal to W-dipping package of reflectors in the footwall to the shear zone.

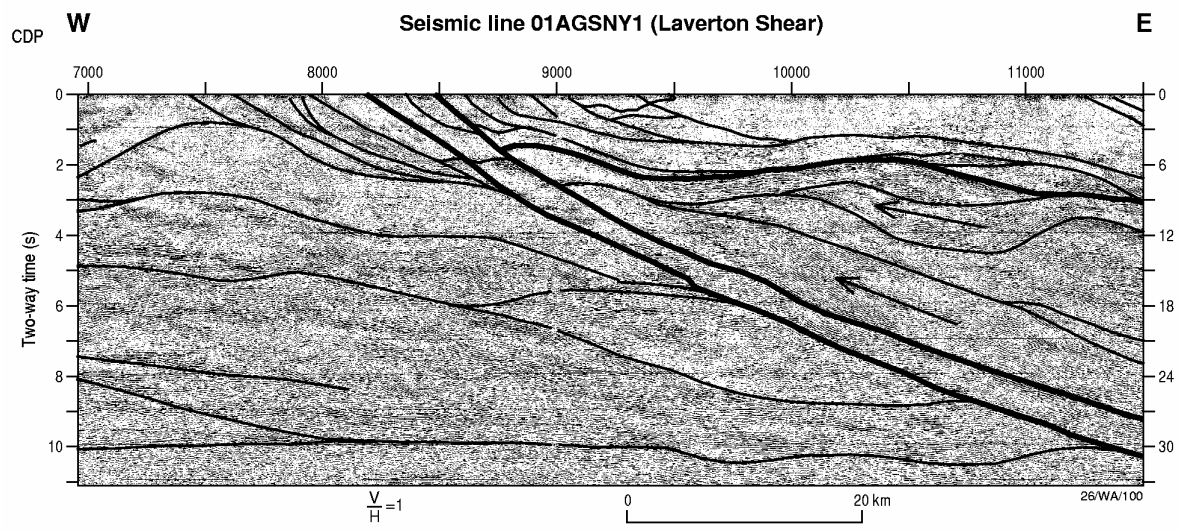

Figure 7. Schematic diagram of wedge-like geometry developed by the intersection of the moderately E-Dipping Laverton shear zone with subhorizontal reflectors in the hangingwall. Fluids from depth are focussed upwards into a narrow neck of the wedge at a depth of ~6-7 km

Similarities and differences between Kalgoorlie region and the Northeastern Yilgarn seismic profiles

It is evident that there are several features of the Northeastern Yilgarn (01AGS-NY1 and 01AGS-NY3) seismic profiles that are similar and some features that are different to those recorded in the Kalgoorlie region seismic profiles. Some of the similarities include:

- A well-defined crustal profile comprising a variably reflective upper crust, a middle crust containing numerous thrust duplexes, and a lower crust with predominantly sub-horizontal reflectors. Both regions are consistent with the middle crustal layer representing west-directed imbrication, essentially resulting in a stacked duplex geometry.
- A well-defined Moho that is generally planar, and dipping very shallowly to the east. Ramps in the Moho are evident at the down-dip extensions of the Ida and Laverton deep crustal structures.
- The greenstones and their intrusive granitoid plutons form a 4 to 7 km thick layer in the upper part of the crust in both regions. If regionally extensive komatiites are interpreted to represent a time marker and lithostratigraphic correlations of Hallberg (1985), Rattenbury (1993), Krapez *et al*. (2000) and Brown *et al*. (2001) are correct, there are significant differences in the lithostratigraphy of both regions and implicate either extensive thrust imbrication or tectonic interwedging.
- Both regions contain major E-dipping, deep crustal structures that penetrate the lower crust and possibly the mantle; the Ida Fault in the Kalgoorlie region and the Mt George, Laverton and Yamarna shear zones in the northeastern Yilgarn. The Laverton and Yamarna shear zones are the most prominent structures in the northeastern Yilgarn. The Ida Fault and Laverton shear zones record significant normal movement following earlier imbrication, suggesting that extensional collapse may have been important late in the tectonic history of the eastern Yilgarn.

Some of the differences include:

- One the most prominent features of the Kalgoorlie region seismic profiles is a regional detachment surface at the base of the greenstones and under some of the granite domes

(e.g., Drummond *et al*., 2000; Korsch *et al*., 2001; Goleby *et al*., 2002). Although in places along the 01AGS-NY1 seismic profile there are sub-horizontal and antiformal reflectors at the interpreted base of the greenstones, this surface is not regionally extensive and cannot be interpreted as a regional detachment surface.

- The Kalgoorlie region is characterised by several W-dipping major shear zones (e.g., Bardoc-Boorara), whereas W-dipping structures are uncommon on the Northeastern Yilgarn profiles. In the Kalgoorlie region, some of the W-dipping structures (e.g., Bardoc-Boorara Shear) truncate the detachment surface and their interaction with the E-dipping Ida Fault form the basis for the 'Y-front' geometry used by Upton *et al*. (1997) and Hall (1998) to explain the formation of large hydrothermal fluid cells within the upper crust. In the Northeastern Yilgarn there are no major W-dipping structures in the upper crust. There are, however, several W-dipping packages of reflectivity that are geometrically linked to the major E-dipping deep-crustal penetrating shear zones. In the Northeastern Yilgarn a 'Y-front' geometry cannot control the location of major orogenic Au mineralising systems.
- Although there is no 'Y-front' geometry along the Northeastern Yilgarn profiles, there are unusual wedge-like geometries on the hanging wall of the Laverton and Yamarna shear zones. These wedge geometries are apparent at the base of the upper crust where zones of sub-horizontal reflectors appear to be truncated by the major E-dipping, crustal-scale structures.

Implications of the Northeastern Yilgarn seismic reflection survey for orogenic Au mineral systems

There are a number of implications for orogenic Au mineralising systems from the Northeastern Yilgarn seismic reflection survey. These include:

- The unifying deformation feature of the eastern Yilgarn Craton is the major east-west compressive event that was superimposed on previously deformed cratonic elements. Recent studies in the Leonora-Laverton region indicate previously unrecognized complexity in the deformation sequence (e.g., Davis, 2001; Witt *et al*., 2001; Blewett *et al*., submitted). For instance, the presence of ca. 2755 Ma Mo-Au mineralisation in the Leonora area (Witt *et al*., 2001) reflects deformation and hydrothermal fluid flow at least 50 m.y. prior to much of the greenstone stratigraphy in the Kalgoorlie region. Much of this work suggests additional extensional episodes prior to, during and after the major contractional event (e.g., Davis, 2001; Blewett *et al*., this volume).
- The major east-west contractional event (D2) resulted in development of regional upright north-northwest-trending folds, and coincided with the uplift of granitoid-core anticlines and development of a pervasive metamorphic foliation (Swager, 1997). Hammond and Nisbet (1992) suggested that the regional antiforms were related to major thrusting, and this view is consistent with the seismic data from both the Kalgoorlie region (Drummond *et al*., 2000) and the 3D model developed for the Northeastern Yilgarn (Blewett *et al*., 2002). The timing of D2 is, however, contentious, with Swager (1997) suggesting ca. 2665 Ma and Krapez *et al*. (2000) suggesting ca. <2650 Ma.
- The presence of three major E-dipping, deep-crustal structures in the Northeastern Yilgarn. These include the Laverton and Yamarna shear zones that appear to penetrate the lower crust, are interpreted to truncate the prominent sub-horizontal reflectivity in the lower crust and, at least for the Laverton shear zone, possibly correlate with ramping down of the Moho. To the west of the 01AGS-NY1 seismic transect, the down-dip extension of the E-dipping Ida Fault is also associated with an apparent deepening of the Moho from west to east. The timing of the possible displacement of the Moho at the down-dip extension of the Ida and Laverton shear zones is, however, unresolved. The ramping of the Moho may

indicate late extension associated with orogenic collapse, or may be related to post-Archaean processes. The sub-horizontal reflectivity of the lower crust and presence of major deep-crustal structures on the NY1 and EGY1 profiles are similar to the seismic reflectivity pattern of Phanerozoic orogenic belts that have undergone orogenic collapse accompanied by low- to medium-P granulite facies metamorphism (e.g., Meissner *et al*., 1991; Rey, 1993). In contrast, a poorly reflective lower crust has been reported for areas that have not been affected by orogenic thickening processes (Rey, 1993), suggesting that the orogeny could be at the origin of the seismic fabric of the lower crust. In addition, the reflectivity pattern of regions where late orogenic extension has been demonstrated generally retains the character attributed to the later stages of compressional deformation (e.g., Appalachians: Quinlan *et al*., 1992; Beaumont and Quinlan, 1994). The reflectivity pattern in the eastern Yilgarn, therefore, may reflect processes during thermal and mechanical reequilibration of orogenically thickened crust. Alternatively, the apparent ramping of the Moho may be related to previously unrecognized post-Archaean deformation.

- The major E-dipping structures are potentially important conduits for fluids involved in the development of orogenic Au mineralising systems. Major orogenic Au deposits in the Northeastern Yilgarn are spatially associated with major structures. For instance, the Laverton tectonic zone is a highly-mineralised structural corridor containing the world-class Sunrise-Cleo and Wallaby deposits and many other smaller deposits. Some of the other major structures (e.g., Celia, Kilkenny and Mt George shear zones) do not appear to be as well endowed with respect to gold as the Laverton structure and this may reflect the deep-crustal through-going nature of the Laverton structural corridor. The prominence of the Yamarna shear zone, and its similarity to the highly-mineralised Laverton shear zone, may indicate that the Yamarna greenstone belt also potentially contains gold mineralisation.
- There is no evidence for a major 'Y-front' geometry in the Northeastern Yilgarn seismic profiles. This region is characterised instead by unusual wedge-like geometries developed in the hanging wall of the Laverton and Yamarna shear zones (Figure 7). The implications of this wedge-like geometry in terms of promoting focussed fluid flow and/or fluid mixing are not known, however, such geometries are possible where there is interaction between pre-existing structures and later west-directed compression. This wedge-like geometry may explain the endowment of the Laverton Domain. The funnelling effect caused by this wedge-like geometry may have focussed and concentrated deeper crustal fluids upwards towards the apex of the wedge (i.e., the Laverton shear zone and its hanging wall rocks that host major deposits, including Wallaby and Sunrise-Cleo).
- The 01AGS-NY1 seismic reflection profile shows a marked partitioning of the crust into three broad domains through the greenstone belt from the Raeside Batholith to Diorite Hill. The three domains are bounded by the Kilkenny shear zone and the Laverton shear zone (Figure 8). Between these shear zones, the upper crust is characterised by broad, open, flat structures. This style is partly a function of the oblique section of the profile with respect to regional strike. However, this style is believed to be real because few major faults transect the area, and the known surface geology of this area contains some of the most complete stratigraphic sequences of the profile area. In contrast, to the west of the Kilkenny shear zone, and to the east to the Laverton shear zone, the geometry of the upper crust is characterised by thrust? imbricates, with abundant well-develop seismic reflectors and roll-over anticlines developed in the hanging wall of major faults. In these areas, major faults transect the upper and middle crust. The Celia shear zone is a major fault that lies within the broad domain. It is difficult to interpret on the seismic reflection data and it does not have the rollover anticlines that typify the other through-going structures in the adjacent domains.

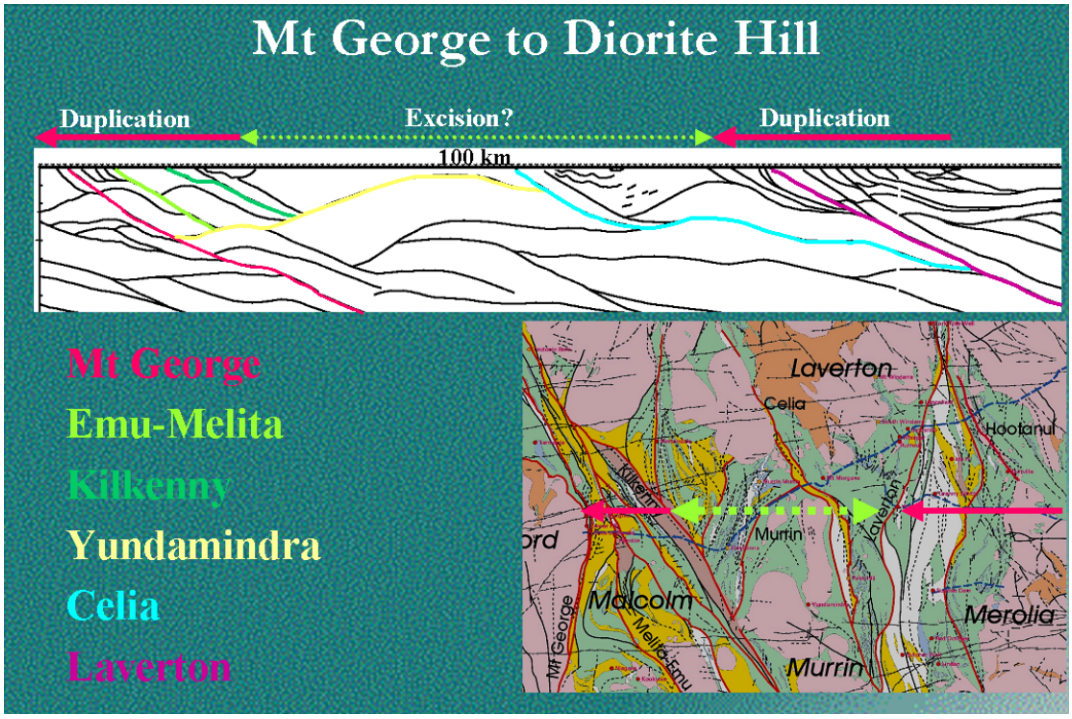

Figure 8. Interpreted section of the 01AGS-NY1 seismic reflection profile from the Raeside Batholith to Diorite Hill showing a marked partitioning of the crust into three broad domains through the Leonora-Laverton greenstone belt. The three domains are bounded by the Kilkenny shear zone and the Laverton shear zone

In summary, there are a number of implications for orogenic Au mineralising systems from the deep seismic reflection profiles. Potentially, the most significant implication is the presence of the major, deep-crustal Yamarna shear zone and associated complex structural corridor. The striking similarity of this structure with the highly mineralised Laverton shear zone suggests that similar geodynamic processes, and possibly similar fluid flow patterns, took place during the development of the Yamarna shear zone.

Acknowledgments

We would like to thank Leonie Jones, Tania Fomin and Ed Chudyk for processing the seismic reflection data, and Alan Whitaker and Russell Korsch for discussions. Kevin Cassidy, Richard Blewett, David Champion and Bruce Goleby publish with the permission of the Chief Executive Officer of Geoscience Australia. This report is a contribution to the *pmd**CRC Y2 project.

References

Archibald, N.J., 1998. 3D geology and tectonic synthesis of the Kalgoorlie Terrane. *in* Wood, S.E., ed., Geodynamics and Gold Exploration in the Yilgarn, Workshop Abstracts. *Australian Geodynamics Cooperative Research Centre, Western Australia*, 17-22.

Beaumont, C. and Quinlan, G., 1994. A geodynamic framework for interpreting crustal-scale seismic-reflectivity patterns in compressional orogens. *Geophysics Journal International*, **116**, 754-783.

Blewett, R.S., Champion, D.C., Whitaker, A.J., Bell, B., Nicoll, M., Goleby, B.R., Cassidy, K.F. and Groenewald, P.B., 2002. Three dimensional (3D) model of the Leonora-Laverton transect area: implications for Eastern Goldfields tectonics and mineralisation. *Geoscience Australia, Record*, **2002/18**, 83-100.

Blewett, R.S., Champion, D.C., Cassidy, K.F., Goleby, B.R., Bell, B., Groenewald, P.B., Nicoll, M. and Whitaker, A.J., 2003. Implications of the northeastern Yilgarn seismic traverse to the Leonora-Laverton three dimensional (3D) model. (*this volume*).

Blewett, R.S., Cassidy, K.F., Champion, D.C., Henson, P.A., Goleby, B.R., Jones, L. and Groenewald, P.B., submitted. The Wangkathaa Orogeny: an example of episodic regional 'D_2' in the late Archaean Eastern Goldfields Province, Western Australia. *Precambrian Research*.

Brown, S.J.A., Krapez, B., Beresford, S.W., Cassidy, K.F., Champion, D.C., Barley, M.E. and Cas, R.A.F., 2001. Archaean volcanic and sedimentary environments of the Eastern Goldfields Provionce, Western Australia – A field guide. *Western Australia Geological Survey, Record*, **2001/13**, 66p.

Calvert, A.J. and Ludden, J.N., 1999. Archean continental assembly in the southeastern Superior Province of Canada. *Tectonics*, **18**, 412-429.

Cook, F., Brown, L.D., Kaufman, S., Oliver, J. and Von Tish, D., 1981. COCORP seismic profiling of the Appalachian orogen beneath the coastal plain of Georgia. *Geological Society of America, Bulletin*, **92**, 738-748.

Cox, S.F., 1999. Deformational controls on the dynamics of fluid flow in mesothermal gold systems. *in* McCaffrey, K.J.W., Lonergan, L. and Wilkinson, J.J., eds., Fractures, Fluid Flow and Mineralization. *Geological Society, London, Special Publication*, **155**, 123-140.

Davis, B.K., 2001. Complexity of tectonic history in the Eastern Goldfields Province, Yilgarn Craton. *in* Cassidy, K.F., Dunphy, J.M. and Van Kranendonk, M.J., eds., 4th International Archaean Symposium, Extended Abstracts. *AGSO – Geoscience Australia Record*, **2001/37**, 423-425.

De Boorder, H., Sparkman, W., White, S.H. and Wortell, M.J.R., 1998. Late Cenozoic mineralization, orogenic collapse, and slab detachment in the European Alpine belt. *Earth and Planetary Science Letters*, **164**, 569-575.

Drummond, B.J. and Goleby, B.R., 1993. Seismic reflection images of the major ore-controlling structures in the Eastern Goldfields Province, Western Australia. *Exploration Geophysics*, **24**, 473-478.

Drummond, B.J. and Goleby, B.R., 1998. Yilgarn crustal structure revealed in five seismic profiles. *in* Wood, S.E., ed., Geodynamics and Gold Exploration in the Yilgarn, Workshop Abstracts. *Australian Geodynamics Cooperative Research Centre*, 23-31.

Drummond, B.J., Goleby, B.R. and Swager, C.P., 2000. Crustal signature of Late Archaean tectonic episodes in the Yilgarn craton, Western Australia: evidence from deep seismic sounding. *Tectonophysics*, **329**, 193-221.

Eisenlohr, B.N., Groves, D.I. and Partington, G.A., 1989. Crustal-scale shear zones and their significance to Archaean gold mineralization in Western Australia. *Mineralium Deposita*, **24**, 1-8.

Ganchin, Y.V., Smithson, S.B., Morozov, I.B., Smythe, D.K., Garipov, V.Z., Karaev, N.A. and Kristofferson, Y., 1998. Seismic studies around the Kola superdeep borehole, Russia. *Tectonophysics*, **288**, 1-16.

Goldfarb, R.J., Groves, D.I. and Gardoll, S., 2001. Orogenic gold and geologic time: A global synthesis. *Ore Geology Reviews*, **18**, 1-75.

Goleby, B.R., Shaw, R.D., Wright, C., Kennett, B.L.N. and Lambeck, K., 1989. Geophysical evidence for 'thick skinned' crustal deformation in central Australia. *Nature*, **337**, 325-330.

Goleby, B.R., Rattenbury, M.S., Swager, C.P., Drummond, B.J., Williams, P.R., Sheraton, J.E. and Heinrich, C.A., 1993. Archaean crustal structure from seismic reflection profiling, Eastern Goldfields, Western Australia. *Australian Geological Survey Organisation, Record*, **1993/15**, 54p.

Goleby, B.R., Drummond, B.J., Owen, A., Yeates, A.N., Jackson, J., Swager, C. and Upton, P., 1997. Structurally controlled mineralization in Australia – How seismic profiling helps find minerals: Recent case histories. *in* Gubins, A.G., ed., Proceedings of Exploration '97. *Fourth Decennial International Conference on Mineral Exploration: GEO F/X, Toronto*, 409-420.

Goleby, B.R., Bell, B., Korsch, R.J., Sorjonen-Ward, P., Groenewald, P.B., Wyche, S., Bateman, R., Fomin, T., Witt, W., Walshe, J., Drummond, B.J. and Owen, A.J., 2000. Crustal structure and fluid flow in the Eastern Goldfields, Western Australia. *Australian Geological Survey Organisation, Record*, **2000/34**, 109p.

Goleby, B.R., Korsch, R.J., Fomin, T., Bell, B., Nicoll, M.G., Drummond, B.J. and Owen, A.J., 2002. A preliminary 3D geological model of the Kalgoorlie region, Yilgarn Craton, Western Australia based on deep seismic reflection and potential field data. *Australian Journal of Earth Sciences*, **49**, 917-933.

Groves, D.I., Goldfarb, R.J., Knox-Robinson, C.M., Ojala, J., Gardoll, S., Yun, G.Y. and Holyland, P., 2000. Late-kinematic timing of orogenic gold deposits and significance for computer-based exploration techniques with emphasis on the Yilgarn Block, Western Australia. *Ore Geology Reviews*, **17**, 1-38.

Hagemann, S.G. and Cassidy, K.F., 2000. Archaean orogenic lode gold deposits. *in* Hagemann, S.G. and Brown, P.E., eds,. Gold in 2000. *Reviews in Economic Geology*, **13**, 9-62.

Hall, G., 1998. Autochthonous model for gold metallogenesis and exploration in the Yilgarn. *in* Wood, S.E., ed., Geodynamics and Gold Exploration in the Yilgarn, Workshop Abstracts. *Australian Geodynamics Cooperative Research Centre, Western Australia*, 32-35.

Hallberg, J.A., 1985. *Geology and Mineral Deposits of the Leonora – Laverton area, Northeastern Yilgarn Block, Western Australia*. Hesperian Press, Carlisle, Western Australia, 140p.

Hammond, R.L. and Nisbet, B.W., 1992. Towards a structural and tectonic framework for the Norseman-Wiluna greenstone belt. *in* GLOVER, J.E. and HO, S.E., eds., The Archaean: Terrains, Processes and Metallogeny. *University of Western Australia, Geology Department (Key Centre) and Extension, Publication*, **22**, 39-50.

Hodgson, C.J., 1989. The structure of shear-related, vein-type gold deposits: A review. *Ore Geology Reviews*, **4**, 231-273.

Hurich, C.A., Smithson, S.B., Fountain, D.M. and Humphreys, M.C., 1985. Seismic evidence of mylonite reflectivity and deep structure in the Kettle dome metamorphic core complex, Washington. *Geology*, **13**, 577-580.

Jamison, W.R., 1993. Mechanical stability of the triangle zone: the backthrust wedge. *Journal of Geophysical Research*, **98B**, 20015-20032.

Jones, T. and Nur, A., 1982. Seismic velocity and anisotropy in mylonites and the reflectivity of deep crustal fault zones. *Geology*, **10**, 260-263.

Jones, L.E.A., Chudyk, E., Goleby, B.R., Johnstone, D.W. and Barton, T.J., 2002. Seismic data acquisition and processing – 2001 Northeastern Yilgarn Seismic Reflection Survey (L154). *Geoscience Australia, Record*, **2002/18**, 111-118.

Kerrich, R., 1989. Geodynamic setting and hydraulic regimes: shear zone hosted mesothermal gold deposits. *in* Bursnall, J.T., ed., Mineralization and Shear Zones, *Geological Association of Canada, Short Course Notes*, **6**, p.89-128.

Korsch, R.J., Goleby, B.R., Fomin, T. and Bell, B., 2001. Imaging the Kalgoorlie region using seismic and gravity techniques. *in* Cassidy, K.F., Dunphy, J.M. and Van Kranendonk,

M.J., eds., 4th International Archaean Symposium, Extended Abstracts. *AGSO – Geoscience Australia Record*, **2001/37**, 516-518.

Krapez, B., Brown, S.J.A., Hand, J., Barley, M.E. and Cas, R.A.F., 2000. Age constraints on recycled crustal and supracrustal sources of Archaean metasedimentary sequences, Eastern Goldfields Province, Western Australia: evidence from SHRIMP zircon dating. *Tectonophysics*, **322**, 89-133.

Meissner, R., Wever, TH. and Sadowiak, P., 1991. Continetial collisions and seismic signature. *Geophysics Journal International*, **105**, 15-23.

Neumayr, P. and Hagemann, S.G., 2002. Hydrothermal fluid evolution within the Cadillac Tectonic Zone, Abitibi greenstone belt, Canada: Relationship to auriferous fluids in adjacent second- and third-order shear zones. *Economic Geology*, **97**, 1203-1225.

Oliver, N.H.S., 2001. Linking of regional and local hydrothermal systems in the mid-crust by shearing and faulting. *Tectonophysics*, **335**, 147-161.

Quinlan, G.M., Hall, J., Williams, H., Wright, J.A., Colman-Sadd, S.P., O'Brien, S.J., Stockmal, G.S. and Marilloez, P., 1992. LITHOPROBE onshore seismic reflection transects across the Newfoundland Appalachians. *Canadian Journal of Earth Sciences*, **29**, 1865-1877.

Quinlan, G.M., Beuamont, C. and Hall, J., 1993. Tectonic model for crustal seismic reflectivity patterns in compressional orogens. *Geology*, **21**, 663-666.

Rattenbury, M. S., 1993. Tectonostratigraphic terranes in the northern Eastern Goldfields. *in* Williams, P.R. and Haldane, J.A., compilers, An international conference on the Crustal Evolution, Metallogeny and Exploration of the Eastern Goldfields, Extended Abstracts, *Australian Geological Survey Organisation Record*, **1993/54**, 29-32.

Rey, P., 1993. Seismic and tectono-metamorphic characters of the lower continental crust in Phanerozoic areas: a consequence of post-thickening extension. *Tectonics*, **12**, 580-590.

Robert, F., 1990. Structural setting and control of gold-quartz veins of the Val d'Or area, southeastern Abitibi subprovince. *in* Ho, S.E., Robert, F. and Groves, D.I., compilers, Gold and base-metal mineralization in the Abitibi subprovince, Canada, with emphasis on the Quebec segment. *Geology Department and University Extension, The University of Western Australia, Publication*, **24**, 167-209.

Smithson, S.B., Wenzel, F., Ganchin, Y.V. and Morozov, I.B., 2000. Seismic studies at Kola and KTB deep scientific boreholes: velocities, reflections, fluids and crustal composition. *Tectonophysics*, **329**, 301-317.

Sorjonen-Ward, P., Zhang, Y. and Zhao, C., 2002. Numerical modelling of orogenic processes and gold mineralisation in the southeastern part of the Yilgarn Craton, Western Australia. *Australian Journal of Earth Sciences*, **49**, 935-964.

Strayer, L.M., Hudleston, P.J. and Lorig, L.J., 2001. A numerical model of deformation and fluid-flow in an evolving thrust wedge. *Tectonophysics*, **335**, 121-145.

Swager, C.P., 1997. Tectono-stratigraphy of late Archaean greenstone terrains in the southern Eastern Goldfields, Western Australia. *Precambrian Research*, **83**, 11-41.

Upton, P., Hobbs, B., Ord, A., Zhang, Y., Drummond, B. and Archibald, N., 1997. Thermal and deformation modelling of the Yilgarn Deep Seismic transect. *Geodynamics and Ore Deposits Conference, Australian Geodynamics Cooperative Research Centre, Ballarat, Victoria*, 22-25.

Witt, W.K., Stein, H.J., Cassidy, K.F., Black, L., Champion, D.C. and Fletcher, I.R., 2001. A >2.75 Ga basement enclave at Leonora: a domain of uplift and 2.75 Ga gold within the 2.71-2.66 Ga Eastern Goldfields Province. *AGU Chapman Conference, Extended Abstracts*.

Wyman, D.A., Kerrich, R. and Groves, D.I., 1999. Lode gold deposits and Archean mantle plume-island arc interaction, Abitibi Subprovince, Canada. *The Journal of Geology*, **107**, 715-725.

